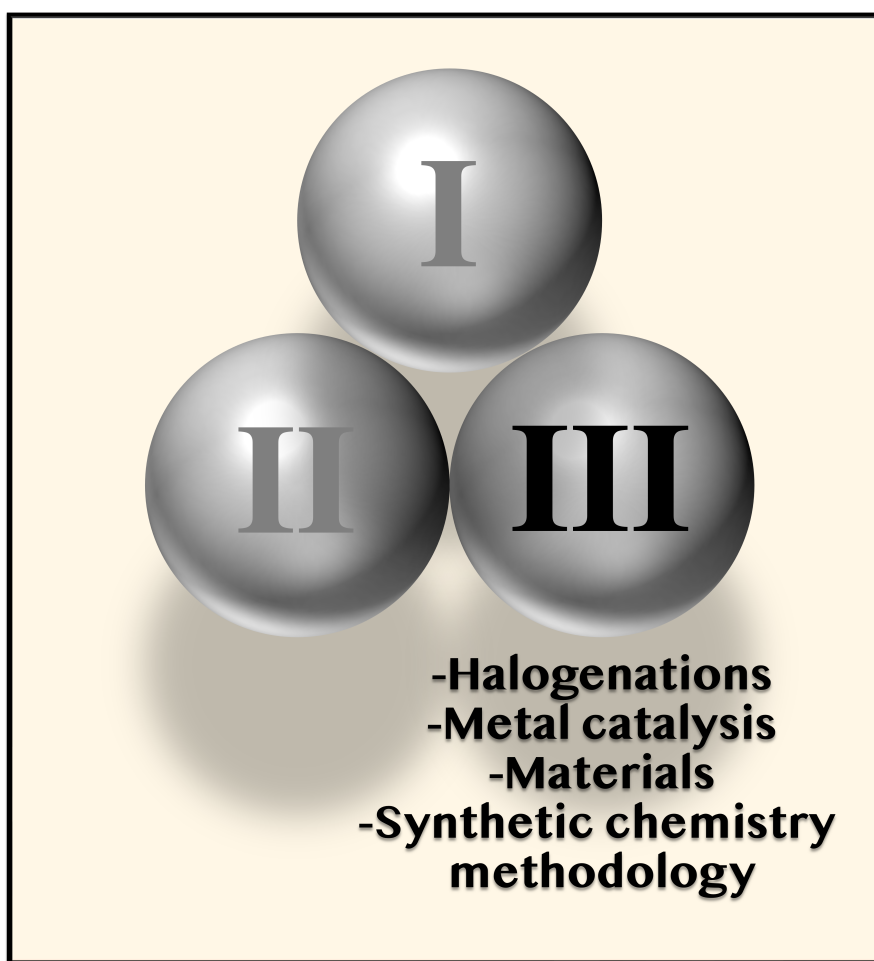




Mechanochemistry III

Edited by José G. Hernández and Lars Borchardt



Imprint

Beilstein Journal of Organic Chemistry

www.bjoc.org

ISSN 1860-5397

Email: journals-support@beilstein-institut.de

The *Beilstein Journal of Organic Chemistry* is published by the Beilstein-Institut zur Förderung der Chemischen Wissenschaften.

Beilstein-Institut zur Förderung der Chemischen Wissenschaften
Trakehner Straße 7–9
60487 Frankfurt am Main
Germany
www.beilstein-institut.de

The copyright to this document as a whole, which is published in the *Beilstein Journal of Organic Chemistry*, is held by the Beilstein-Institut zur Förderung der Chemischen Wissenschaften. The copyright to the individual articles in this document is held by the respective authors, subject to a Creative Commons Attribution license.

The cover image, copyright 2022 José G. Hernández, is licensed under the Creative Commons Attribution 4.0 license (<https://creativecommons.org/licenses/by/4.0/>). The reuse, redistribution or reproduction requires that the author, source and license are credited. The cover image shows the “three-balls” symbol recurrently used to denote mechanochemical transformations.



Dissecting Mechanochemistry III

Lars Borchardt^{*1} and José G. Hernández^{*2}

Editorial

Open Access

Address:

¹Department of Inorganic Chemistry, Ruhr-Universität Bochum, Universitätsstrasse 150, 44801 Bochum, Germany and ²Grupo Ciencia de los Materiales, Instituto de Química, Facultad de Ciencias Exactas y Naturales, Universidad de Antioquia, Calle 70 No 52-21, Medellín, Colombia

Email:

Lars Borchardt^{*} - lars.borchardt@rub.de; José G. Hernández^{*} - joseg.hernandez@udea.edu.co

^{*} Corresponding author

Beilstein J. Org. Chem. **2022**, *18*, 1454–1456.

<https://doi.org/10.3762/bjoc.18.150>

Received: 12 September 2022

Accepted: 04 October 2022

Published: 12 October 2022

Guest Editors: L. Borchardt and J. G. Hernández

© 2022 Borchardt and Hernández; licensee Beilstein-Institut.

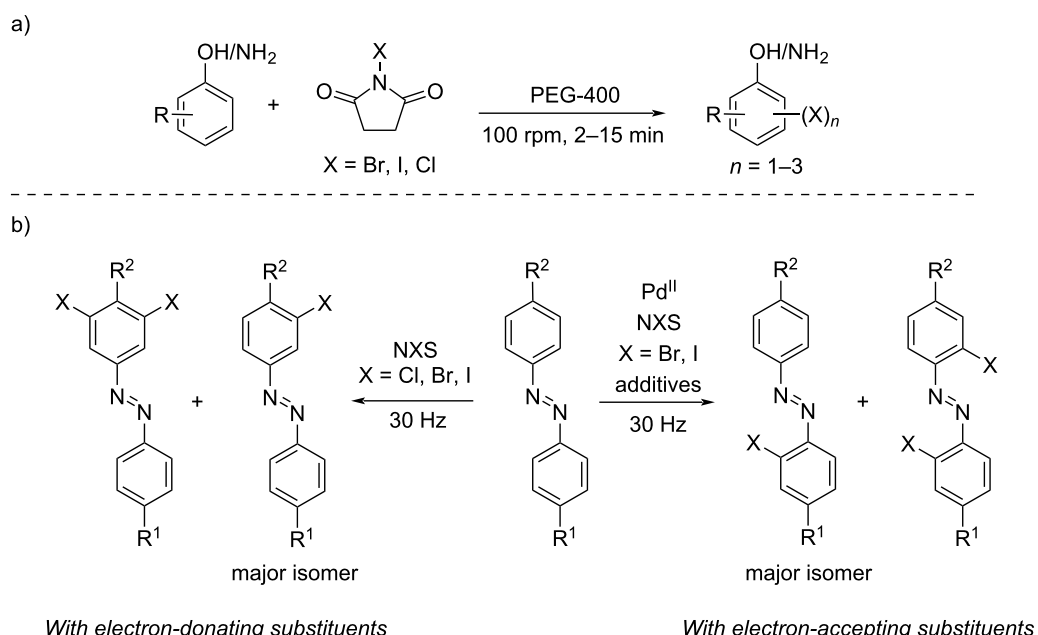
License and terms: see end of document.

In the past ten years, the use of mechanochemical techniques (e.g., grinding, milling, extrusion, pulsed ultrasonication, resonant acoustic mixing, etc.) have widespread in the field of organic chemistry, enabling the development of new and more sustainable protocols for chemical synthesis [1,2]. Within this period, the *Beilstein Journal of Organic Chemistry* has organized two Thematic Issues (i.e., Mechanochemistry and Mechanochemistry II) to facilitate the open dissemination of the best research in the field of synthetic organic mechanochemistry. The great success of these past initiatives encouraged us to organize Mechanochemistry III, a new Thematic Issue in which the readership of the journal will find a collection of full research papers, letters and, for the first time, a Perspective article.

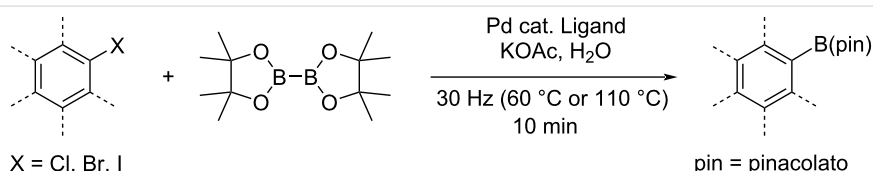
In more detail, the readers will find new mechanochemical protocols for the halogenation of organic substrates. For example, Banerjee and co-workers reported the mono-, di-, and trihalogenation of aromatics by controlling the stoichiometry of the *N*-halosuccinimide (NXS) and PEG-400 as the grinding auxiliary in a mechanical grinder (Scheme 1a) [3].

N-Halosuccinimides were also key reagents to develop the mechanochemical halogenation of azobenzenes as studied by Ćurić and co-workers [4]. They demonstrated how, depending on the azobenzene structure, the halogenation of the C–H bonds with NBX occurred in the presence of Pd(II) catalysts or under metal-free conditions (Scheme 1b). Similarly, in the absence of metal catalysts, *N*-fluorobenzenesulfonimide (NFSI) was found to act as a mild fluorinating reagent for activated aromatics by mechanochemistry [5]. Such a collective effort to access halogenated substrates is understandable, owning the synthetic value of organic halides as substrates in multiple reactions. For instance, within this Thematic Issue, the synthetic relevance of aryl halides was evidenced during the development of a protocol for the solid-state palladium-catalyzed borylation reported by Kubota, Ito, and co-workers (Scheme 2) [6].

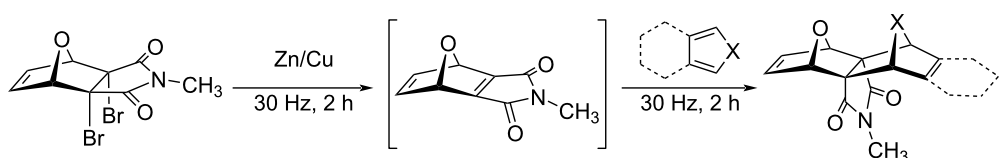
Moreover, Štrbac and Margetić used dibrominated polycyclic imides as substrates to generate reactive alkenes, which could be trapped in situ by several dienes through Diels–Alder cycloadditions by ball milling (Scheme 3) [7].



Scheme 1: a) Mechanochemical PEG-400-assisted halogenation of phenols and anilines using NXS. b) Halogenation of azobenzenes with NXS.



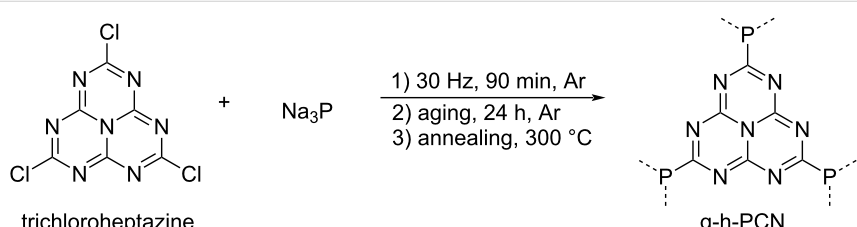
Scheme 2: Mechanochemical palladium-catalyzed borylation protocol of aryl halides.



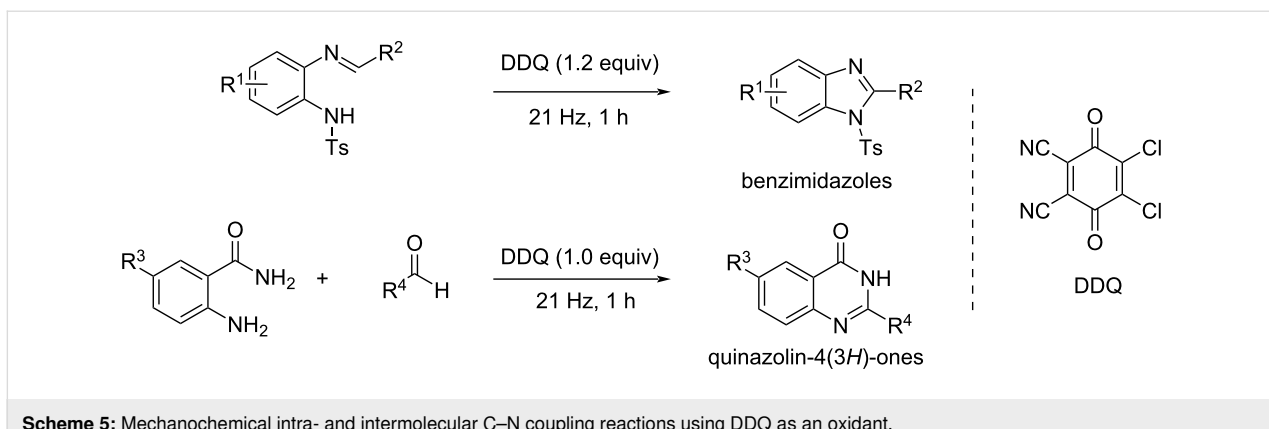
Scheme 3: 1,2-Debromination of polycyclic imides, followed by in situ trapping of the dienophile by several dienes.

Further, Moores and co-workers synthesized phosphorus-bridged heptazine-based carbon nitrides (g-h-PCN) from an initial mechanical treatment of trichloroheptazine and Na_3P ,

once again highlighting the importance of halogenated organic molecules as building blocks for graphitic heptazine materials (Scheme 4) [8].



Scheme 4: Synthesis of g-h-PCN from sodium phosphide and trichloroheptazine mediated by mechanochemistry.

**Scheme 5:** Mechanochemical intra- and intermolecular C–N coupling reactions using DDQ as an oxidant.

Another halogenated molecule, 2,3-dichloro-5,6-dicyano-1,4-benzoquinone (DDQ), proved to be an appropriate oxidant for C–N couplings towards the synthesis of 1,2-disubstituted benzimidazoles and quinazolin-4(3*H*)-one derivatives under mechanochemical conditions, as evidenced by Mal and co-workers (Scheme 5) [9].

However, the findings within Mechanochemistry III span beyond the synthesis or the use of halogenated compounds and include the mechanochemical preparation of isocyanides [10], formylated and acetylated amines [11], and the mechanosynthesis of unsymmetrical salens ligands for preparing metal–salen catalysts [12]. This illustrates the broad applicability of mechanochemical activation to advance chemical synthesis on various fronts. Therefore, we hope you enjoy reading the variety of manuscripts in this Thematic Issues as much as we enjoyed editing it, which was only possible thanks to the impeccable assistance by the Editorial Team of the Beilstein-Institut.

Lars Borchardt and José G. Hernández

Bochum, Medellín, October 2022

ORCID® iDs

Lars Borchardt - <https://orcid.org/0000-0002-8778-7816>

José G. Hernández - <https://orcid.org/0000-0001-9064-4456>

References

1. Friščić, T.; Mottillo, C.; Titi, H. M. *Angew. Chem., Int. Ed.* **2020**, *59*, 1018–1029. doi:10.1002/anie.201906755
2. Ardila-Fierro, K. J.; Hernández, J. G. *ChemSusChem* **2021**, *14*, 2145–2162. doi:10.1002/cssc.202100478
3. Das, D.; Bhosle, A. A.; Chatterjee, A.; Banerjee, M. *Beilstein J. Org. Chem.* **2022**, *18*, 999–1008. doi:10.3762/bjoc.18.100
4. Barišić, D.; Pajić, M.; Halasz, I.; Babić, D.; Ćurić, M. *Beilstein J. Org. Chem.* **2022**, *18*, 680–687. doi:10.3762/bjoc.18.69
5. Hernández, J. G.; Ardila-Fierro, K. J.; Barišić, D.; Geneste, H. *Beilstein J. Org. Chem.* **2022**, *18*, 182–189. doi:10.3762/bjoc.18.20
6. Kubota, K.; Baba, E.; Seo, T.; Ishiyama, T.; Ito, H. *Beilstein J. Org. Chem.* **2022**, *18*, 855–862. doi:10.3762/bjoc.18.86
7. Štrbac, P.; Margetić, D. *Beilstein J. Org. Chem.* **2022**, *18*, 746–753. doi:10.3762/bjoc.18.75
8. Fiss, B. G.; Douglas, G.; Ferguson, M.; Becerra, J.; Valdez, J.; Do, T.-O.; Friščić, T.; Moores, A. *Beilstein J. Org. Chem.* **2022**, *18*, 1203–1209. doi:10.3762/bjoc.18.125
9. Bera, S. K.; Bhanja, R.; Mal, P. *Beilstein J. Org. Chem.* **2022**, *18*, 639–646. doi:10.3762/bjoc.18.64
10. Basoccu, F.; Cuccu, F.; Casti, F.; Mocci, R.; Fattuoni, C.; Porcheddu, A. *Beilstein J. Org. Chem.* **2022**, *18*, 732–737. doi:10.3762/bjoc.18.73
11. Casti, F.; Mocci, R.; Porcheddu, A. *Beilstein J. Org. Chem.* **2022**, *18*, 1210–1216. doi:10.3762/bjoc.18.126
12. Zuo, S.; Zheng, S.; Liu, J.; Zou, A. *Beilstein J. Org. Chem.*, in press.

License and Terms

This is an open access article licensed under the terms of the Beilstein-Institut Open Access License Agreement (<https://www.beilstein-journals.org/bjoc/terms>), which is identical to the Creative Commons Attribution 4.0 International License

(<https://creativecommons.org/licenses/by/4.0/>). The reuse of material under this license requires that the author(s), source and license are credited. Third-party material in this article could be subject to other licenses (typically indicated in the credit line), and in this case, users are required to obtain permission from the license holder to reuse the material.

The definitive version of this article is the electronic one which can be found at:

<https://doi.org/10.3762/bjoc.18.150>



Multi-faceted reactivity of *N*-fluorobenzenesulfonimide (NFSI) under mechanochemical conditions: fluorination, fluoro-demethylation, sulfonylation, and amidation reactions

José G. Hernández^{*1,2,§}, Karen J. Ardila-Fierro³, Dajana Barišić¹ and Hervé Geneste^{*4}

Full Research Paper

Open Access

Address:

¹Division of Physical Chemistry, Ruder Bošković Institute, Bijenička c. 54, 10000 Zagreb, Croatia, ²current address Instituto de Química, Facultad de Ciencias Exactas y Naturales, Universidad de Antioquia, Calle 70 No 52-21, Medellín, Colombia, ³Division of Materials Chemistry, Ruder Bošković Institute, Bijenička c. 54, 10000 Zagreb, Croatia and ⁴AbbVie Deutschland GmbH & Co. KG, Neuroscience Research, D-67008 Ludwigshafen, Germany

Email:

José G. Hernández^{*} - jhernand@irb.hr; Hervé Geneste^{*} - herve.geneste@abbvie.com

* Corresponding author

§ current email address: joseg.hernandez@udea.edu.co

Keywords:

amidation; ball mill; fluorination; *in situ* monitoring; mechanochemistry; NFSI; Raman monitoring; sulfonylation

Beilstein J. Org. Chem. **2022**, *18*, 182–189.

<https://doi.org/10.3762/bjoc.18.20>

Received: 26 November 2021

Accepted: 26 January 2022

Published: 07 February 2022

This article is part of the thematic issue "Mechanochemistry III".

Associate Editor: L. Vaccaro

© 2022 Hernández et al.; licensee Beilstein-Institut.

License and terms: see end of document.

Abstract

In the search for versatile reagents compatible with mechanochemical techniques, in this work we studied the reactivity of *N*-fluorobenzenesulfonimide (NFSI) by ball milling. We corroborated that, by mechanochemistry, NFSI can engage in a variety of reactions such as fluorinations, fluorodemethylations, sulfonylations, and amidations. In comparison to the protocols reported in solution, the mechanochemical reactions were accomplished in the absence of solvents, in short reaction times, and in yields comparable to or higher than their solvent-based counterparts.

Introduction

Mechanosynthesis of organic molecules and materials using mechanochemical techniques such as ball milling, extrusion, grinding, etc. [1–3] have enabled the development of known and new chemical transformations in a more sustainable fashion [4]. Commonly, mechanochemical reactions by ball milling involve the mechanical treatment of at least one solid reagent in the

presence of other solid, liquid or gaseous reaction partners or additives [5,6]. Due to the particular reaction conditions in which mechanochemical reactions by milling are carried out, reagents need to exhibit stability under environments of mechanical stress, while at the same time enough reactivity to engage in chemical transformations. In the search for solid

reagents compatible with mechanochemical techniques, we became interested in evaluating the behavior of *N*-fluorobenzene-sulfonimide (NFSI) under ball-milling conditions. NFSI is a colorless crystalline powder (mp 114–116 °C), bench-stable, and an easy-to-handle reagent, which, due to its commercial availability, has been extensively used as a fluorinating agent in solution [7–9]. Additionally, NFSI has also been explored as an oxidant, amidation reagent [9–11], and phenylsulfonyl group transfer reagent [12,13].

In the field of mechanochemistry, the usefulness of *N*-fluorobenzenesulfonimide has been exemplified in the asymmetric fluorination of β -keto esters (Scheme 1a) [14], and in diastereoselective fluorinations (Scheme 1b) [15], which complemented mechanochemical fluorinations carried out with other reagents, such as AgF [16], 1-chloromethyl-4-fluoro-1,4-diazoniabicyclo[2.2.2]octane bis(tetrafluoroborate) (Selectfluor®) [17–20], among other fluorinating reagents [21].

However, as shown above, examples using NFSI by mechanochemistry are scarce and they have mostly been focused on the fluorinations of enolizable substrates. These considerations led us to explore the behavior of NFSI in fluorinations of activated arenes under ball-milling conditions towards an eventual implementation of mechanochemistry in late-stage C–H functionalizations [22,23]. In particular, efficient fluorination protocols are long sought after in several areas of science, including medicinal chemistry [24]. Next to fluorination, in this work, we also have investigated NFSI as a source for

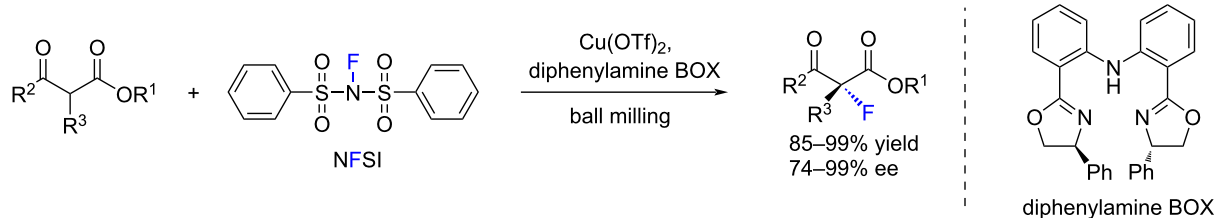
mechanochemical sulfonylation of imidazoles and amidation reactions.

Results and Discussion

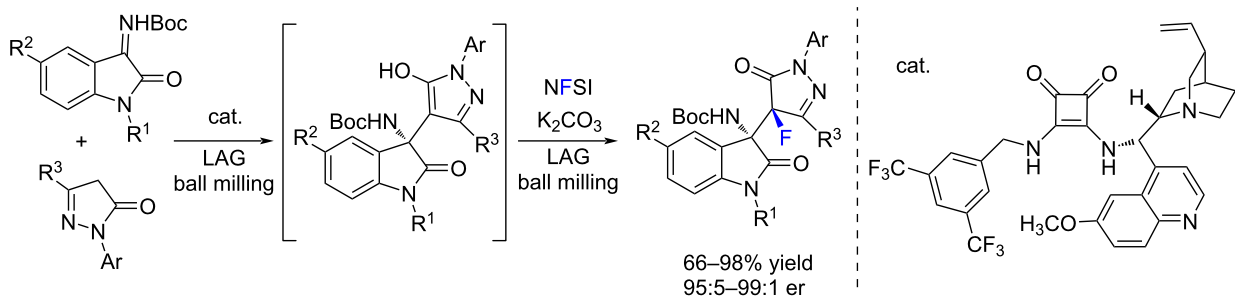
Previous reports in the absence of solvent have shown that NFSI promotes aromatic fluorination at temperatures between 80 °C and 105 °C [25]. To commence, we focused on the reaction between arenes **1a–c** and NFSI by ball milling in the absence of external heating (Scheme 2a). To conduct a high-throughput screening we initially carried out the milling experiments in Eppendorf vials before using standard milling jars made of stainless steel or poly(methyl methacrylate) (PMMA). This simple approach accelerated the optimization of the milling and reaction parameters [26]. From a sustainable point of view, experimenting in small scale could prevent waste production and increase safety. However, miniaturization of mechanochemical reactions could also be an alternative to working with precious or expensive reagents and to facilitate monitoring of the reactions [27].

Under such reaction conditions anisole (**1a**) did not undergo fluorination even in the presence of two equivalents of NFSI. However, more activated 1,3-dimethoxybenzene (**1b**) gave a mixture of principally monofluorinated products **2b** and **2b'**. Reacting 1,3,5-trimethoxybenzene (**1c**) and NFSI (1.0 equiv) also gave preferentially monofluorinated product **2c** in 51% yield. Analysis of the milled mixture by ^1H and ^{19}F NMR spectroscopy also revealed the presence of difluorinated products **2c'** and **2c''**. The product composition of the reaction of **1c** with

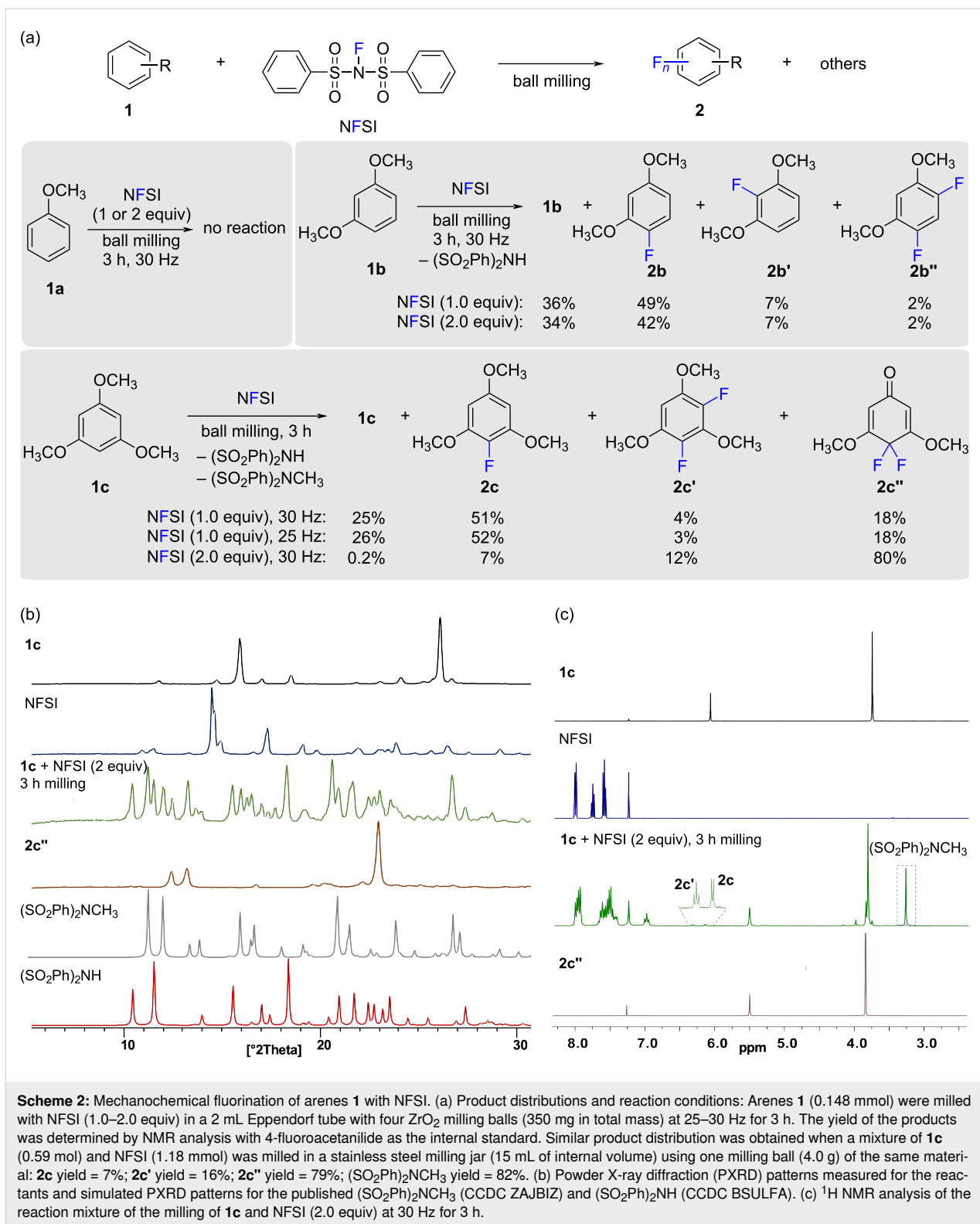
a) mechanochemical asymmetric fluorination of β -keto esters [14].



b) mechanochemical asymmetric organocatalytic Mannich reaction/fluorination [15].



Scheme 1: Examples of mechanochemical reactions using NFSI.



Scheme 2: Mechanochemical fluorination of arenes **1** with NFSI. (a) Product distributions and reaction conditions: Arenes **1** (0.148 mmol) were milled with NFSI (1.0–2.0 equiv) in a 2 mL Eppendorf tube with four ZrO_2 milling balls (350 mg in total mass) at 25–30 Hz for 3 h. The yield of the products was determined by NMR analysis with 4-fluoroacetanilide as the internal standard. Similar product distribution was obtained when a mixture of **1c** (0.59 mol) and NFSI (1.18 mmol) was milled in a stainless steel milling jar (15 mL of internal volume) using one milling ball (4.0 g) of the same material: **2c** yield = 7%; **2c'** yield = 16%; **2c''** yield = 79%; $(SO_2Ph)_2NCH_3$ yield = 82%. (b) Powder X-ray diffraction (PXRD) patterns measured for the reactants and simulated PXRD patterns for the published $(SO_2Ph)_2NCH_3$ (CCDC ZAJBIZ) and $(SO_2Ph)_2NH$ (CCDC BSULFA). (c) 1H NMR analysis of the reaction mixture of the milling of **1c** and NFSI (2.0 equiv) at 30 Hz for 3 h.

NFSI (1.0 equiv) remained unchanged at lower milling speeds (25 Hz vs 30 Hz), but the use of two equivalents of NFSI afforded 4,4-difluoro-3,5-dimethoxy-2,5-cyclohexadienone (**2c''**) as the major product in 80% yield (Scheme 2a). Mecha-

nistically, formation of **2c''** from 1,3,5-trimethoxybenzene (**1c**) requires a fluorodemethylation pathway to be operational under the ball-milling conditions, for example through the reaction of product **2c** with the second equivalent of NFSI. In solution,

1,3,5-trimethoxybenzene (**1c**) has been reported to undergo fluorodemethylation when reacted with Selectfluor®, however the authors mentioned that “the fate of the methyl group lost in the conversion” of **2c** to **2c''** “remain[ed] obscure” [28]. In our case, we anticipated that formation of **2c''** could be accompanied by concomitant formation of $(\text{PhSO}_2)_2\text{NH}$ and $(\text{PhSO}_2)_2\text{NCH}_3$ derived from NFSI and **1c**. For the analysis of the reaction mixture we selected powder X-ray diffraction (PXRD), a rapid analytical technique that has proven useful for the structural characterization of crystalline organic solids and which requires minimal sample preparation [29]. Pleasingly, analysis of the milled mixture (**1c** + NFSI) by PXRD evidenced the existence of diffraction reflections corresponding to crystalline $(\text{PhSO}_2)_2\text{NH}$, $(\text{PhSO}_2)_2\text{NCH}_3$, and product **2c''** (Scheme 2b) [30]. Additionally, ^1H NMR spectroscopy confirmed the presence of $(\text{PhSO}_2)_2\text{NCH}_3$ in the reaction mixture after the milling process (Scheme 2c) [31], in yields that matched the ones for **2c''** (Scheme 2a).

To get some insights into the mechanochemical reaction of **1c** with NFSI we have performed *in situ* reaction monitoring of the milling process by Raman spectroscopy [32,33]. In an experiment milling **1c** with NFSI (1 equiv) we observed the consumption of NFSI after ca. 30 min of milling as evidenced by a reduction in the intensity of the band at 1197 cm^{-1} of NFSI (Figure S3 in Supporting Information File 1). However, the very strong bands around 998 cm^{-1} (in-plane bending; phenyl ring), 1177 cm^{-1} (stretching; SO_2), and 1583 cm^{-1} (stretching; phenyl ring) of NFSI and byproducts [$(\text{PhSO}_2)_2\text{NH}$ [34], and $(\text{PhSO}_2)_2\text{NCH}_3$], prevented the observation of the less Raman active fluorinated products **2c** and **2c''**. Even though **1c** and NFSI are solids ($\text{mp}_{\mathbf{1c}} = 50\text{--}53^\circ\text{C}$; $\text{mp}_{\text{NFSI}} = 114\text{--}116^\circ\text{C}$), rheological changes of the reaction mixture upon milling and formation of liquid **2c** rendered a sticky reaction mixture, which

affected the quality of the Raman monitoring (Figures S3 and S4 in Supporting Information File 1). To mitigate this, the milling experiment was repeated using silica gel (SiO_2) as a milling auxiliary. The use of SiO_2 did not affect significantly the product composition of the reaction as determined by NMR analysis of an independent experiment milling **1c** and NFSI (2.0 equiv) at 30 Hz for 3 h. This reaction gave a mixture of **2c''**, **2c'**, and **2c** in a ratio of 79:16:5 vs a ratio of 80:12:7 in the absence of SiO_2 (Scheme 2a). Moreover, the presence of SiO_2 improved the absorption of reactants and rendered a reaction mixture physically more appropriate for the milling process, which in turn enabled a better monitoring of the transformation and favored the reaction to be completed in shorter milling times (Figure 1a and Figure S5 in Supporting Information File 1). The mechanochemical reaction of **1c** with NFSI (2 equiv) was also monitored revealing that the consumption of NFSI required ca. 30 min of milling (Figure 1b and Figure S5 in Supporting Information File 1).

Other substrates such as naphthalene and *N*-Boc-aniline proved unreactive under the milling conditions with NFSI. However, the more activated arene 2-naphthol underwent double fluorination affording 1,1-difluoronaphthalen-2(1*H*)-one as the major product (i.e., 29% yield using 1.0 equiv of NFSI and 51% yield using 2.0 equiv of NFSI after 3 h of milling at 30 Hz).

After having studied the ability of NFSI to participate in fluorination and fluorodemethylation reactions, we evaluated the capacity of NFSI to act as a sulfonyl source. For this, we reacted a mixture of NFSI and imidazole (**3a**) by ball milling. Analysis by NMR spectroscopy of the crude reaction mixture showed that 1-(benzenesulfonyl)imidazole (**4a**) had been formed in 41% yield (Scheme 3a).

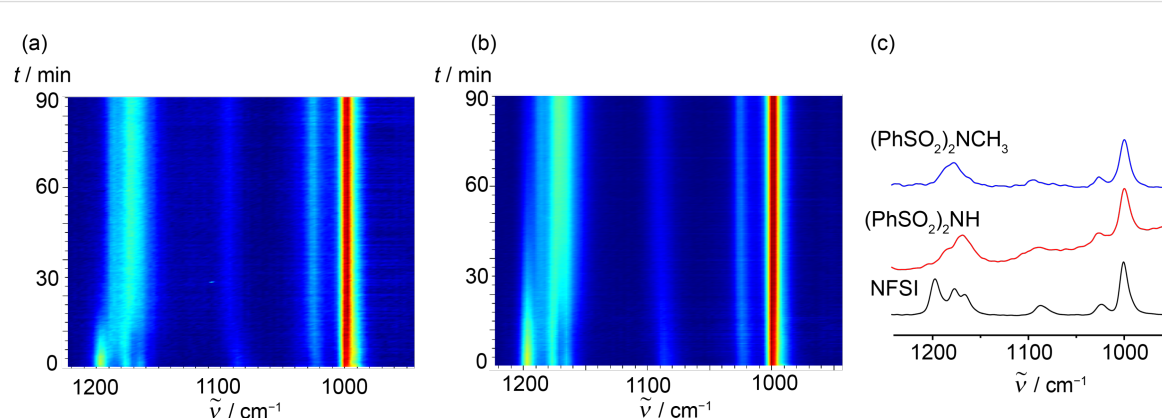
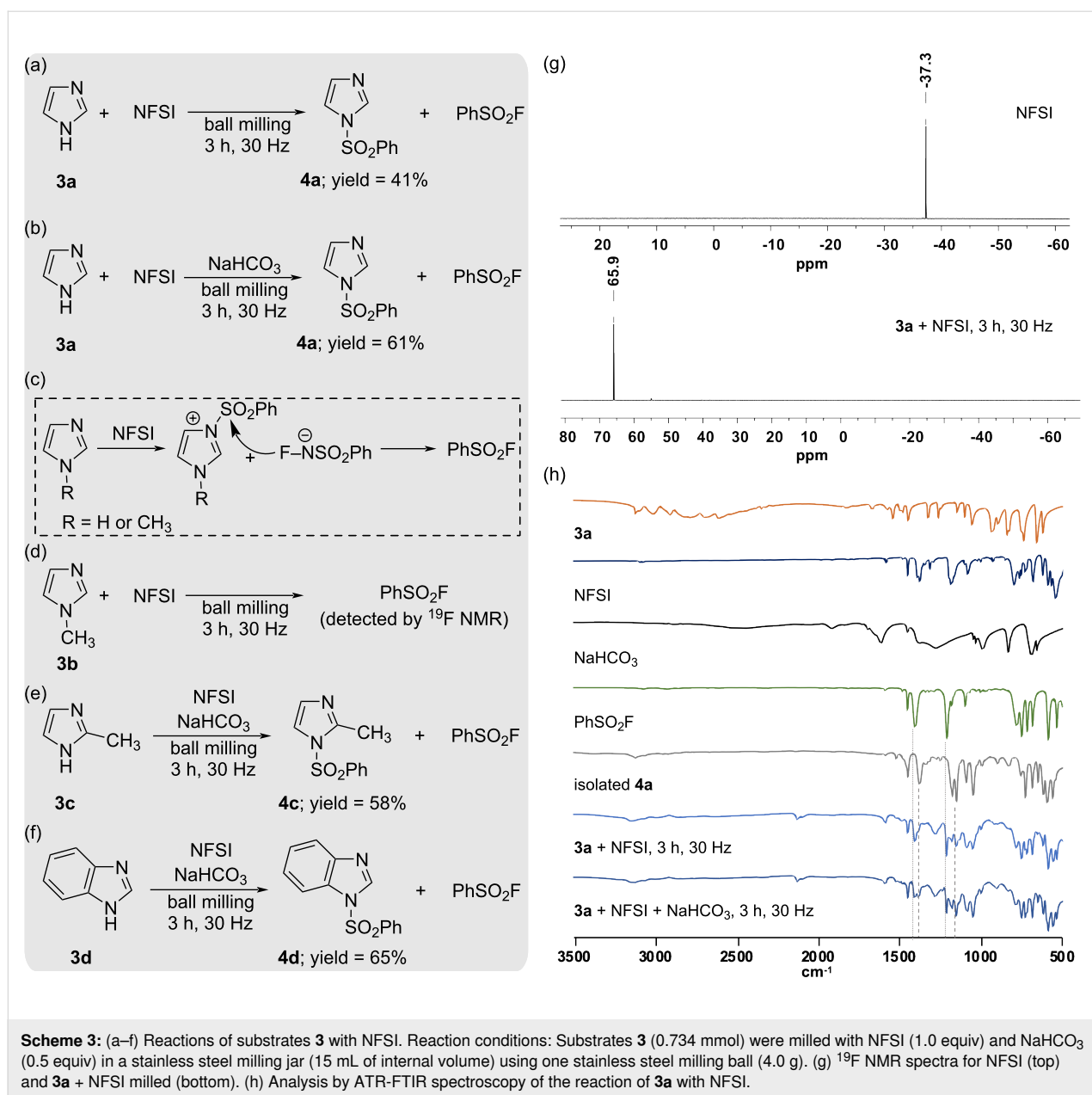


Figure 1: Time-resolved 2D plots of the mechanochemical reaction of: (a) **1c** (0.59 mmol), NFSI (1.0 equiv), and SiO_2 (300 mg). (b) **1c** (0.59 mmol), NFSI (2.0 equiv), and SiO_2 (300 mg). Both reactions were carried out at 30 Hz using milling jars made of PMMA (15 mL of internal volume) with one ZrO_2 milling ball (3.4 g). (c) Raman spectra of pure NFSI, $(\text{PhSO}_2)_2\text{NH}$, and $(\text{PhSO}_2)_2\text{NCH}_3$.



Scheme 3: (a–f) Reactions of substrates **3** with NFSI. Reaction conditions: Substrates **3** (0.734 mmol) were milled with NFSI (1.0 equiv) and NaHCO₃ (0.5 equiv) in a stainless steel milling jar (15 mL of internal volume) using one stainless steel milling ball (4.0 g). (g) ¹⁹F NMR spectra for NFSI (top) and **3a + NFSI milled** (bottom). (h) Analysis by ATR-FTIR spectroscopy of the reaction of **3a** with NFSI.

Complementarily, ¹⁹F NMR spectroscopy of the crude reaction mixture evidenced a distinctive peak at 65.8 ppm in the ¹⁹F NMR spectrum (Scheme 3g), which was assigned to phenylsulfonyl fluoride (PhSO₂F) [35], a byproduct often obtained in reactions with NFSI [36,37]. Trying to improve the rheology of the reaction mixture and to increase the basicity of the medium, we milled **3a** and NFSI in the presence of NaHCO₃, which had a positive effect affording product **4a** in 61% yield (Scheme 3b), which is significantly higher than the 46% yield reported in CH₃CN after 12 h at 80 °C [38]. The generation of **4a** upon milling was demonstrated after immediate analysis of the milled sample by ATR-FTIR spectroscopy (Scheme 3h).

Formation of **4a** could have occurred from the direct reaction of the N–H nitrogen of **3a** with NFSI, which would agree with the propensity for NFSI to react with some hard oxygen and nitrogen nucleophiles at the sulfur atom instead of at the fluorine atom [39,40]. Similarly, NFSI has also been reported to act as a transfer of the sulfonyl moiety from NFSI to carbon centers [12,13]. Alternatively, **4a** could have been formed from the reaction of imidazole (**3a**) with the in situ formed PhSO₂F. To better understand the formation of PhSO₂F during the milling of NFSI with **3a**, we reacted its N-methylated derivative **3b**, a substrate unable to undergo the sulfonylation pathway with NFSI. We hypothesized that PhSO₂F could have been generated after an initial reaction of the nitrogen with the lone electron pair in

imidazole at the sulfonyl group of the NFSI (Scheme 3c), mimicking the reactivity of pyridine derivatives with NFSI, which are known to generate phenylsulfonyl fluoride via a transient generation of *N*-sulfonylpyridinium salts [37].

Analysis by ^{19}F NMR spectroscopy of the crude reaction mixture of **3b** and NFSI revealed the presence of PhSO_2F (Scheme 3d), thus confirming the capacity of the nitrogen with the lone electron pair in **3b**, and probably in **3a**, to react with NFSI at the sulfonyl group to facilitate the formation of phenylsulfonyl fluoride (Scheme 3c). Other imidazole derivatives such as 2-methylimidazole (**3c**) and benzimidazole (**3d**) also underwent sulfonylation affording products **4c** and **4d** in 58% yield and 65% yield, respectively (Scheme 3e and 3f).

Finally, to corroborate that other known chemical pathways for NFSI, including amidation reactions, could be accessible under mechanochemical conditions we studied the reaction of 1-acetylindole (**5**) with NFSI. In solution (i.e., dichloroethane, 60 °C, 24 h, Ar atmosphere), **5** undergoes regioselective C-3 amidation with NFSI using catalytic amounts of K_2CO_3 [41]. An initial attempt to carry out the reaction by ball milling **5**, NFSI (2 equiv), and K_2CO_3 (10 mol %) for 3 h afforded only traces of the aminated product **6**. To assist the metal-free amidation of the aromatic C–H bond in **5**, we repeated the milling experiment at 40 °C using a heat gun to increase the temperature of the milling jar (see Supporting Information File 1, Figure S2) [42], which gave a mixture of **5** and **6** (ratio 85:15). The same experiment at 60 °C led to the full consumption of **5** after 1.5 h of milling and product **6** could be isolated in moderate 37% yield (Scheme 4). Formation of **6** in the absence of external heating was also possible after lengthening the milling time to 16 h, such an experiment afforded a mixture of **5** and **6** (ratio 60:40). In comparison, in dichloroethane at 40 °C the reaction of **5** and NFSI only afforded amidated product **6** in 4% after 24 h of reaction [41].

Conclusion

In this study we evaluated the multifaceted reactivity of NFSI under mechanochemical conditions. We observed that NFSI was compatible with the ball-milling reaction conditions. Addi-

tionally, we corroborated that, by mechanochemistry, NFSI can engage in a variety of reactions known in solution such as fluorinations, fluorodemethylations, sulfonylations, and amidations. These transformations could be accomplished in short milling times in the absence of solvent. Being a crystalline material [43] and a Raman and IR active molecule [44,45], NFSI enabled the monitoring of the reactions by ex situ PXRD and IR spectroscopy, as well as by in situ Raman spectroscopy. Such a monitoring enabled us to understand background reactions such as the fluorodemethylation pathway underwent by 1,3,5-trimethoxybenzene (**1c**) when reacted with NFSI, which was found to proceed via initial formation of monofluorinated product **2c**. In general, NFSI could participate in the chemical transformations by ball milling without the need for external heating, however, the amidation of 1-acetylindole (**5**) was found to proceed more efficiently under simultaneous thermal milling conditions. Altogether, the results of this work expand the applicability of NFSI by mechanochemistry beyond fluorination reactions of enolizable substrates and might facilitate the application of NFSI in new reactions by ball milling in the future. Ongoing work on the development of similar mechanochemical reactions using NFSI are being investigated in our laboratories.

Supporting Information

Supporting Information File 1

Experimental details, characterization data and copies of spectra.

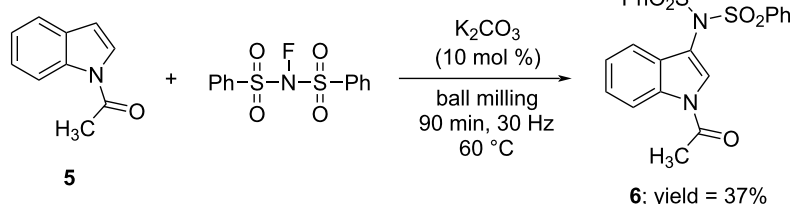
[<https://www.beilstein-journals.org/bjoc/content/supplementary/1860-5397-18-20-S1.pdf>]

Acknowledgements

We thank Dr. Ivan Halasz (Ruđer Bošković Institute) for helpful discussions and proofreading.

Funding

This research was possible thanks to the financial support from AbbVie Deutschland GmbH & Co. D.B. thanks the financial



Scheme 4: Regioselective C-3 mechanochemical amidation of **5** with NFSI.

support provided by the Croatian Science Foundation (grant No. IP-2019-04-9951).

ORCID® IDs

José G. Hernández - <https://orcid.org/0000-0001-9064-4456>
 Karen J. Ardila-Fierro - <https://orcid.org/0000-0002-5801-5534>
 Dajana Barišić - <https://orcid.org/0000-0003-3017-7061>
 Hervé Geneste - <https://orcid.org/0000-0002-2808-1573>

References

1. Tan, D.; Friščić, T. *Eur. J. Org. Chem.* **2018**, 18–33. doi:10.1002/ejoc.201700961
2. Howard, J. L.; Cao, Q.; Browne, D. L. *Chem. Sci.* **2018**, 9, 3080–3094. doi:10.1039/c7sc05371a
3. Achar, T. K.; Bose, A.; Mal, P. *Beilstein J. Org. Chem.* **2017**, 13, 1907–1931. doi:10.3762/bjoc.13.186
4. Ardila-Fierro, K. J.; Hernández, J. G. *ChemSusChem* **2021**, 14, 2145–2162. doi:10.1002/cssc.202100478
5. Ying, P.; Yu, J.; Su, W. *Adv. Synth. Catal.* **2021**, 363, 1246–1271. doi:10.1002/adsc.202001245
6. Bolm, C.; Hernández, J. G. *Angew. Chem., Int. Ed.* **2019**, 58, 3285–3299. doi:10.1002/anie.201810902
7. Bizet, V. *Synlett* **2012**, 23, 2719–2720. doi:10.1055/s-0032-1317348
8. Umemoto, T.; Yang, Y.; Hammond, G. B. *Beilstein J. Org. Chem.* **2021**, 17, 1752–1813. doi:10.3762/bjoc.17.123
9. Gu, Q.; Vessally, E. *RSC Adv.* **2020**, 10, 16756–16768. doi:10.1039/d0ra00324g
10. Li, Y.; Zhang, Q. *Synthesis* **2015**, 47, 159–174. doi:10.1055/s-0034-1379396
11. Sushmita; Aggarwal, T.; Kumar, S.; Verma, A. K. *Org. Biomol. Chem.* **2020**, 18, 7056–7073. doi:10.1039/d0ob01429j
12. Collman, J. P.; Zhong, M.; Boulatov, R. *J. Chem. Res., Synop.* **2000**, 230–231. doi:10.3184/030823400103167093
13. Roy, A.; Schneller, S. W. *Org. Lett.* **2005**, 7, 3889–3891. doi:10.1021/o1051297e
14. Wang, Y.; Wang, H.; Jiang, Y.; Zhang, C.; Shao, J.; Xu, D. *Green Chem.* **2017**, 19, 1674–1677. doi:10.1039/c6gc03306g
15. Krištofíková, D.; Mečiarová, M.; Rakovský, E.; Šebesta, R. *ACS Sustainable Chem. Eng.* **2020**, 8, 14417–14424. doi:10.1021/acssuschemeng.0c04260
16. Hernández, J. G.; Butler, I. S.; Friščić, T. *Chem. Sci.* **2014**, 5, 3576–3582. doi:10.1039/c4sc01252f
17. Howard, J. L.; Sagatov, Y.; Repusseau, L.; Schotten, C.; Browne, D. L. *Green Chem.* **2017**, 19, 2798–2802. doi:10.1039/c6gc03139k
18. Howard, J. L.; Nicholson, W.; Sagatov, Y.; Browne, D. L. *Beilstein J. Org. Chem.* **2017**, 13, 1950–1956. doi:10.3762/bjoc.13.189
19. Howard, J. L.; Sagatov, Y.; Browne, D. L. *Tetrahedron* **2018**, 74, 3118–3123. doi:10.1016/j.tet.2017.11.066
20. Cao, Q.; Howard, J. L.; Crawford, D. E.; James, S. L.; Browne, D. L. *Green Chem.* **2018**, 20, 4443–4447. doi:10.1039/c8gc02036a
21. Riley, W.; Jones, A. C.; Singh, K.; Browne, D. L.; Stuart, A. M. *Chem. Commun.* **2021**, 57, 7406–7409. doi:10.1039/d1cc02587b
22. Ni, S.; Hribersek, M.; Baddigam, S. K.; Ingner, F. J. L.; Orthaber, A.; Gates, P. J.; Pilarski, L. T. *Angew. Chem., Int. Ed.* **2021**, 60, 6660–6666. doi:10.1002/anie.202010202
23. Börgel, J.; Ritter, T. *Chem* **2020**, 6, 1877–1887. doi:10.1016/j.chempr.2020.07.007
24. Britton, R.; Gouverneur, V.; Lin, J.-H.; Meanwell, M.; Ni, C.; Pupo, G.; Xiao, J.-C.; Hu, J. *Nat. Rev. Methods Primers* **2021**, 1, 47. doi:10.1038/s43586-021-00042-1
25. Andreev, R. V.; Borodkin, G. I.; Shubin, V. G. *Russ. J. Org. Chem.* **2009**, 45, 1468–1473. doi:10.1134/s107042800910008x
26. Martina, K.; Rotolo, L.; Porcheddu, A.; Delogu, F.; Bysouth, S. R.; Cravotto, G.; Colacino, E. *Chem. Commun.* **2018**, 54, 551–554. doi:10.1039/c7cc07758k
27. Lampronti, G. I.; Michalchuk, A. A. L.; Mazzeo, P. P.; Belenguer, A. M.; Sanders, J. K. M.; Bacchi, A.; Emmerling, F. *Nat. Commun.* **2021**, 12, 6134. doi:10.1038/s41467-021-26264-1
28. Banks, R. E.; Besheesh, M. K.; Górski, R. W.; Lawrence, N. J.; Taylor, A. J. *Fluorine Chem.* **1999**, 96, 129–133. doi:10.1016/s0022-1139(99)00064-0
29. Karki, S.; Fábián, L.; Friščić, T.; Jones, W. *Org. Lett.* **2007**, 9, 3133–3136. doi:10.1021/o1071329t
30. Cotton, F. A.; Stokely, P. F. *J. Am. Chem. Soc.* **1970**, 92, 294–302. doi:10.1021/ja00705a012
31. Chen, L.; Lang, H.; Fang, L.; Yu, J.; Wang, L. *Eur. J. Org. Chem.* **2014**, 6385–6389. doi:10.1002/ejoc.201402919
32. Gracin, D.; Štrukil, V.; Friščić, T.; Halasz, I.; Užarević, K. *Angew. Chem., Int. Ed.* **2014**, 53, 6193–6197. doi:10.1002/anie.201402334
33. Lukin, S.; Užarević, K.; Halasz, I. *Nat. Protoc.* **2021**, 16, 3492–3521. doi:10.1038/s41596-021-00545-x
34. Castro, J. L.; Lopez-Ramirez, M. R.; Arenas, J. F.; Otero, J. C. *J. Raman Spectrosc.* **2012**, 43, 857–862. doi:10.1002/jrs.3107
35. Davies, A. T.; Curto, J. M.; Bagley, S. W.; Willis, M. C. *Chem. Sci.* **2017**, 8, 1233–1237. doi:10.1039/c6sc03924c
36. Tang, R.-J.; Luo, C.-P.; Yang, L.; Li, C.-J. *Adv. Synth. Catal.* **2013**, 355, 869–873. doi:10.1002/adsc.201201133
37. Meanwell, M.; Nodwell, M. B.; Martin, R. E.; Britton, R. *Angew. Chem., Int. Ed.* **2016**, 55, 13244–13248. doi:10.1002/anie.201606323
38. Jie, K.; Wang, Y.; Huang, L.; Guo, S.; Cai, H. *J. Sulfur Chem.* **2018**, 39, 465–471. doi:10.1080/17415993.2018.1480725
39. Antelo, J. M.; Crugeiras, J.; Leis, J. R.; Ríos, A. *J. Chem. Soc., Perkin Trans. 2* **2000**, 2071–2076. doi:10.1039/b003982i
40. Rozatian, N.; Hodgson, D. R. W. *Chem. Commun.* **2021**, 57, 683–712. doi:10.1039/d0cc06339h
41. Liu, H.-H.; Wang, Y.; Deng, G.; Yang, L. *Adv. Synth. Catal.* **2013**, 355, 3369–3374. doi:10.1002/adsc.201300767
42. Seo, T.; Toyoshima, N.; Kubota, K.; Ito, H. *J. Am. Chem. Soc.* **2021**, 143, 6165–6175. doi:10.1021/jacs.1c00906
43. Lennartson, A.; Hakansson, M. CCDC 840301: Experimental Crystal Structure Determination. 2011; <https://www.ccdc.cam.ac.uk/structures/search?id=doi:10.5517/ccx6dhz&sid=DataCite>. doi:10.5517/ccx6dhz
44. <https://www.sigmaaldrich.com/deepweb/assets/sigmaaldrich/quality/spectra/125/072/FTIR006130.pdf> (accessed Jan 16, 2022).
45. <https://www.sigmaaldrich.com/deepweb/assets/sigmaaldrich/quality/spectra/606/858/RAIR011023.pdf> (accessed Jan 16, 2022).

License and Terms

This is an open access article licensed under the terms of the Beilstein-Institut Open Access License Agreement (<https://www.beilstein-journals.org/bjoc/terms>), which is identical to the Creative Commons Attribution 4.0 International License (<https://creativecommons.org/licenses/by/4.0>). The reuse of material under this license requires that the author(s), source and license are credited. Third-party material in this article could be subject to other licenses (typically indicated in the credit line), and in this case, users are required to obtain permission from the license holder to reuse the material.

The definitive version of this article is the electronic one which can be found at:

<https://doi.org/10.3762/bjoc.18.20>



DDQ in mechanochemical C–N coupling reactions

Shyamal Kanti Bera[†], Rosalin Bhanja[†] and Prasenjit Mal^{*}

Full Research Paper

Open Access

Address:

School of Chemical Sciences, National Institute of Science Education and Research (NISER), An OCC of Homi Bhabha National Institute, Bhubaneswar, PO Bhimpur-Padanpur, Via Jatni, District Khurda, Odisha 752050, India

Email:

Prasenjit Mal^{*} - pmal@niser.ac.in

^{*} Corresponding author [†] Equal contributors

Keywords:

ball mill; 1*H*-benzo[*d*]imidazole; C(sp²)–H amidation; DDQ; mechanochemistry; quinazolin-4(3*H*)-one

Beilstein J. Org. Chem. **2022**, *18*, 639–646.

<https://doi.org/10.3762/bjoc.18.64>

Received: 11 March 2022

Accepted: 20 May 2022

Published: 01 June 2022

This article is part of the thematic issue "Mechanochemistry III".

Guest Editors: J. G. Hernández and L. Borchardt

© 2022 Bera et al.; licensee Beilstein-Institut.

License and terms: see end of document.

Abstract

2,3-Dichloro-5,6-dicyano-1,4-benzoquinone (DDQ) is a commonly known oxidant. Herein, we report that DDQ can be used to synthesize 1,2-disubstituted benzimidazoles and quinazolin-4(3*H*)-ones via the intra- and intermolecular C–N coupling reaction under solvent-free mechanochemical (ball milling) conditions. In the presence of DDQ, the intramolecular C(sp²)–H amidation of *N*-(2-(arylideneamino)phenyl)-*p*-toluenesulfonamides leads to 1,2-disubstituted benzimidazoles and the one-pot coupling of 2-aminobenzamides with aryl/alkyl aldehydes resulted in substituted quinazolin-4(3*H*)-one derivatives in high yields.

Introduction

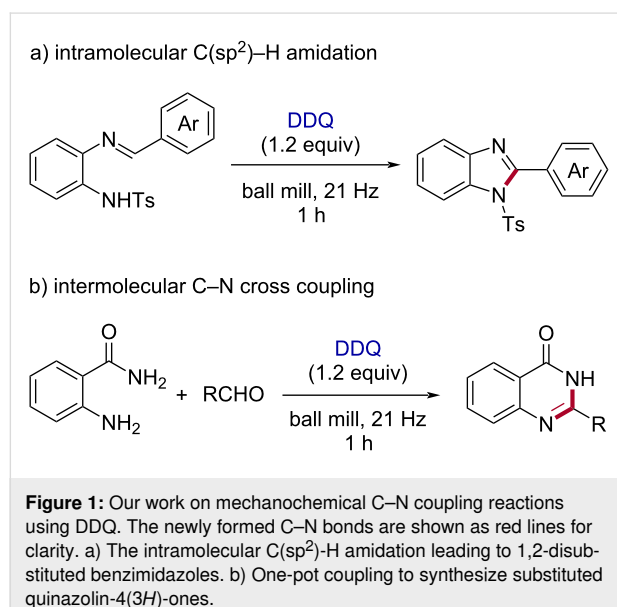
The reawakening approaches to use solvent-free and environmentally benign conditions in organic synthesis have facilitated new opportunities [1–4]. The research area of mechanochemistry [5,6] mainly focuses on conducting synthetic transformations in solid-state or solvent-free conditions. Mechanochemistry is one of the emerging avenues in chemistry that can make the world more sustainable by following the “Twelve Principles of Green Chemistry” [2]. Mechanochemistry is one of the ten innovative technologies that IUPAC recognized [7]. To perform organic transformations in a greener way, the mechanochemical methods can also be considered as one of the alternative approaches [8–10]. The one-pot multicomponent synthesis of important heterocycles can be the state of art prac-

tice by applying the strategies like domino, cascade, or tandem [11–13]. These environmentally friendly approaches set forth the journey of facilitating sustainable systems by using mechanochemical methods to access small organic compounds [3].

Due to the high reduction potential of the quinone moiety in 2,3-dichloro-5,6-dicyano-1,4-benzoquinone (DDQ), it was well established as a hydride transfer reagent in various organic reactions [14,15]. Generally, DDQ assists in dehydrogenation reactions in organic synthesis [16]. In this context, various carbon–heteroatom bond formation reactions such as C–P [17], C–O [18–20], and C–S [21] were achieved using DDQ as an

oxidant [22,23]. In addition, the utilization of DDQ as a photoredox catalyst [24] and co-catalyst [25,26] have also been documented in organic synthesis [27]. DDQ-mediated oxidative C–N cross-coupling reactions are well known, but limited reports are available for reactions carried out under solvent-free conditions [28,29].

However, improving environmentally benign methods [30,31] of C–N bond synthesis is of enormous significance [32–34]. In comparison to the metal-mediated C–N coupling reactions [35], the direct C–H amination is vital to provide many amine derivatives by sustainable methods [36,37]. The dehydrogenative C–N cross-coupling reactions from unreactive N–H and C–H bonds can lead to various nitrogen-containing heterocycles [32,38]. Herein, we disclose the DDQ-mediated oxidative C–N coupling toward the synthesis of 1,2-disubstituted benzimidazoles [39] under mechanochemical (ball milling) conditions (Figure 1a). In addition, the one-pot coupling of 2-aminobenzamides with aryl/alkyl aldehydes in the presence of DDQ resulted in substituted quinazolin-4(3H)-one [40] derivatives (Figure 1b).



Results and Discussion

Towards the optimization study, (*E*)-*N*-(2-((2-bromobenzylidene)amino)phenyl)-4-methylbenzenesulfonamide (**1a**) was considered as a model substrate for the synthesis of 2-(2-bromophenyl)-1-tosyl-1*H*-benzo[*d*]imidazole (**2a**, Table 1). Initially, with 1.0 equiv of DDQ, product **2a** was obtained in 88% yield (Table 1, entry 1). However, in the presence of 1.2 equiv, the yield of **2a** increased to 97% (Table 1, entry 2). Further, with the increase of the amount of DDQ to 1.5 equiv, no further improvement was obtained (Table 1, entry 3). In addition, we

have screened several iodine oxidation reagents, but none of them gave better yields (Table 1, entries 4–7). On the other hand, oxone as an oxidant yielded product **2a** with up to 43% yield (Table 1, entry 8). Similarly, we have optimized the reaction conditions for the synthesis of 2-phenylquinazolin-4(3*H*)-one (**5a**) from anthranilamide and benzaldehyde under the solvent-free conditions (Table S1, Supporting Information File 1). Notably, the use of 1.0 equiv of DDQ as oxidant, afforded the product 2-phenylquinazolin-4(3*H*)-one (**5a**) in 98% yield within 1 h. However, when reducing the amount of DDQ to 0.5 equiv the of product **5a** decreased to 48%. On the other hand, increasing the amount of DDQ to 1.2 equiv resulted in 98% yield of the product (Supporting Information File 1, Table S1, entries 1 and 3). Further studies revealed that other commonly used oxidants such as PIDA and oxone gave 30% and 61% the desired product, respectively (Supporting Information File 1, Table S1, entries 4 and 5). When molecular iodine or NIS were used as oxidants, product **5a** was obtained in 83% and 80% yield, respectively (Supporting Information File 1, Table S1, entries 6 and 7). However, the yield of the desired product **5a** slightly decreased to 92% with lowering of the operating milling frequency from 21 to 16 Hz (Supporting Information File 1, Table S1, entry 9). On the other hand, the yield of product **5a** was unaffected by increasing the operating frequency from 21 Hz to 25 Hz (Supporting Information File 1, Table S1, entry 8).

Table 1: Optimization of the reaction conditions.^a

Entry	Reagent (equiv)	Yield (%) ^b
1	DDQ (1.0)	88
2	DDQ (1.2)	97
3	DDQ (1.5)	96
4	NIS (1.2)	65
5	I ₂ (1.2)	32
6	I ₂ (1.2)/K ₂ CO ₃ (1.2)	23
7	PIDA (1.2)	60
8	oxone (1.2)	43

^aReaction conditions: 0.14 mmol of **1a** and 0.167 mmol of DDQ (1.2 equiv) under solvent-free conditions were milled at 21 Hz in a 10 mL milling jar containing one stainless-steel grinding ball (15 mm in diameter) for 1 h. ^bYield of the isolated product after purification through silica-gel column chromatography.

1,2-Disubstituted benzimidazoles are heterocyclic scaffolds holding a broad range of biological activities [41–43]. For ex-

ample, telmisartan, a 1,2-disubstituted benzimidazole derivative, is extensively used as an antihypertensive agent [44]. The substrate scope for the synthesis of variously substituted benzimidazoles is shown in Figure 2. Benzimidazoles with a variety of aryl substituents (such as bromo, nitro, chloro, and 2,4,6-trimethyl) in the 2-position of the benzimidazole (**2a–d,g**) were obtained in good yields. Furthermore, the synthesis of the corresponding benzimidazoles with fused aromatic systems in the 2-position such as anthracenyl (**2e**) and naphthyl (**2f**) proved to be efficient. Similarly, the 5,6-dimethyl- or 5,6-dichloro-1,2-disubstituted benzimidazoles **2i**, **2j**, and **2k** were synthesized with 82, 85, and 79% yield, respectively. In addition, the structure of the synthesized 2-(4-(phenylethynyl)phenyl)-substituted product **2h** was established from the X-ray crystallography data.

Various methodologies are available in the literature toward constructing quinazolin-4(3*H*)-one derivatives [40,45,46].

Quinazolin-4(3*H*)-ones and its derivatives possess several biological activities such as antibacterial [47], antiviral [48], anti-tumor [49,50], antimalarial [51], anti-inflammatory [52], etc. We therefore investigated the scope of the one-pot coupling of 2-aminobenzamides with aryl/alkyl aldehydes in the presence of DDQ under the optimized mechanochemical conditions and the results are shown in Figure 3.

Unsubstituted anthranilamides reacted smoothly with various substituted aldehydes (containing a bromo, fluoro, hydroxy, chloro, ethyl, or methyl group) affording the corresponding products **5b–g** with good to excellent yields. Also, 3,4,5-trimethoxy-, 2,4,6-trimethyl-, anthracene-9-yl-, and naphthalene-1-yl-substituted benzaldehydes were well tolerated and gave the desired products **5h–k** with high yields. In this context, biphenyl aldehyde with a chloro group was efficiently converted to **5l** with 93% yield. Furthermore, aromatic aldehydes

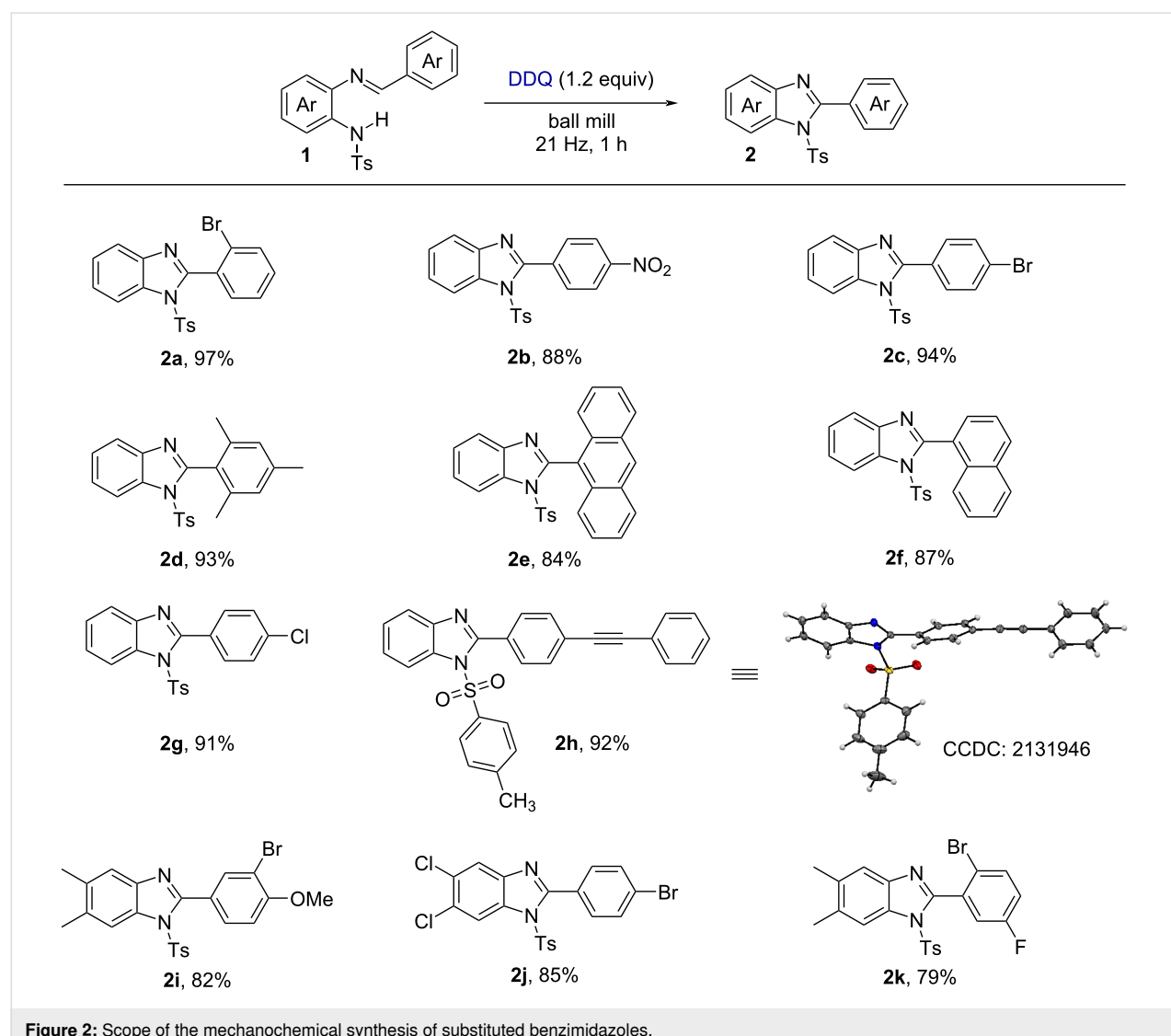


Figure 2: Scope of the mechanochemical synthesis of substituted benzimidazoles.

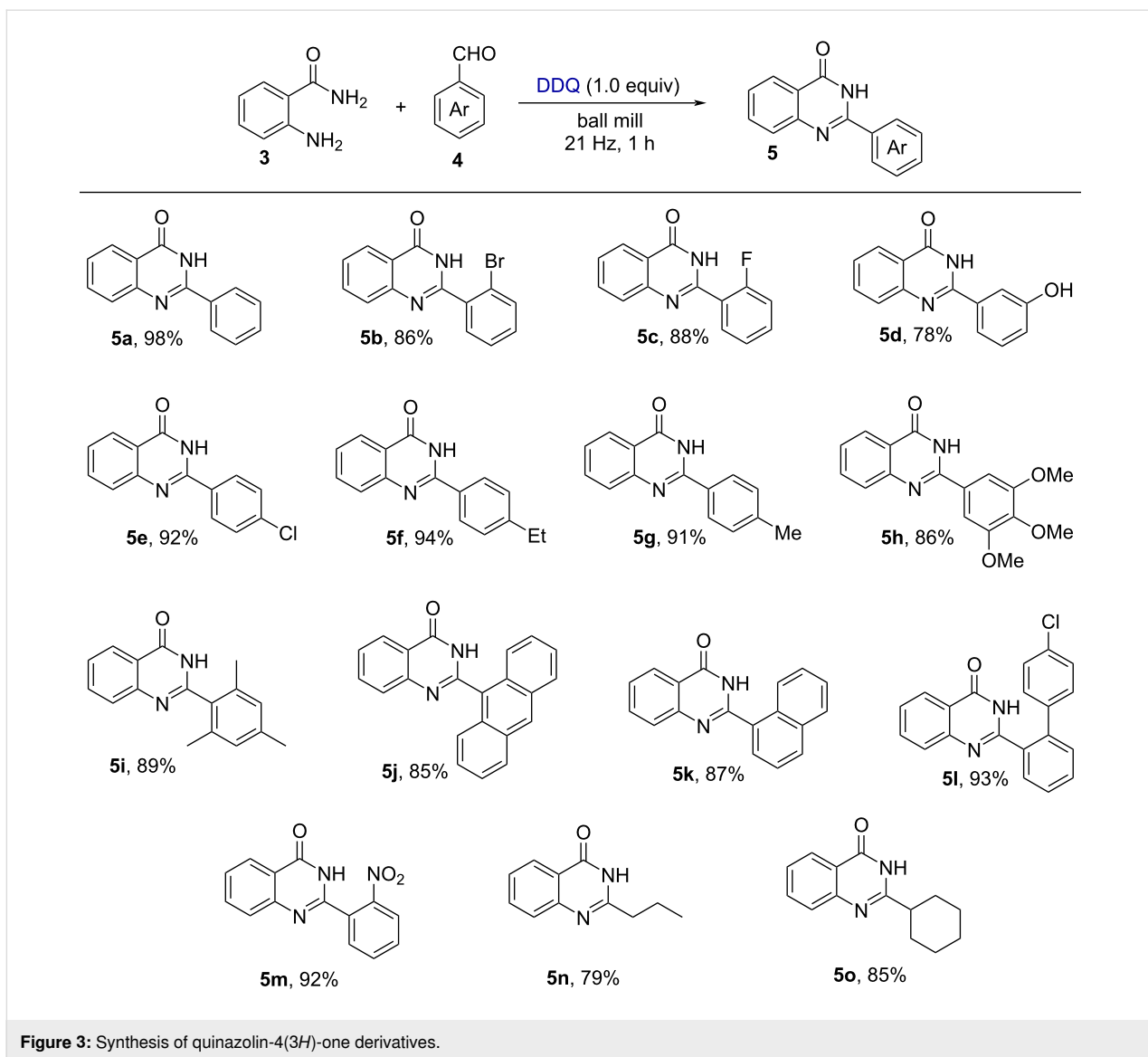


Figure 3: Synthesis of quinazolin-4(3H)-one derivatives.

having a strong electron-withdrawing group (such as NO_2) were smoothly converted to the corresponding products **5m** with 92% yield, respectively. In addition to this, aliphatic aldehydes (cyclohexanecarbaldehyde, butyraldehyde) were well tolerated under the standard reaction conditions to produce the product **5n** and **5o** with good yield.

The substrate scope of this methodology was extended to chloro and fluoro-substituted anthranilamides and aldehydes (Figure 4). Initially, 2-amino-5-fluorobenzamide was reacted with various benzaldehydes having bromo, ethyl, methyl, styryl, and cyclohexyl groups to produce the respective cyclized products **6b–f** with good to excellent yields. Similarly, biphenyl aldehydes with -OMe and -COMe groups were well tolerated under the standard reaction conditions and delivered the corresponding products **6g** and **6h** with 83 and 85% yields, respec-

tively. In addition, we have also explored the substrate scope with 2-amino-5-chlorobenzamide and various aldehydes. Benzaldehyde containing fluoro, bromo, ethyl, and anthryl groups led to the corresponding products **6j**, **6k**, **6l**, and **6p** in good to excellent yield. Aliphatic aldehydes such as butyraldehyde gave the cyclized product **6m** with an 86% yield. In this regard, an -OMe and -COMe group-containing biphenyl aldehyde resulted in the corresponding products **6n** and **6o** with 79 and 82% yields, respectively. Nitro and fluoro-substituted aromatic aldehydes efficiently reacted with the chloro and fluoro-substituted anthranilamides and delivered the corresponding products **6q** and **6r** with good yields.

To understand the reaction mechanism, we have performed radical trapping experiments using TEMPO and BHT in the reaction of substrate **1c** (Figure 5a). Under the standard reac-

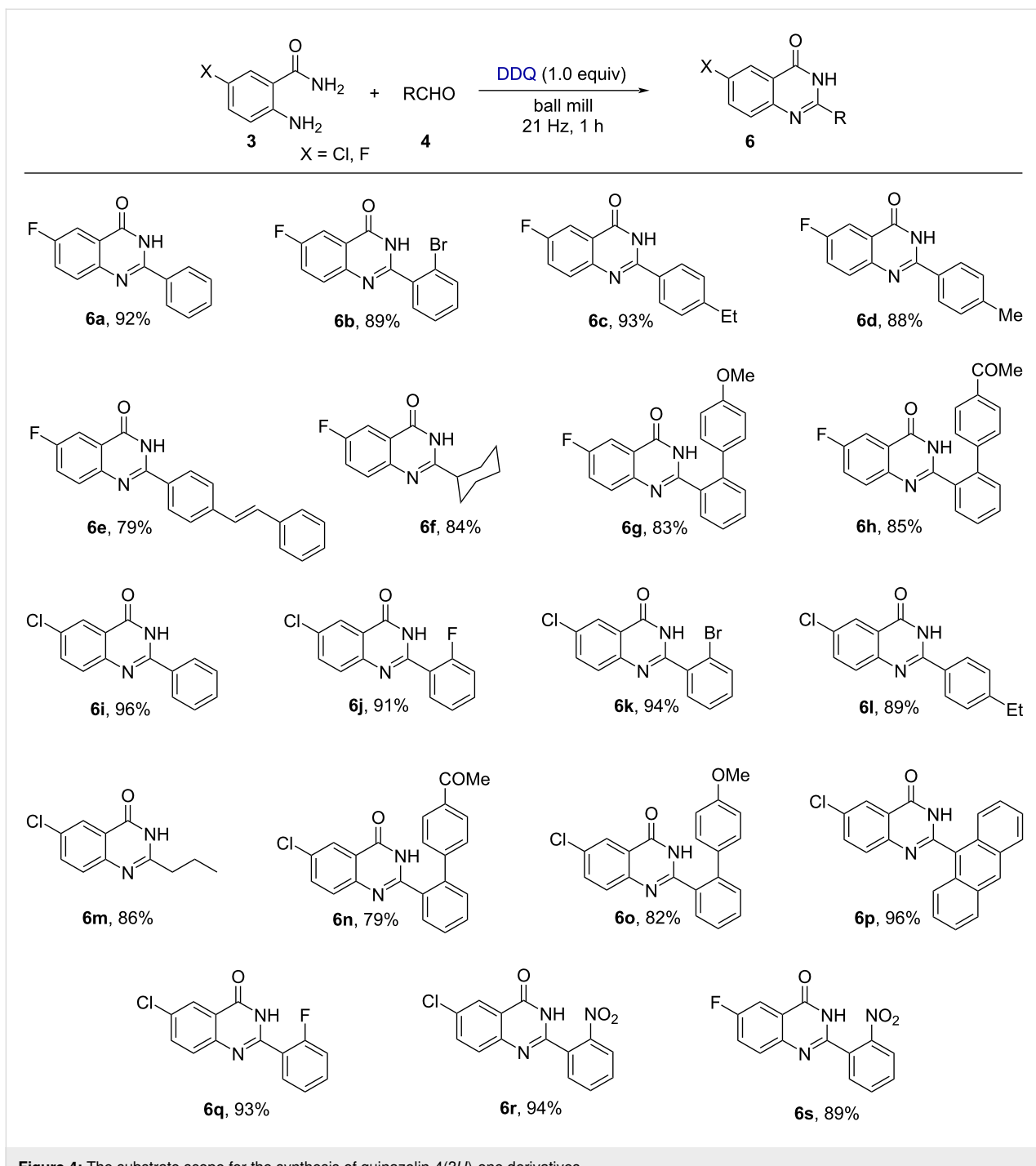


Figure 4: The substrate scope for the synthesis of quinazolin-4(3H)-one derivatives.

tion conditions in the presence of TEMPO or BHT, the expected product **2c** was formed in 66 and 72% yields. These results indicate that a radical pathway may not be involved in the reaction. So, based on literature reports [53–55], we have proposed a reaction mechanism in Figure 5b. Initially, DDQ abstracts a hydride ion from substrate **1a** to generate the intermediate **A**. Then intermediate **A** undergoes an electrophilic intramolecular cyclization to form the cationic intermediate **B**,

followed by hydride abstraction to generate the desired product **2a**. On the other hand, the formation of quinazolin-4(3H)-ones starts with the formation of an imine intermediate and then it will follow the similar mechanistic pathway.

To explore the synthetic utility of the oxidative C–N cross-coupling reaction, we have performed the large-scale synthesis under the solvent-free (ball milling) conditions as shown in

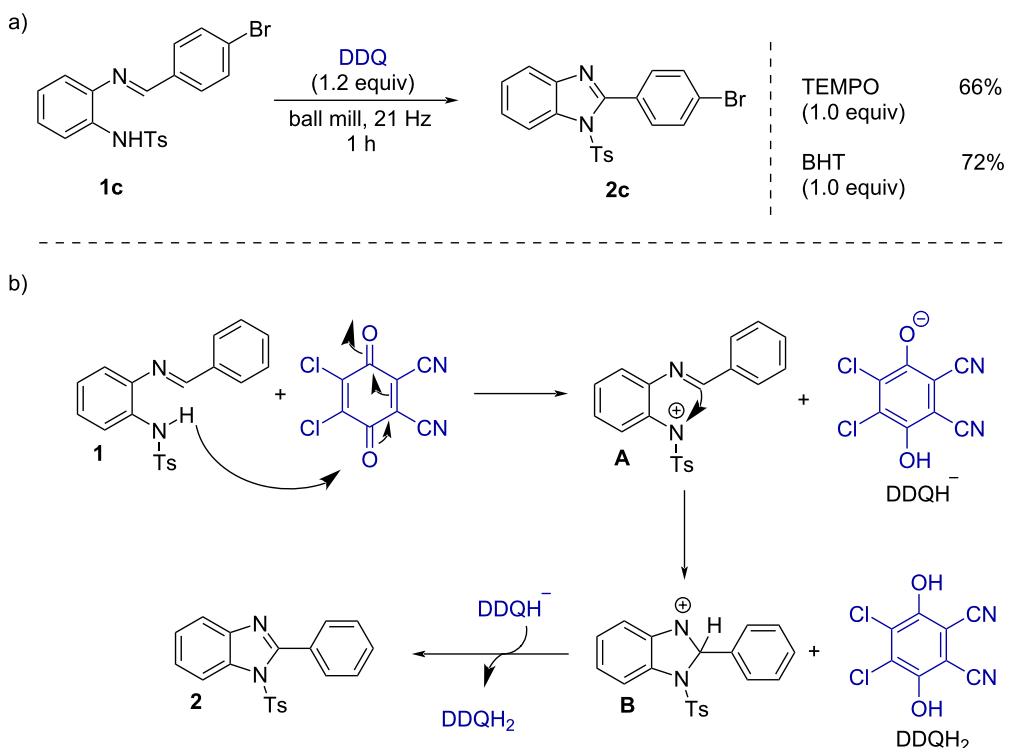


Figure 5: a) Control experiment and b) Plausible mechanism.

Figure 6. In this context, milling of the substrate (*E*)-*N*-(2-((4-bromobenzylidene)amino)phenyl)-4-methylbenzenesulfonamide (**1c**, 2.795 mmol) in the presence of 1.2 equiv of DDQ

delivered 1.098 g (92%) of the cyclized product 2-(4-bromophenyl)-1-tosyl-1*H*-benzo[*d*]imidazole (**2c**). Similarly, we also carried out the large-scale synthesis with 4.04 mmol each of

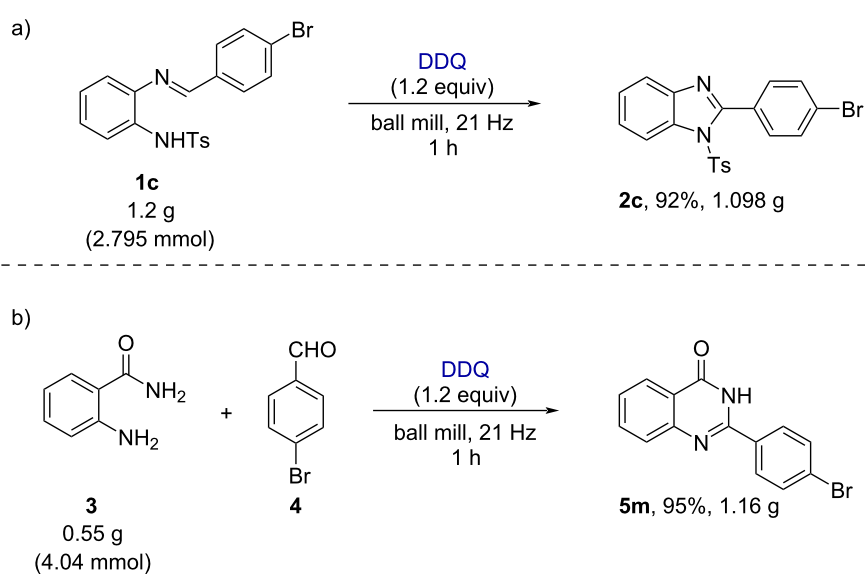


Figure 6: Large-scale synthesis. a) 1,2-Disubstituted benzimidazoles. b) Substituted quinazolin-4(3*H*)-ones. Reaction conditions: reactants were milled at 21 Hz in a 25 mL milling jar containing one stainless-steel grinding ball (15 mm in diameter).

anthranilamide and 4-bromobenzaldehyde (**4**), which produced 1.16 g (95%) of the desired product 2-(4-bromophenyl)quinazolin-4(3*H*)-one (**5m**).

Conclusion

In summary, we have successfully developed efficient methodologies for synthesizing 1,2-disubstituted benzimidazoles and quinazolin-4(3*H*)-one derivatives under mechanochemical (ball milling at 21 Hz) conditions in the presence of DDQ. The developed methodology can be considered as a green and eco-friendly methodology due to its solvent-free and metal-free nature. So, it can also be regarded as an alternative pathway to the traditional solution-based protocols. We anticipate that our developed strategy will have a substantial impact on the field of organic synthesis.

Supporting Information

Supporting Information File 1

Experimental details, characterization data, copies of NMR spectra and X-ray crystallography details.

[<https://www.beilstein-journals.org/bjoc/content/supplementary/1860-5397-18-64-S1.pdf>]

Funding

SKB thank DST (INSPIRE) and RB thank CSIR (India) for fellowships.

ORCID® IDs

Prasenjit Mal - <https://orcid.org/0000-0002-7830-9812>

References

1. Hernández, J. G.; Bolm, C. *J. Org. Chem.* **2017**, *82*, 4007–4019. doi:10.1021/acs.joc.6b02887
2. Ardila-Fierro, K. J.; Hernández, J. G. *ChemSusChem* **2021**, *14*, 2145–2162. doi:10.1002/cssc.202100478
3. Egorov, I. N.; Santra, S.; Kopchuk, D. S.; Kovalev, I. S.; Zyryanov, G. V.; Majee, A.; Ranu, B. C.; Rusinov, V. L.; Chupakhin, O. N. *Green Chem.* **2020**, *22*, 302–315. doi:10.1039/c9gc03414e
4. Tan, D.; Friščić, T. *Eur. J. Org. Chem.* **2018**, 18–33. doi:10.1002/ejoc.201700961
5. Wang, G.-W. *Chem. Soc. Rev.* **2013**, *42*, 7668–7700. doi:10.1039/c3cs35526h
6. Mateti, S.; Mathesh, M.; Liu, Z.; Tao, T.; Ramireddy, T.; Glushenkov, A. M.; Yang, W.; Chen, Y. I. *Chem. Commun.* **2021**, *57*, 1080–1092. doi:10.1039/d0cc06581a
7. Gomollón-Bel, F. *Chem. Int.* **2019**, *41* (2), 12–17. doi:10.1515/ci-2019-0203
8. Bose, A.; Mal, P. *Beilstein J. Org. Chem.* **2019**, *15*, 881–900. doi:10.3762/bjoc.15.86
9. Achar, T. K.; Bose, A.; Mal, P. *Beilstein J. Org. Chem.* **2017**, *13*, 1907–1931. doi:10.3762/bjoc.13.186
10. O'Neill, R. T.; Boulatov, R. *Nat. Rev. Chem.* **2021**, *5*, 148–167. doi:10.1038/s41570-020-00249-y
11. Lou, S.-J.; Mao, Y.-J.; Xu, D.-Q.; He, J.-Q.; Chen, Q.; Xu, Z.-Y. *ACS Catal.* **2016**, *6*, 3890–3894. doi:10.1021/acscatal.6b00861
12. Das, D.; Bhosle, A. A.; Panjikar, P. C.; Chatterjee, A.; Banerjee, M. *ACS Sustainable Chem. Eng.* **2020**, *8*, 19105–19116. doi:10.1021/acssuschemeng.0c07465
13. Bera, S. K.; Mal, P. *J. Org. Chem.* **2021**, *86*, 14144–14159. doi:10.1021/acs.joc.1c01742
14. Alsharif, M. A.; Raja, Q. A.; Majeed, N. A.; Jassas, R. S.; Alsimarree, A. A.; Sadiq, A.; Naeem, N.; Mughal, E. U.; Alsantali, R. I.; Moussa, Z.; Ahmed, S. A. *RSC Adv.* **2021**, *11*, 29826–29858. doi:10.1039/d1ra04575j
15. Wendlandt, A. E.; Stahl, S. S. *Angew. Chem., Int. Ed.* **2015**, *54*, 14638–14658. doi:10.1002/anie.201505017
16. Cheng, D.; Wu, L.; Deng, Z.; Xu, X.; Yan, J. *Adv. Synth. Catal.* **2017**, *359*, 4317–4321. doi:10.1002/adsc.201700853
17. Chen, Q.; Wen, C.; Wang, X.; Yu, G.; Ou, Y.; Huo, Y.; Zhang, K. *Adv. Synth. Catal.* **2018**, *360*, 3590–3594. doi:10.1002/adsc.201800804
18. Li, J.-S.; Xue, Y.; Fu, D.-M.; Li, D.-L.; Li, Z.-W.; Liu, W.-D.; Pang, H.-L.; Zhang, Y.-F.; Cao, Z.; Zhang, L. *RSC Adv.* **2014**, *4*, 54039–54042. doi:10.1039/c4ra08627a
19. Yi, H.; Liu, Q.; Liu, J.; Zeng, Z.; Yang, Y.; Lei, A. *ChemSusChem* **2012**, *5*, 2143–2146. doi:10.1002/cssc.201200458
20. Pan, D.; Pan, Z.; Hu, Z.; Li, M.; Hu, X.; Jin, L.; Sun, N.; Hu, B.; Shen, Z. *Eur. J. Org. Chem.* **2019**, 5650–5655. doi:10.1002/ejoc.201900773
21. Li, C.; Li, J.; Tan, C.; Wu, W.; Jiang, H. *Org. Chem. Front.* **2018**, *5*, 3158–3162. doi:10.1039/c8qo00799c
22. Yan, B.; Fu, Y.; Zhu, H.; Chen, Z. *J. Org. Chem.* **2019**, *84*, 4246–4262. doi:10.1021/acs.joc.9b00231
23. Zhai, L.; Shukla, R.; Rathore, R. *Org. Lett.* **2009**, *11*, 3474–3477. doi:10.1021/ol901331p
24. Natarajan, P.; König, B. *Eur. J. Org. Chem.* **2021**, 2145–2161. doi:10.1002/ejoc.202100011
25. Song, C.; Dong, X.; Yi, H.; Chiang, C.-W.; Lei, A. *ACS Catal.* **2018**, *8*, 2195–2199. doi:10.1021/acscatal.7b04434
26. Shen, Z.; Dai, J.; Xiong, J.; He, X.; Mo, W.; Hu, B.; Sun, N.; Hu, X. *Adv. Synth. Catal.* **2011**, *353*, 3031–3038. doi:10.1002/adsc.201100429
27. Mandal, T.; Azim, A.; Das, S.; De Sarkar, S. *Asian J. Org. Chem.* **2022**, *11*, e202100601. doi:10.1002/ajoc.202100601
28. Sun, C.; Zheng, L.; Xu, W.; Dushkin, A. V.; Su, W. *Green Chem.* **2020**, *22*, 3489–3494. doi:10.1039/d0gc00372g
29. Hernández, J. G.; Turberg, M.; Schiffrers, I.; Bolm, C. *Chem. – Eur. J.* **2016**, *22*, 14513–14517. doi:10.1002/chem.201603057
30. Li, C.-J. *Chem* **2016**, *1*, 423–437. doi:10.1016/j.chempr.2016.08.007
31. Hermann, G. N.; Bolm, C. *ACS Catal.* **2017**, *7*, 4592–4596. doi:10.1021/acscatal.7b00582
32. Bariwal, J.; Van der Eycken, E. *Chem. Soc. Rev.* **2013**, *42*, 9283–9303. doi:10.1039/c3cs60228a
33. Hartwig, J. F. *Acc. Chem. Res.* **2008**, *41*, 1534–1544. doi:10.1021/ar800098p
34. Majumdar, B.; Sarma, D.; Bhattacharya, T.; Sarma, T. K. *ACS Sustainable Chem. Eng.* **2017**, *5*, 9286–9294. doi:10.1021/acssuschemeng.7b02267
35. Ruiz-Castillo, P.; Buchwald, S. L. *Chem. Rev.* **2016**, *116*, 12564–12649. doi:10.1021/acs.chemrev.6b00512

36. Sun, C.-L.; Shi, Z.-J. *Chem. Rev.* **2014**, *114*, 9219–9280.
doi:10.1021/cr400274j

37. Louillat, M.-L.; Patureau, F. W. *Chem. Soc. Rev.* **2014**, *43*, 901–910.
doi:10.1039/c3cs60318k

38. Carvalho, L. C. R.; Fernandes, E.; Marques, M. M. B. *Chem. – Eur. J.* **2011**, *17*, 12544–12555. doi:10.1002/chem.201101508

39. Maiti, S.; Mal, P. *Adv. Synth. Catal.* **2015**, *357*, 1416–1424.
doi:10.1002/adsc.201401110

40. Alam, M. T.; Maiti, S.; Mal, P. *Beilstein J. Org. Chem.* **2018**, *14*, 2396–2403. doi:10.3762/bjoc.14.216

41. Li, Y.-F.; Wang, G.-F.; He, P.-L.; Huang, W.-G.; Zhu, F.-H.; Gao, H.-Y.; Tang, W.; Luo, Y.; Feng, C.-L.; Shi, L.-P.; Ren, Y.-D.; Lu, W.; Zuo, J.-P. *J. Med. Chem.* **2006**, *49*, 4790–4794. doi:10.1021/jm060330f

42. Valdez, J.; Cedillo, R.; Hernández-Campos, A.; Yépez, L.; Hernández-Luis, F.; Navarrete-Vázquez, G.; Tapia, A.; Cortés, R.; Hernández, M.; Castillo, R. *Bioorg. Med. Chem. Lett.* **2002**, *12*, 2221–2224. doi:10.1016/s0960-894x(02)00346-3

43. Sondhi, S. M.; Rajvanshi, S.; Johar, M.; Bharti, N.; Azam, A.; Singh, A. K. *Eur. J. Med. Chem.* **2002**, *37*, 835–843.
doi:10.1016/s0223-5234(02)01403-4

44. Sharpe, M.; Jarvis, B.; Goa, K. L. *Drugs* **2001**, *61*, 1501–1529.
doi:10.2165/00003495-20011100-00009

45. Parua, S.; Das, S.; Sikari, R.; Sinha, S.; Paul, N. D. *J. Org. Chem.* **2017**, *82*, 7165–7175. doi:10.1021/acs.joc.7b00643

46. Sahoo, S.; Pal, S. *J. Org. Chem.* **2021**, *86*, 18067–18080.
doi:10.1021/acs.joc.1c02343

47. Kung, P.-P.; Casper, M. D.; Cook, K. L.; Wilson-Lingardo, L.; Risen, L. M.; Vickers, T. A.; Ranken, R.; Blyn, L. B.; Wyatt, J. R.; Cook, P. D.; Ecker, D. J. *J. Med. Chem.* **1999**, *42*, 4705–4713.
doi:10.1021/jm9903500

48. Chen, M.; Li, P.; Hu, D.; Zeng, S.; Li, T.; Jin, L.; Xue, W.; Song, B. *Bioorg. Med. Chem. Lett.* **2016**, *26*, 168–173.
doi:10.1016/j.bmcl.2015.11.006

49. Chandrika, P. M.; Yakaiah, T.; Rao, A. R. R.; Narsaiah, B.; Reddy, N. C.; Sridhar, V.; Rao, J. V. *Eur. J. Med. Chem.* **2008**, *43*, 846–852. doi:10.1016/j.ejmchem.2007.06.010

50. Cao, S.-L.; Feng, Y.-P.; Jiang, Y.-Y.; Liu, S.-Y.; Ding, G.-Y.; Li, R.-T. *Bioorg. Med. Chem. Lett.* **2005**, *15*, 1915–1917.
doi:10.1016/j.bmcl.2005.01.083

51. Kikuchi, H.; Yamamoto, K.; Horiowa, S.; Hirai, S.; Kasahara, R.; Hariguchi, N.; Matsumoto, M.; Oshima, Y. *J. Med. Chem.* **2006**, *49*, 4698–4706. doi:10.1021/jm0601809

52. Ozaki, K.-i.; Yamada, Y.; Oine, T.; Ishizuka, T.; Iwasawa, Y. *J. Med. Chem.* **1985**, *28*, 568–576. doi:10.1021/jm50001a006

53. Batra, A.; Singh, K. N. *Eur. J. Org. Chem.* **2020**, 6676–6703.
doi:10.1002/ejoc.202000785

54. Cheng, D.; Bao, W. *J. Org. Chem.* **2008**, *73*, 6881–6883.
doi:10.1021/jo8010039

55. Guo, X.; Zipse, H.; Mayr, H. *J. Am. Chem. Soc.* **2014**, *136*, 13863–13873. doi:10.1021/ja507598y

License and Terms

This is an open access article licensed under the terms of the Beilstein-Institut Open Access License Agreement (<https://www.beilstein-journals.org/bjoc/terms>), which is identical to the Creative Commons Attribution 4.0

International License

(<https://creativecommons.org/licenses/by/4.0>). The reuse of material under this license requires that the author(s), source and license are credited. Third-party material in this article could be subject to other licenses (typically indicated in the credit line), and in this case, users are required to obtain permission from the license holder to reuse the material.

The definitive version of this article is the electronic one which can be found at:

<https://doi.org/10.3762/bjoc.18.64>



Mechanochemical halogenation of unsymmetrically substituted azobenzenes

Dajana Barišić, Mario Pajić, Ivan Halasz, Darko Babić and Manda Ćurić*

Full Research Paper

Open Access

Address:

Division of Physical Chemistry, Ruder Bošković Institute, Bijenička cesta 54, Zagreb, Croatia

Beilstein J. Org. Chem. **2022**, *18*, 680–687.

<https://doi.org/10.3762/bjoc.18.69>

Email:

Manda Ćurić* - curic@irb.hr

Received: 23 March 2022

Accepted: 01 June 2022

Published: 15 June 2022

* Corresponding author

This article is part of the thematic issue "Mechanochemistry III".

Keywords:

azo compounds; halogenation; mechanochemistry;
N-halosuccinimide; palladium(II)

Guest Editors: J. G. Hernández and L. Borchardt

© 2022 Barišić et al.; licensee Beilstein-Institut.

License and terms: see end of document.

Abstract

The direct and selective mechanochemical halogenation of C–H bonds in unsymmetrically substituted azobenzenes using *N*-halosuccinimides as the halogen source under neat grinding or liquid-assisted grinding conditions in a ball mill has been described. Depending on the azobenzene substrate used, halogenation of the C–H bonds occurs in the absence or only in the presence of Pd^{II} catalysts. Insight into the reaction dynamics and characterization of the products was achieved by *in situ* Raman and *ex situ* NMR spectroscopy and PXRD analysis. A strong influence of the different 4,4'-substituents of azobenzene on the halogenation time and mechanism was found.

Introduction

Electrophilic aromatic substitution [1–3] and ligand-directed transition-metal-catalyzed reactions [4–8] are among the most widely used synthetic approaches for the preparation of halogenated arenes. They are important precursors in cross-coupling reactions [9–19] or components of pharmaceuticals and biologically active molecules [20,21]. The synthetic aspects of both approaches in solution are well established.

The need for green and sustainable chemistry [22] has led to the development and synthetic application of solid-state methods [23–46], particularly ball milling [26–46], which has proven to be an environmentally friendly and powerful alternative to

conventional solvent-based protocols, offering unique advantages in terms of sustainability, reaction times, yields, reactant solubility, selectivity, and chemical reactivity. Although ball milling methods are widely used for the synthesis of various classes of compounds [26–46], their application in the synthesis of halogenated arenes is still scarce.

In 2015, Bolm and Hernandez reported the halogenation of 2-phenylpyridine in a ball mill using [Cp*RhCl₂]₂ in combination with AgSbF₆ as catalyst and *N*-halosuccinimide (NXS, X = Br, I) as halogen source [47]. Two years later in 2017, Eslami's group applied a ball-milling method to synthesize aryl

bromides and α -bromoketones with *N*-bromosuccinimide (NBS) and MCM-41-SO₃H catalyst and no liquid additives [48]. In 2018, Wang and co-workers developed the ball-milling protocol for the *ortho*-halogenation of acetanilide with NXS (X = Cl, Br, I) using Pd(OAc)₂ as precatalyst in the presence of *p*-toluenesulfonic acid (TsOH) as an additive under solvent-free conditions [49]. Recently, Mal and Bera reported the utilization of NXS (X = Br, Cl) as bifunctional reagents for the solvent-free synthesis of phenanthridinones via a cascaded oxidative C–N coupling followed by a halogenation reaction [50].

Only recently, our group carried out a detailed synthetic and mechanistic study of the mechanochemical Pd^{II}-catalyzed bromination of unsubstituted azobenzene (**L1**) by *N*-bromosuccinimide (NBS) under neat grinding (NG) and liquid-assisted grinding (LAG) conditions in a ball mill [51]. Insight into the dynamics of the formation of reaction intermediates and products was obtained by *in situ* Raman monitoring that provided information on the nature of the catalytically active Pd^{II} species, cyclopalladated intermediates, and products (Figure 1). The monitoring results confirmed the crucial role of TsOH and acetonitrile (MeCN) as additives in the catalytic bromination of the C–H bond in **L1**. The experimental results were supported by quantum-chemical calculations, which showed that four mechanistic pathways could be involved in this reaction [51]. Three of them involve oxidative addition followed by reductive elimination. Neutral NBS or the hydrogen bond complex NBS…TsOH are bromine donors in two of them, while protonated NBS is engaged in the third. The fourth mechanism proceeds by electrophilic cleavage with neutral NBS or the hydrogen bond complex NBS…TsOH as a bromine source.

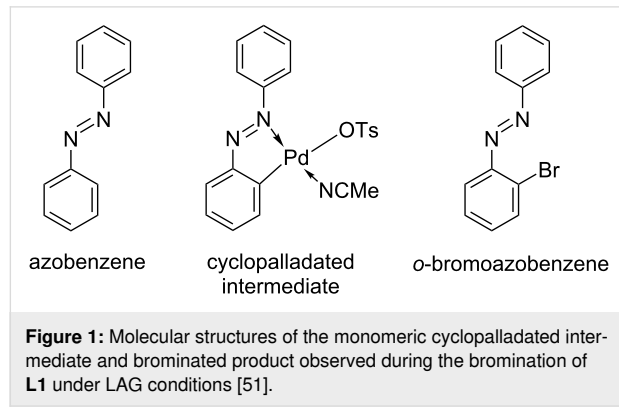


Figure 1: Molecular structures of the monomeric cyclopalladated intermediate and brominated product observed during the bromination of **L1** under LAG conditions [51].

Here we present the mechanochemical selective halogenation of unsymmetrically substituted azobzenes by NXS (X = Cl, Br, or I). The liquid-assisted grinding of *para*-halogenated derivatives of azobenzene with NXS and Pd(OAc)₂ as precatalyst in the presence of TsOH and MeCN as solid and liquid additives, respectively, led to the *ortho*-halogenated products relative to

the azo group of the azobzenes. *In situ* Raman monitoring of these reactions confirmed that the most favorable reaction pathway is via the monomeric cyclopalladated intermediate, as in the halogenation reaction of unsubstituted **L1** [51]. While the reactions of **L1** and its *para*-halogenated derivatives were unsuccessful without the Pd^{II} catalyst and TsOH, the halogenation of azobzenes with the strong electron-donating substituents in the *para* position occurred in the absence of the added Pd^{II} catalyst and additives, in the *ortho* position to the substituent, which is typical for the products of electrophilic aromatic substitution.

In addition, an additive- and solvent-free protocol without the added Pd^{II} catalyst was developed for the selective imidation of azobzenes containing a dimethylamino group as substituent in the *para* position to the azo group.

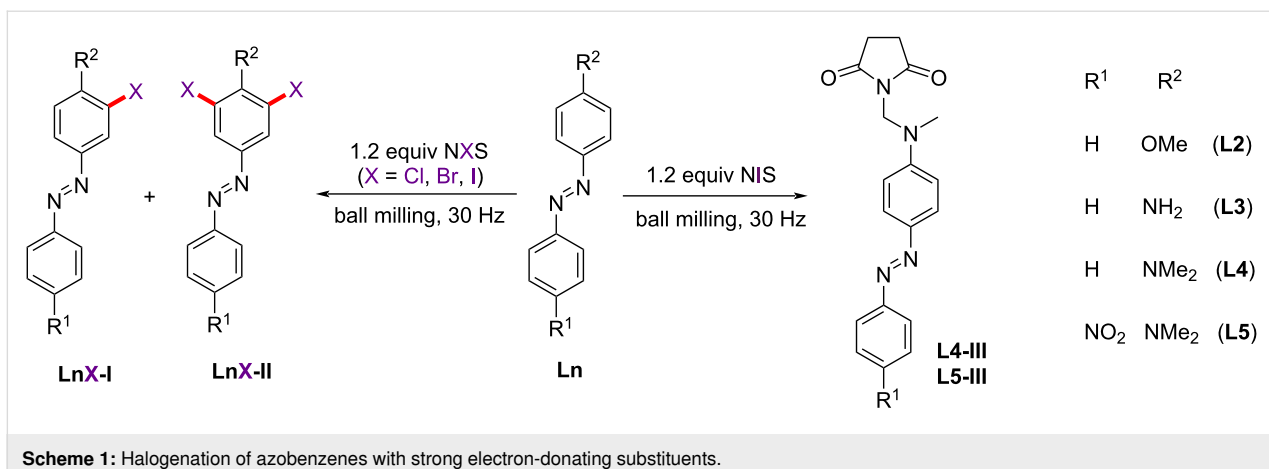
Results and Discussion

Inspired by our findings on the mechanochemical halogenation of **L1** [51] and the report of Ma and Tian on the bromination of symmetric and unsymmetric azobzenes in MeCN [52], we investigated how substituents of different donor strength affect the selectivity, reactivity, and reaction pathways of halogenation of azobenzene substrates under mechanochemical conditions.

Halogenation of azobzenes with strong electron-donating substituents

In contrast to the reactions of **L1** [51], the halogenation of azobenzene substrates containing strong electron-donating substituents (4-methoxyazobenzene (**L2**), 4-aminoazobenzene (**L3**), 4-dimethylaminoazobenzene (**L4**), and 4-(dimethylamino)-4'-nitroazobenzene (**L5**)) with NXS (X = Cl and Br) occurred in the absence of the added Pd^{II} catalyst and additives. These reactions in most cases produced electrophilic substitution products that were halogenated in the *ortho* position(s) relative to the electron-donating substituent (Scheme 1 and Table 1), as confirmed by Raman (Figures S14–S22 in Supporting Information File 1) and NMR spectroscopy (Figures S40–S76 in Supporting Information File 1). All experiments were performed without additional oxidants and solid or liquid additives. The presence of the Pd^{II}-catalyst in the reactions of **L2–5** with NXS resulted predominantly in **LnX-I** products or a mixture of products that were mono- or dihalogenated at the *ortho* and *meta*-position(s) relative to the electron-donating substituent, which may be attributed to competition between Pd^{II}-catalyzed reactions and uncatalyzed electrophilic substitution.

Our results are consistent with those reported by Sanford's group for the halogenation of various substrates by NXS with and without Pd^{II} catalyst [53]. Most of these reactions were

**Scheme 1:** Halogenation of azobenzenes with strong electron-donating substituents.**Table 1:** Halogenation of azobenzenes with strong electron-donating substituents.^a

Entry	Reactant	NXS	Product	t [h]	Yield [%] ^b
1	L2	NCS	—	7	—
2	L3	NCS	L3Cl-I	1	46 (34)
3	L4	NCS	L4Cl-I	1	85 (73)
4	L5	NCS	L5Cl-I L5Cl-II	15	83 (72) 16 (8) ^c
5	L2	NBS	L2Br-I	15	96 (90)
6	L3	NBS	L3Br-I	1	72 (54)
7	L4	NBS	L4Br-I	1	79 (67)
8	L5	NBS	L5Br-I	7	53 (37)
9	L2	NIS	—	7	—
10	L3	NIS	L3I-I	1	30 (21)
11	L4	NIS	L4-III	1	39 (29)
12	L5	NIS	L5-III	5	38 (31)

^aReaction conditions: 14 mL PMMA jar, mixer mill, one nickel bound tungsten carbide milling ball (7 mm in diameter, 3.9 g), 30 Hz, **L2–5** (0.50 mmol), NXS (0.60 mmol), SiO₂ (250 mg); ^bdetermined by ¹H NMR spectroscopy using 1,4-dinitrobenzene as the internal standard, with isolated yield given in parentheses; ^cyield calculated with respect to **L5**.

carried out in MeCN and AcOH solutions at 100–120 °C. In contrast, the bromination of 4-methoxyazobenzene by NBS in MeCN at ambient temperature, reported by Tian and Ma [52], resulted in an electrophilic monobrominated product as a single isomer in both the catalyzed and uncatalyzed reactions.

Neat grinding of **L3** and **L4** with NCS produced the monochlorinated products **L3Cl-I** and **L4Cl-I** as single isomers within one hour (Table 1, entries 2 and 3). In contrast, the reaction of **L5** with NCS resulted in a mixture of mono- and dichlorinated regioisomers (**L5Cl-I** and **L5Cl-II**) (Scheme 1 and Table 1, entry 4). The chlorination of **L3** substrate with a primary amine

as substituent gave the monochlorinated product **L3Cl-I** in 46% yield, while the yields of **L4Cl-I** and **L5Cl-I** were 85% and 83%, respectively (Table 1, entries 2–4). Although both substrates **L4** and **L5** contain a tertiary amine as a substituent (NMe₂), the chlorination of **L5** proceeded much more slowly (Table 1, entries 3 and 4).

Neither NCS nor NIS yielded halogenated products with substrate **L2** (Table 1, entries 1 and 9). However, the reaction of **L2** with NBS gave the monobrominated product **L2Br-I** in 96% yield after 15 hours of milling (Figure 2, Table 1, entry 5). The yield of this reaction was higher than the analogous reaction in MeCN solution (90% isolated yield under the mechanochemical conditions compared to 72% in MeCN solution) [52]. In situ Raman monitoring of the bromination of **L2** confirmed its conversion to the product **L2Br-I** (Figure 2). The formation of **L2Br-I** was accompanied by the intensity decrease of **L2** ν (N=N) and ν (C–N) bands in the range 1400–1450 and 1080–1200 cm⁻¹, respectively. Compounds **L2** and **L2Br-I** were identified in the reaction mixture by the Raman spectra of isolated **L2** and **L2Br-I** (Figure 2c).

Neat grinding of **L3**, **L4**, and **L5** with NBS also produced the monobrominated products in yields ranging from 53 to 79% within one and seven hours, respectively (Table 1, entries 6–8).

The reaction of **L3** with NIS resulted in the monoiodinated product in a low yield of 30% after one hour of milling (Table 1, entry 10 and Figures S77–S81 in Supporting Information File 1). Interestingly, in the reactions of **L4** and **L5** with NIS, instead of the halogenation of the aromatic C–H bond, imidation of the aliphatic C–H bond was observed. Imides are among the most studied functional groups, and new methods for their preparation, especially by environmentally friendly protocols, are of great synthetic importance in organic chemistry [54].

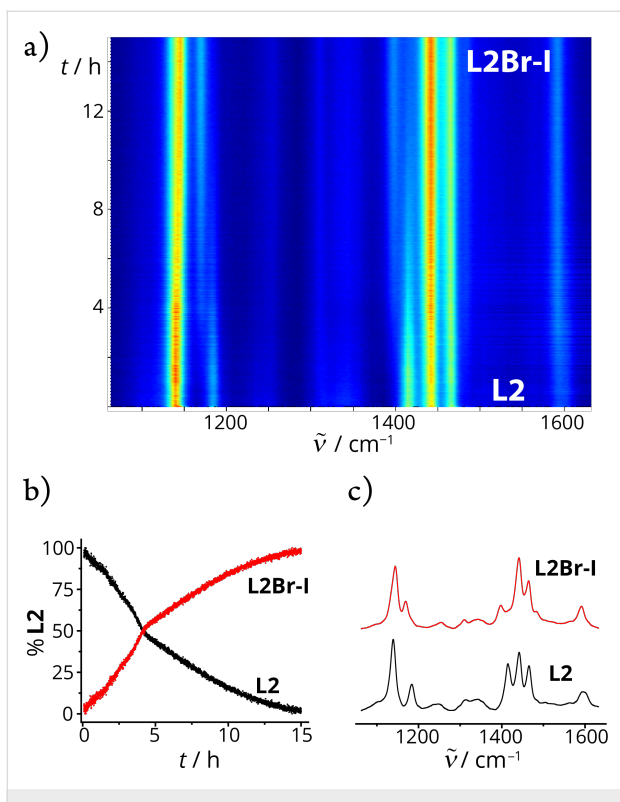


Figure 2: a) Two-dimensional (2D) plot of the time-resolved Raman monitoring of NG of **L2** (0.50 mmol) with NBS (0.60 mmol) and SiO_2 (250 mg). b) Reaction profile derived from multivariate curve analysis – alternating least squares fitting (MCR-ALS analysis). c) Extracted Raman spectra of species observed during Raman monitoring.

The succinimide products **L4-III** and **L5-III** (Table 1, entries 11 and 12) were obtained within one and five hours in 39 and 38% yields, respectively, as confirmed by NMR spectroscopy (Figures S82–S91 in Supporting Information File 1). Additional support for the formation of succinimide products was provided by the molecular structure of **L4-III**, resolved by single-crystal X-ray analysis (Figure 3 and Figure S33 and Table S1 in Supporting Information File 1). The molecular structure of **L4-III** showed that imidation occurred at the methyl group of the NMe_2 substituent. Analogous succinimide species were also observed in the reaction of *N,N*-dimethyl-*p*-toluidine with NIS in ethyl acetate [55] or *N,N*-dimethylamides and *N,N*-dimethylamines with NBS in carbon tetrachloride [56].

The reactivity trend of electron-rich azobenzenes **L2–5** toward NXS was also investigated. Results of competition experiments clearly demonstrated that in the case of NCS their reactivity decreases in the order: **L4** > **L3** > **L5** (Figures S1 and S2 in Supporting Information File 1), in the case of NBS in the order: **L3** > **L4** > **L5** >> **L2** (Figures S3–S6 in Supporting Information File 1), and in the case of NIS in the order: **L4** >> **L5** for the succinimide products (Figure S7 in Supporting Information File 1). The presence of an electron-accepting substituent (NO_2)

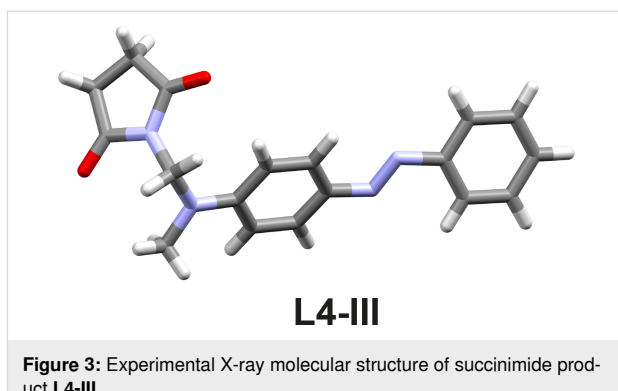


Figure 3: Experimental X-ray molecular structure of succinimide product **L4-III**.

at the *para* position of the second phenyl ring in **L5** significantly slowed the halogenation reaction and impaired the reactivity of the azobenzene. This result suggests that NO_2 has a long-range effect that spreads through the azobenzene skeleton. Compared to the bromination of substrates **L3–5** containing amino substituents, the analogous reaction of **L2** is slower because the methoxy substituent has weaker donor strength than amino substituents [57].

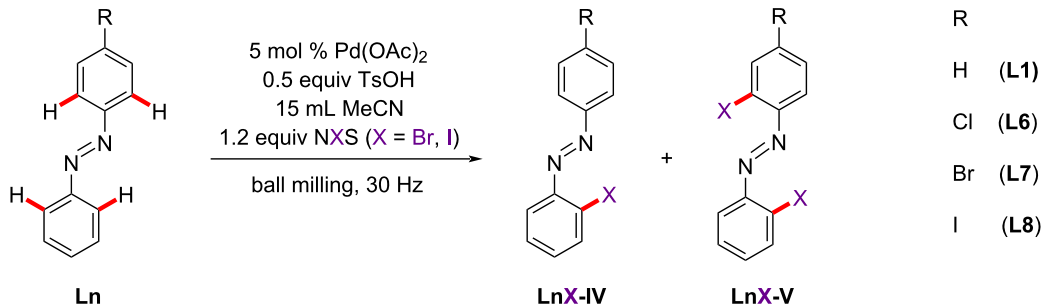
The protocols described above provide a solvent- and additive-free approach without added Pd^{II} catalysts for the halogenation of Csp^2 -H and imidation of Csp^3 -H bonds of azobenzenes with electron-donating substituents by electrophilic activation with NXS.

Halogenation of azobenzenes with electron-accepting substituents

Using the optimal parameters for the mechanochemical bromination and iodination of **L1** [51], we investigated the halogenation of azobenzene substrates with electron-accepting substituents at the *para* position relative to the azo group: 4-chloroazobenzene (**L6**), 4-bromoazobenzene (**L7**), and 4-iodoazobenzene (**L8**) (Scheme 2 and Table 2).

The synthetic protocols included milling the mixture of **Ln**/NXS/TsOH 1:1.2:0.5 equiv, 5 mol % $\text{Pd}(\text{OAc})_2$ precatalyst, and 15 μL MeCN as liquid additive. Under these conditions, the reactions of **L6–8** with NBS resulted in moderate to good yields of monobrominated products **LnBr-IV** (Table 2, entries 6–8).

The bromination of **L6–8** occurred regioselectively at the *ortho* position of the unsubstituted phenyl ring, as shown by NMR spectroscopy (Figures S92–S103 in Supporting Information File 1). The reaction times required for bromination increased in the order **L1** < **L6** < **L7** = **L8** (Table 2, entries 5–8). Dibrominated products **LnBr-V** were not detected in any of these reactions. Since the complex $\text{Pd}(\text{OTs})_2(\text{MeCN})_2$ was identified as the active catalyst, formed *in situ*, in the bromination reaction of

Scheme 2: Pd^{II} -catalyzed halogenation of azobenzene and its *para*-halogenated derivatives.Table 2: Pd^{II} -catalyzed halogenation of **L1** [51] and its *para*-halogenated derivatives (**L6–8**).^a

Entry	Reactant	NXS	Product	<i>t</i> [h]	Yield [%] ^b
1	L1 [51]	NCS	—	17	—
2	L6	NCS	—	17	—
3	L7	NCS	—	17	—
4	L8	NCS	—	17	—
5	L1 [51]	NBS	L1Br-IV	4	83 (74)
6	L6	NBS	L6Br-IV	6	73 (59)
7	L7	NBS	L7Br-IV	8	72 (60)
8	L8	NBS	L8Br-IV	8	62 (55)
9	L1 [51]	NIS	L1I-IV L1I-V	4	38 (35) 43 (28) ^c
10	L6	NIS	L6I-IV L6I-V	6	66 (63) 17 (11) ^c
11	L7	NIS	L7I-IV L7I-V	5	69 (59) 19 (8) ^c
12	L8	NIS	L8I-IV L8I-V	7	52 (45) 19 (17) ^c

^aReaction conditions: 14 mL PMMA jar, mixer mill, one nickel bound tungsten carbide milling ball (7 mm in diameter, 3.9 g), 30 Hz, **L1** and **L6–8** (0.50 mmol), $\text{Pd}(\text{OAc})_2$ (5 mol %), NXS (0.60 mmol), TsOH (0.25 mmol), MeCN (15 μ L), SiO_2 (250 mg); ^bdetermined by ^1H NMR spectroscopy using 1,4-dinitrobenzene as the internal standard, with isolated yield given in parentheses; ^cyield calculated with respect to **L1** or **L6–8**.

L1 [51], the analogous reactions of **L6–8** were carried out using $\text{Pd}(\text{OTs})_2(\text{MeCN})_2$ as the catalyst instead of $\text{Pd}(\text{OAc})_2$. As expected, the yields of **LnBr-IV** products were comparable to those obtained in the reactions with the $\text{Pd}(\text{OAc})_2$ precatalyst.

The Pd^{II} -catalyzed iodination of **L6–8** was conducted with *N*-iodosuccinimide (NIS) as the iodine source. The reaction time for the iodination of **L6** was the same as for the analogous bromination reaction (Table 2, entry 10). Iodination of **L7** and **L8** was completed within five and seven hours, respectively

(Table 2, entries 11 and 12). Unlike bromination, iodination of **L6–8** with NIS resulted in a mixture of the mono- and diiodinated products at the *ortho* positions of one or both phenyl rings (**LnI-IV** and **LnI-V**, Scheme 2 and Table 2, entries 10–12), as confirmed by NMR spectroscopy (Figures S104–S130 in Supporting Information File 1). Compared to **L1** [51], iodination of its *para*-halogenated derivatives resulted in lower yields of diiodinated products (Table 2, entries 9–12) since the activation/halogenation of the C–H bond occurs preferentially at the un-substituted azobenzene phenyl ring [57].

The reactions of **L6–8** with *N*-chlorosuccinimide (NCS) gave no chlorinated product, which was also observed in the reaction of **L1** with NCS (Table 2, entries 1–4) [51].

Since the monomeric monopalladated tosylate complex of azobenzene **II-I** was identified as an intermediate in the solid-state bromination of **L1** (Figure 1) [51], the analogous complexes of **L6** and **L7** were prepared to investigate whether the halogenation of the *para*-halogenated azobenzene derivatives follows the reaction pathway of the bromination of **L1**. The molecular structures of the isolated monopalladated tosylate complexes **I6-I** and **I7-I** solved from laboratory powder X-ray diffraction (PXRD) data (Figure 4 and Figures S31 and S32 in Supporting Information File 1), are similar to that of complex **II-I** [51] in which the palladium center is bound to the MeCN and tosylate (OTs) via nitrogen and oxygen, respectively, and to the azobenzene via the azo nitrogen and a carbon atom of the unsubstituted phenyl ring. The tosylate ion is at the *trans* position to the carbon atom.

In situ Raman monitoring of the bromination of **L6–8** in the presence of 30 mol % Pd^{II} catalyst revealed a new band around 1380 cm^{-1} (Figure 5a and Figures S23–S27 in Supporting Information File 1). It was assigned to the characteristic $\nu(\text{N}=\text{N})$ bands of the **In-I** intermediates, confirming that the bromination of **L6–8** proceeds via monopalladated **In-I** intermediates as

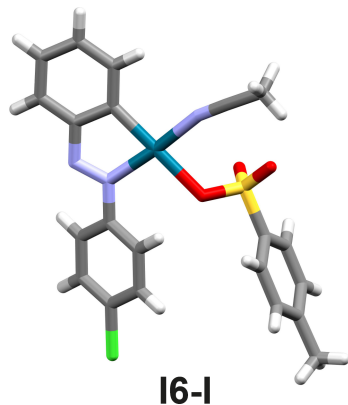


Figure 4: Experimental X-ray molecular structure of the intermediate **I6-I**.

in the reactions of **L1** (Figure 5a and Figures S23–S27 in Supporting Information File 1) [51].

To gain insight into the dynamics of the formation of cyclopalladated intermediates **In-I**, LAG reactions of $\text{Pd}(\text{OAc})_2$ with **L6–8** and TsOH were performed using 25 μL of MeCN as a liquid additive in a molar ratio of 1:1:1 ($\text{Ln}/\text{Pd}(\text{OAc})_2/\text{TsOH}$). In situ Raman monitoring of C–H bond activation was possible for **L6** and **L7**, while in the case of **L8**, fluorescence prevented a more detailed insight into this reaction. The monitoring results confirmed the complete conversion of azobenzenes **L6** and **L7** to their monopalladated products after about one hour of milling, as well as a reaction course similar to that of the analogous reaction of **L1** [51] (Figure 5b and Figure S28 in Supporting Information File 1).

The isolated cyclopalladated intermediates **I6-I** and **I7-I** were tested as catalysts for the bromination of **L6** and **L7**. The yields of halogenated products in these reactions are 64% for **L6Br-I** and 70% for **L7Br-I**, which are close to those obtained in the analogous reactions with $\text{Pd}(\text{OAc})_2$ as precatalyst, as confirmed by NMR spectroscopy.

The results of in situ and ex situ spectroscopic monitoring along with the structural characterization of the intermediates have shown that the mechanism of the halogenation of azobenzenes with electron-accepting substituents is consistent with the proposed mechanistic schemes for the bromination of the unsubstituted azobenzene **L1** [51]. Thus, the halogenation of **L6–8** begins with the formation of the catalytically active Pd^{II} species, $\text{Pd}(\text{OTs})_2(\text{MeCN})_2$, from $\text{Pd}(\text{OAc})_2$, TsOH , and MeCN. It is followed by the formation of monomeric cyclopalladated intermediates **In-I**, at which halogenation occurs. Based on the similarities between the halogenation of **L6–8** and the bromination of **L1** [51], we assumed that the four mechanistic pathways considered for the bromination of **I1-I** are also possible for the halogenation of **I6-I**, **I7-I**, and **I8-I** [51].

In addition, we also investigated the reactivity trend of azobenzene **L1** and its *para*-halogenated derivatives **L6–8** toward NBS or NIS. The competition experiments showed that the azobenzenes with electron-withdrawing substituents are much less reactive to halogenation than **L1**. The reactivity of azobenzenes in the case of NBS decreases in this order: **L1** >> **L6** > **L7** \approx **L8** (Figures S8–S10 in Supporting Information File 1), and in the case of NIS in the order: **L1** >> **L6** \approx **L8** > **L7** (Figures S11–S13 in Supporting Information File 1), indi-

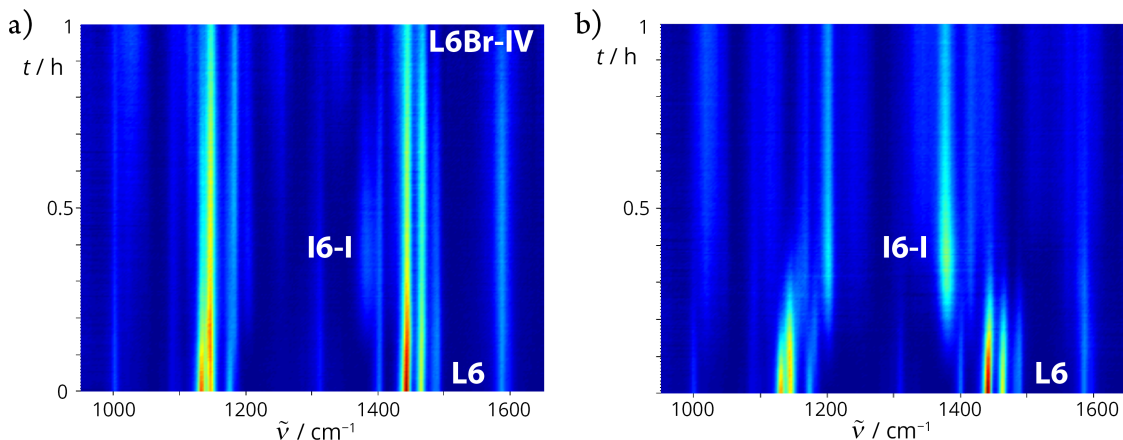


Figure 5: a) In situ observation of **I6-I** during the time-resolved Raman monitoring of LAG of **L6** (0.50 mmol) with NBS (0.6 mmol), TsOH (0.25 mmol), $\text{Pd}(\text{OAc})_2$ (30 mol %), MeCN (15 μL), and SiO_2 (250 mg). b) Two-dimensional (2D) plot of the time-resolved Raman monitoring of LAG of **L6** (0.40 mmol) with $\text{Pd}(\text{OAc})_2$ (0.42 mmol), TsOH (0.42 mmol), MeCN (0.48 mmol, 25 μL), and SiO_2 (250 mg). Only Raman spectra before fluorescence are shown in both parts.

cating that the Pd^{II} -catalyzed halogenation of azobenzenes is strongly influenced by the nature of the azobenzene substituents.

Conclusion

We have applied a mechanochemical protocol for the halogenation of 4,4'-functionalized azobenzenes in a ball mill under NG or LAG conditions, using NXS (X = Cl, Br, and I) as the halogen source.

Halogenation of azobenzenes with strong electron-donating groups was carried out without an added Pd^{II} catalyst. These transformations, which take place via electrophilic aromatic substitution, resulted in products halogenated in the *ortho* position to the electron-donating groups. The reactions of azobenzenes containing a dimethylamino group as substituent with NIS led to imidation products. A different reactivity of the dimethylamino group compared to the other substituents was also observed in these reactions.

On the other hand, the halogenation of *para*-halogenated azobenzenes required the presence of the Pd^{II} catalyst and TsOH as additive. In situ spectroscopic monitoring of these reactions revealed that the Pd^{II} -catalyzed halogenation proceeds via monomeric cyclopalladated intermediates formed by activation of the C–H bond in azobenzenes with the in situ generated $\text{Pd}(\text{OTs})_2(\text{MeCN})_2$ catalyst. The described results indicate a strong dependence of the halogenation outcome of C–H bonds in 4,4'-functionalized azobenzenes on the nature of their substituents.

Supporting Information

Supporting Information File 1

Detailed experimental procedures, complete characterization data for new compounds, X-ray structures of compounds, and the results of in situ Raman monitoring.
[<https://www.beilstein-journals.org/bjoc/content/supplementary/1860-5397-18-69-S1.pdf>]

Supporting Information File 2

X-ray crystallographic data.
[<https://www.beilstein-journals.org/bjoc/content/supplementary/1860-5397-18-69-S2.cif>]

Funding

Financial support was provided by Croatian Science Foundation (grant No. IP-2019-04-9951 and grant No. IP-2020-02-1419).

ORCID® iDs

Dajana Barišić - <https://orcid.org/0000-0003-3017-7061>
Darko Babić - <https://orcid.org/0000-0002-8832-3183>
Manda Ćurić - <https://orcid.org/0000-0003-1861-9269>

References

1. Taylor, R. *Electrophilic Aromatic Substitution*; John Wiley & Sons: New York, NY, USA, 1990.
2. De la Mare, P. B. D. *Electrophilic Halogenation*; Cambridge University Press: New York, NY, USA, 1976.
3. Börgei, J.; Tanwar, L.; Berger, F.; Ritter, T. *J. Am. Chem. Soc.* **2018**, *140*, 16026–16031. doi:10.1021/jacs.8b09208
4. Ackermann, L. *Chem. Rev.* **2011**, *111*, 1315–1345. doi:10.1021/cr100412j and references cited therein.
5. Lyons, T. W.; Sanford, M. S. *Chem. Rev.* **2010**, *110*, 1147–1169. doi:10.1021/cr900184e and references cited therein.
6. Liu, X.-H.; Park, H.; Hu, J.-H.; Hu, Y.; Zhang, Q.-L.; Wang, B.-L.; Sun, B.; Yeung, K.-S.; Zhang, F.-L.; Yu, J.-Q. *J. Am. Chem. Soc.* **2017**, *139*, 888–896. doi:10.1021/jacs.6b11188
7. Powers, D. C.; Ritter, T. *Nat. Chem.* **2009**, *1*, 302–309. doi:10.1038/nchem.246
8. Zhu, R.-Y.; Saint-Denis, T. G.; Shao, Y.; He, J.; Sieber, J. D.; Senanayake, C. H.; Yu, J.-Q. *J. Am. Chem. Soc.* **2017**, *139*, 5724–5727. doi:10.1021/jacs.7b02196
9. Petrone, D. A.; Ye, J.; Lautens, M. *Chem. Rev.* **2016**, *116*, 8003–8104. doi:10.1021/acs.chemrev.6b00089
10. Nattmann, L.; Saeb, R.; Nöthling, N.; Cornell, J. *Nat. Catal.* **2020**, *3*, 6–13. doi:10.1038/s41929-019-0392-6
11. Ayogu, J. I.; Onoabedje, E. A. *Catal. Sci. Technol.* **2019**, *9*, 5233–5255. doi:10.1039/c9cy01331h
12. Zhai, Y.; Chen, X.; Zhou, W.; Fan, M.; Lai, Y.; Ma, D. *J. Org. Chem.* **2017**, *82*, 4964–4969. doi:10.1021/acs.joc.7b00493
13. Hartwig, J. F. Palladium-Catalyzed Synthesis of Aryl Ethers and Related Compounds Containing S and Se. In *Handbook of Organopalladium Chemistry for Organic Synthesis*; Negishi, E., Ed.; Wiley-Interscience: New York, NY, USA, 2002; pp 1051–1106. doi:10.1002/0471212466.ch43
14. Stille, J. K. *Angew. Chem., Int. Ed. Engl.* **1986**, *25*, 508–524. doi:10.1002/anie.198605081
15. Heck, R. F. *Synlett* **2006**, 2855–2860. doi:10.1055/s-2006-951536
16. Suzuki, A. *Chem. Commun.* **2005**, 4759–4763. doi:10.1039/b507375h
17. Muci, A. R.; Buchwald, S. L. Practical Palladium Catalysts for C–N and C–O Bond Formation. In *Cross-Coupling Reactions*; Miyaura, N., Ed.; Topics in Current Chemistry, Vol. 219; Springer: Berlin, Heidelberg, 2002; pp 131–209. doi:10.1007/3-540-45313-x_5
18. Hartwig, J. F. *Synlett* **2006**, 1283–1294. doi:10.1055/s-2006-939728
19. Hartwig, J. F. *Nature* **2008**, *455*, 314–322. doi:10.1038/nature07369
20. Evans, D. A.; Katz, J. L.; Peterson, G. S.; Hintermann, T. *J. Am. Chem. Soc.* **2001**, *123*, 12411–12413. doi:10.1021/ja011943e
21. Pelletier, J. C.; Youssefeyeh, R. D.; Campbell, H. F. Substituted Saturated and Unsaturated Indole Quinoline and Benzazepine Carboxamides and Their Use as Pharmacological Agents. U.S. Pat. Appl. US4920219A, April 24, 1990.
22. Li, C.-J.; Trost, B. M. *Proc. Natl. Acad. Sci. U. S. A.* **2008**, *105*, 13197–13202. doi:10.1073/pnas.0804348105
23. Cliffe, M. J.; Mottillo, C.; Stein, R. S.; Bučar, D.-K.; Friščić, T. *Chem. Sci.* **2012**, *3*, 2495–2500. doi:10.1039/c2sc20344h

24. Juribašić Kulcsár, M.; Halasz, I.; Budimir, A.; Užarević, K.; Lukin, S.; Monas, A.; Emmerling, F.; Plavec, J.; Ćurić, M. *Inorg. Chem.* **2017**, *56*, 5342–5351. doi:10.1021/acs.inorgchem.7b00422

25. Monas, A.; Užarević, K.; Halasz, I.; Juribašić Kulcsár, M.; Ćurić, M. *Chem. Commun.* **2016**, *52*, 12960–12963. doi:10.1039/c6cc06062e

26. James, S. L.; Adams, C. J.; Bolm, C.; Braga, D.; Collier, P.; Friščić, T.; Grepioni, F.; Harris, K. D. M.; Hyett, G.; Jones, W.; Krebs, A.; Mack, J.; Maini, L.; Orpen, A. G.; Parkin, I. P.; Shearouse, W. C.; Steed, J. W.; Waddell, D. C. *Chem. Soc. Rev.* **2012**, *41*, 413–447. doi:10.1039/c1cs15171a

27. Wang, G.-W. *Chem. Soc. Rev.* **2013**, *42*, 7668–7700. doi:10.1039/c3cs35526h

28. Porcheddu, A.; Colacino, E.; De Luca, L.; Delogu, F. *ACS Catal.* **2020**, *10*, 8344–8394. doi:10.1021/acscatal.0c00142 and references cited therein.

29. Schumacher, C.; Hernández, J. G.; Bolm, C. *Angew. Chem., Int. Ed.* **2020**, *59*, 16357–16360. doi:10.1002/anie.202003565

30. Hernández, J. G.; Bolm, C. *J. Org. Chem.* **2017**, *82*, 4007–4019. doi:10.1021/acs.joc.6b02887 and references cited therein.

31. Hernández, J. G. *Chem. – Eur. J.* **2017**, *23*, 17157–17165. doi:10.1002/chem.201703605 and references cited therein.

32. Zhao, S.; Li, Y.; Liu, C.; Zhao, Y. *Tetrahedron Lett.* **2018**, *59*, 317–324. doi:10.1016/j.tetlet.2017.12.021

33. Howard, J. L.; Cao, Q.; Browne, D. L. *Chem. Sci.* **2018**, *9*, 3080–3094. doi:10.1039/c7sc05371a and references cited therein.

34. Andersen, J.; Mack, J. *Green Chem.* **2018**, *20*, 1435–1443. doi:10.1039/c7gc03797j

35. Pickhardt, W.; Grätz, S.; Borchardt, L. *Chem. – Eur. J.* **2020**, *26*, 12903–12911. doi:10.1002/chem.202001177 and references cited therein.

36. Ingner, F. J. L.; Giustra, Z. X.; Novosedlik, S.; Orthaber, A.; Gates, P. J.; Dyrager, C.; Pilarski, L. T. *Green Chem.* **2020**, *22*, 5648–5655. doi:10.1039/d0gc02263b

37. Hermann, G. N.; Unruh, M. T.; Jung, S.-H.; Krings, M.; Bolm, C. *Angew. Chem., Int. Ed.* **2018**, *57*, 10723–10727. doi:10.1002/anie.201805778

38. Cheng, H.; Hernández, J. G.; Bolm, C. *Org. Lett.* **2017**, *19*, 6284–6287. doi:10.1021/acs.orglett.7b02973

39. Cheng, H.; Hernández, J. G.; Bolm, C. *Adv. Synth. Catal.* **2018**, *360*, 1800–1804. doi:10.1002/adsc.201800161

40. Hermann, G. N.; Bolm, C. *ACS Catal.* **2017**, *7*, 4592–4596. doi:10.1021/acscatal.7b00582

41. Hermann, G. N.; Jung, C. L.; Bolm, C. *Green Chem.* **2017**, *19*, 2520–2523. doi:10.1039/c7gc00499k

42. Yu, J.; Yang, X.; Wu, C.; Su, W. *J. Org. Chem.* **2020**, *85*, 1009–1021. doi:10.1021/acs.joc.9b02951

43. Rightmire, N. R.; Hanusa, T. P. *Dalton Trans.* **2016**, *45*, 2352–2362. doi:10.1039/c5dt03866a

44. Juribašić, M.; Užarević, K.; Gracin, D.; Ćurić, M. *Chem. Commun.* **2014**, *50*, 10287–10290. doi:10.1039/c4cc04423a

45. Bjelopetrović, A.; Lukin, S.; Halasz, I.; Užarević, K.; Đilović, I.; Barišić, D.; Budimir, A.; Juribašić Kulcsár, M.; Ćurić, M. *Chem. – Eur. J.* **2018**, *24*, 10672–10682. doi:10.1002/chem.201802403

46. Bjelopetrović, A.; Robić, M.; Halasz, I.; Babić, D.; Juribašić Kulcsár, M.; Ćurić, M. *Organometallics* **2019**, *38*, 4479–4484. doi:10.1021/acs.organomet.9b00626

47. Hernández, J. G.; Bolm, C. *Chem. Commun.* **2015**, *51*, 12582–12584. doi:10.1039/c5cc04423e

48. Ghanbari, N.; Ghafuri, H.; Esmaili Zand, H. R.; Eslami, M. *SynOpen* **2017**, *1*, 143–146. doi:10.1055/s-0036-1590959

49. Liu, Z.; Xu, H.; Wang, G.-W. *Beilstein J. Org. Chem.* **2018**, *14*, 430–435. doi:10.3762/bjoc.14.31

50. Bera, S. K.; Mal, P. *J. Org. Chem.* **2021**, *86*, 14144–14159. doi:10.1021/acs.joc.1c01742

51. Barišić, D.; Halasz, I.; Bjelopetrović, A.; Babić, D.; Ćurić, M. *Organometallics* **2022**, *41*, 1284–1294. doi:10.1021/acs.organomet.1c00698

52. Ma, X.-T.; Tian, S.-K. *Adv. Synth. Catal.* **2013**, *355*, 337–340. doi:10.1002/adsc.201200902

53. Kalyani, D.; Dick, A. R.; Anani, W. Q.; Sanford, M. S. *Tetrahedron* **2006**, *62*, 11483–11498. doi:10.1016/j.tet.2006.06.075

54. de Figueiredo, R. M.; Suppo, J.-S.; Campagne, J.-M. *Chem. Rev.* **2016**, *116*, 12029–12122. doi:10.1021/acs.chemrev.6b00237

55. Xu, X.-J.; Amuti, A.; Wusiman, A. *Adv. Synth. Catal.* **2020**, *362*, 5002–5008. doi:10.1002/adsc.2020000796

56. Caristi, C.; Ferlazzo, A.; Gattuso, M. *J. Chem. Soc., Perkin Trans. 1* **1984**, 281–285. doi:10.1039/p19840000281

57. Bjelopetrović, A.; Barišić, D.; Duvnjak, Z.; Džajić, I.; Juribašić Kulcsár, M.; Halasz, I.; Martínez, M.; Budimir, A.; Babić, D.; Ćurić, M. *Inorg. Chem.* **2020**, *59*, 17123–17133. doi:10.1021/acs.inorgchem.0c02418

License and Terms

This is an open access article licensed under the terms of the Beilstein-Institut Open Access License Agreement (<https://www.beilstein-journals.org/bjoc/terms>), which is identical to the Creative Commons Attribution 4.0 International License

(<https://creativecommons.org/licenses/by/4.0/>). The reuse of material under this license requires that the author(s), source and license are credited. Third-party material in this article could be subject to other licenses (typically indicated in the credit line), and in this case, users are required to obtain permission from the license holder to reuse the material.

The definitive version of this article is the electronic one which can be found at:

<https://doi.org/10.3762/bjoc.18.69>



A trustworthy mechanochemical route to isocyanides

Francesco Basocci[†], Federico Cuccu[†], Federico Casti, Rita Mocci, Claudia Fattuoni and Andrea Porcheddu^{*}

Full Research Paper

Open Access

Address:

Dipartimento di Scienze Chimiche e Geologiche, Università degli Studi di Cagliari, Cittadella Universitaria, Monserrato, 09042 Cagliari, Italy

Email:

Andrea Porcheddu^{*} - porcheddu@unica.it

* Corresponding author † Equal contributors

Keywords:

green chemistry; isocyanide; isonitriles; mechanochemistry

Beilstein J. Org. Chem. **2022**, *18*, 732–737.

<https://doi.org/10.3762/bjoc.18.73>

Received: 05 April 2022

Accepted: 10 June 2022

Published: 22 June 2022

This article is part of the thematic issue "Mechanochemistry III".

Guest Editors: J. G. Hernández and L. Borchardt

© 2022 Basocci et al.; licensee Beilstein-Institut.

License and terms: see end of document.

Abstract

Isocyanides are hardly produced, dramatically sensitive to purification processes, and complex to handle as synthetic tools. Notwithstanding, they represent one of the most refined and valuable compounds for accessing sophisticated and elegant synthetic routes. A unique interest has always been addressed to their production, though their synthetic pathways usually involve employing strong conditions and toxic reagents. The current paper intends to provide a conceptually innovative synthetic protocol for mechanochemical isocyanide preparation, simultaneously lowering the related reagents' toxicity and improving their purification in a straightforward procedure.

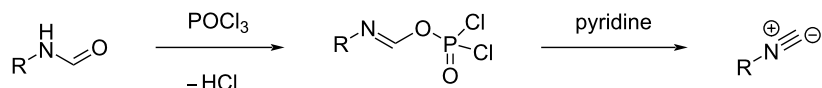
Introduction

Isocyanides were first discovered more than a century ago by Lieke in Göttingen after having handled allyl iodide and potassium cyanide to synthesize crotonic acid. This attempt, instead, brought to the accidental synthesis of an isocyanide which was recognizable by its revolting smell, as reported by Lieke [1]. A deepening of the topic arrived, though, only in the following century, when a natural and potential pharmaceutical compound was discovered, namely xanthocillin [2]. Finally, after two decades, the first synthetic approaches were reported by Ugi and Hofmann (Scheme 1) [3,4], who described their characteristic odour as “horrible” and “extremely distressing”. With such a breakthrough, isonitriles gained wide popularity in organic synthesis due to their extreme versatility [5–7]. Espe-

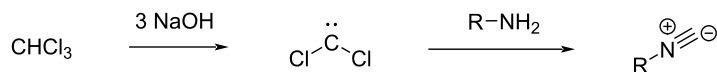
cially, they are often used in heterocycles formation [8,9], multicomponent strategies [10,11], polymers production [12,13], and metal complexation [14,15].

The molecular structure is composed of an N–C planar triple bond where the nitrogen atom assumes a positive charge due to the fourth bond with a carbon chain, which could be aliphatic or aromatic. In contrast, the carbon of the functional group bears a negative localized charge [16]. Apparently unstable and unreasonable, this is the most likely and plausible resonance structure because the other hypothesised form, where the carbenic counterpart does not respect the octet rule, is less favoured (Figure 1).

Ugi synthetic route



Hofmann synthetic route



Scheme 1: Historic synthetic approaches.

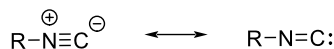


Figure 1: Resonance forms of isocyanides.

The synthetic approaches to this core are multiple, but numerous drawbacks severely limit their output. Common pathways generally involve formamides; one of the most known is Ugi's method [17] which is based on the dehydration of a primary formamide with POCl_3 in the presence of a base. Apart from phosphorus-mediated compounds, phosgene or diphosgene [18] work well, despite being still affected by the same limitations of POCl_3 . Therefore, organic chemists decided to move to other safer shores, so different dehydrating agents were also proposed. Tosyl chloride [19,20] and TCT (1,3,5-trichlorotriazine) [21] proved to be valuable alternatives to the aforementioned phosphorous compounds due to their powerful dehydrating ability. Lastly, Burgess reagent has been reported as a mild and selective dehydrating compound for formamides [22,23]. As we previously mentioned, the Hofmann isocyanide synthesis is a historical approach which our group revised mechanically [24]. Following this line, an eco-friendlier Ugi's isocyanide synthesis will be depicted in this article (Scheme 2).

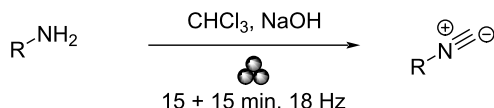
Results and Discussion

At the beginning of this project, we envisioned the feasibility of producing isocyanides from primary formamides by using anhydrides as dehydrating agents. Therefore, we focused our attention on acetic, trifluoroacetic, and isatoic anhydrides to achieve this. First attempts were made on acetic and trifluoroacetic anhydrides. The best results were obtained when a stoichiometric ratio between the anhydride and the reference compound, *N*-benzylformamide (**1f**), was milled with 2 equivalents of triethylamine or *N*-methylimidazole as bases. Despite slightly performing as a method, the reaction mixture was "too liquid" for running a mechanochemical reaction. This is why a solid anhydride, like the isatoic one, captured our interest, but unfortunately, the results were unsatisfying.

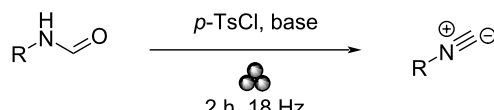
A second idea relied on traditional coupling reagents, especially carbodiimides (DIC and DCC) [25] and CDI [26-29]. The former should generate a urea derivative whilst the latter should produce CO_2 and imidazole as byproducts. In both cases, the reaction driving force is the production of thermodynamically stable products. However, they did not bring any advantage compared to acetic anhydride. Considering that CDI is activated in an acid environment, adding a catalytic amount of NaHSO_4 was necessary. Since isocyanides are sensitive to acids, this approach was ruled out a priori. Aware of these issues, we were discouraged from employing *p*-tosylimidazole as well, since it requires acid activation to be effective as a dehydrating agent.

Accordingly, we moved our interest to DIC and DCC compounds, used in stoichiometric quantity and in the presence of 1 equivalent of NEt_3 . Unfortunately, their use formed the desired product only in traces, so we finally decided to converge our efforts on the use of tosyl chloride as previously reported [19,30]. We found in it the most suitable agent for synthesising isocyanides when combined with a basic milieu. Among the immense variety of compounds that can be employed as bases, only a few are reported to catalyse such a process: pyridine [31] and triethylamine [32] are the most repre-

mechanochemical Hofmann reinterpretation (previous work)



mechanochemical Ugi reinterpretation (this work)



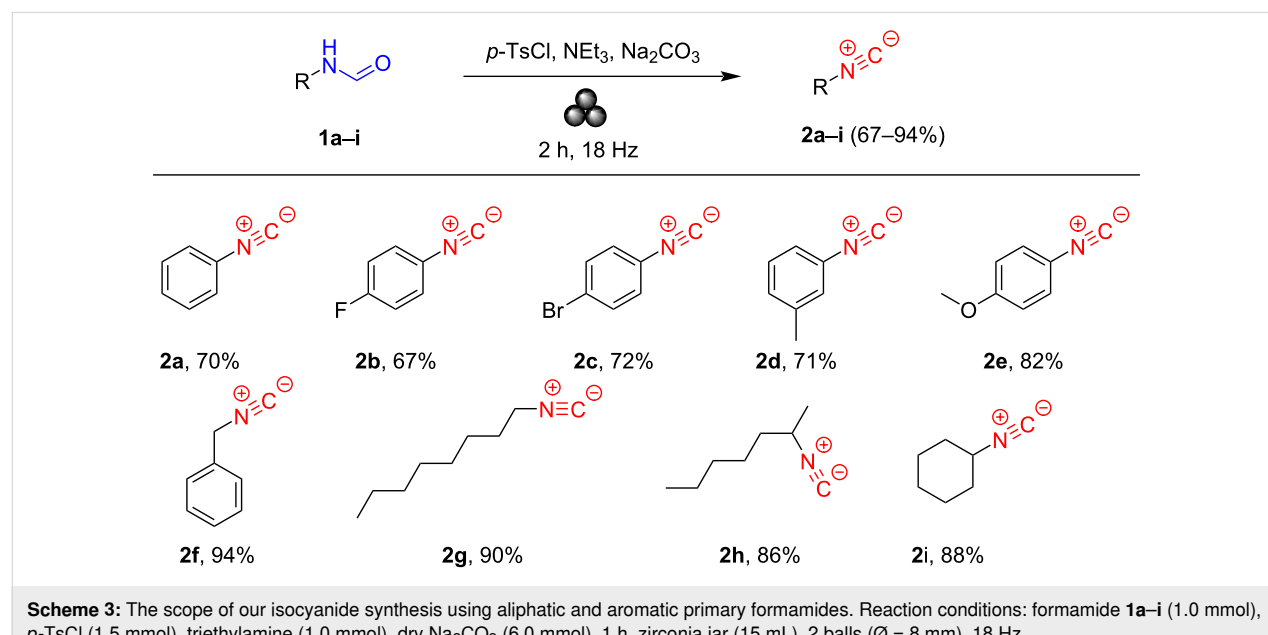
Scheme 2: Comparison between the previous mechanochemical synthetic pathway [24] and the new adapted one in this work.

sentative ones. Their reactivity can be attributed to their probable reaction mechanism where the nitrogen atom not only promotes the enolate derivative formation as already described in literature [33,34] but it may also generate a positively charged intermediate at the transition state [35], enhancing the nucleophilic substitution. Obviously, pyridine handling is associated with many risks, mainly concerning human health [36]. Consequently, our idea was to substitute pyridine with *N*-methylimidazole because their basicity and physical state are analogous. When the reactions between the formamide and different equivalents (from 1 to 6) of *N*-methylimidazole were carried out, the outcomes were not as good as those already documented with pyridine in the literature. Possible explanations for this phenomenon are either a different electronic distribution between the two heterocycles or the absence of intermolecular interactions caused by the solvent.

The association of triethylamine, *p*-tosyl chloride, and **1f** gave the best results, so, following this trend, we started the optimisation process. First attempts involved a 1:1:2 ratio between formamide **1f**, *p*-tosyl chloride, and triethylamine which resulted in an approximately 40% yield of isocyanide **2f** (GC–MS analysis). Unexpectedly, the addition of Lewis acids, namely LiCl and $\text{BF}_3\cdot\text{Et}_2\text{O}$, did not improve the enolate generation. The next step was searching the optimal conditions for a better conversion of **1f** in **2f**. These were found in the 1:2:7 ratios of the three components with the addition of 400 mg of NaCl as a grinding auxiliary (0.5 h, 36 Hz, Table S1 in Supporting Information File 1). So, we then looked for a solid base to use in place of triethylamine, avoiding the use of further additives. Unluckily, neither solid inorganic bases such Na, K, and

Cs carbonates [37], Mg and Ba oxides, nor organic bases like potassium *tert*-butoxide and imidazole proved to be as effective as triethylamine. Much to our surprise, we observed that the association between only 1 equivalent of triethylamine and 6 equivalents of sodium carbonate brought a good conversion rate of **1f** in **2f** at a frequency of 36 Hz after 1 h (70%, GC–MS analysis). Reducing the amount of sodium carbonate did not provide any advantage. Interestingly, using anhydrous sodium carbonate instead of its hydrated form improved reaction yields, likely due to the hydrolysis of tosyl chloride. With these data in hand, we then opted for refining other mechanochemical parameters such as frequency and reaction time. We attempted to emulate milder operating conditions as previously established in our paper [24] because of their high degradation rate [38] and instability [39]. Our idea found a match in the experimental data, confirming the total conversion of **1f** to **2f** after 1 h at 18 Hz.

With this comprehensive insight, we applied the described method to both aliphatic and aromatic substrates **1a–i** (Scheme 3). The conversion was almost complete for the aliphatic compounds **1f–i**, with yields from very high to excellent. On the other side, for the aromatic starting compounds **1a–e**, the reaction did not exceed the maximum of 82% yield obtained for **2e**. It should be emphasized that the preparation of aromatic isocyanides has always been a challenging process from a synthetic point of view. Such a different fashion can be ascribed to the diverse electronic distribution between aliphatic and aromatic formamides. Concerning aromatic amides, the presence of electron-withdrawing (EWG) or electron-donating groups (EDG) further affect the tautomeric equilibrium, promoting or



weakening the reactivity of the substrates. In this case, the yields are high for EDGs (**2d,e**), while from good to high for the EWGs (**2b,c**). To confirm what has been previously stated, isonitrile **2a** was recovered in lower yields than compound **2e** (Scheme 3).

At the end of the reaction, adding 0.5 equivalents of water for a 15 minute grinding step was necessary to hydrolyse the *p*-tosyl chloride excess. Our approach for the removal of the unreacted *p*-tosyl chloride was demonstrated to be the most feasible and eco-friendly compared with the reported techniques, which imply the use of cellulose with a large excess of pyridine [40] and the need for flash chromatography [41].

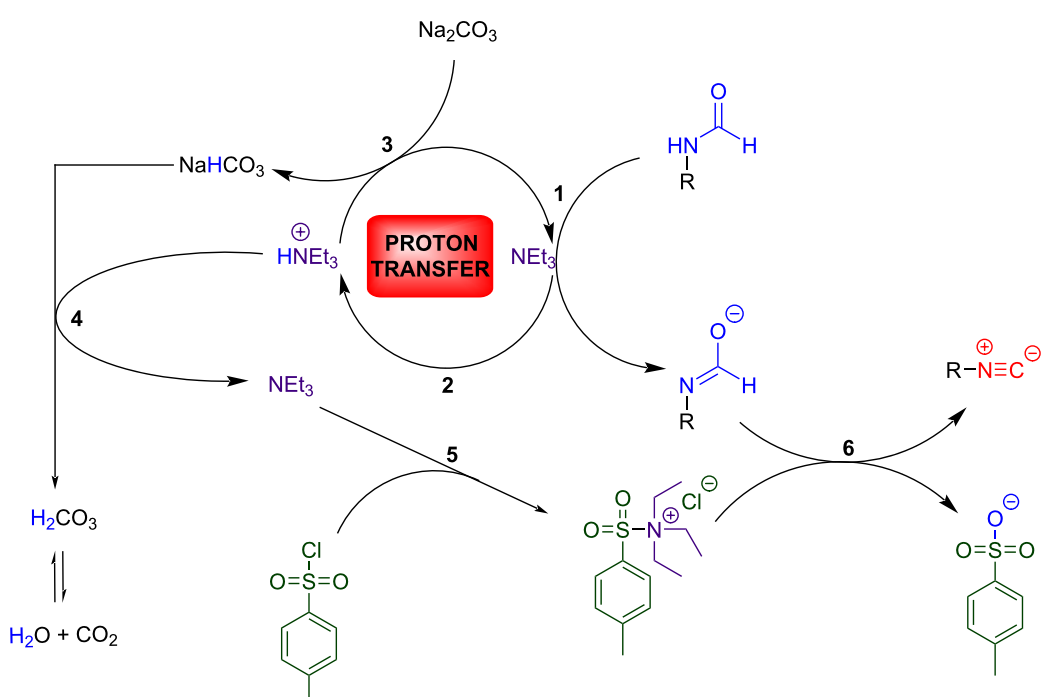
Afterwards, the mixture was recovered as a solid in a beaker, shredded in *n*-heptane, and filtered on paper. The organic solution only contained the desired product and various quantities of starting material, depending on the formamide employed. A short silica pad was then used to increase the isocyanide purity (Figure 2), even though, in some cases, a small amount of sulphonyl derivatives or solvent residues can be spotted. These little impurities are due to the isocyanide instability and difficulty in being held.

In light of what was said above, it makes sense to hypothesise a possible reaction mechanism (Scheme 4). The single equivalent of triethylamine should be able to activate



Figure 2: The purification process of a brownish isocyanide on a short silica pad.

the tautomerism of the formamide through an acid-base reaction [33,42-45]. The triethylammonium salt produced can be restored as triethylamine through the action of Na_2CO_3 . This proton transfer allows the formation of NaHCO_3 , which



Scheme 4: Suggested proton transfer mechanism.

should still be sufficiently basic for deprotonating again the regenerated ammonium species, releasing H₂O in the process.

Conclusion

Even though there is a tremendous interest in the synthesis of isocyanides, only few procedures have been developed since their discovery. Since so many troublesome downsides characterise them, any possible alternative synthetic route has been unfairly put aside. Nonetheless, we demonstrated the feasibility of their synthesis through a greener procedure employing cheap reagents such as sodium carbonate [46] and waste materials deriving from industry such as TsCl (mechanochemical approach: EcoScale → 81; E-Factor → 9.5; in-solution approach: EcoScale → 55; E-Factor → 131.1; see Supporting Information File 1 for more details) [47,48]. Not only did we plummet the reaction expenditures, but we also undoubtedly proved that our method could be entirely exerted in the solid phase through mechanochemical activation. In conclusion, we hope that our synthetic strategy could be considered a significant step toward a less impacting and more extensive research on isocyanide chemistry.

Supporting Information

Supporting Information File 1

Experimental.

[<https://www.beilstein-journals.org/bjoc/content/supplementary/1860-5397-18-73-S1.pdf>]

Acknowledgements

We acknowledge the CeSAR (Centro Servizi Ricerca d'Ateneo) core facility of the University of Cagliari and Dr. Sandrina Lampis for assistance with the generation of the ¹H and ¹³C NMR spectroscopic data.

Funding

This research was funded by MIUR Italy, PRIN 2017 project (grant number: 2017B7MMJ5_001) “MultiFunctional poLymer cOmposites based on groWn matERials (MIFLOWER) and Fondazione di Sardegna (FdS, F72F20000230007)

ORCID® IDs

Francesco Basocu - <https://orcid.org/0000-0002-5480-1044>
 Federico Cuccu - <https://orcid.org/0000-0003-1249-4856>
 Federico Casti - <https://orcid.org/0000-0002-0530-3700>
 Rita Mocci - <https://orcid.org/0000-0002-8249-9735>
 Claudia Fattuoni - <https://orcid.org/0000-0002-6956-7967>
 Andrea Porcheddu - <https://orcid.org/0000-0001-7367-1102>

Preprint

A non-peer-reviewed version of this article has been previously published as a preprint: <https://doi.org/10.3762/bxiv.2022.21.v1>

References

1. Lieke, W. *Ann. Chem. Pharm.* **1859**, *112*, 316–321. doi:10.1002/jlac.18591120307
2. Scheuer, P. J. *Acc. Chem. Res.* **1992**, *25*, 433–439. doi:10.1021/ar00022a001
3. Ugi, I.; Fetzer, U.; Eholzer, U.; Knupfer, H.; Offermann, K. *Angew. Chem., Int. Ed. Engl.* **1965**, *4*, 472–484. doi:10.1002/anie.196504721
4. Hofmann, A. W. *Grundlagen der organischen Chemie*; Verlag Sauerländer: Aarau, Switzerland, 1970.
5. El Kaïm, L.; Grimaud, L. *Eur. J. Org. Chem.* **2014**, 7749–7762. doi:10.1002/ejoc.201402783
6. El Kaïm, L.; Grimaud, L.; Patil, P. *Synlett* **2012**, *23*, 1361–1363. doi:10.1055/s-0031-1290939
7. Passerini, M.; Simone, L. *Gazz. Chim. Ital.* **1921**, *51*, 126–129.
8. Liu, N.; Chao, F.; Liu, M.-G.; Huang, N.-Y.; Zou, K.; Wang, L. *J. Org. Chem.* **2019**, *84*, 2366–2371. doi:10.1021/acs.joc.8b03242
9. Bienaymé, H.; Bouzid, K. *Tetrahedron Lett.* **1998**, *39*, 2735–2738. doi:10.1016/s0040-4039(98)00283-4
10. Leonardi, M.; Villacampa, M.; Menéndez, J. C. *Chem. Sci.* **2018**, *9*, 2042–2064. doi:10.1039/c7sc05370c
11. Rudick, J. G.; Shaabani, S.; Dömling, A. *Front. Chem. (Lausanne, Switz.)* **2020**, *7*, 918. doi:10.3389/fchem.2019.00918
12. Ramozzi, R.; Chéron, N.; Braïda, B.; Hiberty, P. C.; Fleurat-Lessard, P. *New J. Chem.* **2012**, *36*, 1137–1140. doi:10.1039/c2nj40050b
13. Arshady, R.; Zecca, M.; Corain, B. *React. Polym.* **1993**, *20*, 147–173. doi:10.1016/0923-1137(93)90090-3
14. Singleton, E.; Oosthuizen, H. E. *Adv. Organomet. Chem.* **1983**, *22*, 209–310. doi:10.1016/s0065-3055(08)60404-9
15. Bassett, J.-M.; Farrugia, L. J.; Stone, F. G. A. *J. Chem. Soc., Dalton Trans.* **1980**, 1789–1790. doi:10.1039/dt9800001789
16. Kessler, M.; Ring, H.; Trambarulo, R.; Gordy, W. *Phys. Rev.* **1950**, *79*, 54–56. doi:10.1103/physrev.79.54
17. Ugi, I.; Meyr, R. *Chem. Ber.* **1960**, *93*, 239–248. doi:10.1002/cber.19600930136
18. Weber, W. P.; Gokel, G. W.; Ugi, I. K. *Angew. Chem., Int. Ed. Engl.* **1972**, *11*, 530–531. doi:10.1002/anie.197205301
19. Okada, I.; Kitano, Y. *Synthesis* **2011**, 3997–4002. doi:10.1055/s-0031-1289592
20. Stephens, C. R.; Bianco, E. J.; Pilgrim, F. J. *J. Am. Chem. Soc.* **1955**, *77*, 1701–1702. doi:10.1021/ja01611a102
21. Porcheddu, A.; Giacomelli, G.; Salaris, M. *J. Org. Chem.* **2005**, *70*, 2361–2363. doi:10.1021/jo047924f
22. Creedon, S. M.; Crowley, H. K.; McCarthy, D. G. *J. Chem. Soc., Perkin Trans. 1* **1998**, 1015–1018. doi:10.1039/a708081f
23. Rappai, J. P.; Karthikeyan, J.; Prathapan, S.; Unnikrishnan, P. A. *Synth. Commun.* **2011**, *41*, 2601–2606. doi:10.1080/00397911.2010.515333
24. Mocci, R.; Murgia, S.; De Luca, L.; Colacino, E.; Delogu, F.; Porcheddu, A. *Org. Chem. Front.* **2018**, *5*, 531–538. doi:10.1039/c7qo01006k

25. Marquarding, D.; Gokel, G.; Hoffman, P.; Ugi, I. *Isonitrile Chemistry*; Academic Press: New York, NY, USA, 1971; p 133.
doi:10.1016/b978-0-12-706150-4.50012-5

26. Armstrong, A.; Li, W. *N,N'-Carbonyldiimidazole. Encyclopedia of Reagents for Organic Synthesis*; John Wiley & Sons, 2007.
doi:10.1002/9780470842898.rc024.pub2

27. Métro, T.-X.; Martinez, J.; Lamaty, F. *ACS Sustainable Chem. Eng.* **2017**, *5*, 9599–9602. doi:10.1021/acssuschemeng.7b03260

28. Konnert, L.; Gonnet, L.; Halasz, I.; Suppo, J.-S.; de Figueiredo, R. M.; Campagne, J.-M.; Lamaty, F.; Martinez, J.; Colacino, E. *J. Org. Chem.* **2016**, *81*, 9802–9809. doi:10.1021/acs.joc.6b01832

29. Métro, T.-X.; Bonnamour, J.; Reidon, T.; Duprez, A.; Sarpoulet, J.; Martinez, J.; Lamaty, F. *Chem. – Eur. J.* **2015**, *21*, 12787–12796. doi:10.1002/chem.201501325

30. Hoy, D. J.; Poziomek, E. J. Isocyanide Synthesis. *US Army Edgewood Arsenal Chemical Research and Development Laboratories Technical Report*; Edgewood Arsenal: Maryland, USA, 1965.

31. Waibel, K. A.; Nickisch, R.; Möhl, N.; Seim, R.; Meier, M. A. R. *Green Chem.* **2020**, *22*, 933–941. doi:10.1039/c9gc04070f

32. Patil, P.; Ahmadian-Moghaddam, M.; Dömling, A. *Green Chem.* **2020**, *22*, 6902–6911. doi:10.1039/d0gc02722g

33. Shipilovskikh, S. A.; Vaganov, V. Y.; Denisova, E. I.; Rubtsov, A. E.; Malkov, A. V. *Org. Lett.* **2018**, *20*, 728–731.
doi:10.1021/acs.orglett.7b03862

34. Appel, R.; Kleinstueck, R.; Ziehn, K.-D. *Chem. Informationsdienst, Org. Chem.* **1971**, *2*, 25.
doi:10.1002/chin.197125230

35. Zarchi, M. A. K.; Aslani, M. J. *Appl. Polym. Sci.* **2012**, *124*, 3456–3462.
doi:10.1002/app.35425

36. Yang, X.; Ding, X.; Zhou, L.; Fan, H.-h.; Wang, X.; Ferronato, C.; Chovelon, J.-M.; Xiu, G. *Water Res.* **2020**, *171*, 115378.
doi:10.1016/j.watres.2019.115378

37. Ortiz-Trankina, L. N.; Crain, J.; Williams, C.; Mack, J. *Green Chem.* **2020**, *22*, 3638–3642. doi:10.1039/d0gc01116a

38. Spallarossa, M.; Wang, Q.; Riva, R.; Zhu, J. *Org. Lett.* **2016**, *18*, 1622–1625. doi:10.1021/acs.orglett.6b00483

39. van der Heijden, G.; Jong, J. A. W.; Ruijter, E.; Orru, R. V. A. *Org. Lett.* **2016**, *18*, 984–987. doi:10.1021/acs.orglett.6b00091

40. Schoonover, D. V.; Gibson, H. W. *Tetrahedron Lett.* **2017**, *58*, 242–244. doi:10.1016/j.tetlet.2016.12.014

41. Morita, J.-i.; Nakatsui, H.; Misaki, T.; Tanabe, Y. *Green Chem.* **2005**, *7*, 711–715. doi:10.1039/b505345e

42. Ugi, I.; Meyr, R. *Chem. Ber.* **1960**, *93*, 239–248.
doi:10.1002/cber.19600930136

43. Ugi, I.; Meyr, R. *Angew. Chem.* **1958**, *70*, 702–703.
doi:10.1002/ange.19580702213

44. Wang, X.; Wang, Q.-G.; Luo, Q.-L. *Synthesis* **2015**, 49–54.
doi:10.1055/s-0034-1379111

45. Keita, M.; Vandamme, M.; Mahé, O.; Paquin, J.-F. *Tetrahedron Lett.* **2015**, *56*, 461–464. doi:10.1016/j.tetlet.2014.11.128

46. Thieme, C. Sodium Carbonates. *Ullmann's Encyclopedia of Industrial Chemistry*; John Wiley & Sons. doi:10.1002/14356007.a24_299

47. Tosyl Chloride. ECHA European Chemicals Agency.
<https://echa.europa.eu/it/substance-information/-/substanceinfo/100.002.441> (accessed March 31, 2022).

48. Ager, D. J.; Pantaleone, D. P.; Henderson, S. A.; Katritzky, A. R.; Prakash, I.; Walters, D. E. *Angew. Chem., Int. Ed.* **1998**, *37*, 1802–1817.
doi:10.1002/(sici)1521-3773(19980803)37:13/14<1802::aid-anie1802>3.0.co;2-9

License and Terms

This is an open access article licensed under the terms of the Beilstein-Institut Open Access License Agreement (<https://www.beilstein-journals.org/bjoc/terms>), which is identical to the Creative Commons Attribution 4.0 International License (<https://creativecommons.org/licenses/by/4.0>). The reuse of material under this license requires that the author(s), source and license are credited. Third-party material in this article could be subject to other licenses (typically indicated in the credit line), and in this case, users are required to obtain permission from the license holder to reuse the material.

The definitive version of this article is the electronic one which can be found at:

<https://doi.org/10.3762/bjoc.18.73>



Complementarity of solution and solid state mechanochemical reaction conditions demonstrated by 1,2-debromination of tricyclic imides

Petar Štrbac and Davor Margetić*§

Full Research Paper

Open Access

Address:

Ruder Bošković Institute, Bijenička cesta 54, HR-10002 Zagreb, Croatia

Email:

Davor Margetić* - margetid@irb.hr

* Corresponding author

§ Tel.: +385-1-468-0197; fax: +385-1-456-1008

Keywords:

ball milling; cycloaddition; debromination; Diels–Alder reaction; mechanochemistry

Beilstein J. Org. Chem. **2022**, *18*, 746–753.

<https://doi.org/10.3762/bjoc.18.75>

Received: 26 March 2022

Accepted: 15 June 2022

Published: 24 June 2022

This article is part of the thematic issue "Mechanochemistry III".

Guest Editors: J. G. Hernández and L. Borchardt

© 2022 Štrbac and Margetić; licensee Beilstein-Institut.

License and terms: see end of document.

Abstract

The solution phase 1,2-debromination of polycyclic imides using the Zn/Ag couple was successfully transferred to solid state mechanochemical conditions. The Zn/Ag couple was replaced by the Zn/Cu couple which was prepared without any metal activation by *in situ* ball milling of zinc and copper dusts. The advantage of the ball milling process is that the whole procedure is operationally very simplified. The reactive alkene generated was trapped *in situ* by several dienes and the respective Diels–Alder cycloadducts were obtained. It was demonstrated that mechanochemical milling offers complementary conditions to solution (thermal) reaction by allowing chemical transformations to proceed which were not possible in solution and vice versa.

Introduction

The complementarity of reaction conditions [1–3] where the reaction takes place under some, but not under other conditions, or where a chemical reaction proceeds in a different way or mechanism is a useful feature in synthetic organic chemistry. Advantageously, more difficult substrates or limitations of the conditions can be overcome by the change of the reaction methods. One of the emerging synthetic methods is mechanochemistry [4–7], a greener alternative to carry out synthesis which complements heating, irradiation and electrochemistry as methods of chemical activation [8]. Based upon our

experience in applications of this method to organic synthesis [9–12], we recognized its potential for the adjustment of conditions in zinc-mediated debromination reactions.

Highly reactive dienophiles such as polycyclic molecules given in Figure 1 are interesting reactive intermediates which could be applied in the Diels–Alder reactions of less reactive or thermally susceptible dienes. Often, these are generated *in situ* and trapped with dienes in a single pot, such as 7-oxanorbornadiene imides **1–3**. For instance, a synthetic methodology for the prep-

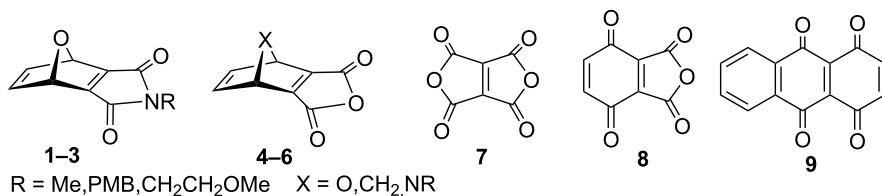


Figure 1: Highly reactive dienophiles.

aration of **1–3** was developed by Warrener and co-workers by a Zn/Ag couple debromination [13–15]. However, this methodology has some disadvantages, such as tedious preparation of the catalyst, the use of dry solvent and expensive silver acetate as well as side-reactions with solvent.

An alternative method for the synthesis 7-oxanorbornadiene-2,3-anhydrides and imides is via retro Diels–Alder reaction employing the flash vacuum pyrolysis (FVP) technique [16]. However, the FVP also has disadvantages such as limited scope of functionalities which can withstand harsh conditions (temperature) and the inability to control the elimination process [17].

The objective of this work was to establish whether the 1,2-debromination with the Zn/Ag couple could be carried out under solvent-free conditions in a ball mill and whether the tedious Zn/Ag couple preparation procedure [18] could be simplified by *in situ* generation of the catalyst. Moreover, in the debromination of norbornene imide **11**, the expected Diels–Alder adduct with furan was not obtained, but compound **12** incorporating a tetrahydrofuran ring at position 2, presumably by radical reaction (Figure 2) [19,20]. We envisaged that the absence of solvent under mechanochemical conditions should prevent the formation of products from tetrahydrofuran and therefore allow cycloaddition to take place.

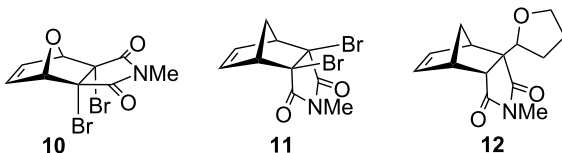


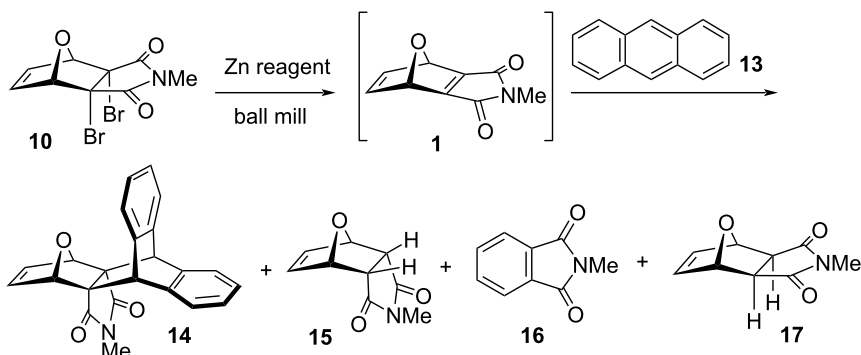
Figure 2: Dibromide substrates and product **12**.

Results and Discussion

Reaction optimization

Anthracene addition to dibromide **10** (Scheme 1) was used as the model reaction. Along with cycloadduct **14**, three known side-products were obtained: *endo*-product **15** (hydrogenolysed inverted **10**), *N*-methylphthalimide (**16**) and **17** (hydrogenolysed **10**). Their ratio varied with the reaction conditions (Supporting Information, Table S1) and results of the optimizations are collected in Table 1.

The results of the optimization experiments showed that the solution reaction conditions could be transferred to mechanochemical conditions without significant loss of reactivity and identical side-products were formed. Initial experiments were performed with the Zn/Ag couple prepared by a usual procedure from Zn and silver acetate. Several simplifications of the Zn/Ag couple preparation were tested and showed that simple



Scheme 1: Mechanochemical reaction of **10** with anthracene.

Table 1: Optimization of reaction conditions for reaction of **10** with anthracene.^a

Entry	Catalyst	Additives	Time [h]	Conversion ^b	Yield 14 [%] ^c
1	Zn/Ag couple		0.5	81	2
2	Zn/Ag couple	NaCl	0.5	quant	8
3	Zn/Ag couple	LAG THF	0.5	quant	58
4	Zn/Ag couple	LAG THF, NaCl	0.5	96	33
5	Zn dust, Ag wire		0.5	NR ^d	
6	Zn dust, Ag wire	LAG THF	0.5	33	27
7	Zn dust, Ag wire	LAG MeOH	1	quant	64
8	Zn dust, Ag wire	LAG MeCN	1	88	63
9	Zn activ., Ag wire	LAG THF, NaCl	0.5	quant	56
10	Zn dust, silvergal		0.5	NR	
11	Zn dust, silvergal	LAG THF	1	50	40
12	Zn activated		0.5	NR	
13	Zn dust		0.5	NR	
14	Zn dust	LAG THF	0.5	12	4
15	Zn dust, Cu dust	LAG THF	0.5	55	50
16	Zn dust, Cu dust	LAG THF	0.75	97	64
17	Zn dust, Cu dust	LAG THF ZnBr ₂	1	quant	67
18	Zn dust, Cu dust	LAG THF ^e	1	66	48
19	Zn dust, Cu dust	LAG THF^e	2	quant	76 (42)
Reactions in solution		Solvent			
20	Zn/Ag couple	dry THF, Ar	1	quant	86
21	Zn dust, Cu dust	dry THF	1	NR	
22	Zn dust, Cu dust	THF, ultrasound	1.5	NR	

^aRetsch MM400, 30 Hz, stainless steel 10 mL, one 12 mm SS ball; dibromide (50 mg); anthracene (132 mg, 5 equiv); reducing agent/catalyst (75 mg); silvergal = Ag/Cu powder 70% Ag; LAG THF η = 0.66 $\mu\text{L}\cdot\text{mg}^{-1}$; ^bNMR analysis; ^cNMR yields, isolated yield in parentheses; ^dNR = no reaction;

^eLAG THF η = 0.33 $\mu\text{L}\cdot\text{mg}^{-1}$.

milling with Zn dust and Ag dust or wire can be also applied (Table 1, entries 5–8) [21]. Further improvement in the procedure was the replacement of the Ag dust with Cu dust. This combination of metals worked well, and the best conditions were obtained with the addition of a small amount of THF (liquid assisted grinding, LAG) [22], η = 0.5 $\mu\text{L}\cdot\text{mg}^{-1}$ (Table 1, entry 19). In contrast, the solution reaction catalyzed by Zn/Cu dust was totally ineffective (Table 1, entry 21), even with the agitation by ultrasound (Table 1, entry 22). The ratios of side-products vary depending on the reaction conditions (Table S1, Supporting Information File 1). The *endo*-product **15** was dominant in the neat grinding experiment (Table 1, entry 1), whereas phthalimide **16** dominates when NaCl was employed as grinding auxiliary (Table 1, entries 2 and 4). The addition of ZnBr₂ (which is formed in the reaction and postulated that it could facilitate the oxa-ring opening of **15** to **16**) [13] did not notably increase the amount of phthalimide, indicating that rather deoxygenation leading to **16** is facilitated by the Zn/Cu couple [23]. When LAG THF reactions were carried out without anthracene, **15** was major product, whereas **16** is the major

product in LAG MeOH milling (Supporting Information File 1, Table S1).

Scope of the reaction

With the optimized conditions established, the scope of the reaction and its synthetic utility were investigated employing various dienes such as furan (**18**), 1,3-diphenylisobenzofuran (**24**) (DPIBF) and substituted anthracenes **31**, **36** and **39** (Figure 3). Exclusive norbornene *exo*- π selectivity [24] was observed in all cycloaddition reactions.

Selected five-membered dienes were subjected to established the Zn/Cu mechanochemical conditions (Figure 3). The furan reaction under ball milling conditions led to a mixture of *exo,exo*- and *exo,endo*-cycloadducts **19** and **20** in a 0.8:1 ratio. This is in contrast to classical conditions with the Zn/Ag couple in THF, where the ratio is different (0.6:1), and slightly more in favor of the unsymmetrical adduct **20**. On the other hand, the reaction of cyclopentadiene (**21**) provided the linear *exo,exo*-cycloadduct **22** as the major product, together with the 2:1

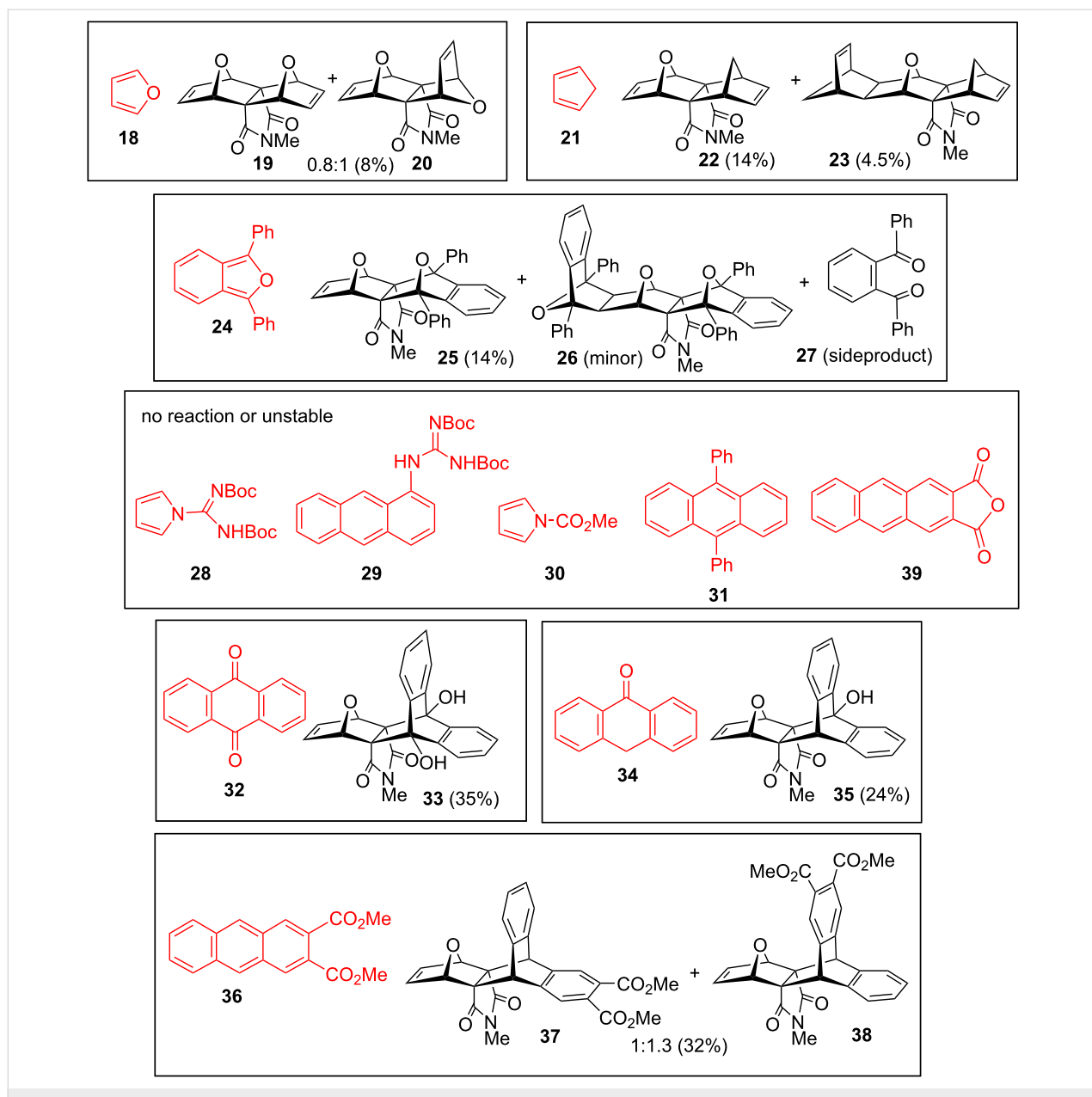


Figure 3: Scope of the Zn/Cu reaction with dibromide **10** (dienes are colored in red).

adduct **23**. In this reaction, identical stereospecificity was obtained by employment of the Zn/Ag couple in THF [19].

Linear *exo,exo*-product **25** was obtained exclusively in the reaction with DPIBF **24**, which is in accordance to the stereospecificity of cycloadditions reported by Sasaki [25] where the linear adduct is greatly preferred over bent. An interesting feature of the ¹H NMR spectrum is the very low-field position of the phenyl protons (8.15 ppm), not common for DPIBF adducts with 7-oxanorbornenes (usually below 8 ppm) [26,27]. Double adduct **26** was detected as minor product (evidenced by the lack of olefinic and presence of the *endo* protons at 2.64 ppm),

whereas the DPIBF sideproduct in this reaction is 1,2-dibenzoylbenzene (**27**). The mechanism for the formation of **27** from DPIBF is not elucidated, but we confirmed that the reaction does not proceed by milling of DPIBF with Zn/Cu dust alone, indicating that the presence of the dibromide substrate is essential. Product **27** was also found in the reaction of bicyclo[2.2.2]dibromide **42** (Scheme 3), which suggests that the mechanism may involve radical anion intermediates. This result further supports a single electron transfer (SET) and radical anion mechanism which was postulated earlier for the Zn/Ag debromination reaction and was supported by a CH₃OD trapping experiment [13]. Thus, DPIBF in this reaction acts both as

Diels–Alder trap reagent for reactive alkene [28] as well as radical anion quencher [29,30].

The *N,N*-Boc-protected *N*-amidinylpyrrole **28** [31] and 1-guanidinoanthracene (**29**) [10,32] have functional groups which were not tolerated under the debromination conditions and intractable mixtures of products were obtained. Carbomethoxypyrrrole (**30**) was less susceptible to the reaction conditions, but unreactive. In these reactions, *N*-methylphthalimide (**16**) was obtained as the major product.

Interestingly, when 9,10-diphenylanthracene (**31**) was subjected to milling with **10**, the expected cycloadduct was not detected and **31** has remained unchanged, indicating its lower reactivity in comparison to anthracene (presumably due to steric reasons [33], the presence of phenyl substituents at reacting carbons). Instead, small amounts of another cycloadduct were obtained. It was found that this is the product arising from anthraquinone (**32**), which was present as an impurity in **31**. Independent milling of **10** with anthraquinone afforded dihydroxy cycloadduct **33** (in 35% yield) indicating that in the reaction conditions of the anthraquinone \leftrightarrow 9,10-dihydroxyanthracene (DHA) equilibrium is shifted towards DHA [34,35]. To prove this premise, anthraquinone alone was ball milled, however, unreacted material was recovered and the formation of 9,10-dihydroxyanthracene was not spectroscopically detected. An analogous hydroxy adduct **35** was produced in the reaction with anthrone (**34**). When the reaction of anthraquinone was carried in THF solution (reflux, 1 h), dibromide **10** remained unchanged. However, a small amount of **33** was formed in refluxing THF by the use of the Zn/Ag couple in the case of anthraquinone. These results indicate that the Zn/Cu catalyst in solid state is much more effective than Zn/Cu or Zn/Ag in THF solution, and that ball milling offers different reaction outcomes and as such complements solution chemistry.

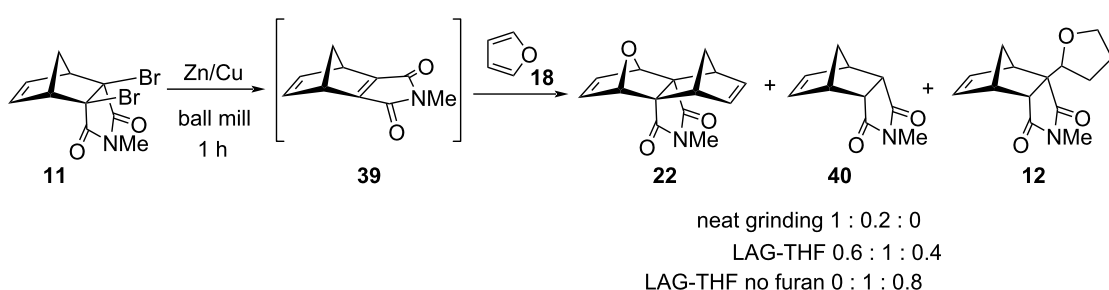
The reaction with 2,3-dicarbomethoxyanthracene (**36**) afforded two isomeric cycloadducts **37** and **38** in a 1:1.3 ratio (inseparable mixture, 32% overall yield). The minor isomer has a linear

structure with carbomethoxy groups in the equatorial plane as depicted for **37**, whereas in the major isomer **38** the carbomethoxy groups are positioned in axial plane of the molecule. The bent structure of **38** was established by ¹H NMR analysis and comparison with product **10**. The most indicative signals are of *N*-methyl groups, which are at an almost identical position for the bent isomer **38** (2.36 ppm), as in products **10** and **33** (2.38 and 2.37 ppm, respectively). The chemical shift of the NMe group in linear product **36** is affected by anthracene carbomethoxy 2,3-substituents and is shifted towards lower magnetic field (2.42 ppm). Furthermore, the highest lying aromatic multiplet of **38** is similarly positioned as for **10** (7.06 and 7.08 ppm, respectively), whereas the chemical shift of the methyl ester groups in **38** is closer to the starting anthracene **36** (3.87 ppm and 3.85 ppm in **38** and **37** vs 3.97 ppm in **36**). When 2,3-anthracene anhydride (**39**) was subjected to ball milling, a complex mixture of products was obtained, indicating that the anhydride functionality is not compatible to the reaction conditions.

Product **22** could be also obtained by cycloaddition parity reversal principle [16,36], employing norbornene dibromide **11** and furan (**18**). Ball milling reaction without THF (neat grinding) provided **22** as the major product, together with a minor amount of dehalogenated product **40** (Scheme 2). When THF was added for LAG, milling again gave **22**, but it was accompanied with a larger amount of **40** and some side-product **12**. A control LAG milling experiment without furan led to **40** and a significant amount of **12**. These experiments emphasize the complementarity of ball milling conditions with solution chemistry (in solution, only THF side-product **12** was obtained). Interestingly, small amounts of THF (used for LAG) were not detrimental for the reaction outcome in ball mill.

The bicyclo[2.2.2] system

Besides the bicyclo[2.2.1] system (7-oxa or 7-methano), the reactivity of the bicyclo[2.2.2] moiety was investigated. Dibromide **42** was prepared by Diels–Alder reaction of anthracene (**13**) and 2,3-dibromo-*N*-methylmaleimide (**41**) (Scheme 3).



Scheme 2: Mechanocatalytic reaction of **11** with furan.

Heating of the reactants at 180 °C for 10 min provided the required cycloadduct **42** (98% yield). When **42** was subjected to Zn/Cu debromination in a ball mill in the presence of anthracene (conditions a), imide **44** was the major product accompanied by a small amount of janusene imide derivative **45** (7:1 ratio). The formation of the intermediate alkene **43** was observed spectroscopically only in the milling reaction of **42** alone (an indicative ¹H NMR signal of bicyclo[2.2.1] moiety at 5.28 ppm). Cycloreversion side-reaction in mechanochemical conditions [37] was noticed for dibromide **42**, which led to mixtures consisting some janusene **45**. Thus, milling of **42** with Zn/Cu without anthracene (**13**) (conditions b) provided a mixture of **43/44/45/anthracene** in a 1:5:1:2 ratio) and milling of **42** alone without metal dust (conditions c) gave anthracene. Furthermore, alkene trapping with DPIBF provided 1:1 cycloadduct **46** as a single isomer (possessing linear structure as indicated by ¹H NMR chemical shift of methyl group at 1.96 ppm). There is a large up-field shift of two aromatic protons of the anthracene moiety (6.31 ppm) arising from the magnetic shielding of phenyl groups. Analogously to the reaction of DPIBF with **10** (Figure 3), 1,2-dibenzoylbenzene (**27**) was found in the reaction mixture (Scheme 3). Starting from **42** in identical mechanochemical conditions, furan cycloadduct **14** was not formed, just **43** and **44** (6:1 ratio) and anthracene (**13**) were obtained. Our results demonstrate that the bicyclo[2.2.2] system is less reactive in comparison to the 7-oxabicyclo[2.2.1] system. Ball milling did not provide any cycloadduct even in the presence of 20-fold molar excess of furan and the alterna-

tive synthetic route (cycloaddition parity reversal) [16,17] for **14** was not viable.

Conclusion

The 1,2-debromination reactions employing the Zn/Ag couple could be effectively carried out in a ball mill, with advantageous employment of the Zn/Cu couple prepared in situ, avoiding the use of dry solvent precautions and tedious Zn/Ag couple preparation, in a simple procedure. It is an example of organic reactions in solution that could be transferred to greener conditions. The reaction works in some instances when classical conditions failed, and as such it offers a complementary synthetic approach towards required molecules.

Supporting Information

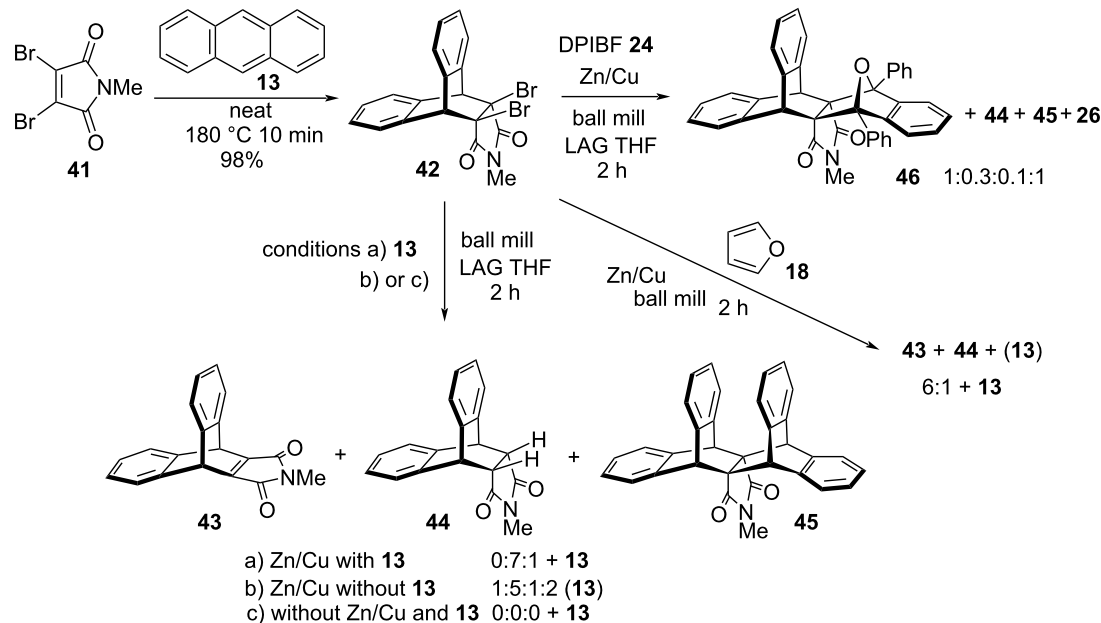
Supporting Information File 1

Details of experimental procedures and characterization data of selected compounds.

[<https://www.beilstein-journals.org/bjoc/content/supplementary/1860-5397-18-75-S1.pdf>]

Funding

This work is funded by the Croatian Science Foundation (grant No. IP-2018-01-3298, Cycloaddition strategies towards polycyclic guanidines (CycloGu)). Poster presented at the ACS 25th



Scheme 3: Reactivity of bicyclo[2.2.2] dibromide **42** with dienes.

Annual Green Chemistry & Engineering Conference, June 14–18, 2021.

ORCID® IDs

Petar Štrbac - <https://orcid.org/0000-0001-7410-744X>
Davor Margetić - <https://orcid.org/0000-0002-1039-6569>

References

- McAtee, R. C.; McClain, E. J.; Stephenson, C. R. J. *Trends Chem.* **2019**, *1*, 111–125. doi:10.1016/j.trechm.2019.01.008
- Sambagio, C.; Noël, T. *Trends Chem.* **2020**, *2*, 92–106. doi:10.1016/j.trechm.2019.09.003
- Wallace, S.; Balskus, E. P. *Curr. Opin. Biotechnol.* **2014**, *30*, 1–8. doi:10.1016/j.copbio.2014.03.006
- James, S. L.; Adams, C. J.; Bolm, C.; Braga, D.; Collier, P.; Friščić, T.; Grepioni, F.; Harris, K. D. M.; Hyett, G.; Jones, W.; Krebs, A.; Mack, J.; Maini, L.; Orpen, A. G.; Parkin, I. P.; Shearouse, W. C.; Steed, J. W.; Waddell, D. C. *Chem. Soc. Rev.* **2012**, *41*, 413–447. doi:10.1039/c1cs15171a
- Wang, G.-W. *Chem. Soc. Rev.* **2013**, *42*, 7668–7700. doi:10.1039/c3cs35526h
- Stolle, A.; Ranu, B., Eds. *Ball Milling Towards Green Synthesis: Applications, Projects, Challenges*; Green Chemistry Series, Vol. 31; Royal Society of Chemistry: Cambridge, UK, 2015. doi:10.1039/9781782621980
- Margetić, D.; Štrukil, V. *Mechanochemical Organic Synthesis*; Elsevier: Amsterdam, Netherlands, 2016. doi:10.1016/c2014-0-01621-8
- Howard, J. L.; Cao, Q.; Browne, D. L. *Chem. Sci.* **2018**, *9*, 3080–3094. doi:10.1039/c7sc05371a
- Dud, M.; Briš, A.; Jušinski, I.; Gracin, D.; Margetić, D. *Beilstein J. Org. Chem.* **2019**, *15*, 1313–1320. doi:10.3762/bjoc.15.130
- Dud, M.; Glasovac, Z.; Margetić, D. *Tetrahedron* **2019**, *75*, 109–115. doi:10.1016/j.tet.2018.11.038
- Portada, T.; Margetić, D.; Štrukil, V. *Molecules* **2018**, *23*, 3163. doi:10.3390/molecules23123163
- Briš, A.; Dud, M.; Margetić, D. *Beilstein J. Org. Chem.* **2017**, *13*, 1745–1752. doi:10.3762/bjoc.13.169
- Warrener, R. N.; Maksimovic, L. *Tetrahedron Lett.* **1994**, *35*, 2389–2392. doi:10.1016/0040-4039(94)85227-8
- Warrener, R. N.; Maksimovic, L.; Butler, D. N. *J. Chem. Soc., Chem. Commun.* **1994**, 1831–1832. doi:10.1039/c39940001831
- Warrener, R. N.; Pitt, I. G.; Russell, R. A. *Aust. J. Chem.* **1991**, *44*, 1293–1305. doi:10.1071/ch9911293
- Margetić, D.; Warrener, R. N.; Sun, G.; Butler, D. N. *Tetrahedron* **2007**, *63*, 4338–4346. doi:10.1016/j.tet.2007.03.009
- Margetić, D.; Butler, D. N.; Warrener, R. N.; Murata, Y. *Tetrahedron* **2011**, *67*, 1580–1588. doi:10.1016/j.tet.2010.12.032
- Clark, R. D.; Heathcock, C. H. *J. Org. Chem.* **1976**, *41*, 636–643. doi:10.1021/jo00866a012
- Warrener, R. N.; Elsey, G. M.; Maksimovic, L.; Johnston, M. R.; Kennard, C. H. L. *Tetrahedron Lett.* **1995**, *36*, 7753–7756. doi:10.1016/0040-4039(95)01617-q
- Matsuo, Y.; Zhang, Y.; Nakamura, E. *Org. Lett.* **2008**, *10*, 1251–1254. doi:10.1021/o1800143b
- Cao, Q.; Stark, R. T.; Fallis, I. A.; Browne, D. L. *ChemSusChem* **2019**, *12*, 2554–2557. doi:10.1002/cssc.201900886
- Friščić, T.; Trask, A. V.; Jones, W.; Motherwell, W. D. S. *Angew. Chem., Int. Ed.* **2006**, *45*, 7546–7550. doi:10.1002/anie.200603235
- Yide, X.; Qingqing, G.; Naizheng, H. *Huaxue Xuebao* **1983**, *41*, 934–938.
- Margetić, D.; Warrener, R. N. *Croat. Chem. Acta* **2003**, *76*, 357–363.
- Sasaki, T.; Kanematsu, K.; Iizuka, K. *Heterocycles* **1975**, *3*, 109–112. doi:10.3987/r-1975-02-0109
- Eda, S.; Eguchi, F.; Haneda, H.; Hamura, T. *Chem. Commun.* **2015**, *51*, 5963–5966. doi:10.1039/c5cc00077g
- Blatter, K.; Schlüter, A.-D. *Chem. Ber.* **1989**, *122*, 1351–1356. doi:10.1002/cber.19891220719
- Marchand, A. P.; Namboothiri, I. N. N.; Ganguly, B.; Watson, W. H.; Bodige, S. G. *Tetrahedron Lett.* **1999**, *40*, 5105–5109. doi:10.1016/s0040-4039(99)00888-6
- Ohyashiki, T.; Nunomura, M.; Katoh, T. *Biochim. Biophys. Acta, Biomembr.* **1999**, *1421*, 131–139. doi:10.1016/s0005-2736(99)00119-4
- Žamojć, K.; Zdrowowicz, M.; Rudnicki-Velasquez, P. B.; Krzymiński, K.; Zaborowski, B.; Niedziałkowski, P.; Jacewicz, D.; Chmurzyński, L. *Free Radical Res.* **2017**, *51*, 38–46. doi:10.1080/10715762.2016.1262541
- Parr, B. T.; Economou, C.; Herzon, S. B. *Nature* **2015**, *525*, 507–510. doi:10.1038/nature14902
- Antol, I.; Glasovac, Z.; Murata, Y.; Hashikawa, Y.; Margetić, D. *ChemistrySelect* **2022**, *7*, e202200633. doi:10.1002/slct.202200633
- Huynh, V. N.; Leitner, M.; Bhattacharyya, A.; Uhlstein, L.; Kreitmeier, P.; Sakrausky, P.; Rehbein, J.; Reiser, O. *Commun. Chem.* **2020**, *3*, 158. doi:10.1038/s42004-020-00407-9
- Koerner, M.; Rickborn, B. J. *Org. Chem.* **1989**, *54*, 6–9. doi:10.1021/jo0262a003
- Koerner, M.; Rickborn, B. J. *Org. Chem.* **1990**, *55*, 2662–2672. doi:10.1021/jo00296a024
- Butler, D. N.; Margetić, D.; O'Neill, P. J. C.; Warrener, R. N. *Synlett* **2000**, 98–100. doi:10.1055/s-2000-6445
- Murata, Y.; Kato, N.; Fujiwara, K.; Komatsu, K. *J. Org. Chem.* **1999**, *64*, 3483–3488. doi:10.1021/jo990013z

License and Terms

This is an open access article licensed under the terms of the Beilstein-Institut Open Access License Agreement (<https://www.beilstein-journals.org/bjoc/terms>), which is identical to the Creative Commons Attribution 4.0 International License (<https://creativecommons.org/licenses/by/4.0>). The reuse of material under this license requires that the author(s), source and license are credited. Third-party material in this article could be subject to other licenses (typically indicated in the credit line), and in this case, users are required to obtain permission from the license holder to reuse the material.

The definitive version of this article is the electronic one which can be found at:

<https://doi.org/10.3762/bjoc.18.75>



Palladium-catalyzed solid-state borylation of aryl halides using mechanochemistry

Koji Kubota^{*1,2}, Emiru Baba¹, Tamae Seo¹, Tatsuo Ishiyama¹ and Hajime Ito^{*1,2}

Letter

Open Access

Address:

¹Division of Applied Chemistry, Graduate School of Engineering, Hokkaido University, Sapporo, Hokkaido 060-8628, Japan and

²Institute for Chemical Reaction Design and Discovery (WPI-ICReDD), Hokkaido University, Sapporo, Hokkaido 060-8628, Japan

Email:

Koji Kubota^{*} - kbt@eng.hokudai.ac.jp; Hajime Ito^{*} - hajito@eng.hokudai.ac.jp

* Corresponding author

Keywords:

ball mill; borylation; cross-coupling; mechanochemistry; solid-state reaction

Beilstein J. Org. Chem. **2022**, *18*, 855–862.

<https://doi.org/10.3762/bjoc.18.86>

Received: 18 April 2022

Accepted: 09 June 2022

Published: 18 July 2022

This article is part of the thematic issue "Mechanochemistry III".

Guest Editors: J. G. Hernández and L. Borchardt

© 2022 Kubota et al.; licensee Beilstein-Institut.

License and terms: see end of document.

Abstract

This study describes the solid-state palladium-catalyzed cross-coupling between aryl halides and bis(pinacolato)diboron using ball milling. The reactions were completed within 10 min for most aryl halides to afford a variety of synthetically useful arylboronates in high yields. Notably, all experimental operations could be performed in air, and did not require the use of large amounts of dry and degassed organic solvents. The utility of this method was further demonstrated by gram-scale synthesis under solvent-free, mechanochemical conditions.

Introduction

Arylboronic acid and its derivatives are indispensable reagents in modern synthetic chemistry because they have been frequently used for the preparation of many bioactive molecules, natural products, and functional organic materials, typically through Suzuki–Miyaura coupling [1–7]. The palladium-catalyzed boryl substitution of aryl halides with boron reagents, termed Miyaura–Ishiyama borylation, is an efficient method for synthesizing arylboronates with high functional group compatibility [8–14]. To date, many palladium-based catalytic systems

in solution for the borylation of aryl halides have been reported [8–14]. However, these solution-based reactions usually require long reaction times and significant amounts of dry and degassed organic solvents. Additionally, to avoid the deterioration of reactivity due to moisture and oxygen, conventional protocols require synthesis techniques that involve the use of high-vacuum Schlenk lines and/or glove boxes, which are costly and require special training to handle. Thus, the development of an operationally simple, solvent-free palladium-catalyzed boryla-

tion process applicable for a wide range of aryl halides would greatly improve the practicality of the desired arylboronic acid derivatives.

Nechaev et al. reported the first solvent-free protocol for the palladium-catalyzed Miyaura–Ishiyama borylation of aryl halides in a test tube [15]. They found that a $\text{Pd}(\text{dba})_2/\text{DPEphos}$ catalytic system was effective for aryl bromides, and aryl chlorides reacted more efficiently when XPhos was used as the ligand [15]. Although their achievements are remarkable, this protocol is only applicable to liquid substrates, which can serve as reactants and solvents (neat liquid conditions). In addition, a long reaction time (12 h) is required to complete the reaction [15]. A general and efficient solvent-free borylation protocol that can be applied to liquid as well as solid aryl halides remains undeveloped.

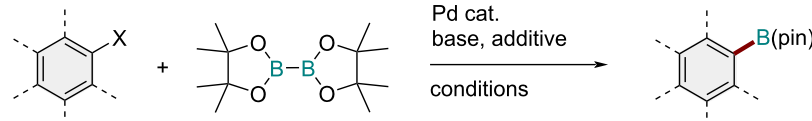
Recently, mechanochemical synthesis using ball milling has attracted considerable attention as an efficient solvent-free synthetic technique [16–33]. Notably, the strong mechanical agitation provided by ball milling enables efficient solid-state organic transformations. Thus far, mechanochemical palladium-catalyzed cross-coupling reactions such as Suzuki–Miyaura [34–47], Buchwald–Hartwig [48–52], Sonogashira [53–56], Negishi [57], Mizoroki–Heck [58–60], and C–S bond-forming [61] reactions have been developed. Our group has also been interested in this class of mechanochemical transformations, particularly in the development of cross-coupling reactions that proceed in the solid state [43–50]. These mechanochemical cross-coupling reactions often show much faster reaction kinetics than those under conventional solution-based conditions because of the high concentration; further, the experimental operations can be carried out in air. Considering these achievements, including our recent success in solid-state cross-coupling chemistry, we envisioned that this mechanochemical strategy could be applied to the palladium-catalyzed borylation of aryl halides [8–14]. The

development of a solid-state borylation protocol could provide a practical solution to the many issues associated with conventional solution-based protocols (Scheme 1).

Results and Discussion

Initially, we conducted an optimization study on the mechanochemical cross-coupling between 2-bromo-6-methoxynaphthalene (**1a**, 0.3 mmol) and bis(pinacolato)diboron (**2**, 1.2 equiv) in the presence of $\text{Pd}(\text{OAc})_2$ (2 mol %), KOAc (3.0 equiv), and H_2O (60 μL) as a liquid additive [43–45] (Table 1). The reactions were conducted in a Retch MM400 ball mill in a stainless-steel milling jar (1.5 mL) at 30 Hz using one stainless-steel ball (diameter: 5 mm) for 10 min. We used a commercially available temperature-controllable heat gun that was placed directly above the ball-milling jar to control the reaction temperature [45]. Reactions were performed using a heat gun with a preset temperature of 100 °C, and the internal temperature of the reaction mixture (60 °C) was assessed by thermography immediately after opening the milling jar (see Supporting Information File 1 for details). First, we tested various phosphine ligands [62] for this reaction (Table 1, entries 1–8). Interestingly, we found that tri-*tert*-butylphosphonium tetrafluoroborate (*t*-Bu₃P·HBF₄) provided the borylation product **3a** in excellent yield (92%, Table 1, entry 1), with a small amount of the protonation product **4a** (5%, entry 1). When the reaction was stopped after 5 min, only a 26% yield of **3a** was obtained (Table 1, entry 2). The use of 1,1'-bis(diphenylphosphino)ferrocene (dpff), which is the optimal ligand under the original conditions for the solution-based protocol [8], provided only trace amounts of **3a** (1%, Table 1, entry 3). Reactions with DPEphos and XPhos, which are the optimal ligands for neat liquid conditions reported by Nechaev [15], also yielded only poor results (Table 1, entries 4 and 5). Other monophosphine ligands, such as SPhos, PCy₃, and PAd₃, did not improve the yield of **3a** (Table 1, entries 6–8). The amount of H_2O added was important for the efficiency of the reaction. Decreasing the

palladium-catalyzed borylation of aryl halides (Miyaura–Ishiyama borylation)



in solution: well-studied

- long reaction time
- potentially harmful solvent
- complicated synthesis techniques using Schlenk lines and/or glove boxes

in the solid state: this study

- fast and efficient
- no reaction solvent required
- ball milling: all operations can be carried out in air without necessitating special synthetic techniques

Scheme 1: Development of the first solid-state palladium-catalyzed borylation protocol of aryl halides using mechanochemistry.

Table 1: Optimization of the reaction conditions.^a

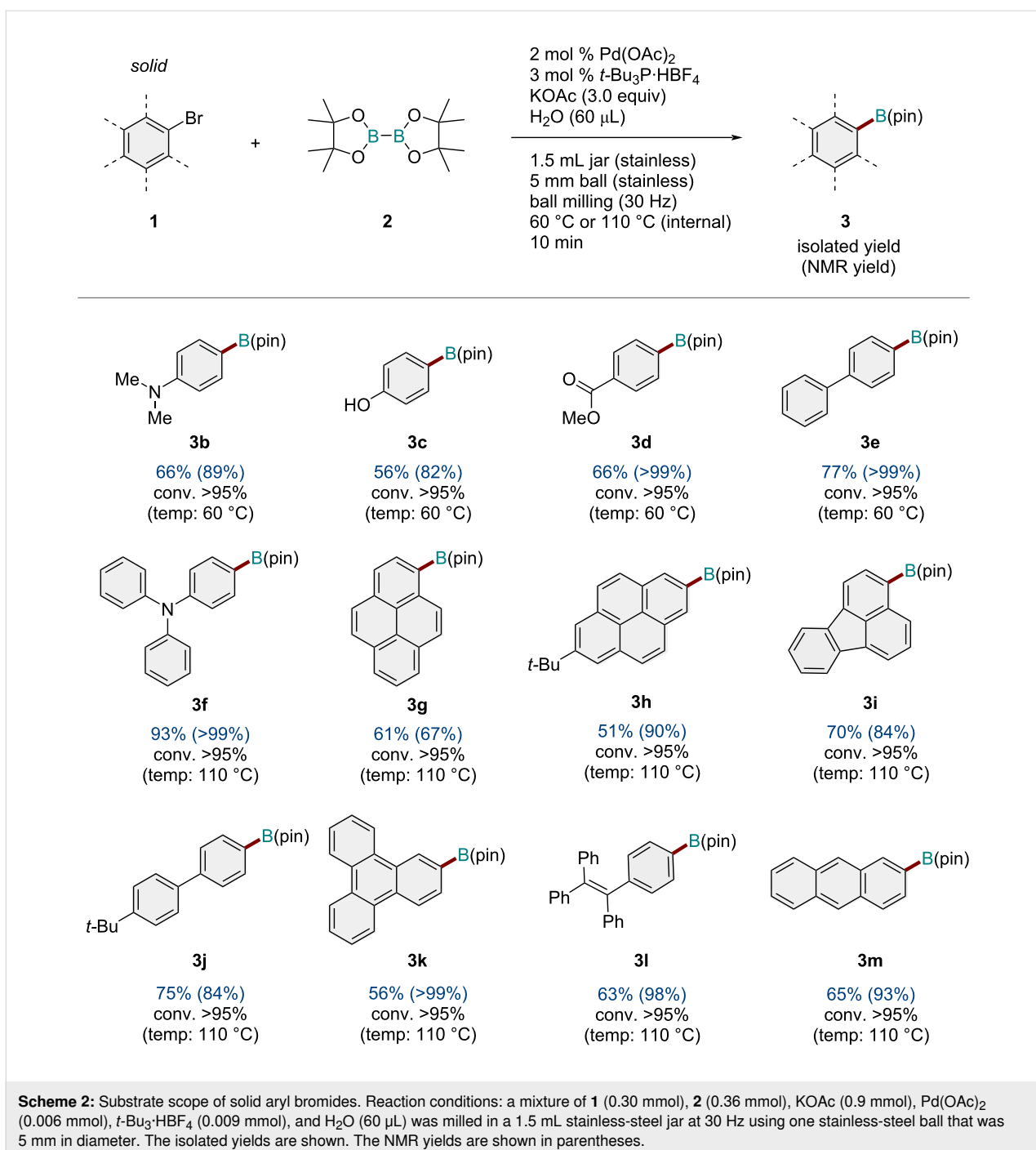
Entry	Ligand	Amount of H ₂ O (µL)	Internal temp (°C)	Time (min)	Yield of 3a (%) ^b	Yield of 4a (%) ^b
1	<i>t</i> -Bu ₃ P·HBF ₄	60	60	10	92	5
2	<i>t</i> -Bu ₃ P·HBF ₄	60	60	5	26	1
3	dppf	60	60	10	1	<1
4	DPEphos	60	60	10	<1	<1
5	XPhos	60	60	10	5	<1
6	SPhos	60	60	10	2	<1
7	PCy ₃	60	60	10	5	<1
8	PAd ₃	60	60	10	6	<1
9	<i>t</i> -Bu ₃ P·HBF ₄	40	60	10	68	3
10	<i>t</i> -Bu ₃ P·HBF ₄	0	60	10	8	1
11	<i>t</i> -Bu ₃ P·HBF ₄	60	110	10	90	6
12	<i>t</i> -Bu ₃ P·HBF ₄	60	30	10	6	1
13	<i>t</i> -Bu ₃ P·HBF ₄	60	30	90	41	2

^aReaction conditions: a mixture of **1a** (0.30 mmol), **2** (0.36 mmol), KOAc (0.9 mmol), Pd(OAc)₂ (0.006 mmol), ligand (0.009 mmol), and H₂O was milled in a 1.5 mL stainless-steel jar at 30 Hz with one stainless-steel ball that was 5 mm in diameter. ^bDetermined by GC analysis using an internal standard.

amount of H₂O to 40 µL led to a lower yield of **3a** (68%; Table 1, entry 9). The reaction without H₂O afforded **3a** in only 8% yield (Table 1, entry 10). Finally, we investigated the effect of the reaction temperature. The reaction at a higher temperature (110 °C) also provided **3a** in a good yield (90%; Table 1, entry 11), but when the reaction was carried out at 30 °C, the yield was very low (6%; Table 1, entry 12). A longer reaction time (90 min) at 30 °C afforded **3a** in a moderate yield (41%; Table 1, entry 13). Note that no homocoupling product of **1a**

was formed, or only trace amounts (<1%) were formed in all cases.

Under the optimized reaction conditions (Table 1, entry 1), we explored the substrate scope of aryl bromides for the solid-state borylation (Scheme 2). The reactions of aryl bromides bearing electron-donating and electron-withdrawing groups at the *para* position (**1b–d**) proceeded smoothly to afford the corresponding arylboronates (**3b–d**) in good to high yields. 4-Bromo-

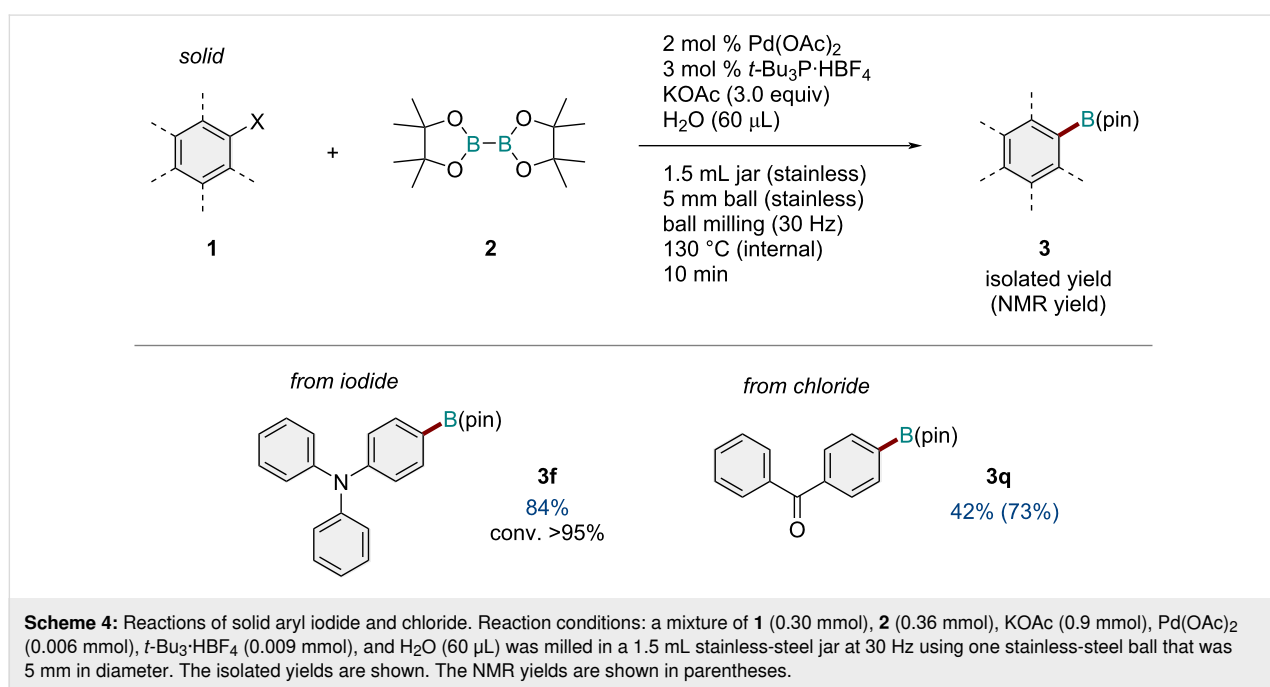
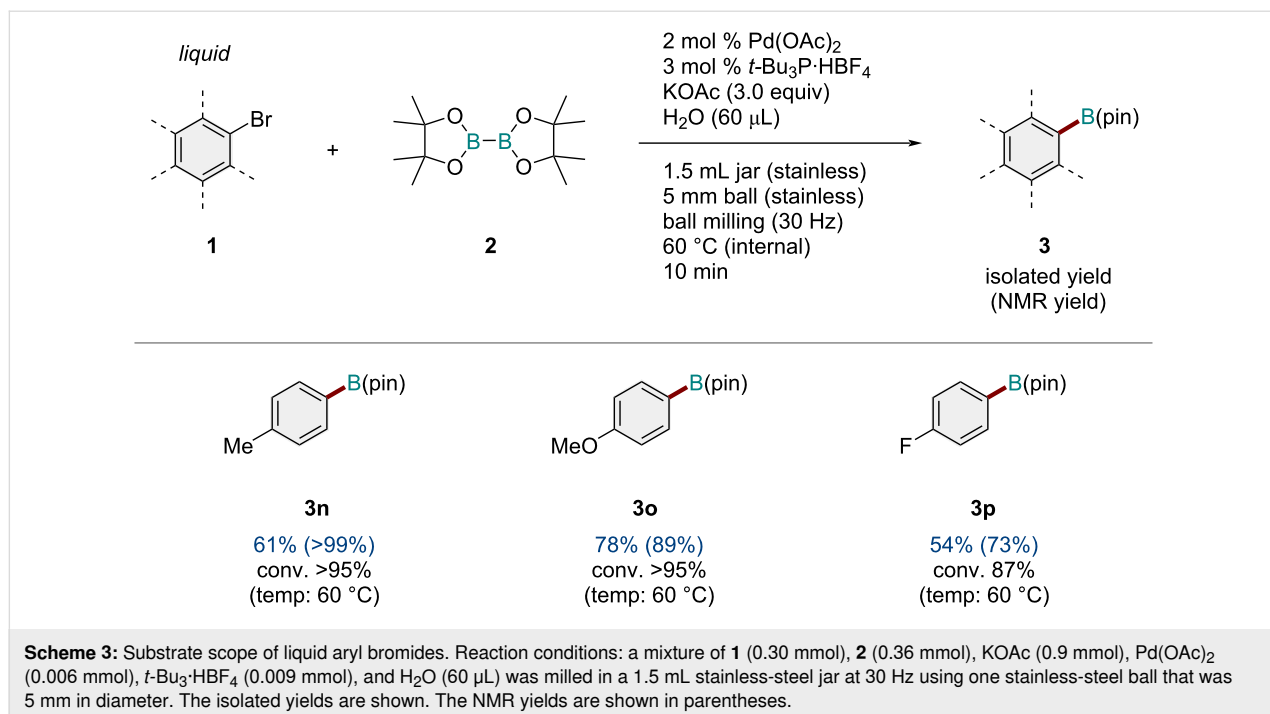


Scheme 2: Substrate scope of solid aryl bromides. Reaction conditions: a mixture of **1** (0.30 mmol), **2** (0.36 mmol), KOAc (0.9 mmol), $\text{Pd}(\text{OAc})_2$ (0.006 mmol), $t\text{-Bu}_3\text{P}\cdot\text{HBF}_4$ (0.009 mmol), and H_2O (60 μL) was milled in a 1.5 mL stainless-steel jar at 30 Hz using one stainless-steel ball that was 5 mm in diameter. The isolated yields are shown. The NMR yields are shown in parentheses.

biphenyl (**1e**) also underwent borylation efficiently to form the borylation product (**3e**) in excellent yield. We found that substrates bearing relatively large conjugated structures (**1f–m**) tended to show low reactivity under the optimized conditions at 60 $^{\circ}\text{C}$, but the reactions proceeded smoothly at 110 $^{\circ}\text{C}$. For example, the bromo-substituted triphenylamine (**1f**), pyrene (**1g** and **1h**), fluoranthene (**1i**), biphenyl (**1j**), triphenylene (**1k**), tetraphenylethylene (**1l**), and anthracene (**1m**) reacted with diboron **2** to form the desired products (**3f–m**) in high yields.

Next, the substrate scope of liquid aryl bromides was investigated (Scheme 3). We found that the present mechanochemical conditions were applicable to the solid substrate and various liquid substrates (**1n–p**), and the desired borylation products (**3n–p**) were obtained in good yields.

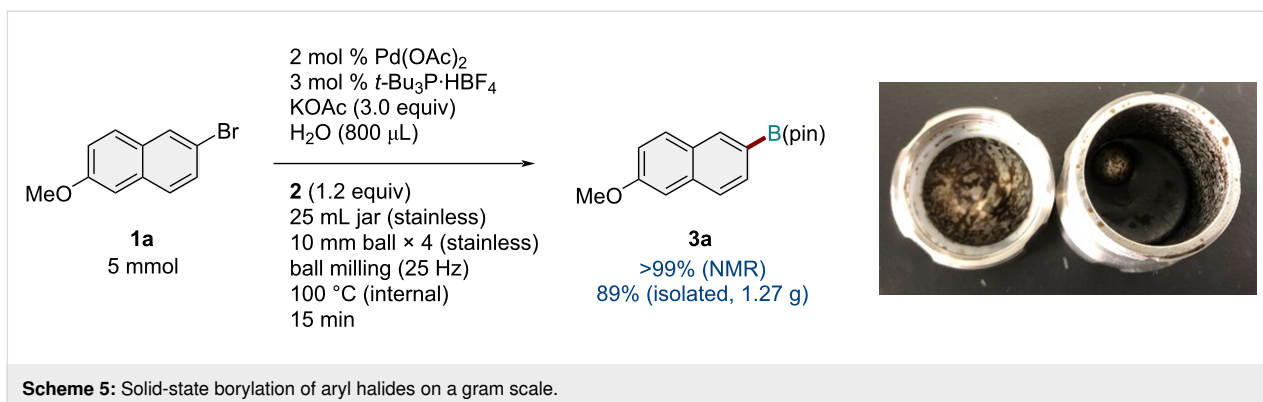
We also investigated the solid-state borylation reactions of aryl iodides and chlorides (Scheme 4). The reaction of 4-iodo-*N,N*-diphenylaniline (**1q**) under the optimized conditions at 130 $^{\circ}\text{C}$



for 30 min proceeded smoothly and provided the desired product **3f** in high yield (84%). Also, the reaction of (4-chlorophenyl)(phenyl)methanone (**1r**) afforded the corresponding product **3q** in good yield.

To demonstrate the practical utility of the developed protocol, the solid-state borylation reaction was investigated on a gram scale (Scheme 5). We carried out the reaction of **1a** at 5 mmol

in the presence of the optimized catalytic system using a 25 mL stainless-steel jar and four stainless-steel balls (diameter: 10 mm) at 25 Hz and a preset heat-gun temperature of 150 °C. The gram-scale borylation proceeded efficiently and afforded the borylation product **3a** in high yield, which was comparable to the yield obtained at the 0.3 mmol scale. We confirmed by thermography that the internal temperature after the reaction was approximately 100 °C.

**Scheme 5:** Solid-state borylation of aryl halides on a gram scale.

Conclusion

In summary, we have developed the first protocol for the solid-state palladium-catalyzed borylation of aryl halides. This mechanochemical protocol allows the synthesis of various aryl boronates in high yields within a short reaction time (within 10 min). Notably, the borylation reactions can be conducted without the use of organic solvents, and all synthetic operations can be carried out in air without the requirement of Schlenk-line techniques or glovebox operations. Therefore, the present solid-state approach is a practical and sustainable method to complement conventional solution-based protocols. The application of this method to the solid-state borylation of insoluble substrates for the synthesis of new arylboronates that are difficult to prepare by other means is currently under investigation.

Supporting Information

Supporting Information File 1

Experimental procedures, experimental set-ups, characterization data, and NMR spectra.

[<https://www.beilstein-journals.org/bjoc/content/supportive/1860-5397-18-86-S1.pdf>]

Acknowledgements

We thank Otsuka Chemical Co., Ltd. for their cooperation and helpful discussion.

Funding

This work was financially supported by the Japan Society for the Promotion of Science (JSPS) via KAKENHI grants 22H00318 and 21H01926; by the JST via CREST grant JPMJCR19R1; FOREST grant JPMJFR20I1; and by the Institute for Chemical Reaction Design and Discovery (ICReDD) established by the World Premier International Research Initiative (WPI), MEXT, Japan.

ORCID® iDs

Koji Kubota - <https://orcid.org/0000-0003-1522-291X>
Hajime Ito - <https://orcid.org/0000-0003-3852-6721>

References

- Hall, D. G., Ed. *Boronic Acids: Preparation and Application in Organic Synthesis, Medicine and Materials*, 2nd ed.; Wiley-VCH: Weinheim, Germany, 2011. doi:10.1002/9783527639328
- Diner, C.; Szabó, K. J. *J. Am. Chem. Soc.* **2017**, *139*, 2–14. doi:10.1021/jacs.6b10017
- Diaz, D. B.; Yudin, A. K. *Nat. Chem.* **2017**, *9*, 731–742. doi:10.1038/nchem.2814
- Touchet, S.; Carreaux, F.; Carboni, B.; Bouillon, A.; Boucher, J.-L. *Chem. Soc. Rev.* **2011**, *40*, 3895–3914. doi:10.1039/c0cs00154f
- Smoum, R.; Rubinstein, A.; Dembitsky, V. M.; Srebnik, M. *Chem. Rev.* **2012**, *112*, 4156–4220. doi:10.1021/cr608202m
- Mellerup, S. K.; Wang, S. *Trends Chem.* **2019**, *1*, 77–89. doi:10.1016/j.trechm.2019.01.003
- Budiman, Y. P.; Westcott, S. A.; Radius, U.; Marder, T. B. *Adv. Synth. Catal.* **2021**, *363*, 2224–2255. doi:10.1002/adsc.202001291
- Ishiyama, T.; Murata, M.; Miyaura, N. *J. Org. Chem.* **1995**, *60*, 7508–7510. doi:10.1021/jo00128a024
- Ishiyama, T.; Itoh, Y.; Kitano, T.; Miyaura, N. *Tetrahedron Lett.* **1997**, *38*, 3447–3450. doi:10.1016/s0040-4039(97)00642-4
- Ishiyama, T.; Ishida, K.; Miyaura, N. *Tetrahedron* **2001**, *57*, 9813–9816. doi:10.1016/s0040-4020(01)00998-x
- Chow, W. K.; Yuen, O. Y.; Choy, P. Y.; So, C. M.; Lau, C. P.; Wong, W. T.; Kwong, F. Y. *RSC Adv.* **2013**, *3*, 12518–12539. doi:10.1039/c3ra22905j
- Barroso, S.; Joksch, M.; Puylaert, P.; Tin, S.; Bell, S. J.; Donnellan, L.; Duguid, S.; Muir, C.; Zhao, P.; Farina, V.; Tran, D. N.; de Vries, J. G. *J. Org. Chem.* **2021**, *86*, 103–109. doi:10.1021/acs.joc.0c01758
- Murata, M.; Oyama, T.; Watanabe, S.; Masuda, Y. *J. Org. Chem.* **2000**, *65*, 164–168. doi:10.1021/jo991337q
- Kubota, K.; Iwamoto, H.; Ito, H. *Org. Biomol. Chem.* **2017**, *15*, 285–300. doi:10.1039/c6ob02369j
- Dzhevakov, P. B.; Topchiy, M. A.; Zharkova, D. A.; Morozov, O. S.; Asachenko, A. F.; Nechaev, M. S. *Adv. Synth. Catal.* **2016**, *358*, 977–983. doi:10.1002/adsc.201500844

16. James, S. L.; Adams, C. J.; Bolm, C.; Braga, D.; Collier, P.; Friščić, T.; Grepioni, F.; Harris, K. D. M.; Hyett, G.; Jones, W.; Krebs, A.; Mack, J.; Maini, L.; Orpen, A. G.; Parkin, I. P.; Shearouse, W. C.; Steed, J. W.; Waddell, D. C. *Chem. Soc. Rev.* **2012**, *41*, 413–447. doi:10.1039/c1cs15171a

17. Bowmaker, G. A. *Chem. Commun.* **2013**, *49*, 334–348. doi:10.1039/c2cc35694e

18. Wang, G.-W. *Chem. Soc. Rev.* **2013**, *42*, 7668–7700. doi:10.1039/c3cs35526h

19. Hernández, J. G.; Bolm, C. *J. Org. Chem.* **2017**, *82*, 4007–4019. doi:10.1021/acs.joc.6b02887

20. Stolle, A.; Szuppa, T.; Leonhardt, S. E. S.; Ondruschka, B. *Chem. Soc. Rev.* **2011**, *40*, 2317–2329. doi:10.1039/c0cs00195c

21. Kubota, K.; Ito, H. *Trends Chem.* **2020**, *2*, 1066–1081. doi:10.1016/j.trechm.2020.09.006

22. Howard, J. L.; Cao, Q.; Browne, D. L. *Chem. Sci.* **2018**, *9*, 3080–3094. doi:10.1039/c7sc05371a

23. Braga, D.; Maini, L.; Grepioni, F. *Chem. Soc. Rev.* **2013**, *42*, 7638–7648. doi:10.1039/c3cs60014a

24. Achar, T. K.; Bose, A.; Mal, P. *Beilstein J. Org. Chem.* **2017**, *13*, 1907–1931. doi:10.3762/bjoc.13.186

25. Do, J.-L.; Friščić, T. *ACS Cent. Sci.* **2017**, *3*, 13–19. doi:10.1021/acscentsci.6b00277

26. Métra, T.-X.; Martinez, J.; Lamaty, F. *ACS Sustainable Chem. Eng.* **2017**, *5*, 9599–9602. doi:10.1021/acssuschemeng.7b03260

27. Eguaogie, O.; Vyle, J. S.; Conlon, P. F.; Gilea, M. A.; Liang, Y. *Beilstein J. Org. Chem.* **2018**, *14*, 955–970. doi:10.3762/bjoc.14.81

28. Bolm, C.; Hernández, J. G. *Angew. Chem., Int. Ed.* **2019**, *58*, 3285–3299. doi:10.1002/anie.201810902

29. Friščić, T.; Mottillo, C.; Titi, H. M. *Angew. Chem., Int. Ed.* **2020**, *59*, 1018–1029. doi:10.1002/anie.201906755

30. Andersen, J.; Mack, J. *Green Chem.* **2018**, *20*, 1435–1443. doi:10.1039/c7gc03797j

31. Porcheddu, A.; Colacino, E.; De Luca, L.; Delogu, F. *ACS Catal.* **2020**, *10*, 8344–8394. doi:10.1021/acscatal.0c00142

32. Leitch, J. A.; Browne, D. L. *Chem. – Eur. J.* **2021**, *27*, 9721–9726. doi:10.1002/chem.202100348

33. Kaupp, G. *CrystEngComm* **2009**, *11*, 388–403. doi:10.1039/b810822f

34. Schneider, F.; Ondruschka, B. *ChemSusChem* **2008**, *1*, 622–625. doi:10.1002/cssc.200800086

35. Cravotto, G.; Garella, D.; Tagliapietra, S.; Stolle, A.; Schüßler, S.; Leonhardt, S. E. S.; Ondruschka, B. *New J. Chem.* **2012**, *36*, 1304–1307. doi:10.1039/c2nj40064b

36. Nielsen, S. F.; Peters, D.; Axelsson, O. *Synth. Commun.* **2000**, *30*, 3501–3509. doi:10.1080/00397910008087262

37. Klingensmith, L. M.; Leadbeater, N. E. *Tetrahedron Lett.* **2003**, *44*, 765–768. doi:10.1016/s0040-4039(02)02645-x

38. Bernhardt, F.; Trotzki, R.; Szuppa, T.; Stolle, A.; Ondruschka, B. *Beilstein J. Org. Chem.* **2010**, *6*, No. 7. doi:10.3762/bjoc.6.7

39. Schneider, F.; Szuppa, T.; Stolle, A.; Ondruschka, B.; Hopf, H. *Green Chem.* **2009**, *11*, 1894–1899. doi:10.1039/b915744c

40. Schneider, F.; Stolle, A.; Ondruschka, B.; Hopf, H. *Org. Process Res. Dev.* **2009**, *13*, 44–48. doi:10.1021/op800148y

41. Jiang, Z.-J.; Li, Z.-H.; Yu, J.-B.; Su, W.-K. *J. Org. Chem.* **2016**, *81*, 10049–10055. doi:10.1021/acs.joc.6b01938

42. Báti, G.; Csókás, D.; Yong, T.; Tam, S. M.; Shi, R. R. S.; Webster, R. D.; Pápai, I.; García, F.; Stuparu, M. C. *Angew. Chem., Int. Ed.* **2020**, *59*, 21620–21626. doi:10.1002/anie.202007815

43. Seo, T.; Ishiyama, T.; Kubota, K.; Ito, H. *Chem. Sci.* **2019**, *10*, 8202–8210. doi:10.1039/c9sc02185j

44. Seo, T.; Kubota, K.; Ito, H. *J. Am. Chem. Soc.* **2020**, *142*, 9884–9889. doi:10.1021/jacs.0c01739

45. Seo, T.; Toyoshima, N.; Kubota, K.; Ito, H. *J. Am. Chem. Soc.* **2021**, *143*, 6165–6175. doi:10.1021/jacs.1c00906

46. Takahashi, R.; Seo, T.; Kubota, K.; Ito, H. *ACS Catal.* **2021**, *11*, 14803–14810. doi:10.1021/acscatal.1c03731

47. Kubota, K.; Kondo, K.; Seo, T.; Ito, H. *Synlett* **2022**, *33*, 898–902. doi:10.1055/a-1748-3797

48. Kubota, K.; Seo, T.; Koide, K.; Hasegawa, Y.; Ito, H. *Nat. Commun.* **2019**, *10*, No. 111. doi:10.1038/s41467-018-08017-9

49. Kubota, K.; Takahashi, R.; Uesugi, M.; Ito, H. *ACS Sustainable Chem. Eng.* **2020**, *8*, 16577–16582. doi:10.1021/acssuschemeng.0c05834

50. Kubota, K.; Endo, T.; Uesugi, M.; Hayashi, Y.; Ito, H. *ChemSusChem* **2022**, *15*, e202102132. doi:10.1002/cssc.202102132

51. Shao, Q.-L.; Jiang, Z.-J.; Su, W.-K. *Tetrahedron Lett.* **2018**, *59*, 2277–2280. doi:10.1016/j.tetlet.2018.04.078

52. Cao, Q.; Nicholson, W. I.; Jones, A. C.; Browne, D. L. *Org. Biomol. Chem.* **2019**, *17*, 1722–1726. doi:10.1039/c8ob01781f

53. Fulmer, D. A.; Shearouse, W. C.; Medonza, S. T.; Mack, J. *Green Chem.* **2009**, *11*, 1821–1825. doi:10.1039/b915669k

54. Liang, Y.; Xie, Y.-X.; Li, J.-H. *J. Org. Chem.* **2006**, *71*, 379–381. doi:10.1021/jo051882t

55. Thorwirth, R.; Stolle, A.; Ondruschka, B. *Green Chem.* **2010**, *12*, 985–991. doi:10.1039/c000674b

56. Gao, Y.; Feng, C.; Seo, T.; Kubota, K.; Ito, H. *Chem. Sci.* **2022**, *13*, 430–438. doi:10.1039/d1sc05257h

57. Cao, Q.; Howard, J. L.; Wheatley, E.; Browne, D. L. *Angew. Chem., Int. Ed.* **2018**, *57*, 11339–11343. doi:10.1002/anie.201806480

58. Declerck, V.; Colacino, E.; Bantrell, X.; Martinez, J.; Lamaty, F. *Chem. Commun.* **2012**, *48*, 11778–11780. doi:10.1039/c2cc36286d

59. Tullberg, E.; Schacher, F.; Peters, D.; Frejd, T. *Synthesis* **2006**, 1183–1189. doi:10.1055/s-2006-926371

60. Tullberg, E.; Peters, D.; Frejd, T. *J. Organomet. Chem.* **2004**, 689, 3778–3781. doi:10.1016/j.jorganochem.2004.06.045

61. Jones, A. C.; Nicholson, W. I.; Smallman, H. R.; Browne, D. L. *Org. Lett.* **2020**, *22*, 7433–7438. doi:10.1021/acs.orglett.0c02418

62. Tang, W.; Keshipeddy, S.; Zhang, Y.; Wei, X.; Savoie, J.; Patel, N. D.; Yee, N. K.; Senanayake, C. H. *Org. Lett.* **2011**, *13*, 1366–1369. doi:10.1021/ol2000556

License and Terms

This is an open access article licensed under the terms of the Beilstein-Institut Open Access License Agreement (<https://www.beilstein-journals.org/bjoc/terms>), which is identical to the Creative Commons Attribution 4.0 International License (<https://creativecommons.org/licenses/by/4.0>). The reuse of material under this license requires that the author(s), source and license are credited. Third-party material in this article could be subject to other licenses (typically indicated in the credit line), and in this case, users are required to obtain permission from the license holder to reuse the material.

The definitive version of this article is the electronic one which can be found at:

<https://doi.org/10.3762/bjoc.18.86>



Automated grindstone chemistry: a simple and facile way for PEG-assisted stoichiometry-controlled halogenation of phenols and anilines using *N*-halosuccinimides

Dharmendra Das, Akhil A. Bhosle, Amrita Chatterjee ^{*} and Mainak Banerjee ^{*}

Full Research Paper

Open Access

Address:

Department of Chemistry, BITS Pilani, K. K. Birla Goa Campus, Goa 403 726, India

Email:

Amrita Chatterjee ^{*} - amrita@goa.bits-pilani.ac.in; Mainak Banerjee ^{*} - mainak@goa.bits-pilani.ac.in

^{*} Corresponding author

Keywords:

automated grinding; chemoselectivity; mechanochemistry; *N*-bromosuccinimide; PEG-400; regioselectivity; stoichiometry-controlled halogenation

Beilstein J. Org. Chem. **2022**, *18*, 999–1008.

<https://doi.org/10.3762/bjoc.18.100>

Received: 12 June 2022

Accepted: 27 July 2022

Published: 09 August 2022

This article is part of the thematic issue "Mechanochemistry III".

Guest Editors: J. G. Hernández and L. Borchardt

© 2022 Das et al.; licensee Beilstein-Institut.

License and terms: see end of document.

Abstract

A simple electrical mortar–pestle was used for the development of a green and facile mechanochemical route for the catalyst-free halogenation of phenols and anilines via liquid-assisted grinding using PEG-400 as the grinding auxiliary. A series of mono-, di-, and tri-halogenated phenols and anilines was synthesized in good to excellent yields within 10–15 min in a chemoselective manner by controlling the stoichiometry of *N*-halosuccinimides (NXS, X = Br, I, and Cl). It was observed that PEG-400 plays a key role in controlling the reactivity of the substrates and to afford better regioselectivity. Almost exclusive *para*-selectivity was observed for the aromatic substrates with free *o*- and *p*-positions for mono- and dihalogenations. As known, the decarboxylation (or desulfonation) was observed in the case of salicylic acids and anthranilic acids (or sulfanilic acids) leading to 2,4,6-trihalogenated products when 3 equiv of NXS was used. Simple instrumentation, metal-free approach, cost-effectiveness, atom economy, short reaction time, and mild reaction conditions are a few noticeable merits of this environmentally sustainable mechanochemical protocol.

Introduction

Aryl halides are valuable compounds with potent bioactivities [1–5] (Figure 1) and are utilized as crucial precursors for various metal-catalyzed cross-coupling reactions [6–9]. They are frequently used as synthetic intermediates in several value-added syntheses of natural products, pharmaceuticals, agrochemicals, and advanced materials [10–14]. The ubiquity of

halogen atoms in these synthetic building blocks urges the development of efficient, sustainable, and mild methods for aromatic halogenation.

The century-old classical method of using hazardous and corrosive reagents X₂ (X = Br, Cl) suffers from low atom economy

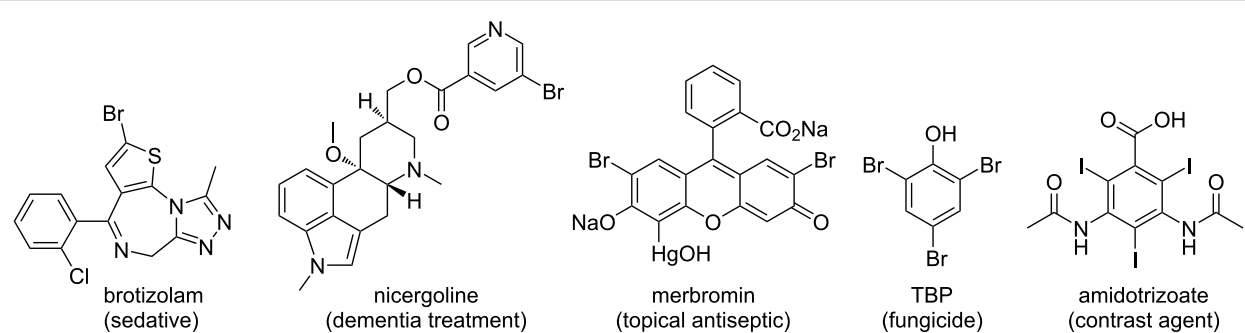
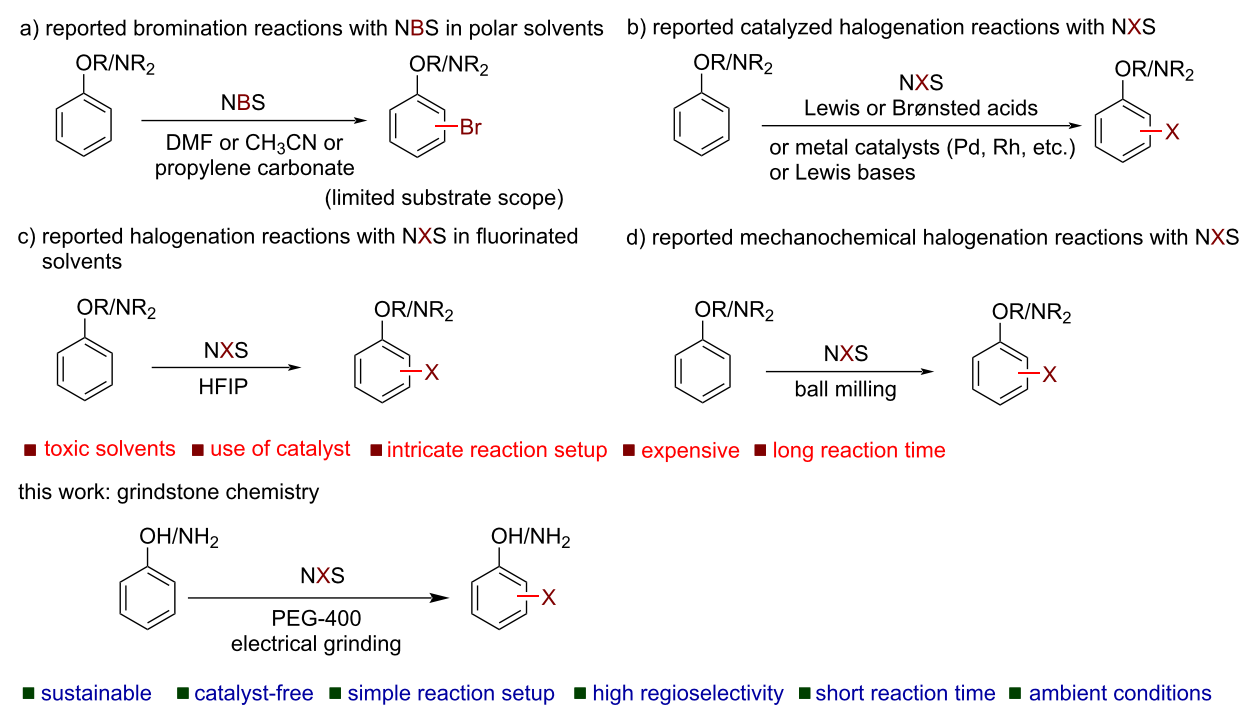


Figure 1: Representative examples of important halogen-containing aryl derivatives.

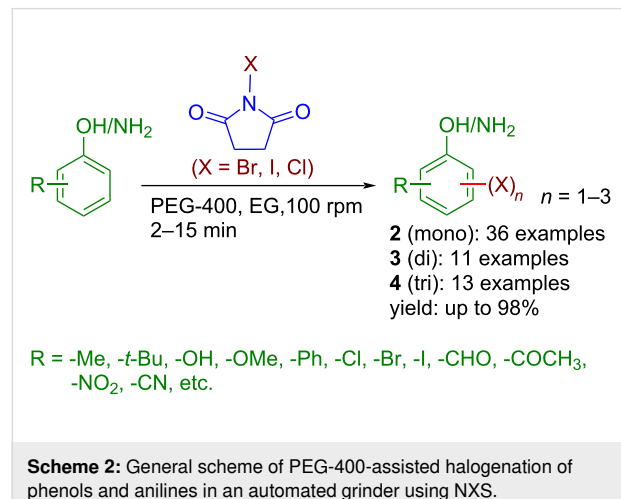
(<50%), formation of corrosive byproducts (e.g., HBr) [15,16], which cause serious environmental issues. To mitigate the problem, several mild and operationally safe halogenating agents have been successfully introduced to replace X_2 [17–31]. Among them, the use of *N*-halosuccinimides has turned out to be a viable alternative to X_2 because of their low-cost, ease of handling, and possible recycling of the byproduct succinimide [24–31]. In several earlier cases, the bromination with *N*-bromosuccinimide (NBS) was carried out in toxic polar solvents (e.g., DMF), but no iodinated or chlorinated products were obtained because of the low reactivity of NIS and NCS (Scheme 1a) [24–27]. In recent time, the use of Lewis or Brønsted acids, Lewis bases, and transition-metal catalysts (Pd, Rh, Fe, etc.) were em-

ployed to boost the reactivity of NXS (Scheme 1b) [32–43]. However, the use of toxic and expensive metals, high catalyst loading, and heating conditions are some sheer hurdles to achieving sustainability. Among notable other catalyst-free methods, the use of costly and low boiling hexafluoroisopropanol (HFIP) as solvent offered the *para*-selective halogenation of activated aromatic systems (Scheme 1c) [44]. It is noteworthy to mention that over-halogenation of activated systems like phenols and anilines, due to the high reactivity and availability of multiple sites for substitution, often leads to an inseparable mixture of halogenated products [27,28]. Thus, a cheaper and sustainable method for a regioselective halogenation in a controlled manner is a worthy pursuit.



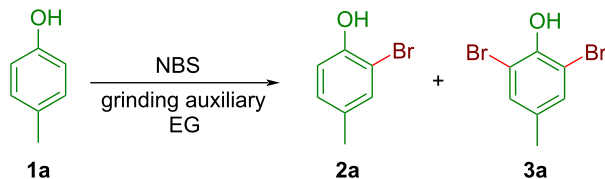
Scheme 1: Strategies for halogenation of aromatic compounds using NXS.

In recent times, mechanochemistry [45,46], achieved by mechanical grinding or milling, has garnered massive interest among chemists owing to its green attributes like solvent-free, clean, atom economic, and time-efficient, and has been identified by the IUPAC as one of 10 world-changing technologies [47]. While milling has received more focus, the simpler form of mechanochemistry, Toda et al.'s "grindstone chemistry" [48] has also been proved as a useful technique for various organic transformations [49]. It is generally carried out by hand-grinding which is not only a labor-intensive process but also raises some concerns on the reaction kinetics, reproducibility, and scalability. An alternative and efficient way of grinding is the use of automation instead of manual intervention. Notably, an industrial-scale synthesis is possible by the suitable choice of a large automated grindstone apparatus. However, there are only limited examples of the use of automated grindstone chemistry [50]. Notably, a few mechanochemical methods are available for aromatic halogenation using NXS (Scheme 1d) [51–53]. However, the solvent-free protocol reported by Mal and co-workers requires several hours for halogenation [51], whereas Ghafuri and co-workers' method requires the use of a solid acid catalyst [52], apart from the use of high-cost, high-end milling equipment which limits to laboratory scale only. Therefore, developing an operationally simple, environmentally benign protocol, potentially useful for the batch-scale synthesis of aryl halides is highly desirable. From our past experience, we realized a liquid-assisted grinding expedites a reaction to several folds [54–56]. In this regard, PEG-400 is widely preferred due to its biodegradable and benign nature and often offers excellent outcomes where other grinding auxiliaries failed to deliver [56,57]. Herein, we report a sustainable and facile aromatic (mono-, di-, and tri-) halogenation protocol by controlling the stoichiometry of the *N*-halosuccinimide and PEG-400 as the grinding auxiliary in an electrical grinder (Scheme 2).



Results and Discussion

At the outset, the optimization of the reaction conditions was carried out using *p*-cresol (**1a**) as the model substrate with 1.1 equiv of *N*-bromosuccinimide (NBS) for attempted monobromination. They were ground together at the speed of 100 rpm in an electrical grinder (EG) of Agate-made under neat conditions for 30 min. The reaction was incomplete and a mixture containing some starting material (**1a**), two other spots which are identified as *o*-monobromo (**2a**) as major (57%), and *o*-dibrominated *p*-cresol (**3a**) as minor (20%) constituents, was obtained (Table 1, entry 1). Next, the reaction mixture was ground under LAG conditions with ethanol and an improved yield (77%) of the monobromo product **2a**, with a reduced amount of **3a** (12%), and a nominal recovery of the starting material were observed (Table 1, entry 2). Incomplete consumption of starting phenol **1a** was primarily due to over bromination. The LAG in the presence of water afforded relatively inferior results than EtOH (Table 1, entry 3). The use of ethylene glycol and glycerol as the grinding matrix showed improved yields with the monobromo product **2a** formed in 81% and 85% yield, respectively within 10 min (Table 1, entries 4 and 5). Next, liquid polyethylene glycol, PEG-400 was selected as the LAG agent keeping all other parameters the same. Interestingly, the monobrominated product **2a** was obtained almost exclusively in an excellent yield (91%) within just 5 min of grinding (Table 1, entry 6). The attempted model reaction under solid-state grinding using silica gel was sluggish and it afforded **2a** and **3a** in a 3:2 ratio in lower yields (Table 1, entry 7). Under PEG-400-assisted grinding conditions, a study was conducted to determine the suitable stoichiometry of NBS for the bromination reaction. The study revealed that the increased or decreased stoichiometry of NBS adversely affects the reaction outcome leading to either incomplete conversion (Table 1, entries 8 and 9) or to a low yield of the desired monobromo product due to over-bromination (Table 1, entry 10). On the other hand, increasing the grinding speed (120 rpm) did not increase the yield of the desired product or expedite the reaction (Table 1, entry 11). Whereas upon lowering the grinding speed (70 rpm), the yield of the desired monobromo product decreased marginally, and the reaction took a long time for complete conversion (Table 1, entry 12). Next, a short study was conducted by carrying out the reactions on the model substrate **1a** in the solution phase to understand the advantage of grinding over conventional ways (Table S1 in Supporting Information File 1). Again, PEG-400 was found suitable as the solvent (1–2 mL per mmol of *p*-cresol) for the monobromination of *p*-cresol, but the reactions took several hours for completion and showed inferior chemoselectivity producing dibrominated product **3a** in higher quantity in the solution phase (Table S1, entries 6 and 7 in Supporting Information File 1). However, a thick immiscible mixture was formed when only 0.2 mL of PEG-400

Table 1: Optimization of the reaction conditions for the bromination with NBS.^a

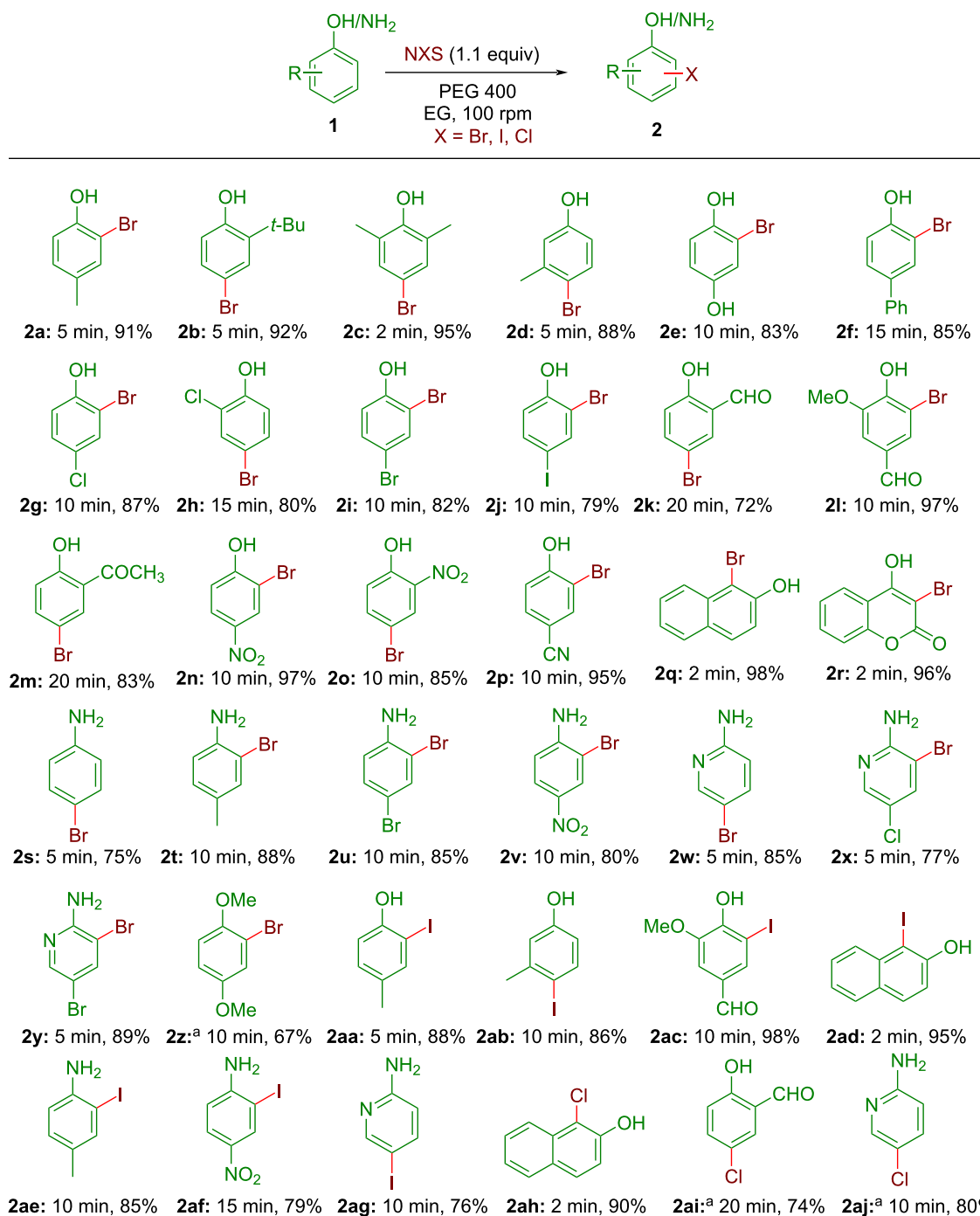
Entry	Grinding media ^b	Equiv of NBS	Grinding speed (rpm)	Time (min)	Yield ^c (%)	
					2a	3a
1	NG	1.1	100	10	57 ^d	20
2	EtOH	1.1	100	10	77 ^d	12
3	H ₂ O	1.1	100	10	63 ^d	15
4	ethylene glycol	1.1	100	10	81 ^d	06
5	glycerol	1.1	100	10	85	05
6	PEG-400	1.1	100	5	91	03
7	SiO ₂	1.1	100	30	45 ^d	28
8	PEG-400	0.9	100	10	62 ^d	–
9	PEG-400	1.0	100	5	84 ^d	03
10	PEG-400	1.2	100	5	78 ^d	08
11	PEG-400	1.1	120	5	89	04
12	PEG-400	1.1	70	15	86	03

^a1 mmol of **1a** and 1.1 mmol NBS are taken for EG; ^b0.2 mL of solvent (300 mg for SiO₂) per mmol of **1a** was used for LAG; ^cisolated yields; ^dsome amount of starting phenol **1a** was also isolated. NG: neat grinding.

were used and the reaction could not proceed to completion (Table S1, entry 8 in Supporting Information File 1). Further, during aqueous work-up at least 10% loss of the water-soluble crude product **2a** was observed in the conventional solution-phase reactions leading to a drop in the isolated yields. Based on the above observations, the optimal reaction conditions for the electrophilic monobromination was set as to grind the substrates (1 mmol) in an automated grinder with 1.1 mmol of NBS at 100 rpm in PEG-400 (0.2 mL per mmol of the substrate) as a grinding auxiliary.

We next explored the substrate scope of the catalyst-free monobromination under the optimized reaction conditions to validate the effectiveness of our method using an indigenous electrical grinder. The results are summarized in Scheme 3. At the outset, several electron-rich and electron-deficient phenol derivatives were converted to the corresponding monobrominated products **2a–r** in high to excellent yields upon employing 1.1 equiv of NBS as the brominating agent and PEG-400 (0.2 mL per mmol of phenols) as the LAG agent. As mentioned, PEG-400 allows the formation of a free-flowing liquid mixture and the reactions were mostly completed within 2–15 min of grinding in an Agate mortar–pestle. In each case, once the reaction got over, the crude product was directly slurried by the addition of silica gel (230–400 mesh, approximately 1 g) and purified by flash chro-

matography eluting with varying proportions of EtOAc/petroleum ether; thus, a typical work-up step was avoided. Moreover, up to 95% of the side product succinimide was also isolated, and considering its possible conversion to NBS [44] it is an attribute to this green protocol by lowering the E-factor. The products were well-characterized by ¹H NMR, ¹³C NMR, IR, and CHN analysis. The NMR spectra of the synthesized compounds matched well with the reported data indicating their successful formation. As such not much substituent effect was seen and the protocol worked well for phenols having electron-donating groups (EDG, products **2b–e**, Scheme 3) or even strong electron-withdrawing groups (EWG, products **2n–p**, Scheme 3) affording high yields of the corresponding monobrominated products. The reaction of halogen-substituted phenols also showed higher yields with no exchange of halogen atoms during the course of the reaction (products **2g–j**, Scheme 3). As expected, exclusive *ortho*-bromination to the phenolic hydroxy group was observed for 4-phenylphenol indicating this electrophilic halogenation is selective to electron-rich aromatic rings only (product **2f**, Scheme 3). Also, aromatic halogenation prevails over α -halogenation of a ketomethyl group as was demonstrated by the formation of product **2m** as the sole product for the bromination of 2'-hydroxyacetophenone (product **2m**, Scheme 3). Notably, easily oxidizable groups like –CHO remained unaffected under the reaction conditions (product **2k**



Scheme 3: Monohalogenation of phenols and anilines by automated grinding with NXS. All yields refer to the isolated products. Note a: Reactions were carried out in the presence of 10 mol % of conc. H_2SO_4 .

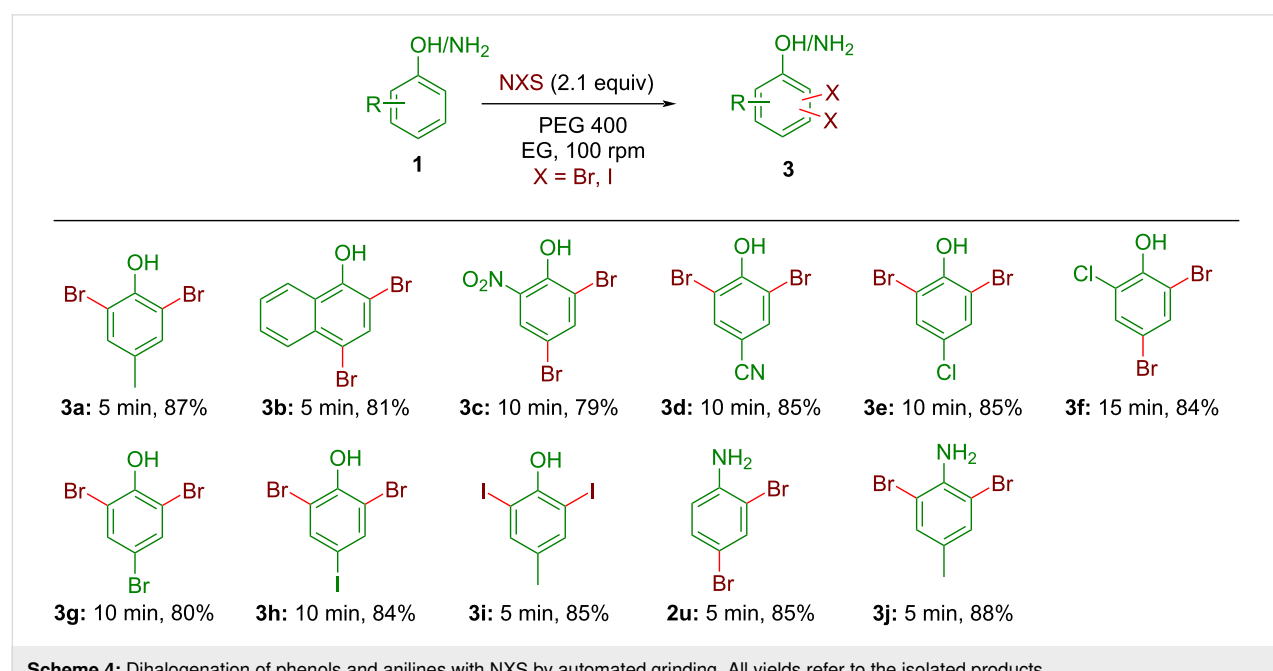
and **2l**, Scheme 3). It is worthy to mention that the bromination on 2-naphthol and coumarin was extremely fast affording >95% yields within just 2 min of grinding (products **2q** and **2r**, Scheme 3). Next, a series of aniline derivatives were taken as the substrates for this electrophilic bromination by NBS. To our delight, the corresponding bromo derivatives were formed in

high yields (75–89%) within 5–15 min of grinding (products **2s–y**, Scheme 3). Once again, no prominent substituent effect was observed in terms of yields or reaction time. Next, we focused our attention on expanding the substrate scope to other electron-rich aromatic systems. The bromination of hydroquinone dimethyl ether was sluggish and a moderate yield

(67%) of the desired monobromo derivative **2z** was achieved only after 30 min of rigorous grinding. However, a negligible conversion was observed for *p*-xylene or mesitylene even after grinding for an hour. Therefore, we restricted our study to the halogenation of phenols and anilines only. Subsequently, a short series of monoiodo derivatives was successfully prepared in high to excellent yields from phenols and anilines by adding 1.1 equiv of NIS with PEG-400 as the LAG agent (product **2aa–ag**, Scheme 3). Notably, both Br- and I-substituents are mainly used as the substrates for cross-coupling reactions indicating the usefulness of the current protocol for quick access to these halo derivatives. Encouraged by this, we attempted monochlorination with selected phenols and anilines. The first attempt with 2-naphthol afforded the desired chloro derivative **2ah** in high yield within 2 min. However, unlike in the case of NBS and NIS, the chlorination by NCS was often found sluggish and complete conversion was not observed even after vigorous grinding for 30 min. Nonetheless, the addition of a catalytic amount of H_2SO_4 (10 mol %) was sufficient to activate NCS and the corresponding chloro derivatives were obtained in good yields (product **2ai** and **2aj**, Scheme 3). It is worthy to note that PEG-400 as the grinding auxiliary not only expedited the reaction but also played a key role in availing better regioselectivity. A very high *para*-selectivity was observed for both phenols and aniline substrates with free *o*- and *p*-positions in the case of bromination as well as iodination (product **2b**, **2d**, **2h**, **2k**, **2s**, **2w**, **2ab**, **2ag**, etc. in Scheme 3). In some cases, the formation of negligible amounts of dihalo derivatives (3–5%) could not be avoided. Only for the attempted monobromination of unsubstituted phenol, the addition of 1.1 equiv of NBS

afforded a mixture of products with reduced regioselectivity to the expected *p*-bromophenol (yield: 62%). From the mechanistic point of view, it is expected that a standard electrophilic aromatic substitution pathway was followed for the halogenation using NXS (X = Br, I, or Cl). Presumably, PEG-400 with several -O- and terminal -OH functionalities helps to enhance the polarization of the N–X bond. Thus, the formation of the halonium ion (X^+) in the reaction medium is faster and stabilized by solvation to offer an extra bit of time for the attack of phenol (or aniline) preferably through *p*-position leading to the formation of the thermodynamically stable halo derivative via a σ -complex formation. The high concentration of substrates and reagents in the close proximity in this solvent-less process and grinding force could be the other reasons for the fast reaction kinetics.

The initial optimization study showed that the presence of excess NBS could increase the yield of undesired dibromo products (Table 1, entry 10). Encouraged by this, a short series of dihalogenated derivatives was prepared under optimized grinding conditions by just changing the stoichiometry of NXS from 1 equiv to 2 equiv (X = Br, I) (Scheme 4). Several electron-rich (products **3a** and **3k**, Scheme 4) and electron-deficient (product **3c–h**, Scheme 4) phenols and anilines were successfully converted to the corresponding dibromo derivatives in good to excellent yields within 5–15 min when 2.1 equiv of NBS were used (Scheme 4). The formation of the corresponding monobromo products was not observed. Similarly, *p*-cresol (**1a**) was converted to the corresponding diiodo derivative **3i** in high yield by using 2.1 equiv of NIS indicating the generality of this

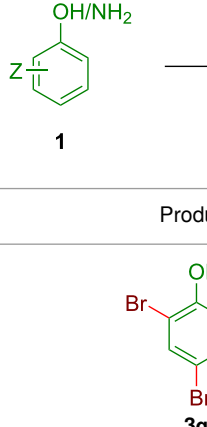
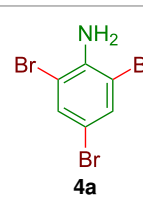
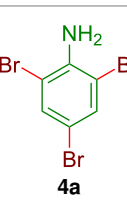
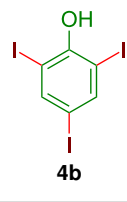
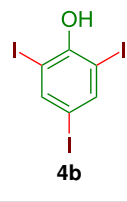
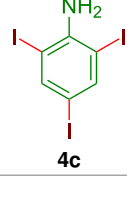
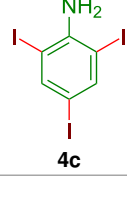


synthetic protocol. Next, the attempted dihalogenation of aniline derivatives also worked well to afford the desired products in high yields (products **2u** and **3j** in Scheme 4). In all cases, no prominent substituent effect was observed in terms of yields and reaction time.

Next, we planned to further diversify this halogenation protocol via automated grinding for the facile access to trihalogenated derivatives by the use of 3 equiv of *N*-halosuccinimides (X = Br, I) (Table 2). Notably, trihalo phenols and anilines are commercial products and used as intermediates of pharmaceutical and agrochemical products. The basic substrates phenol (entry 1, Table 2) and aniline (entry 5, Table 2) afforded the 2,4,6-tribromo derivatives in the presence of NBS in

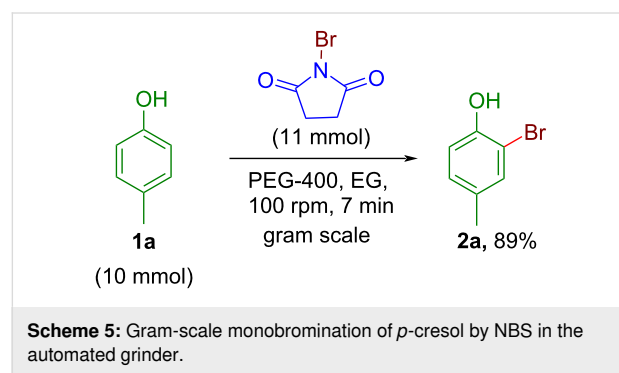
excellent yields just by grinding for 5 min. Similarly, 3 equiv of NIS ensured the formation of 2,4,6-triiodo derivatives in over 90% yields (entries 8 and 11, Table 2). As known, easy decarboxylation (or desulfonylation) was observed for phenols and anilines with carboxylic acid (-CO₂H) or sulfonic acid (-SO₃H) groups both at *o*- or *p*-positions leading to the formation of 2,4,6-trihalo phenols and anilines in excellent yields within just 10 min (Table 2) [58]. Thus simple control of the stoichiometry of NXS could offer the versatility in obtaining mono-, di-, or trihalo derivatives as per the requirement within a very short time, which is a sheer advantage of this mechanochemical method. A further study of mechanochemical decarboxylative aromatic halogenations is underway in our laboratory.

Table 2: Trihalogenation of phenols and anilines with NXS by automated grinding.^a

Entry	Z	Product	Time (min)	Yield (%)		
					1	4
1	H		05	94		
2	<i>o</i> -CO ₂ H		10	86		
3	<i>p</i> -CO ₂ H		10	89		
4	<i>p</i> -SO ₃ H		10	85		
5	H		05	95		
6	<i>p</i> -CO ₂ H		10	90		
7	<i>p</i> -SO ₃ H		05	92		
8	H		05	94		
9	<i>p</i> -CO ₂ H		05	93		
10	<i>p</i> -SO ₃ H		05	95		
11	H		05	92		
12	<i>p</i> -CO ₂ H		05	95		
13	<i>p</i> -SO ₃ H		05	97		

^aAll yields refer to the isolated products.

The scalability of any synthetic protocol is a necessary attribute to access its potential from the laboratory scale to a pilot-scale synthesis. A gram-scale synthesis was conducted with 1.08 g of *p*-cresol (**1a**, 10 mmol) and 1.96 g NBS (11 mmol) in PEG-400 as grinding auxiliary (Scheme 5). The obtained yield of the gram-scale (10 mmol, 89%) synthesis for the monobromo product **2a** was found to be more or less comparable with the yield of small-scale synthesis (1 mmol, 91%). However, the reactions took a slightly longer time (7 min) than the small-scale synthesis. The demonstration of gram-scale reaction implies the potential application of the new protocol in large-scale synthesis with adequate grinding equipment.



Lastly, a comparative study of available methods for *N*-halosuccinimide-aided electrophilic halogenations with our auto-grinding protocol was conducted (Table S2 in Supporting Information File 1). It suggested that the present green method is comparable or better than several other conventional methods in terms of the reaction time, substrate scope, regioselectivity, etc. Moreover, a low E-factor in the range of 2.1–3.6 ensures that the current method could potentially replace the existing conventional methods for the aromatic halogenation of phenols and anilines. Notably, a cost-comparison of our method and the other mechanochemical method by Ghafuri and co-workers was done to understand that the current method is approximately 6 times more cost-effective; besides, the time required for the synthesis of the solid acid catalyst and the cost of high-end milling instruments are additional considerations for that method [52].

Conclusion

In conclusion, we have developed a facile and sustainable mechanochemical route for the catalyst-free halogenation of phenol and aniline derivatives using *N*-halosuccinimides as the reagent. In the protocol, PEG-400 was used as an LAG agent and the reactions were conducted in an automated grinder in open-air at room temperature for quick access to halogenated derivatives. A wide range of substrates was compatible with NXS (X = Br, I, Cl) for electrophilic aryl halogenation without

much substituent effect and by just controlling the stoichiometry of NXS a series of mono-, di-, and trihalogenated phenols and anilines were obtained in a chemoselective manner in good to excellent yields within 2–15 min of grinding. Spontaneous decarboxylation (or desulfonation) was observed in the case of salicylic acids or anthranilic acids leading to 2,4,6-trihalo derivatives when 3 equiv of NXS were used. PEG-400 plays a key role for faster reaction kinetics and to afford better regioselectivity. Almost exclusive *p*-selectivity was observed for the aromatic substrates with free *ortho*- and *para*-positions. The gram-scale reaction shows similar efficiency like smaller batches indicating easy scale-up of this protocol. The method is environmentally friendly and cost-effective having key attributes like simple instrumentation, no aqueous workup, short reaction time, and mild reaction conditions.

Experimental

General procedure for monohalogenation of phenols and anilines

The phenol derivative (**1**, 1.0 mmol) was taken in an Agate mortar attached to an electrical grinder, PEG-400 (0.2 mL) was added as LAG agent, and to the mixture, NBS (1.1 mmol) was added in several portions over 5 min under continuous grinding by a pestle at 100 rpm. The electrical grinding was continued for the specific time period (as mentioned in Scheme 3) and the completion of the reaction was monitored by checking TLC after 2 min, 5 min, 10 min, 15 min as applicable for the reaction. After complete conversion was observed, 0.8–1 g of silica gel (230–400 mesh) was added and the slurry was subjected to flash chromatography and eluted with a mixture of EtOAc/petroleum ether to afford the pure monobromo phenol derivative. The side product succinimide was subsequently eluted using MeOH/CHCl₃ 1:10

Supporting Information

Supporting Information File 1

Experimental procedures, spectral data, tables, and copies of spectra.

[<https://www.beilstein-journals.org/bjoc/content/supplementary/1860-5397-18-100-S1.pdf>]

Funding

SERB, India (project no. EMR/2016/002253) is gratefully acknowledged for financial support. M. B. is grateful to SERB, India (project no. EMR/2016/002253) for financial support, and D. D. is indebted to SERB and BITS, Pilani for research fellowships. A.A.B. is thankful to BITS, Pilani for SRFship.

Acknowledgements

We acknowledge the Central Instrumentation Facilities of BITS-Pilani, Pilani campus and K. K. Birla Goa campus, and Central Analytical Laboratory of BITS-Pilani, Hyderabad campus for NMR spectroscopy.

ORCID® iDs

Dharmendra Das - <https://orcid.org/0000-0002-2478-1257>
 Amrita Chatterjee - <https://orcid.org/0000-0001-8666-2723>
 Mainak Banerjee - <https://orcid.org/0000-0002-6833-5531>

Preprint

A non-peer-reviewed version of this article has been previously published as a preprint: <https://doi.org/10.3762/bxiv.2022.49.v1>

References

- Neilson, A. H., Ed. *Organic Bromine and Iodine Compounds; The Handbook of Environmental Chemistry*, Vol. 3R; Springer: Berlin, Heidelberg, 2003. doi:10.1007/978-3-540-37055-0
- Öztaşkin, N.; Çetinkaya, Y.; Taslimi, P.; Göksu, S.; Gülcin, İ. *Bioorg. Chem.* **2015**, *60*, 49–57. doi:10.1016/j.bioorg.2015.04.006
- Liu, M.; Hansen, P. E.; Lin, X. *Mar. Drugs* **2011**, *9*, 1273–1292. doi:10.3390/md9071273
- Jesus, A.; Correia-da-Silva, M.; Afonso, C.; Pinto, M.; Cidade, H. *Mar. Drugs* **2019**, *17*, 73. doi:10.3390/17020073
- Gribble, G. W. *J. Chem. Educ.* **2004**, *81*, 1441–1449. doi:10.1021/ed081p1441
- Ruiz-Castillo, P.; Buchwald, S. L. *Chem. Rev.* **2016**, *116*, 12564–12649. doi:10.1021/acs.chemrev.6b00512
- Sun, C.-L.; Shi, Z.-J. *Chem. Rev.* **2014**, *114*, 9219–9280. doi:10.1021/cr400274j
- Tellis, J. C.; Kelly, C. B.; Primer, D. N.; Jouffroy, M.; Patel, N. R.; Molander, G. A. *Acc. Chem. Res.* **2016**, *49*, 1429–1439. doi:10.1021/acs.accounts.6b00214
- Weix, D. J. *Acc. Chem. Res.* **2015**, *48*, 1767–1775. doi:10.1021/acs.accounts.5b00057
- Tabassum, S.; Zahoor, A. F.; Ahmad, S.; Noreen, R.; Khan, S. G.; Ahmad, H. *Mol. Diversity* **2022**, *26*, 647–689. doi:10.1007/s11030-021-10195-6
- Jung, N.; Bräse, S. *Eur. J. Org. Chem.* **2009**, 4494–4502. doi:10.1002/ejoc.200900632
- Busacca, C. A.; Fandrick, D. R.; Song, J. J.; Senanayake, C. H. *Adv. Synth. Catal.* **2011**, *353*, 1825–1864. doi:10.1002/adsc.201100488
- Jeschke, P. *Eur. J. Org. Chem.* **2022**, e202101513. doi:10.1002/ejoc.202101513
- Gao, Y.; Feng, C.; Seo, T.; Kubota, K.; Ito, H. *Chem. Sci.* **2022**, *13*, 430–438. doi:10.1039/d1sc05257h
- Taylor, R. *Electrophilic Aromatic Substitution*; John Wiley & Sons: Chichester, UK, 1990.
- Saikia, I.; Borah, A. J.; Phukan, P. *Chem. Rev.* **2016**, *116*, 6837–7042. doi:10.1021/acs.chemrev.5b00400
- Voskressensky, L. G.; Golantsov, N. E.; Maharramov, A. M. *Synthesis* **2016**, *48*, 615–643. doi:10.1055/s-0035-1561503
- Muathen, H. A. *J. Org. Chem.* **1992**, *57*, 2740–2741. doi:10.1021/jo00035a038
- Majetich, G.; Hicks, R.; Reister, S. *J. Org. Chem.* **1997**, *62*, 4321–4326. doi:10.1021/jo970135w
- Roy, S. C.; Guin, C.; Rana, K. K.; Maiti, G. *Tetrahedron Lett.* **2001**, *42*, 6941–6942. doi:10.1016/s0040-4039(01)01412-5
- Naresh, M.; Kumar, M. A.; Reddy, M. M.; Swamy, P.; Nanubolu, J. B.; Narendar, N. *Synthesis* **2013**, *45*, 1497–1504. doi:10.1055/s-0033-1338431
- Li, X.-L.; Wu, W.; Fan, X.-H.; Yang, L.-M. *RSC Adv.* **2013**, *3*, 12091–12095. doi:10.1039/c3ra41664j
- Krishna Mohan, K. V. V.; Narendar, N.; Srinivasu, P.; Kulkarni, S. J.; Raghavan, K. V. *Synth. Commun.* **2004**, *34*, 2143–2152. doi:10.1081/scc-120038491
- Ross, S. D.; Finkelstein, M.; Petersen, R. C. *J. Am. Chem. Soc.* **1958**, *80*, 4327–4330. doi:10.1021/ja01549a053
- Mitchell, R. H.; Lai, Y.-H.; Williams, R. V. *J. Org. Chem.* **1979**, *44*, 4733–4735. doi:10.1021/jo00393a066
- Carreño, M. C.; García Ruano, J. L.; Sanz, G.; Toledo, M. A.; Urbano, A. *J. Org. Chem.* **1995**, *60*, 5328–5331. doi:10.1021/jo00121a064
- Zysman-Colman, E.; Arias, K.; Siegel, J. S. *Can. J. Chem.* **2009**, *87*, 440–447. doi:10.1139/v08-176
- Pingali, S. R. K.; Madhav, M.; Jursic, B. S. *Tetrahedron Lett.* **2010**, *51*, 1383–1385. doi:10.1016/j.tetlet.2010.01.002
- Pramanick, P. K.; Hou, Z.-L.; Yao, B. *Tetrahedron* **2017**, *73*, 7105–7114. doi:10.1016/j.tet.2017.10.073
- Bovonsombat, P.; Teeecomegaet, P.; Kulvaranon, P.; Pandey, A.; Chobtumskul, K.; Tungsirisup, S.; Sophanpanichkul, P.; Losuwanakul, S.; Soimaneewan, D.; Kanjanwongpaisan, P.; Siricharoensang, P.; Choosakoonkriang, S. *Tetrahedron* **2017**, *73*, 6564–6572. doi:10.1016/j.tet.2017.10.005
- Song, S.; Sun, X.; Li, X.; Yuan, Y.; Jiao, N. *Org. Lett.* **2015**, *17*, 2886–2889. doi:10.1021/acs.orglett.5b00932
- Bovonsombat, P.; Ali, R.; Khan, C.; Leykajarakul, J.; Pla-on, K.; Aphimanchindakul, S.; Pungcharoenpong, N.; Timsuea, N.; Arunrat, A.; Punpongjareorn, N. *Tetrahedron* **2010**, *66*, 6928–6935. doi:10.1016/j.tet.2010.06.041
- Racys, D. T.; Sharif, S. A. I.; Pimlott, S. L.; Sutherland, A. *J. Org. Chem.* **2016**, *81*, 772–780. doi:10.1021/acs.joc.5b02761
- Mostafa, M. A. B.; Bowley, R. M.; Racys, D. T.; Henry, M. C.; Sutherland, A. *J. Org. Chem.* **2017**, *82*, 7529–7537. doi:10.1021/acs.joc.7b01225
- Nishii, Y.; Ikeda, M.; Hayashi, Y.; Kawauchi, S.; Miura, M. *J. Am. Chem. Soc.* **2020**, *142*, 1621–1629. doi:10.1021/jacs.9b12672
- Hirose, Y.; Yamazaki, M.; Nogata, M.; Nakamura, A.; Maegawa, T. *J. Org. Chem.* **2019**, *84*, 7405–7410. doi:10.1021/acs.joc.9b00817
- Xu, H.; Hu, L.; Zhu, G.; Zhu, Y.; Wang, Y.; Wu, Z.-G.; Zi, Y.; Huang, W. *RSC Adv.* **2022**, *12*, 7115–7119. doi:10.1039/d2ra00197g
- Xu, X.; Luo, J. *ChemSusChem* **2019**, *12*, 4601–4616. doi:10.1002/cssc.201901951
- Bedford, R. B.; Haddow, M. F.; Mitchell, C. J.; Webster, R. L. *Angew. Chem., Int. Ed.* **2011**, *50*, 5524–5527. doi:10.1002/anie.201101606
- John, A.; Nicholas, K. M. *J. Org. Chem.* **2012**, *77*, 5600–5605. doi:10.1021/jo300713h
- Sun, X.; Sun, Y.; Zhang, C.; Rao, Y. *Chem. Commun.* **2014**, *50*, 1262–1264. doi:10.1039/c3cc47431c
- Schröder, N.; Wencel-Delord, J.; Glorius, F. *J. Am. Chem. Soc.* **2012**, *134*, 8298–8301. doi:10.1021/ja302631j
- Bhardwaj, N.; Singh, A. K.; Tripathi, N.; Goel, B.; Indra, A.; Jain, S. K. *New J. Chem.* **2021**, *45*, 14177–14183. doi:10.1039/d1nj02777h

44. Tang, R.-J.; Milcent, T.; Crousse, B. *J. Org. Chem.* **2018**, *83*, 930–938. doi:10.1021/acs.joc.7b02920

45. Friščić, T.; Mottillo, C.; Titi, H. M. *Angew. Chem., Int. Ed.* **2020**, *59*, 1018–1029. doi:10.1002/anie.201906755

46. Stolle, A.; Ranu, B. C., Eds. *Ball milling towards green synthesis: Applications, projects, challenges*; Green Chemistry Series; Royal Society of Chemistry: Cambridge, UK, 2014. doi:10.1039/9781782621980

47. Gomollón-Bel, F. *Chem. Int.* **2019**, *41* (2), 12–17. doi:10.1515/ci-2019-0203

48. Tanaka, K.; Toda, F. *Chem. Rev.* **2000**, *100*, 1025–1074. doi:10.1021/cr940089p

49. Banerjee, M.; Panjikar, P. C.; Das, D.; Iyer, S.; Bhosle, A. A.; Chatterjee, A. *Tetrahedron* **2022**, *112*, 132753. doi:10.1016/j.tet.2022.132753

50. Das, D.; Bhutia, Z. T.; Panjikar, P. C.; Chatterjee, A.; Banerjee, M. *J. Heterocycl. Chem.* **2020**, *57*, 4099–4107. doi:10.1002/jhet.4106

51. Bose, A.; Mal, P. *Tetrahedron Lett.* **2014**, *55*, 2154–2156. doi:10.1016/j.tetlet.2014.02.064

52. Ghanbari, N.; Ghafuri, H.; Zand, H. R. E.; Eslami, M. *SynOpen* **2017**, *1*, 143–146. doi:10.1055/s-0036-1590959

53. Liu, Z.; Xu, H.; Wang, G.-W. *Beilstein J. Org. Chem.* **2018**, *14*, 430–435. doi:10.3762/bjoc.14.31

54. Bhutia, Z. T.; Prasannakumar, G.; Das, A.; Biswas, M.; Chatterjee, A.; Banerjee, M. *ChemistrySelect* **2017**, *2*, 1183–1187. doi:10.1002/slct.201601672

55. Banerjee, M.; Chatterjee, A.; Kumar, V.; Bhutia, Z. T.; Khandare, D. G.; Majik, M. S.; Roy, B. G. *RSC Adv.* **2014**, *4*, 39606–39611. doi:10.1039/c4ra07058e

56. Das, D.; Bhutia, Z. T.; Chatterjee, A.; Banerjee, M. *J. Org. Chem.* **2019**, *84*, 10764–10774. doi:10.1021/acs.joc.9b01280

57. Declerck, V.; Colacino, E.; Bantrel, X.; Martinez, J.; Lamaty, F. *Chem. Commun.* **2012**, *48*, 11778–11780. doi:10.1039/c2cc36286d

58. Varenikov, A.; Shapiro, E.; Gandelman, M. *Chem. Rev.* **2021**, *121*, 412–484. doi:10.1021/acs.chemrev.0c00813

License and Terms

This is an open access article licensed under the terms of the Beilstein-Institut Open Access License Agreement (<https://www.beilstein-journals.org/bjoc/terms>), which is identical to the Creative Commons Attribution 4.0 International License (<https://creativecommons.org/licenses/by/4.0>). The reuse of material under this license requires that the author(s), source and license are credited. Third-party material in this article could be subject to other licenses (typically indicated in the credit line), and in this case, users are required to obtain permission from the license holder to reuse the material.

The definitive version of this article is the electronic one which can be found at:

<https://doi.org/10.3762/bjoc.18.100>



Mechanochemical bottom-up synthesis of phosphorus-linked, heptazine-based carbon nitrides using sodium phosphide

Blaine G. Fiss^{†1}, Georgia Douglas^{‡1}, Michael Ferguson¹, Jorge Becerra², Jesus Valdez³, Trong-On Do^{*2}, Tomislav Friščić^{*1} and Audrey Moores^{*1,4}

Letter

Open Access

Address:

¹Centre in Green Chemistry and Catalysis, Department of Chemistry, McGill University, 801 Sherbrooke Street West, Montréal, Québec, Canada, ²Department of Chemical Engineering, Laval University, Québec City, Québec, Canada, ³Facility for Electron Microscopy Research (FEMR), McGill University, Montréal, Québec, Canada and ⁴Department of Materials Engineering, McGill University, 3610 University Street, Montréal, Québec, Canada

Email:

Trong-On Do^{*} - trong-on.do@gch.ulaval.ca; Tomislav Friščić^{*} - tomislav.friscic@mcgill.ca; Audrey Moores^{*} - audrey.moores@mcgill.ca

* Corresponding author † Equal contributors

Keywords:

carbon nitride; density functional theory; mechanochemistry; phosphorus; photochemistry

Beilstein J. Org. Chem. **2022**, *18*, 1203–1209.

<https://doi.org/10.3762/bjoc.18.125>

Received: 05 June 2022

Accepted: 15 August 2022

Published: 12 September 2022

This article is part of the thematic issue "Mechanochemistry III".

Guest Editors: J. G. Hernández and L. Borchardt

© 2022 Fiss et al.; licensee Beilstein-Institut.

License and terms: see end of document.

Abstract

Herein, we present the bottom-up, mechanochemical synthesis of phosphorus-bridged heptazine-based carbon nitrides (g-h-PCN). The structure of these materials was determined through a combination of powder X-ray diffraction (PXRD), X-ray photoelectron spectroscopy (XPS), ³¹P magic angle spinning nuclear magnetic resonance (MAS NMR), density functional theory (DFT) and electron energy loss spectroscopy (EELS). Compared to traditional furnace-based techniques, the presented method utilizes milder conditions, as well as shorter reaction times. Both samples of g-h-PCN directly after milling and aging and after an hour of annealing at 300 °C (g-h-PCN300) show a reduction in photoluminescent recombination, as well as a nearly two-time increase in photocurrent under broad spectrum irradiation, which are appealing properties for photocatalysis.

Introduction

The development of heteroatom-doped graphitic carbon nitrides (g-CN) has been a rapidly growing area of research since their first report towards water splitting in 2009 [1]. Since that time, the addition of elements such as boron [2], phosphorus [3-5], sulfur and oxygen [6] have shown to help minimize the bandgap

of these metal-free photocatalysts, as well as improve their overall stability. Traditional routes to incorporate phosphorus have relied on high-temperature [7] or microwave [8] syntheses, and often proceed through the introduction of a phosphorus atom within the heptazine ring, which constitutes the building

block of g-CN, as opposed to in a linking position. Computational studies by Hartley and Martsinovich have investigated the influence of various linkers, including phosphorus atoms, on both the structure and optical behavior of heptazine-based graphitic carbon nitrides [3]. Yet, examples of carbon nitride materials linked together via phosphorus atoms are limited, likely due to challenges in controlling the insertion of phosphorus atoms as linkers under high energy conditions. Mechanochemistry [9–12] has proven to be effective for the synthesis of a variety of polymers [13–17], nanomaterials [18–22], in crystal engineering [23–25], as well as in the synthesis of inorganic materials [26–30] and organic small molecules [31–37]. The ability to avoid bulk solvent and mild reaction conditions allowed by such techniques are beneficial not only from a green chemistry perspective [11], but they also afford conditions conducive to new reactivities and the development of novel materials [9]. Previously, we have explored the synthesis of phosphorus-bridged g-CN-type materials produced from a triazine unit and found that the resulting material featured good photochemical properties (Scheme 1) [38]. Yet, conventional g-CN materials are not based on triazine units, but rather on heptazine ones, thus featuring more open structures. In an effort to replicate a structure closer to known g-CN systems, we explored herein the use of solvent-free, room temperature mechanochemistry to access phosphorus-linked carbon nitride with repeating heptazine units, which were found to show improved photochemistry over pristine graphitic carbon nitride (g-CN). Additionally, the effect of a 1-hour annealing period at 300 °C on the overall structure and photochemical properties of the material was investigated.

Results and Discussion

Employing a similar method to the one previously developed by our group (Scheme 1a) [38], equimolar amounts of sodium

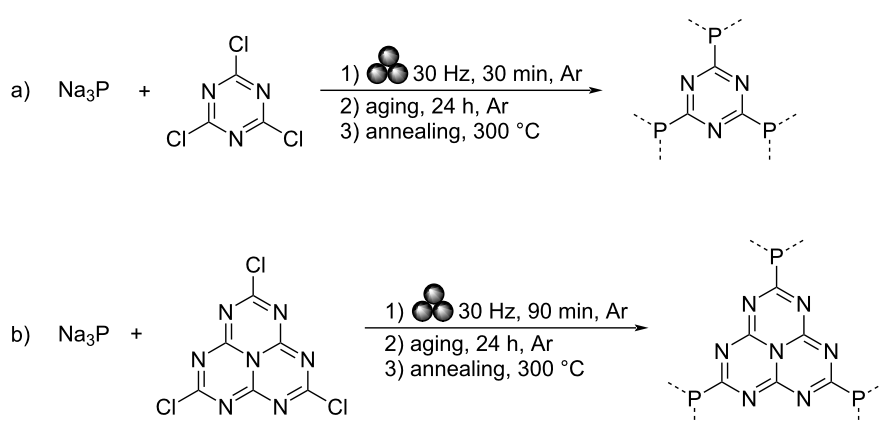
phosphide (Na_3P) and trichlorotriazine were combined in a vibrational ball mill and milled at 30 Hz for 90 minutes under an argon atmosphere (Scheme 1b). As trichloroheptazine was not readily available commercially, it was synthesized from melem in three steps following a known procedure (see Supporting Information File 1 for the detailed procedure) [4]. The milled powder was then allowed to age under an argon atmosphere for 24 hours, prior to washing via centrifugation in a 3:1 by volume mixture of ethanol and deionized (DI) water. This afforded a material referred to below as g-h-PCN. Alternatively, the sample was annealed for 1 hour at 300 °C under a flow of argon gas, affording the material designated g-h-PCN300.

Powder X-ray diffraction (PXRD)

To confirm the formation of a layered structure, powder X-ray diffraction (PXRD) was performed on g-h-PCN and g-h-PCN300 (Figure 1, green and teal). Both g-h-PCN and g-h-PCN300 were largely amorphous but showed two broad Bragg reflections at $2\theta = 16^\circ$ and 28° . This suggests a high thermal stability of the g-h-PCN structure, being formed during the mild milling and aging conditions, with no need for annealing.

X-ray photoelectron spectroscopy (XPS)

To gain insight into the atomic speciation within the structure and establish phosphorus atoms are linkers between heptazine units, X-ray photoelectron spectroscopy (XPS) was used to probe the surface. In g-h-PCN, XPS scans focused on carbon 1s showed three major peaks at 284.7, 286.4, and 288.6 eV, corresponding to $\text{C}=\text{N}$, $\text{C}-\text{OH}$ and $\text{C}=\text{O}$ signals, respectively (Figure 2a), as well as a peak centered on 292.1 eV due to charging effects [39]. The presence of $\text{C}=\text{N}$ bonds established by XPS indicates that the heptazine structure was preserved during milling and aging with Na_3P . Nitrogen 1s focused scans



Scheme 1: a) Mechanocochesical synthesis of g-PCN from sodium phosphide and trichlorotriazine (previous work [38]) and b) g-h-PCN from sodium phosphide and trichloroheptazine (this work).

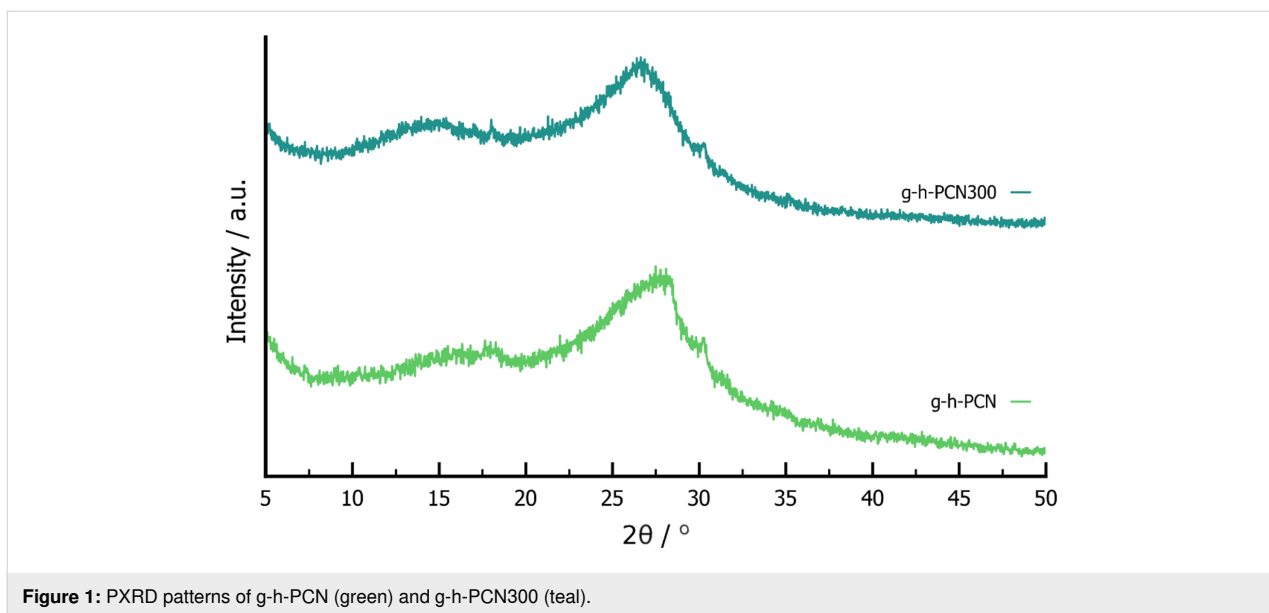


Figure 1: PXRD patterns of g-h-PCN (green) and g-h-PCN300 (teal).

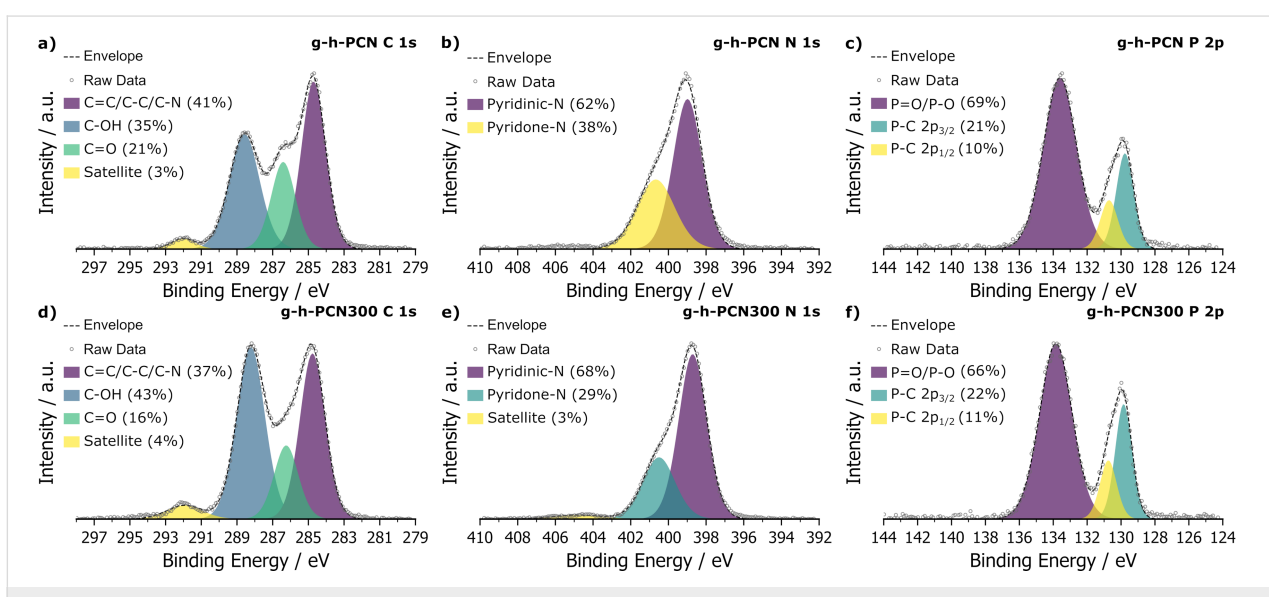


Figure 2: XPS scans of a) C 1s, b) N 1s and c) P 2p for the pre-annealed g-h-PCN and d) C 1s, e) N 1s and f) P 2p focused scans of g-h-PCN300 after annealing at 300 °C for 1 hour.

of g-h-PCN showed a 62% to 38% ratio of pyridinic to pyridone-N type nitrogen environments, centered on 399.0 eV and 400.7 eV, respectively [16,40] (Figure 2b). This suggests that while the majority of the heptazine ring remained pyridinic in nature, partial reduction of the ring structure, due to the reductive nature of Na_3P and mild oxidation during ambient workup following milling and aging, can also have occurred. Additionally, the phosphorus 2p signal in g-h-PCN showed the majority of phosphorus exists as a mixture of P=O and P-O species, with a major peak centered at 133.6 eV (69%, Figure 2c). These species are formed by oxidation with air and hydrolysis upon quenching in water and ethanol at the end of the aging step.

g-h-PCN300 featured the same three major carbon 1s peaks at 284.8, 286.2 and 288.2 eV for $\text{C}=\text{N/C=C}$, C=O and C-OH species, respectively, as well as the charging peak seen in g-h-PCN. In g-h-PCN300, a reduction of the $\text{C}=\text{N}$ ratio to 37%, reduction of C=O character from 21% to 18% compared to g-h-PCN and an increase in C-OH character from 35% to 43% suggests mild hydrolysis, likely of terminal trichloroheptazine, during the annealing step at 300 °C, even under a flow of argon gas (Figure 2d). The nitrogen 1s scans show a similar trend, with the ratio of pyridinic and pyridone nitrogen being 68% and 29%, respectively, compared to 62% and 38% in g-h-PCN (Figure 2e). Phosphorus 2p focused scans of

g-h-PCN300 showed a slight reduction in P–O and P=O bond character from g-h-PCN to g-h-PCN300 down from 69% to 66% (Figure 2f).

Analysis by infrared spectroscopy

The structural motifs seen through XPS were further validated by Fourier-transform infrared attenuated total reflectance (FTIR-ATR) spectroscopy. For g-h-PCN, the sharp absorption band at 800 cm^{-1} was indicative of the heptazine breathing mode, typically seen for nitrogen- and phosphorus-linked C_3N_4 materials (Supporting Information File 1, Figure S3, purple) [41]. The retention of C=N bonds was also further supported by the observation of a series of bands in the range of $1300\text{--}1800\text{ cm}^{-1}$. While the retention of the heptazine ring structure was evident by FTIR-ATR, a low-intensity additional signal at $\approx 950\text{ cm}^{-1}$ is also seen, indicative of the formation of P–C bonds [42], consistent with the results of XPS analysis (Supporting Information File 1, Figure S3, teal). For the g-h-PCN300 material, the overall spectrum showed similar features to that of g-h-PCN, notably retaining the sharp absorption band corresponding to the heptazine breathing mode at 800 cm^{-1} , while also retaining the characteristic P–C vibration at 950 cm^{-1} (Supporting Information File 1, Figure S3, green).

STEM-EELS analysis

The composition and particle morphology were investigated further using scanning tunneling electron microscopy-electron energy loss spectroscopy (STEM-EELS). The STEM-EELS data for a g-h-PCN sample prior to annealing showed equal distribution of carbon and nitrogen with minimal phosphorus present, and particles roughly 400 nm in length (Supporting Information File 1, Figure S4a). Upon annealing at $300\text{ }^\circ\text{C}$ for 1 hour under argon, the phosphorus content is shown to increase, while still remaining partially localized, with the parti-

cles retaining their size and morphology (Supporting Information File 1, Figure S4b).

^{31}P magic angle spinning (MAS) NMR

Bulk solid-state analysis of the heptazine-based materials showed similar resonances to previous work by our group on phosphorus-linked triazine networks [38]. The ^{31}P MAS NMR of g-h-PCN showed a broad resonance centered around -8.9 ppm , with a sharp residual phosphate resonance at 0.9 ppm (Figure 3a). NMR analysis of similar materials, by our group as well as others, suggest that the broad resonance corresponds to a largely amorphous phase with predominately phosphate and phosphite-like environments, with the broad resonance at -8.9 ppm possibly corresponding to hydrated sodium phosphate byproducts [43,44]. The NMR spectrum of the g-h-PCN300 material showed an up-field shift of all main resonances towards -14.4 ppm and -20.6 ppm (Figure 3b). As previously shown by our group [38], such a shift in main resonance positioning is indicative of the organization of the formed sheets, indicating a layered structure.

Computational analysis

The ^{31}P NMR chemical shifts were calculated using the plane-wave density function theory (DFT) code CASTEP v20.11 (see Supporting Information File 1 for full computational details) [45]. In the absence of an experimentally resolved crystal structure for g-h-PCN, we followed a similar methodology to our previous work [38] of substituting bridging nitrogen atoms for phosphorus in previously reported heptazine-based graphitic carbon nitrides. We adapted the ab initio predicted structures for a network of corrugated sheets [46] (Figure 4a and 4b) and planar sheets (Figure 4c) [47]. Additionally, we modelled a chlorine terminated monomeric unit based on an experimentally resolved, nitrogen-bridged, paddlewheel structure (Figure 4d) [48]. Calculations resulted in a single chemical environment for

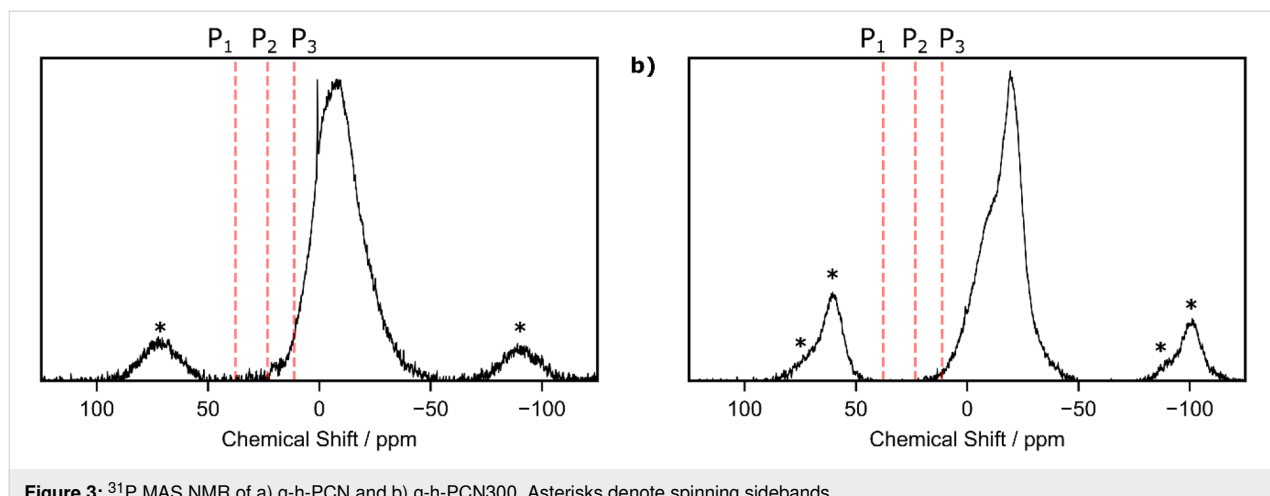


Figure 3: ^{31}P MAS NMR of a) g-h-PCN and b) g-h-PCN300. Asterisks denote spinning sidebands.

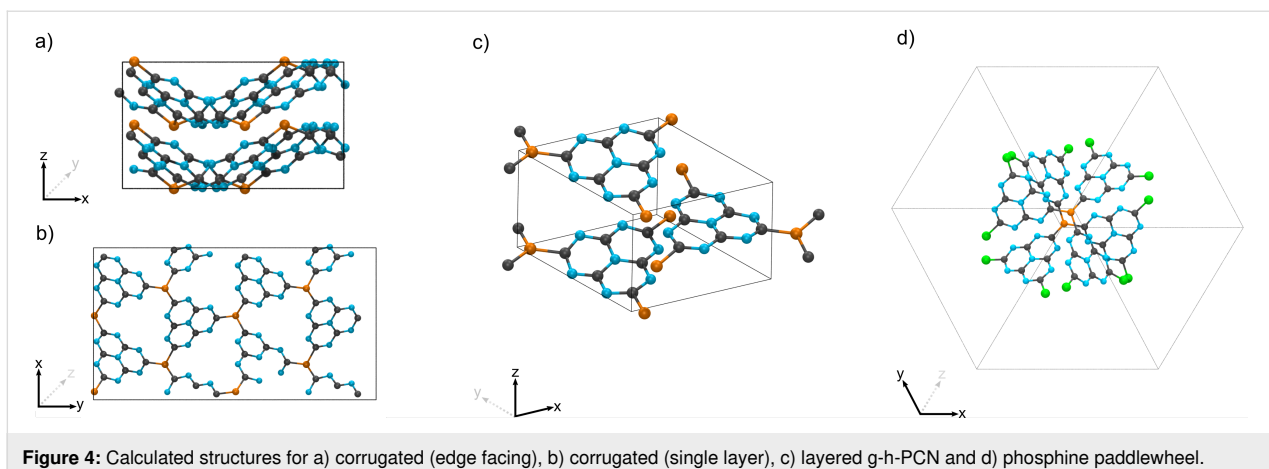


Figure 4: Calculated structures for a) corrugated (edge facing), b) corrugated (single layer), c) layered g-h-PCN and d) phosphine paddlewheel.

the phosphorus atoms in the three model structures. The corrugated and planar network structures have calculated ^{31}P chemical shifts at 37.7 ppm (P_1) and 23.3 ppm (P_2), respectively, while that of the paddlewheel monomer is at 11.2 ppm (P_3). The calculated shifts demonstrate phosphorus environments in the mechanochemically synthesized material are distinct to those calculated in *ab initio* predicted models of the pure reaction product. The variations may be ascribed to the oxygen content found by XPS (Figure 2) or that the mechanochemically synthesized material exists in a different spatial configuration to those previously predicted [46,47].

Thermal stability

Prior to annealing, g-h-PCN was found to show thermal stability upwards of 200 °C through TGA in nitrogen and air (Supporting Information File 1, Figures S6 and S7). The initial loss seen for both samples is attributed to surface-bound water and carbon dioxide. The g-h-PCN300 retains more mass to upwards of 400 °C in both air and nitrogen, however, at higher temperature (>500 °C), g-h-PCN shows an additional loss of \approx 5 wt % compared to g-h-PCN. Overall, under both air and nitrogen, the g-h-PCN retains between 25–35% of its relative mass, up to 800 °C.

Photochemical activity

The photochemical behavior of both g-h-PCN (Supporting Information File 1, Figure S5a, blue trace) and g-h-PCN300 (Figure S5a, green) was investigated by diffuse reflectance spectroscopy (DRS), and compared to that of a pure g-CN sample made by annealing melamine in a loosely capped alumina crucible at 550 °C for 4 hours, with a ramp rate of 5 °C min $^{-1}$ [49]. The g-CN material was found to exhibit an absorption edge at \approx 425 nm (Figure S5a, purple), typical for polymerized and graphitic heptazine materials [50,51]. Both phosphorus-containing structures featured broadened absorption ranges compared to g-CN, with g-h-PCN showing a red-shifted

maximum at \approx 572 nm (Figure S5a, blue) and g-h-PCN300 (Figure S5a, teal) showing a similar, also red-shifted maximum at 525 nm. Additionally, photoluminescence (PL) measurements showed an initially reduced absorption intensity for g-h-PCN (Figure S5b, blue) compared to that of g-CN (Figure S5b, purple) with further reduction notable in absorption for g-h-PCN300 (Figure S5b, teal). This reduction in photoluminescence has previously been reported for phosphorus-doped carbons and carbon nitrides [52], as the addition of Lewis basic heteroatoms improves the stability of excitons, slowing the rate of recombination. Time-resolved lifetimes showed a marked increase upon replacement of the nitrogen linker for phosphorus. Nitrogen-linked g-CN showed exciton lifetimes of 4.2 μ s, while the introduction of a phosphorus linker in g-h-PCN increases the lifetime to 67 μ s, with g-h-PCN300 showing lifetimes of 42 μ s. We have also observed a similar effect in triazine-based phosphorus-linked graphitic CN structures, with lifetimes of 4.7 and 39 μ s seen for g-PCN and g-PCN300, respectively [38].

Improved charge transfer was further confirmed through photocurrent and Nyquist measurements, comparing to pristine g-CN. Photocurrent measurements showed an initial decrease from 10 to \approx 5 μ A for g-h-PCN (Supporting Information File 1, Figure S4c, blue) compared to pristine g-CN (Figure S4c, purple) respectively after 250 s. The g-h-PCN300 material showed increased photocurrent behavior to both g-CN and g-h-PCN, with photocurrent values of \approx 16 μ A (Figure S4c, teal), further demonstrating the benefit of both the presence of phosphorus linkages, as well as thermal annealing for the photoactivity. Finally, Nyquist plots (see Supporting Information File 1, Table S1 for details) of g-h-PCN (Figure S4d, blue) and g-h-PCN300 (Figure S4d, teal) showed lower resistivity compared to pure g-CN (Figure S4d, purple), further supporting the idea that the g-h-PCN series enables better charge mobility due to phosphorus linkages.

Conclusion

Mechanochemistry provided modular, room temperature access to phosphorus-linked carbon nitrides based on heptazine units, through the combination of sodium phosphide and trichloroheptazine. A combination of experimental PXRD, XPS, MAS NMR, as well as theoretical (DFT) approaches confirmed the formation of P–C linkages between repeating heptazine units in the mechanochemically prepared material, with the retention of the heptazine subunits. The introduction of phosphorus linkages reduced photoluminescent recombination and improved exciton lifetimes, when compared to nitrogen-linked g-CN. Overall, this supports future investigations of the room-temperature mechanochemical synthesis of heteroatom containing carbons as well as the benefit of pairing DFT calculations to experimental, structural studies.

Supporting Information

Supporting Information File 1

General methods and materials as well as additional spectra.

[<https://www.beilstein-journals.org/bjoc/content/supplementary/1860-5397-18-125-S1.pdf>]

Acknowledgements

We thank the McGill Institute for Advanced Materials, the Facility for Electron Microscopy Research (FEMR), the MC² facility, McGill University Institute for Advanced Material (MIAM) for the use of their microscopy and spectroscopy equipment.

Funding

We are grateful for the support of the Natural Science and Engineering Research Council of Canada (NSERC) Discovery Grant and Discovery Accelerator Supplement, the Canada Foundation for Innovation (CFI), the McGill Sustainability Systems Initiative (MSSI), the Fonds de Recherche du Québec – Nature et Technologies (FRQNT) – Centre for Green Chemistry and Catalysis (CGCC), the Walter C. Sumner Memorial Fellowship (B. G. F.), McGill University and Université de Laval. This research was enabled in part by support provided by Calcul Québec (<https://www.calculquebec.ca>) and Compute Canada (<https://www.computecanada.ca>).

ORCID® iDs

Blaine G. Fiss - <https://orcid.org/0000-0002-4791-3689>

Georgia Douglas - <https://orcid.org/0000-0002-1538-7223>

Michael Ferguson - <https://orcid.org/0000-0002-5479-1878>

Jorge Becerra - <https://orcid.org/0000-0002-2678-0995>

Trong-On Do - <https://orcid.org/0000-0002-7785-5299>

Tomislav Friščić - <https://orcid.org/0000-0002-3921-7915>

Audrey Moores - <https://orcid.org/0000-0003-1259-913X>

Preprint

A non-peer-reviewed version of this article has been previously published as a preprint: <https://doi.org/10.3762/bxiv.2022.45.v1>

References

1. Wang, X.; Maeda, K.; Thomas, A.; Takanabe, K.; Xin, G.; Carlsson, J. M.; Domen, K.; Antonietti, M. *Nat. Mater.* **2009**, *8*, 76–80. doi:10.1038/nmat2317
2. Guo, Y.; Wang, R.; Wang, P.; Rao, L.; Wang, C. *ACS Sustainable Chem. Eng.* **2019**, *7*, 5727–5741. doi:10.1021/acssuschemeng.8b05150
3. Hartley, G. O.; Martsinovich, N. *Faraday Discuss.* **2021**, *227*, 341–358. doi:10.1039/c9fd00147f
4. Kroke, E.; Schwarz, M.; Horath-Bordon, E.; Kroll, P.; Noll, B.; Norman, A. D. *New J. Chem.* **2002**, *26*, 508–512. doi:10.1039/b111062b
5. Zhang, Y.; Mori, T.; Ye, J.; Antonietti, M. *J. Am. Chem. Soc.* **2010**, *132*, 6294–6295. doi:10.1021/ja101749y
6. Liu, M.; Yang, K.; Li, Z.; Fan, E.; Fu, H.; Zhang, L.; Zhang, Y.; Zheng, Z. *Chem. Commun.* **2022**, *58*, 92–95. doi:10.1039/d1cc05619k
7. Wang, Q.; Gou, H.; Zhu, L.; Huang, H.-T.; Biswas, A.; Chaloux, B. L.; Epshteyn, A.; Yesinowski, J. P.; Liu, Z.; Cody, G.; Ma, M.; Zhao, Z.; Fei, Y.; Prescher, C.; Greenberg, E.; Prakapenka, V. B.; Strobel, T. A. *ACS Mater. Lett.* **2019**, *1*, 14–19. doi:10.1021/acsmaterialslett.9b00010
8. Zou, J.; Yu, Y.; Qiao, K.; Wu, S.; Yan, W.; Cheng, S.; Jiang, N.; Wang, J. *J. Mater. Sci.* **2020**, *55*, 13618–13633. doi:10.1007/s10853-020-04862-6
9. Do, J.-L.; Friščić, T. *ACS Cent. Sci.* **2017**, *3*, 13–19. doi:10.1021/acscentsci.6b00277
10. Friščić, T.; Mottillo, C.; Titi, H. M. *Angew. Chem., Int. Ed.* **2020**, *59*, 1018–1029. doi:10.1002/anie.201906755
11. Ardila-Fierro, K. J.; Hernández, J. G. *ChemSusChem* **2021**, *14*, 2145–2162. doi:10.1002/cssc.202100478
12. James, S. L.; Adams, C. J.; Bolm, C.; Braga, D.; Collier, P.; Friščić, T.; Greponi, F.; Harris, K. D. M.; Hyett, G.; Jones, W.; Krebs, A.; Mack, J.; Maini, L.; Orpen, A. G.; Parkin, I. P.; Shearouse, W. C.; Steed, J. W.; Waddell, D. C. *Chem. Soc. Rev.* **2012**, *41*, 413–447. doi:10.1039/c1cs15171a
13. Ohn, N.; Kim, J. G. *ACS Macro Lett.* **2018**, *7*, 561–565. doi:10.1021/acsmacrolett.8b00171
14. Troschke, E.; Grätz, S.; Lübken, T.; Borchardt, L. *Angew. Chem., Int. Ed.* **2017**, *56*, 6859–6863. doi:10.1002/anie.201702303
15. Casco, M. E.; Kirchhoff, S.; Leistenschneider, D.; Rauche, M.; Brunner, E.; Borchardt, L. *Nanoscale* **2019**, *11*, 4712–4718. doi:10.1039/c9nr01019j
16. Schneidermann, C.; Kensy, C.; Otto, P.; Oswald, S.; Giebelter, L.; Leistenschneider, D.; Grätz, S.; Dörfler, S.; Kaskel, S.; Borchardt, L. *ChemSusChem* **2019**, *12*, 310–319. doi:10.1002/cssc.201801997
17. Fiss, B. G.; Hatherly, L.; Stein, R. S.; Friščić, T.; Moores, A. *ACS Sustainable Chem. Eng.* **2019**, *7*, 7951–7959. doi:10.1021/acssuschemeng.9b00764
18. Moores, A. *Curr. Opin. Green Sustainable Chem.* **2018**, *12*, 33–37. doi:10.1016/j.cogsc.2018.05.004

19. Rak, M. J.; Saadé, N. K.; Friščić, T.; Moores, A. *Green Chem.* **2014**, *16*, 86–89. doi:10.1039/c3gc41827h

20. Malca, M. Y.; Bao, H.; Bastaille, T.; Saadé, N. K.; Kinsella, J. M.; Friščić, T.; Moores, A. *Chem. Mater.* **2017**, *29*, 7766–7773. doi:10.1021/acs.chemmater.7b02134

21. Xu, C.; De, S.; Balu, A. M.; Ojeda, M.; Luque, R. *Chem. Commun.* **2015**, *51*, 6698–6713. doi:10.1039/c4cc09876e

22. Fiss, B. G.; Vu, N.-N.; Douglas, G.; Do, T.-O.; Friščić, T.; Moores, A. *ACS Sustainable Chem. Eng.* **2020**, *8*, 12014–12024. doi:10.1021/acssuschemeng.0c02762

23. Braga, D.; Dichiariante, E.; Grepioni, F.; Lampronti, G. I.; Maini, L.; Mazzeo, P. P.; D'Agostino, S. Mechanical Preparation of Crystalline Materials. An Oxymoron?. In *Supramolecular Chemistry: From Molecules to Nanomaterials*; Steed, J. W.; Gale, P. A., Eds.; Supramolecular Materials Chemistry, Vol. 6; John Wiley & Sons: Hoboken, NJ, USA, 2012; pp 2993–3007. doi:10.1002/9780470661345.smc115

24. Toda, F.; Tanaka, K.; Sekikawa, A. *J. Chem. Soc., Chem. Commun.* **1987**, 279–280. doi:10.1039/c39870000279

25. Friščić, T.; Trask, A. V.; Jones, W.; Motherwell, W. D. S. *Angew. Chem., Int. Ed.* **2006**, *45*, 7546–7550. doi:10.1002/anie.200603235

26. Braga, D.; Giaffreda, S. L.; Grepioni, F.; Pettersen, A.; Maini, L.; Curzi, M.; Polito, M. *Dalton Trans.* **2006**, 1249–1263. doi:10.1039/b516165g

27. Boldyrev, V. V.; Avvakumov, E. G. *Russ. Chem. Rev.* **1971**, *40*, 847–859. doi:10.1070/rc1971v040n10abeh001977

28. Beillard, A.; Bantrel, X.; Métro, T.-X.; Martinez, J.; Lamaty, F. *Chem. Rev.* **2019**, *119*, 7529–7609. doi:10.1021/acs.chemrev.8b00479

29. Rightmire, N. R.; Hanusa, T. P. *Dalton Trans.* **2016**, *45*, 2352–2362. doi:10.1039/c5dt03866a

30. Tan, D.; García, F. *Chem. Soc. Rev.* **2019**, *48*, 2274–2292. doi:10.1039/c7cs00813a

31. Tanaka, K. *Solvent-free organic synthesis*; Wiley-VCH: Weinheim, Germany, 2003. doi:10.1002/3527601821

32. Wang, G.-W. *Chem. Soc. Rev.* **2013**, *42*, 7668–7700. doi:10.1039/c3cs35526h

33. Tan, D.; Friščić, T. *Eur. J. Org. Chem.* **2018**, 18–33. doi:10.1002/ejoc.201700961

34. Wang, G.-W. *Chin. J. Chem.* **2021**, *39*, 1797–1803. doi:10.1002/cjoc.202100085

35. Zhu, S.-E.; Li, F.; Wang, G.-W. *Chem. Soc. Rev.* **2013**, *42*, 7535–7570. doi:10.1039/c3cs35494f

36. Mack, J.; Fulmer, D.; Stofel, S.; Santos, N. *Green Chem.* **2007**, *9*, 1041–1043. doi:10.1039/b706167f

37. Fiss, B. G.; Richard, A. J.; Friščić, T.; Moores, A. *Can. J. Chem.* **2021**, *99*, 93–112. doi:10.1139/cjc-2020-0408

38. Fiss, B.; Douglas, G.; Ferguson, M.; Becerra, J.; Valdez, J.; Do, T.-O.; Friščić, T.; Moores, A. *ChemRxiv* **2022**. doi:10.26434/chemrxiv-2022-15cwv-v2

39. Ronning, C.; Feldermann, H.; Merk, R.; Hofsäss, H.; Reinke, P.; Thiele, J.-U. *Phys. Rev. B* **1998**, *58*, 2207–2215. doi:10.1103/physrevb.58.2207

40. Wang, J.; Senkovska, I.; Oschatz, M.; Lohe, M. R.; Borchardt, L.; Heerwig, A.; Liu, Q.; Kaskel, S. *J. Mater. Chem. A* **2013**, *1*, 10951–10961. doi:10.1039/c3ta11995e

41. Bojdys, M. J.; Müller, J.-O.; Antonietti, M.; Thomas, A. *Chem. – Eur. J.* **2008**, *14*, 8177–8182. doi:10.1002/chem.200800190

42. Kumar, A.; Kumar, P.; Joshi, C.; Manchanda, M.; Boukherroub, R.; Jain, S. L. *Nanomaterials* **2016**, *6*, 59. doi:10.3390/nano6040059

43. Turner, G. L.; Smith, K. A.; Kirkpatrick, R. J.; Oldfield, E. *J. Magn. Reson. (1969–1992)* **1986**, *70*, 408–415. doi:10.1016/0022-2364(86)90129-0

44. MacKenzie, K. J.; Smith, M. E. NMR of Other Commonly Studied Nuclei. *M multinuclear solid-state nuclear magnetic resonance of inorganic materials*; Elsevier: New York, NY, USA, 2002. doi:10.1016/s1470-1804(02)80008-6

45. Clark, S. J.; Segall, M. D.; Pickard, C. J.; Hasnip, P. J.; Probert, M. I. J.; Refson, K.; Payne, M. C. Z. *Kristallogr.* **2005**, *220*, 567–570. doi:10.1524/zkri.220.5.567.65075

46. Gracia, J.; Kroll, P. *J. Mater. Chem.* **2009**, *19*, 3013–3019. doi:10.1039/b821568e

47. Wang, J.; Hao, D.; Ye, J.; Umezawa, N. *Chem. Mater.* **2017**, *29*, 2694–2707. doi:10.1021/acs.chemmater.6b02969

48. Tragl, S.; Gibson, K.; Glaser, J.; Heydenrych, G.; Frenking, G.; Duppel, V.; Simon, A.; Meyer, H.-J. *Z. Anorg. Allg. Chem.* **2008**, *634*, 2754–2760. doi:10.1002/zaac.200800092

49. Yan, S. C.; Li, Z. S.; Zou, Z. G. *Langmuir* **2009**, *25*, 10397–10401. doi:10.1021/la900923z

50. Lin, L.; Ou, H.; Zhang, Y.; Wang, X. *ACS Catal.* **2016**, *6*, 3921–3931. doi:10.1021/acscatal.6b00922

51. Wang, Y.; Wang, X.; Antonietti, M. *Angew. Chem., Int. Ed.* **2012**, *51*, 68–89. doi:10.1002/anie.201101182

52. Ma, X.; Lv, Y.; Xu, J.; Liu, Y.; Zhang, R.; Zhu, Y. *J. Phys. Chem. C* **2012**, *116*, 23485–23493. doi:10.1021/jp308334x

License and Terms

This is an open access article licensed under the terms of the Beilstein-Institut Open Access License Agreement (<https://www.beilstein-journals.org/bjoc/terms>), which is identical to the Creative Commons Attribution 4.0 International License

(<https://creativecommons.org/licenses/by/4.0/>). The reuse of material under this license requires that the author(s), source and license are credited. Third-party material in this article could be subject to other licenses (typically indicated in the credit line), and in this case, users are required to obtain permission from the license holder to reuse the material.

The definitive version of this article is the electronic one which can be found at:

<https://doi.org/10.3762/bjoc.18.125>



From amines to (form)amides: a simple and successful mechanochemical approach

Federico Casti, Rita Mocci* and Andrea Porcheddu*

Full Research Paper

Open Access

Address:

Dipartimento di Scienze Chimiche e Geologiche, Università degli Studi di Cagliari, Cittadella Universitaria, 09042 Cagliari, Italy

Email:

Rita Mocci* - rita.mocci@unica.it; Andrea Porcheddu* - porcheddu@unica.it

* Corresponding author

Keywords:

acetamides; formamides; mechanochemistry; *N*-formylation; *p*-tosylimidazole

Beilstein J. Org. Chem. **2022**, *18*, 1210–1216.

<https://doi.org/10.3762/bjoc.18.126>

Received: 20 May 2022

Accepted: 01 September 2022

Published: 12 September 2022

This article is part of the thematic issue "Mechanochemistry III".

Guest Editors: J. G. Hernández and L. Borchardt

© 2022 Casti et al.; licensee Beilstein-Institut.

License and terms: see end of document.

Abstract

Two easily accessible routes for preparing an array of formylated and acetylated amines under mechanochemical conditions are presented. The two methodologies exhibit complementary features as they enable the derivatization of aliphatic and aromatic amines.

Introduction

The preparation of *N*-formylated and *N*-acetylated amines plays a crucial role in organic synthesis [1–6]. In one respect, it is relevant to protect the amine group straightforwardly and under mild conditions [7,8]. On the other hand, the formamide and acetamide moieties are found in many active pharmaceutical ingredients (APIs) and natural products [1,9]. *N*-Formyl derivatives were used as building blocks in Vilsmeier–Haack reactions [10,11] and for preparing molecule drug substances, various heterocycles, formamidines, isocyanates, and isocyanides [12–17]. The large number of procedures reported in the literature witnesses the relevance of this class of compounds [9,18–26]. However, despite the remarkable advancement in the field, many conventional methodologies proceed at high temperatures and require an expensive catalyst and toxic reagents. In addition, these procedures only work in

substantial excess of formyl or acyl sources, often used as a solvent.

Mechanochemistry has been established as a powerful tool for the rapid, clean, and environmentally friendly synthesis of organic compounds, avoiding bulk solvent and restrictions of solvent-based chemistry [27–34]. In general, mechanochemistry refers to studying solid-state chemical changes promoted by external mechanical energy, such as grinding or milling. A deeper understanding of its mechanistic aspects laid the basis for further growth in this topic, opening new routes to more efficient mechanochemical reactions [35–42].

In our effort to develop green and sustainable methodologies using mechanochemistry [43–46], we recently studied a protocol

for synthesizing isocyanides using *p*-tosyl chloride (Ts-Cl) in basic conditions, starting from the corresponding formamides [47]. In this work, we aimed to set compatible conditions to access formamides, envisioning the possibility of generating the isocyanide in a one-pot, two-step reaction. However, to the best of our knowledge, despite the notable improvement in the mechanochemical synthesis of the amide moiety [44,48–54], no systematic report of *N*-formylation and *N*-acetylation by ball milling has been reported yet. Here, we describe two complementary procedures to prepare formamides and acetamides, applied to primary and secondary aromatic and aliphatic amines. The methodologies directly involve HCO_2H derivatives and $\text{CH}_3\text{CO}_2\text{H}$ and two activating agents for promoting amide coupling.

Results and Discussion

We started our investigation by reacting *p*-methoxyaniline (1.0 mmol) with ammonium formate (3.0 mmol) (Table 1, entry 1) in a zirconia jar in the presence of one milling ball of the same material ($\varnothing = 8$ mm, $m = 3.2$ g) [22,55] in a horizontal vibratory mill at 30 Hz. Under these conditions, we did not detect the formation of the formamide moiety. At the same time, the desired product **2** was obtained in 16% NMR yield when formic acid was added to the reaction mixture (Table 1, entry 2). Switching to sodium sulfate as a grinding additive significantly enhanced the reaction performance (Table 1, entries 3

and 4). At this stage, we wondered, if using a more efficient dehydrating agent would be mandatory for the reaction to occur. Therefore, we turned our attention toward *p*-tosylimidazole (*p*-Ts-Im), a cheap and commercially available reagent directly prepared from *p*-toluensulfonic acid by reaction with 1,1'-carbonyldiimidazole (CDI). The compound proved very effective for dehydrating oximes under mechanochemical acidic Beckmann conditions [44]. Moreover, it represents a suitable and compatible means in the view of a one-pot methodology for preparing isocyanides directly from amines [56].

When the amine **1** was reacted in the presence of Et_3N , HCOOH , and *p*-Ts-Im [58] (Table 1, entry 5), the formamide was accompanied by a significant amount of sulfonamide (formamide/sulfonamide ratio: 70:30). Better results were observed when *p*-Ts-Im was used under acidic conditions (see Table 1, entries 6 and 7). A slight enhancement in yields was observed when 20 balls ($\varnothing = 3$ mm, $m_{\text{tot}} = 6.5$ g) were used instead of one ball.

Recent studies on the effect of the size and number of milling balls pointed out that milling balls of larger diameter led to more rapid transformations [59,60]. On the other side, previously reported procedures revealed a beneficial effect on the reaction rate when the volume fraction occupied by balls inside the reactor increases. In addition, it was found that in some

Table 1: Optimization of reaction conditions for **2**.^{a,b}

Entry	Formic acid (equiv)	Additives (equiv)	Yield of 2 (%) ^c	Ratio 2:2a
1	–	HCOONH_4 (3.0)	–	–
2	1.5	HCOONH_4 (3.0)	16	–
3	1.5	Na_2SO_4 (2.8)	40	–
4	1.5	Na_2SO_4 (2.8)/ MeOH (LAG, $\eta = 0.2$)	45	–
5	1.5	<i>p</i> -Ts-Im/ Et_3N 1:1	56	70:30
6	2	<i>p</i> -Ts-Im (1.0)	75	90:10
7 ^d	2	<i>p</i> -Ts-Im (1.0)	85	88:12
8 ^d	2	<i>p</i> -Ts-Im (0.1)	85	95:5
9 ^d	2	imidazole (1.0)	94	–

^aThe reaction scheme was depicted using the symbolism proposed in [57]. ^bConditions: compound **1** (1.0 mmol, 123.1 mg), formic acid, and additives in the given ratio were milled in a horizontal vibratory mill in a 15 mL ZrO_2 milling jar with one milling ball ($\varnothing = 8$ mm, $m = 3.2$ g) of the same material for 200 minutes at the frequency of 30 Hz. ^cDetermined by ^1H NMR analysis. ^d20 milling balls ($\varnothing = 3.0$ mm, $m_{\text{tot}} = 6.5$ g) were used.

certain transformations, small milling balls are beneficial for the reaction rates since the number of stress events is significantly increased [61,62]. The stress energy appears to be less critical in these processes, and we cannot rule out a thermochemical process [63].

Furthermore, we observed that the reaction efficiently took place even in the presence of a catalytic amount of *p*-Ts-Im without significant differences in the reactivity.

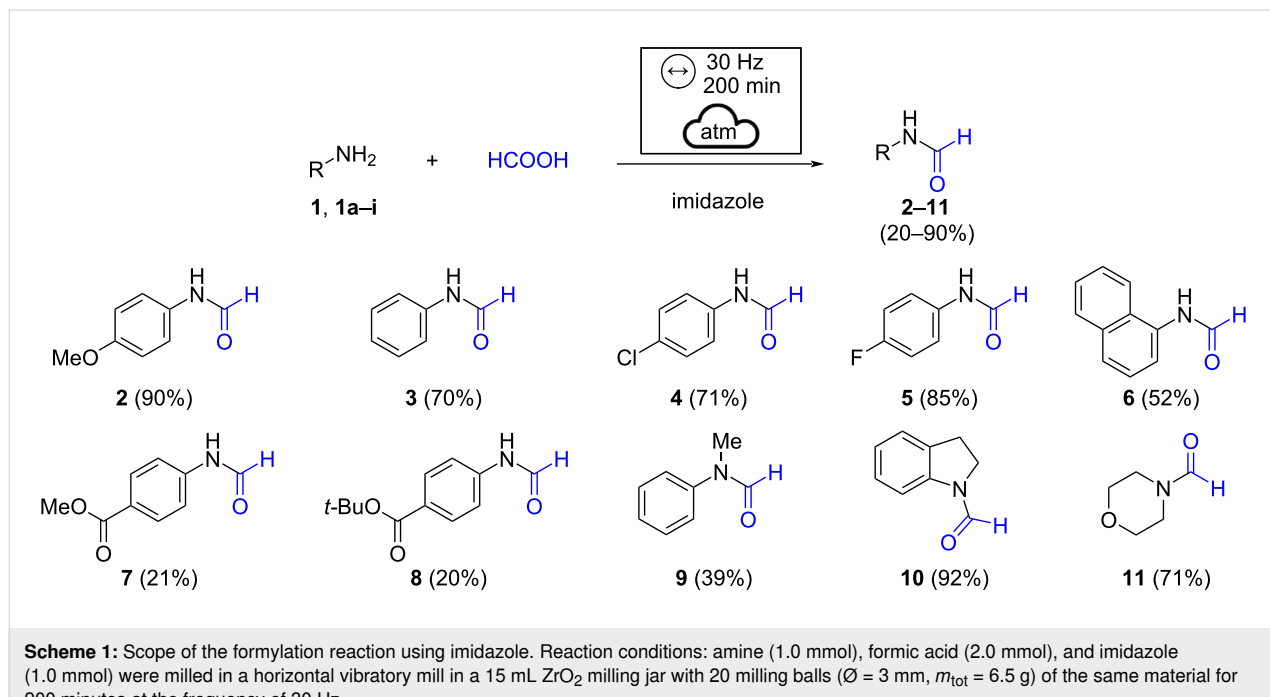
This data led us to question the effective role of *p*-Ts-Im in promoting the formylation reaction, which could exploit its role as the sole solid auxiliary of grinding. *p*-Tosylimidazole releases imidazole as a byproduct during the process. Therefore, we wondered whether imidazole could promote the formation of the target formamide **2**. Imidazole, compared to *p*-tosylimidazole, is a cheaper reagent and makes the final purification process easier.

As a matter of fact, by reacting 1.0 mmol of the model substrate with 2.0 mmol of formic acid and 1.0 mmol of imidazole [23], the product was obtained in better yield and with a higher degree of purity. A control experiment performed by reacting *p*-methoxyaniline (1.0 mmol) and formic acid (2.0 mmol) provided lower conversion into the desired formamide **2** (71% NMR yield, Table S1 in Supporting Information File 1), denoting the input given by imidazole as a promoter of formamide synthesis. Further variation in the ratio of imidazole/formic acid/amine decreases the reaction yield (Table S1 in Supporting Informa-

tion File 1). These data pointed out the importance of working in the presence of an excess of acid and a stoichiometric amount of imidazole.

The better results recorded in the presence of imidazole may be due to different factors. It is known that imidazole can efficiently promote those processes involving proton transfer under mechanochemical conditions. In the solvent-based procedure, imidazole has already been used in combination with DMF, which works as a solvent and source of a formyl group [23]. In that paper, the authors assumed the formation of formylimidazole as an intermediate in the formylation reaction. However, the intermediate was not detected by NMR or GC–MS analysis, possibly due to its instability [64]. Several studies carried out on our reaction crude at different times did not show the presence of compounds traceable to formylimidazole. The imidazole plays a dual role as promoting reagent and solid grinding additive and can be easily removed by aqueous acid workup. The adoption of imidazole as a grinding additive is required to avoid the slurry obtained by mixing amine and acid while allowing the formation of a waxy solid, which is more suitable for a mechanochemical action. With the optimized conditions in hand, the methodology was successfully applied to the synthesis of several formamides starting from a series of aromatic amines (Scheme 1).

The *N*-formyl derivative **3** was prepared in good yields as well as formanilides bearing halogen substituents, which were well tolerated (Scheme 1, products **4** and **5**). *N*-(1-Naphth-



yl)formamide (**6**) was obtained in satisfying yield, while the methyl and *tert*-butyl ester moieties affected the reaction outcome (Scheme 1, amides **7** and **8**). Secondary amines were also tested under the developed conditions; *N*-methylaniline provided the desired product **9** in 39% yield, while outstanding results were achieved in the *N*-formylation of indoline (Scheme 1, formamide **10**). The present methodology could also be effectively applied to the synthesis of *N*-formylmorpholine (Scheme 1, product **11**).

Aliphatic primary amines can be more challenging substrates [22]. In fact, when the reaction was tested with phenylethylamine (**12**), we observed only 10% of conversion into the desired formamide (Table 2, entry 1). We, therefore, chose to resume the use of *p*-Ts-Im, envisioning it could contribute to improving the reactivity. At this point, we reacted the amine **12** (1.0 mmol) with *p*-Ts-Im (1.0 mmol), and formic acid (1.0 or 2.0 mmol, Table 2, compare entries 2 and 3) for 200 minutes at the frequency of 30 Hz and observed a significant improvement on the performance of the reaction. To our delight, the complete conversion into the desired formamide **13** was obtained using 1.5 equivalents of *p*-Ts-Im. Under these experimental conditions, we did not detect the formation of the sulfonamide derivative, preserving complete selectivity towards the target formamide (Table 2, entry 4).

Remarkably, the results remain unchanged regarding yields and purity by shortening the reaction time (Table 2, entry 5). Furthermore, these optimized conditions were applied to other amines that provided us with poor results using the methodology previously described (Scheme 2).

We obtained the formation of formamides **14** and **15** from cyclohexylamine and benzylamine in high yields (Scheme 2). Excellent results were also achieved using secondary aliphatic amines such as dibenzyl- and methylbenzylamine, which provided amides **16** and **17** in 87% and 74% isolated yields, respectively. Furthermore, the methodology allowed us to synthesize a set of aromatic formanilides (amides **18–20**, Scheme 2). Indeed, the deactivated *p*-nitroaniline was successfully converted into the corresponding formamide **19** as was the poorly nucleophilic diphenylamine (Scheme 2, amide **20**).

Lastly, we aimed to apply the procedure to the acylation of a series of amines. To our delight, we successfully extended the methodology to the mechanosynthesis of amides **21–23** (Scheme 2). The best results were obtained when the acetic acid and the *p*-Ts-Im were ball-milled together before adding the suitable amine. In this way, we could acylate primary aromatic and aliphatic amines under the experimental conditions (Scheme 2, amides **21–23**).

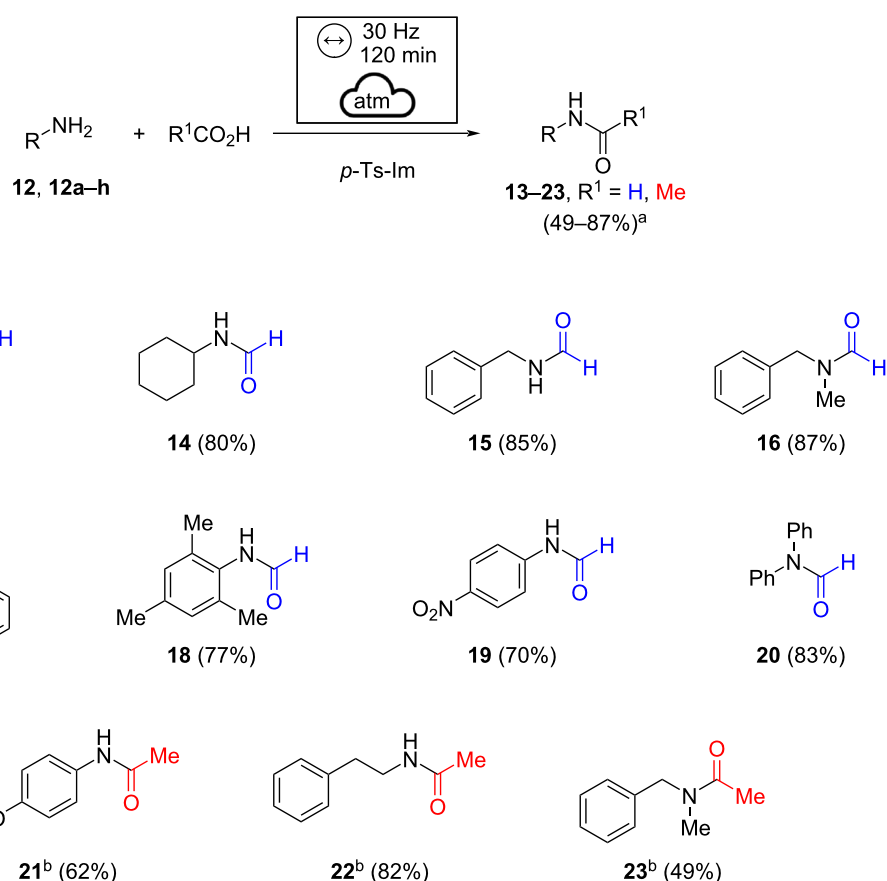
Conclusion

In conclusion, we developed two easily accessible ways to obtain a good number of formylated and acylated amines under mechanochemical conditions. The two methodologies exhibit complementary features as they enable the derivatization of different kinds of amines. Imidazole was found a suitable additive for the *N*-formylation reaction of several aromatic amines. On the other side, *p*-Ts-Im, activated by the acid reagent, proved an efficient activating agent under mild mechanochemical conditions for the formylation and acylation of those amines with less marked or limited (see protonated aliphatic amines) reactivity.

Table 2: Optimization of reaction conditions for product **13**.^a

Entry	Formic acid (equiv)	Additives (equiv)	Yield of 13 (%) ^b
1	2	imidazole (1.0)	10
2	2	<i>p</i> -Ts-Im (1.0)	42
3	1	<i>p</i> -Ts-Im (1.0)	42
4	1.5	<i>p</i> -Ts-Im (1.5)	99
5^c	1.5	<i>p</i>-Ts-Im (1.5)	95

^aAmine **12** (1.0 mmol, 121.2 mg), formic acid, and additives in the given ratio were milled in a horizontal vibratory mill in a 15 mL ZrO₂ milling jar with 20 milling balls (\varnothing = 3 mm, $m_{\text{tot}} = 6.5$ g) of the same material for 200 minutes at the frequency of 30 Hz; ^bdetermined by ¹H NMR analysis; ^cthe mixture was ball-milled for 120 minutes.



Scheme 2: Scope of the formylation reaction using *p*-Ts-Im as activating agent. Reaction conditions: amine (1.0 mmol), formic acid (1.5 mmol), and *p*-Ts-Im (1.5 mmol) were milled in a horizontal vibratory mill in a 15 mL ZrO₂ milling jar with 20 milling balls ($\varnothing = 3$ mm, $m_{\text{tot}} = 6.5$ g) of the same material for 120 minutes at the frequency of 30 Hz. ^aIsolated yields. ^bAcetic acid and *p*-Ts-Im were ball-milled for 10 minutes, then the amine was added, and the mixture was ball-milled for additional 120 minutes.

Supporting Information

Supporting Information File 1

Experimental section and characterization of synthesized compounds.

[<https://www.beilstein-journals.org/bjoc/content/supplementary/1860-5397-18-126-S1.pdf>]

cOmposites based on groWn matERials (MIFLOWER) and Fondazione di Sardegna (FdS, F72F20000230007).

ORCID® iDs

Federico Casti - <https://orcid.org/0000-0002-0530-3700>
 Rita Mocci - <https://orcid.org/0000-0002-8249-9735>
 Andrea Porcheddu - <https://orcid.org/0000-0001-7367-1102>

References

1. Sonawane, R. B.; Rasal, N. K.; Bhange, D. S.; Jagtap, S. V. *ChemCatChem* **2018**, *10*, 3907–3913. doi:10.1002/cctc.201800609
2. Jackson, A.; Meth-Cohn, O. *J. Chem. Soc., Chem. Commun.* **1995**, 1319. doi:10.1039/c39950001319
3. Valeur, E.; Bradley, M. *Chem. Soc. Rev.* **2009**, *38*, 606–631. doi:10.1039/b701677h
4. Sonawane, R. B.; Rasal, N. K.; Jagtap, S. V. *Org. Lett.* **2017**, *19*, 2078–2081. doi:10.1021/acs.orglett.7b00660
5. Chikkulapalli, A.; Aavula, S. K.; Mona NP, R.; C., K.; C.H., V. K.; Sulur G., M.; Sumathi, S. *Tetrahedron Lett.* **2015**, *56*, 3799–3803. doi:10.1016/j.tetlet.2015.04.077

Acknowledgements

We acknowledge the CeSAR (Centro Servizi Ricerca d'Ateneo) core facility of the University of Cagliari, Dr. Sandrina Lampis and Dr. Giulio Ferino for assistance with the generation of the ¹H, ¹³C NMR, and GC–MS spectroscopic data.

Funding

This research was funded by MIUR Italy, PRIN 2017 project (grant number: 2017B7MMJ5_001) “MultiFunctional poLymer

6. Isidro-Llobet, A.; Álvarez, M.; Albericio, F. *Chem. Rev.* **2009**, *109*, 2455–2504. doi:10.1021/cr800323s
7. Sheehan, J. C.; Yang, D.-D. H. *J. Am. Chem. Soc.* **1958**, *80*, 1154–1158. doi:10.1021/ja01538a036
8. Avery, M. A. *J. Med. Chem.* **1999**, *42*, 5285. doi:10.1021/jm990518h
9. Li, C.; Wang, M.; Lu, X.; Zhang, L.; Jiang, J.; Zhang, L. *ACS Sustainable Chem. Eng.* **2020**, *8*, 4353–4361. doi:10.1021/acssuschemeng.9b06591
10. Vilsmeier, A.; Haack, A. *Ber. Dtsch. Chem. Ges. B* **1927**, *60*, 119–122. doi:10.1002/cber.19270600118
11. Downie, I. M.; Earle, M. J.; Heaney, H.; Shuaibar, K. F. *Tetrahedron* **1993**, *49*, 4015–4034. doi:10.1016/s0040-4020(01)89915-4
12. Dömling, A. *Chem. Rev.* **2006**, *106*, 17–89. doi:10.1021/cr0505728
13. Mayer, J.; Umkehrer, M.; Kalinski, C.; Ross, G.; Kolb, J.; Burdack, C.; Hiller, W. *Tetrahedron Lett.* **2005**, *46*, 7393–7396. doi:10.1016/j.tetlet.2005.08.101
14. Picci, G.; Mocci, R.; Ciancaleoni, G.; Lippolis, V.; Zielińska-Blajet, M.; Caltagirone, C. *ChemPlusChem* **2020**, *85*, 1389–1395. doi:10.1002/cplu.202000260
15. Kakehi, A.; Ito, S.; Hayashi, S.; Fujii, T. *Bull. Chem. Soc. Jpn.* **1995**, *68*, 3573–3580. doi:10.1246/bcsj.68.3573
16. Han, Y.; Cai, L. *Tetrahedron Lett.* **1997**, *38*, 5423–5426. doi:10.1016/s0040-4039(97)01206-9
17. Chen, B.-C.; Bednarz, M. S.; Zhao, R.; Sundeen, J. E.; Chen, P.; Shen, Z.; Skoumboidis, A. P.; Barrish, J. C. *Tetrahedron Lett.* **2000**, *41*, 5453–5456. doi:10.1016/s0040-4039(00)00910-2
18. Gerack, C.; McElwee-White, L. *Molecules* **2014**, *19*, 7689–7713. doi:10.3390/molecules19067689
19. Minkin, V. I.; Dorozeenko, G. N. *Russ. Chem. Rev.* **1960**, *29*, 599–618. doi:10.1070/rc1960v029n11abeh001257
20. Dine, T. M. E.; Evans, D.; Rouden, J.; Blanchet, J. *Chem. – Eur. J.* **2016**, *22*, 5894–5898. doi:10.1002/chem.201600234
21. Lanigan, R. M.; Sheppard, T. D. *Eur. J. Org. Chem.* **2013**, 7453–7465. doi:10.1002/ejoc.201300573
22. Ganapati Reddy, P.; Kishore Kumar, G. D.; Baskaran, S. *Tetrahedron Lett.* **2000**, *41*, 9149–9151. doi:10.1016/s0040-4039(00)01636-1
23. Suchý, M.; Elmehriki, A. A. H.; Hudson, R. H. E. *Org. Lett.* **2011**, *13*, 3952–3955. doi:10.1021/ol201475j
24. Kalla, R. M. N.; Lim, J.; Bae, J.; Kim, I. *Tetrahedron Lett.* **2017**, *58*, 1595–1599. doi:10.1016/j.tetlet.2017.03.023
25. Wan, W.; Hou, J.; Jiang, H.; Yuan, Z.; Ma, G.; Zhao, G.; Hao, J. *Eur. J. Org. Chem.* **2010**, 1778–1786. doi:10.1002/ejoc.200901424
26. Chen, Z.; Fu, R.; Chai, W.; Zheng, H.; Sun, L.; Lu, Q.; Yuan, R. *Tetrahedron* **2014**, *70*, 2237–2245. doi:10.1016/j.tet.2014.02.042
27. Porcheddu, A.; Colacino, E.; De Luca, L.; Delogu, F. *ACS Catal.* **2020**, *10*, 8344–8394. doi:10.1021/acscatal.0c00142
28. Ardila-Fierro, K. J.; Hernández, J. G. *ChemSusChem* **2021**, *14*, 2145–2162. doi:10.1002/cssc.202100478
29. Bolt, R. R. A.; Leitch, J. A.; Jones, A. C.; Nicholson, W. I.; Browne, D. L. *Chem. Soc. Rev.* **2022**, *51*, 4243–4260. doi:10.1039/d1cs00657f
30. James, S. L.; Adams, C. J.; Bolm, C.; Braga, D.; Collier, P.; Friščić, T.; Grepioni, F.; Harris, K. D. M.; Hyett, G.; Jones, W.; Krebs, A.; Mack, J.; Maini, L.; Orpen, A. G.; Parkin, I. P.; Shearouse, W. C.; Steed, J. W.; Waddell, D. C. *Chem. Soc. Rev.* **2012**, *41*, 413–447. doi:10.1039/c1cs15171a
31. Stolle, A.; Szuppa, T.; Leonhardt, S. E. S.; Ondruschka, B. *Chem. Soc. Rev.* **2011**, *40*, 2317–2329. doi:10.1039/c0cs00195c
32. Liu, Y.; Lam, A. H. W.; Fowler, F. W.; Lauher, J. W. *Mol. Cryst. Liq. Cryst. Sci. Technol., Sect. A* **2002**, *389*, 39–46. doi:10.1080/713738914
33. Tan, D.; Friščić, T. *Eur. J. Org. Chem.* **2018**, 18–33. doi:10.1002/ejoc.201700961
34. Cuccu, F.; De Luca, L.; Delogu, F.; Colacino, E.; Solin, N.; Mocci, R.; Porcheddu, A. *ChemSusChem* **2022**, e202200362. doi:10.1002/cssc.202200362
35. Boldyreva, E. *Chem. Soc. Rev.* **2013**, *42*, 7719–7738. doi:10.1039/c3cs60052a
36. Howard, J. L.; Sagatov, Y.; Repusseau, L.; Schotten, C.; Browne, D. L. *Green Chem.* **2017**, *19*, 2798–2802. doi:10.1039/c6gc03139k
37. Hwang, S.; Grätz, S.; Borchardt, L. *Chem. Commun.* **2022**, *58*, 1661–1671. doi:10.1039/d1cc05697b
38. Howard, J. L.; Cao, Q.; Browne, D. L. *Chem. Sci.* **2018**, *9*, 3080–3094. doi:10.1039/c7sc05371a
39. Tireli, M.; Juribašić Kulcsár, M.; Cindro, N.; Gracin, D.; Biliškov, N.; Borovina, M.; Čurić, M.; Halasz, I.; Užarević, K. *Chem. Commun.* **2015**, *51*, 8058–8061. doi:10.1039/c5cc01915j
40. Puccetti, F.; Lukin, S.; Užarević, K.; Colacino, E.; Halasz, I.; Bolm, C.; Hernández, J. G. *Chem. – Eur. J.* **2022**, *28*, e202104409. doi:10.1002/chem.202104409
41. Kulla, H.; Fischer, F.; Benemann, S.; Rademann, K.; Emmerling, F. *CrystEngComm* **2017**, *19*, 3902–3907. doi:10.1039/c7ce00502d
42. Michalchuk, A. A. L.; Emmerling, F. *Angew. Chem., Int. Ed.* **2022**, *61*, e202117270. doi:10.1002/anie.202117270
43. Porcheddu, A.; Mocci, R.; Brindisi, M.; Cuccu, F.; Fattuoni, C.; Delogu, F.; Colacino, E.; D'Auria, M. V. *Green Chem.* **2022**, *24*, 4859–4869. doi:10.1039/d2gc00724j
44. Mocci, R.; Colacino, E.; De Luca, L.; Fattuoni, C.; Porcheddu, A.; Delogu, F. *ACS Sustainable Chem. Eng.* **2021**, *9*, 2100–2114. doi:10.1021/acssuschemeng.0c07254
45. Mocci, R.; De Luca, L.; Delogu, F.; Porcheddu, A. *Adv. Synth. Catal.* **2016**, *358*, 3135–3144. doi:10.1002/adsc.201600350
46. Mocci, R.; Murgia, S.; De Luca, L.; Colacino, E.; Delogu, F.; Porcheddu, A. *Org. Chem. Front.* **2018**, *5*, 531–538. doi:10.1039/c7qo01006k
47. Basoccu, F.; Cuccu, F.; Casti, F.; Mocci, R.; Fattuoni, C.; Porcheddu, A. *Beilstein J. Org. Chem.* **2022**, *18*, 732–737. doi:10.3762/bjoc.18.73
48. Declerck, V.; Nun, P.; Martinez, J.; Lamaty, F. *Angew. Chem., Int. Ed.* **2009**, *48*, 9318–9321. doi:10.1002/anie.200903510
49. Gómez-Carpintero, J.; Sánchez, J. D.; González, J. F.; Menéndez, J. C. *J. Org. Chem.* **2021**, *86*, 14232–14237. doi:10.1021/acs.joc.1c02350
50. Métra, T.-X.; Bonnamour, J.; Reidon, T.; Sarpoulet, J.; Martinez, J.; Lamaty, F. *Chem. Commun.* **2012**, *48*, 11781–11783. doi:10.1039/c2cc36352f
51. Štrukil, V.; Bartolec, B.; Portada, T.; Đilović, I.; Halasz, I.; Marjetić, D. *Chem. Commun.* **2012**, *48*, 12100–12102. doi:10.1039/c2cc36613d
52. Porte, V.; Thioly, M.; Pigoux, T.; Métra, T.-X.; Martinez, J.; Lamaty, F. *Eur. J. Org. Chem.* **2016**, 3505–3508. doi:10.1002/ejoc.201600617
53. Bonnamour, J.; Métra, T.-X.; Martinez, J.; Lamaty, F. *Green Chem.* **2013**, *15*, 1116–1120. doi:10.1039/c3gc40302e
54. Métra, T.-X.; Martinez, J.; Lamaty, F. *ACS Sustainable Chem. Eng.* **2017**, *5*, 9599–9602. doi:10.1021/acssuschemeng.7b03260
55. Martina, K.; Baricco, F.; Tagliapietra, S.; Moran, M. J.; Cravotto, G.; Cintas, P. *New J. Chem.* **2018**, *42*, 18881–18888. doi:10.1039/c8nj04240c

56. Basoccu, F.; Cuccu, F.; Casti, F.; Mocci, R.; Fattuoni, C.; Porcheddu, A. *Beilstein J. Org. Chem.* **2022**, *18*, 732–737. doi:10.3762/bjoc.18.73

57. Michalchuk, A. A. L.; Boldyreva, E. V.; Belenguer, A. M.; Emmerling, F.; Boldyreva, V. V. *Front. Chem. (Lausanne, Switz.)* **2021**, *9*, 685789. doi:10.3389/fchem.2021.685789

58. Behrouz, S.; Rad, M. N. S.; Forouhari, E. *J. Chem. Res.* **2016**, *40*, 101–106. doi:10.3184/174751916x14531325057887

59. Michalchuk, A. A. L.; Tumanov, I. A.; Boldyreva, E. V. *CrystEngComm* **2019**, *21*, 2174–2179. doi:10.1039/c8ce02109k

60. Michalchuk, A. A. L.; Tumanov, I. A.; Boldyreva, E. V. *J. Mater. Sci.* **2018**, *53*, 13380–13389. doi:10.1007/s10853-018-2324-2

61. Jicsinszky, L.; Tuza, K.; Cravotto, G.; Porcheddu, A.; Delogu, F.; Colacino, E. *Beilstein J. Org. Chem.* **2017**, *13*, 1893–1899. doi:10.3762/bjoc.13.184

62. Stolle, A.; Schmidt, R.; Jacob, K. *Faraday Discuss.* **2014**, *170*, 267–286. doi:10.1039/c3fd00144j

63. The topic is deeply concerning, but the discussion is still a work in progress. More in-depth studies addressing these issues are beyond the scope of this paper.

64. Kitagwa, T.; Arita, J.; Nagahata, A. *Chem. Pharm. Bull.* **1994**, *42*, 1655–1657. doi:10.1248/cpb.42.1655

License and Terms

This is an open access article licensed under the terms of the Beilstein-Institut Open Access License Agreement (<https://www.beilstein-journals.org/bjoc/terms>), which is identical to the Creative Commons Attribution 4.0

International License

(<https://creativecommons.org/licenses/by/4.0>). The reuse of material under this license requires that the author(s), source and license are credited. Third-party material in this article could be subject to other licenses (typically indicated in the credit line), and in this case, users are required to obtain permission from the license holder to reuse the material.

The definitive version of this article is the electronic one which can be found at:

<https://doi.org/10.3762/bjoc.18.126>



Polymer and small molecule mechanochemistry: closer than ever

José G. Hernández

Perspective

Open Access

Address:

Grupo Ciencia de los Materiales, Instituto de Química, Facultad de Ciencias Exactas y Naturales, Universidad de Antioquia, Calle 70 No 52-21, Medellín, Colombia

Email:

José G. Hernández - joseg.hernandez@udea.edu.co

Keywords:

ball milling; mechanochemistry; mechanophore; polymer; pulsed ultrasonication

Beilstein J. Org. Chem. **2022**, *18*, 1225–1235.

<https://doi.org/10.3762/bjoc.18.128>

Received: 12 May 2022

Accepted: 03 August 2022

Published: 14 September 2022

This article is part of the thematic issue "Mechanochemistry III".

Associate Editor: L. Vaccaro

© 2022 Hernández; licensee Beilstein-Institut.

License and terms: see end of document.

Abstract

The formation and scission of chemical bonds facilitated by mechanical force (mechanochemistry) can be accomplished through various experimental strategies. Among them, ultrasonication of polymeric matrices and ball milling of reaction partners have become the two leading approaches to carry out polymer and small molecule mechanochemistry, respectively. Often, the methodological differences between these practical strategies seem to have created two seemingly distinct lines of thought within the field of mechanochemistry. However, in this Perspective article, the reader will encounter a series of studies in which some aspects believed to be inherently related to either polymer or small molecule mechanochemistry sometimes overlap, evidencing the connection between both approaches.

Introduction

In the past two decades, the growth in popularity of mechanochemistry has been unmistakable. During this time, two main experimental strategies to produce physical and chemical responses in a system when mechanical force is applied have been established. One of them, often called polymer mechanochemistry, relies on the use of polymers to transduce mechanical loads to mechanically sensitive probes (mechanophores) embedded along the polymer chains (Figure 1a) [1-4].

This is mostly accomplished through pulsed ultrasonication, and to a lesser extent by single-molecule force spectroscopy techniques [5,6]. The second approach habitually makes use of ball milling techniques to bring together small molecules (but also inorganic precursors, organometallic complexes, enzymes, monomeric units, or even polymers) in bulk and to provide the energy required for the system to react (Figure 1b and Figure 1c) [7-12]. At times, the methodological differences between both approaches seem to have created two seemingly

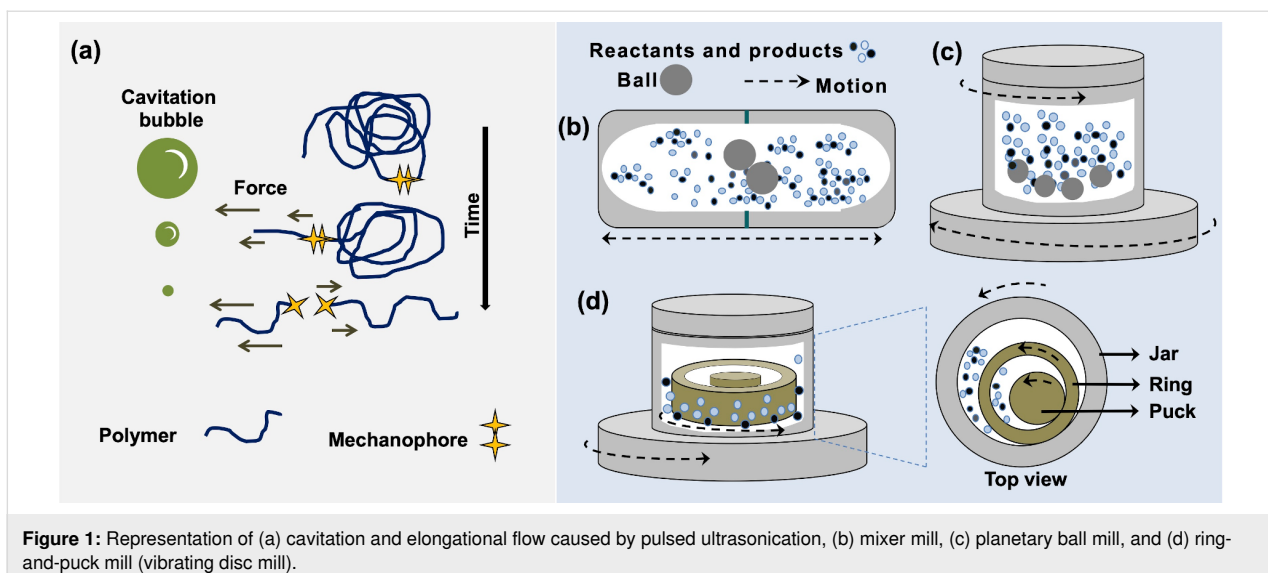


Figure 1: Representation of (a) cavitation and elongational flow caused by pulsed ultrasonication, (b) mixer mill, (c) planetary ball mill, and (d) ring-puck mill (vibrating disc mill).

distinct lines of thought within the field of mechanochemistry, which kept both areas to evolve mostly separately. On the one hand, polymer mechanochemistry by pulsed ultrasonication is believed to exhibit higher control at the microscopic level, for example, by enabling the transduction of mechanical cues with high directionality to the mechanophores [1–4]. In contrast, ball milling protocols have a more evident effect on the macroscopic level of the system, for instance, by causing comminution, amorphization, polymorphic transformations, structural defects, melting of the sample, etc. All these effects superimpose and influence the intrinsic reactivity of the reagents [7].

At present, both mechanochemical approaches have proven highly versatile to activate numerous chemical systems and their applicability is expected to grow. Therefore, understanding the similarities and differences between polymer and small molecule mechanochemistry has become an important subject of academic investigation and constructive discussion in review articles [13,14].

Additionally, questioning the relationship between polymer mechanochemistry and small molecule mechanochemistry has been a recurrent topic mostly addressed at scientific events. The last time I witnessed this discussion was on April 13th, 2022 at the Thieme WebCheminar #2: Mechanochemistry when Prof. Jeffrey S. Moore, the chairperson of the event, rephrased a question from one of the assistants (at 2:22:28 in the video in reference [15]). The question was initially rephrased as to what was the connection between polymer mechanochemistry and small molecule mechanochemistry. On second thoughts, Prof. Moore paraphrased the question further, ending asking if the speakers considered there was a way to use the mechanical

energy in a polymeric material to ultimately have an effect on a small molecule reaction. Interestingly enough, before providing an answer, one of the participants reworded (back) the question one more time as to what was the correlation between polymer and small molecule mechanochemistry [15].

At the event, ideas on how polymer mechanochemistry could bias small molecule reactions were instantaneously provided by Prof. Stephen Craig [15], which included the possibility to mechanically control catalytic cycles in the future by switching the state of reactants or catalysts. Some approximations to this approach have already been realized. For example, some metallopolymer-based systems now enable a controllable release of metal ions by ultrasonication to trigger or catalyze small molecule reactions in solution [16–18]. Complementarily, studies on mechanically releasing cargo and unmasking organocatalytic units embedded in polymers for catalysis in small molecule systems have been discussed [15,19,20]. Moreover, the ability of force to deform the reaction energy landscape and modulate the reversibility of the reactions within proteins has been demonstrated. For example, mechanical force was used to promote the thermodynamically disfavored S_N2 cleavage of an individual protein disulfide bond by poorly nucleophilic organic thiols [21].

On the other hand, as for the connection or correlation between polymer and small molecule mechanochemistry, this Perspective article discusses recent studies, which have found, sometimes inadvertently, links between polymer and small molecule mechanochemistry that could eventually close the apparent gap between both branches. In turn, this might reveal synergistic opportunities to strengthen the field of mechanochemistry as a whole.

Discussion

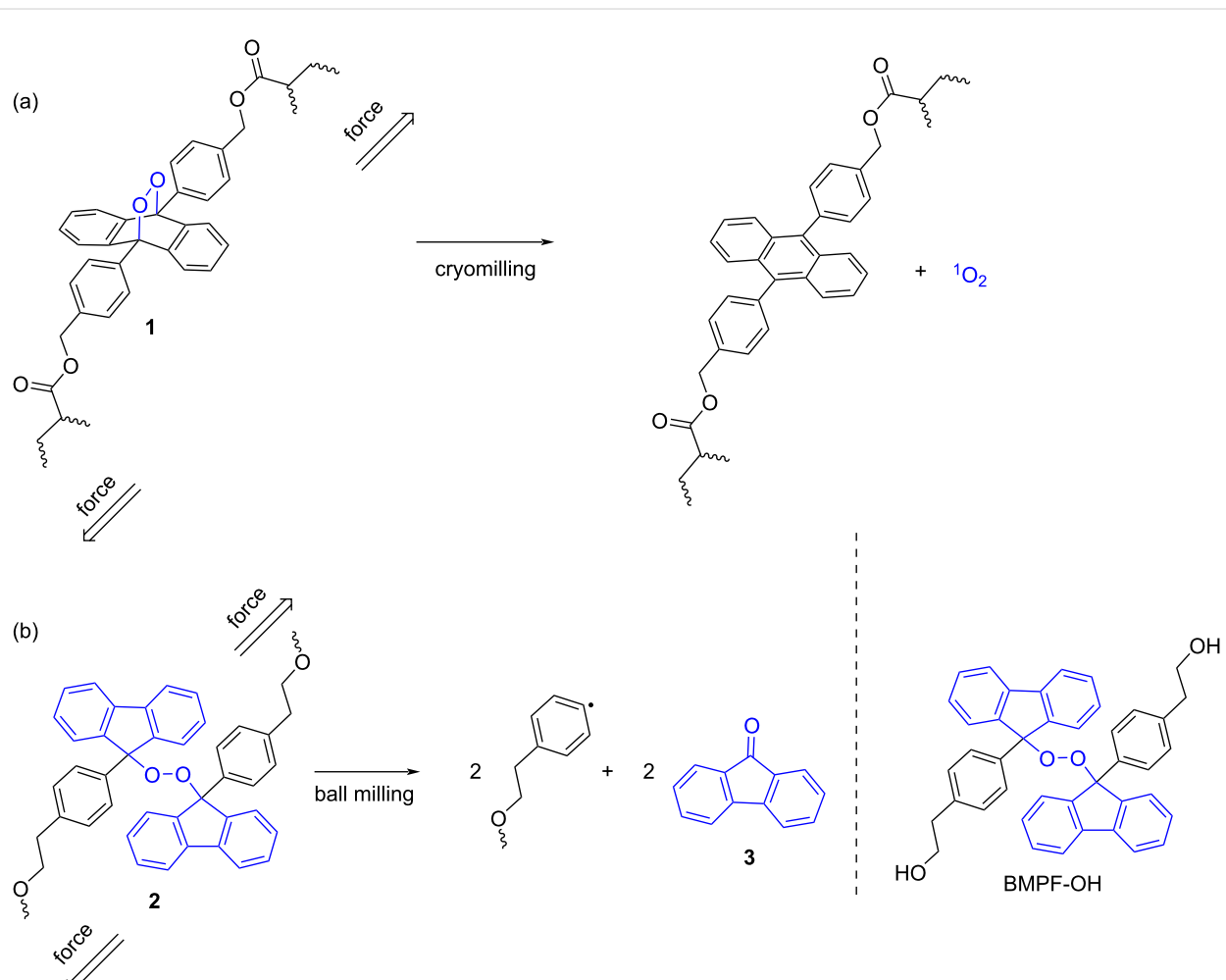
Activation of mechanophores in polymers by ball milling

Mechanochemical activation of mechanophores in polymeric materials is typically carried out by pulsed ultrasonication [5,6]. Under such conditions, the collapse of cavitation bubbles in the liquid medium creates a gradient that exerts mechanical force along the polymer backbone, ultimately reaching and activating the mechanophores within it (Figure 1a). The technical simplicity of the method and the compatibility with spectroscopic analytical techniques for monitoring [22] have made sonication of polymer solutions the primary method in the field of polymer mechanochemistry. However, in recent times, manual grinding and ball milling techniques (Figure 1b and Figure 1c) have also been used as alternatives to activate mechanophores incorporated in polymers. Such an application complements the

original use of ball milling to generate mechanoradicals through homolytic cleavage of the polymer chains [23], a strategy that is still of relevance today [24,25] and also complements the recent application of ball milling for the synthesis of polymers [26].

As an example for the use of ball milling to activate mechanophores incorporated in polymers, Baytekin, Akkaya, and co-workers found that ball milling of the cross-linked polyacrylate polymer **1** could trigger the release of singlet oxygen from the anthracene–endoperoxide mechanophores (Scheme 1a) [27].

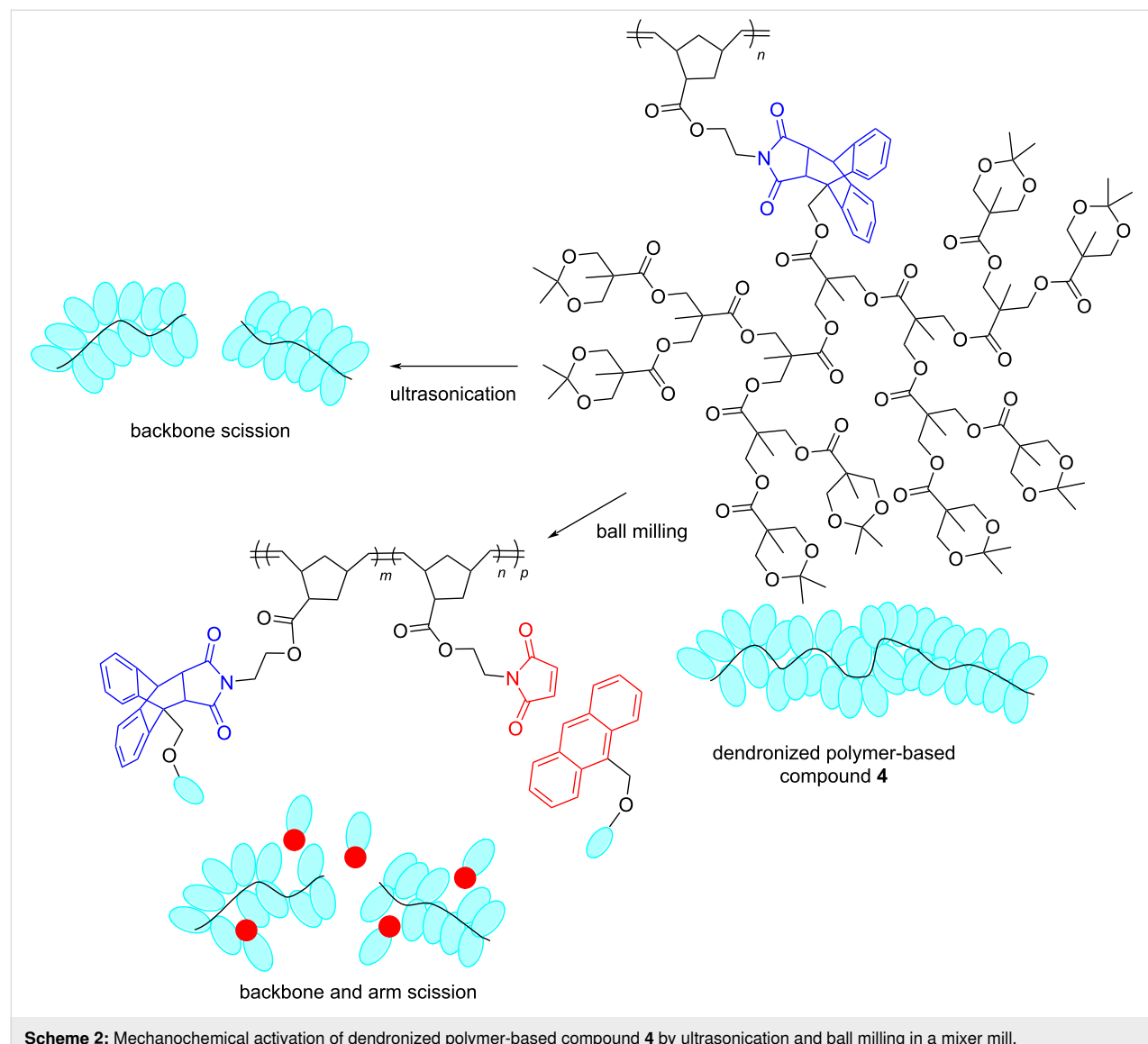
To support the claim that the generation of ${}^1\text{O}_2$ occurred mechanically rather than thermally due to local heat formation by ball collision, the authors tested the mechanochemical reaction under cryogenic ball milling conditions and found that even at low temperature, the mechanical treatment was enough to facilitate the cycloreversion process (Scheme 1a) [27].



Scheme 1: (a) Mechanocleavage of anthracene–endoperoxide mechanophore incorporated in the cross-linked polyacrylate polymer **1** by cryomilling in a mixer mill. (b) Mechanocleavage of a polymer network matrix, bis(9-methylphenyl-9-fluorenyl) peroxide (BMPF)-containing poly(butyl methacrylate) **2**, in a mixer mill.

In a related work, in 2021, Otsuka and co-workers incorporated a BMPF mechanophore into glassy and rubbery polymeric networks such as poly(butyl methacrylate) and a poly(hexyl methacrylate) [28]. Upon treatment of the polymeric material **2** in a mixer mill (Figure 1b), the BMPF units underwent a mechanical homolytic fragmentation of the O–O peroxide bond, releasing fluorescent 9-fluorenone (**3**) via β -scission (Scheme 1b). To highlight the importance of the polymer network in the transduction of the mechanical stimulus to the mechanophore, the authors demonstrated that ball milling monomeric BMPF-OH at 30 Hz for 3 h only generated traces of **3** (1% after isolation). Importantly, the BMPF mechanophore was also proven to be thermally stable up to 110 °C, which supports the conclusion that the mechanical force caused by the grinding was responsible for the activation of the BMPF mechanophores [28].

Comparative studies between ultrasound and ball milling have also demonstrated that both experimental approaches can transduce mechanical force to polymeric materials, sometimes in a complementary manner. For example, in 2021, Noh, Peterson, and Choi investigated the mechanochemical degradation of bottlebrush and dendronized polymers when exposed to ultrasonication in solution and when ball milled in the solid state [29]. The results for bottlebrush polymers demonstrated a more pronounced arm scission by ball milling than by sonication, compared to the extent of backbone rupture. However, for dendronized polymers, arm scission could be accomplished by ball milling but it was not observed in sonication experiments. These observations inspired the synthesis and activation of mechanophores (maleimide–anthracene cycloadducts) in dendronized polymer-based materials such as **4** upon ball milling (Scheme 2).



The differences observed in the activation of polymers such as **4** between ball milling and ultrasonication were associated with the more restricted chain mobility in the solid state and with the dissimilar distribution of mechanical forces on the backbone and arms. With ball milling, these were more pronounced towards the arms of the polymer [29].

Other studies have also provided mounting evidence that ball milling and manual grinding, techniques typically used in small molecule mechanochemistry, could trigger chemical reactions in multimechanophore polymers [30], nonsymmetric mechano-phores embedded in polymer systems [31], and mixtures of mechanochromic polymers [32], among others [33,34]. Therefore, it has been clearly demonstrated that pulsed ultrasound-based, grinding and ball milling techniques are competent in activating polymeric materials and, more importantly, that sometimes the apparent disparity between both approaches can actually lead to complementary reactivity, as discussed above.

Depolymerization of biomacromolecules by mechanical force

In addition to the manipulation of manufactured polymers, ball milling techniques have also been reported to facilitate the depolymerization of biopolymers [35]. On the one hand, the implementation of solvent-free ball milling has enabled to

surpass the insolubility and recalcitrant reactivity of cellulose [36,37], chitin [38,39], and lignin (Figure 2) [40,41].

In addition to allowing solvent-free reactions, mechanical forces generated inside ball mills can depolymerize biomass through cleavage pathways that are different from those found in solution. Computational studies have been a key to understand the role of mechanical force in such reactions and to explain the changes in selectivity under force [42–44]. For example, experimental results have demonstrated that ball milling in a planetary ball mill (Figure 1c) enhances the depolymerization of acid-impregnated chitin more selectively towards glycosidic bond cleavage (i.e., backbone rupture) over amide bond breakage (i.e., deacetylation) [38,45]. Notably, the result is different for the reaction in solution, where scission of both bonds is observed [46]. This difference is believed to be related to the exertion of tensile forces along the glycosidic linkage of the polymer chain during ball milling, which may lower the activation energy for the depolymerization of chitin. Indeed, DFT calculations using the *N*-acetylglucosamine dimer as the model compound showed that the application of pulling forces to selected atoms in the dimer perturb the reaction, making the depolymerization easier to occur [45]. In contrast, no change in the activation energy of the deacetylation step was observed with the introduction of the pulling forces. The decrease in the

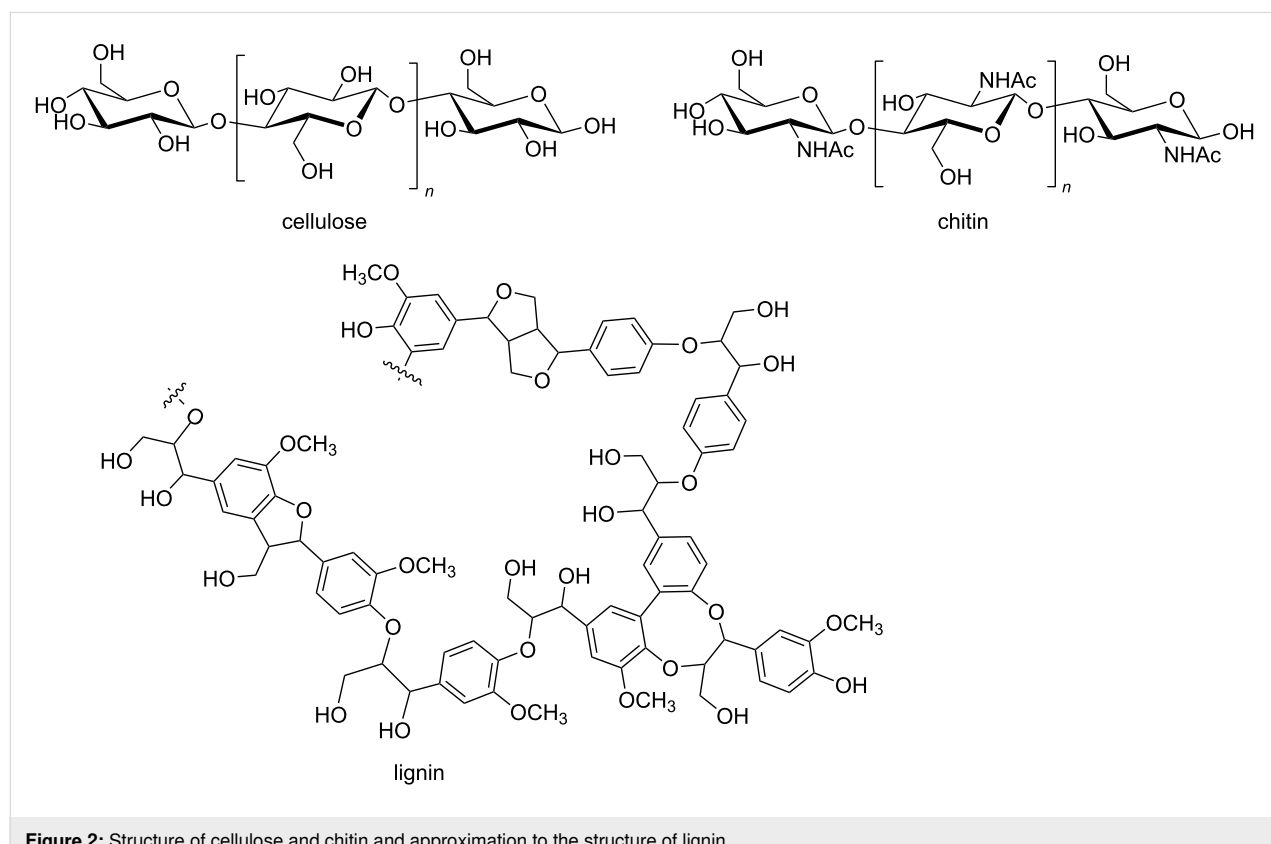
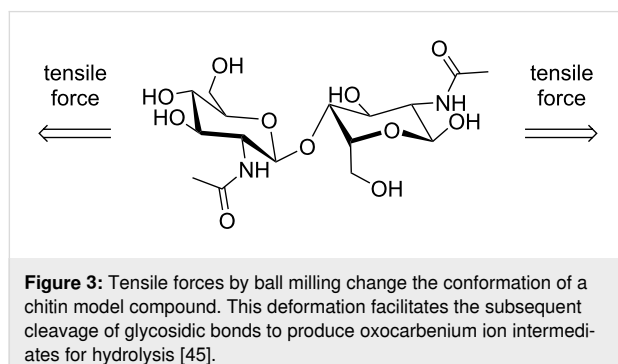


Figure 2: Structure of cellulose and chitin and approximation to the structure of lignin.

activation energy for the mechanochemical depolymerization of chitin was attributed to force-induced conformational changes in the structure, which destabilize the reactant state upon the introduction of a sufficient pulling force (Figure 3).

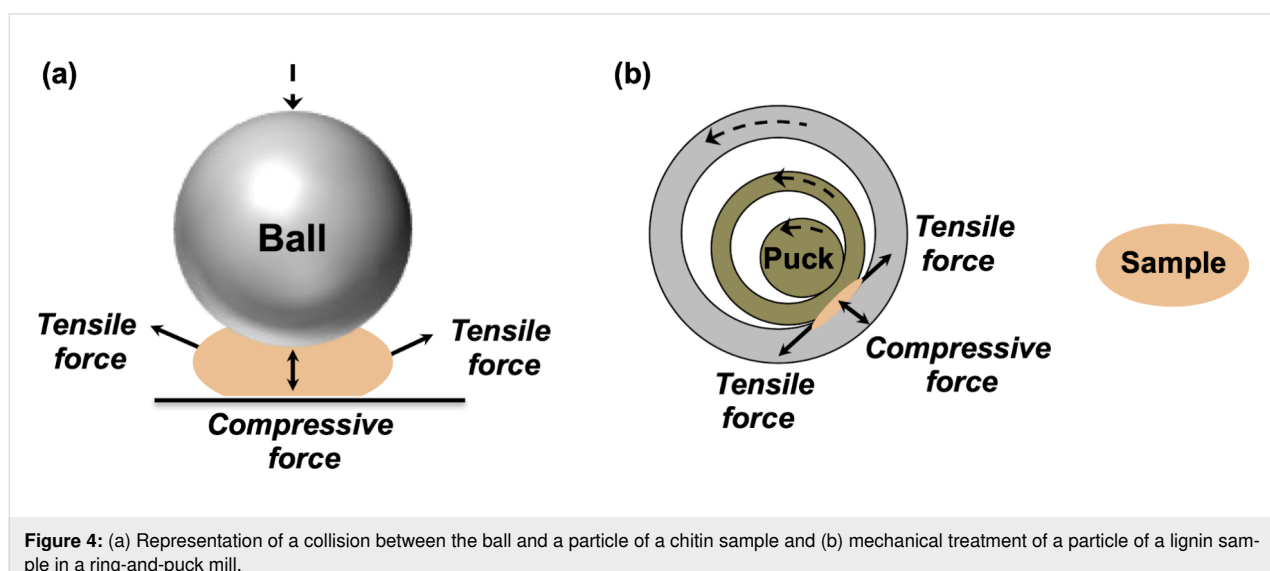


Evidently, ball milling techniques apply forces to the samples in a random fashion, with friction, shearing, and compression being more prominent than pulling forces. Well aware of this, further studies by Kobayashi, Fukuoka, and co-workers on the depolymerization of chitin by ball milling considered not only tensile but also compressive forces transduced by the impact of the balls on the milled sample (Figure 4a) [47].

The computational investigation revealed that ball milling can provide a subnano- to nanonewton order of tensile and compressive forces to activate the biopolymer. Moreover, the results corroborated that tensile force applied in the direction of the polymer chain activates the scission of the glycosidic bonds, but they also showed that the pulling force transduced by ball milling would be insufficient to impact the reaction significantly. Therefore, the depolymerization of chitin was found to be

less frequently influenced by tensile forces. In contrast, compressive forces in the same direction as the collision less strongly activate the chemical bonds, but the large number of this type of collisions in a planetary ball mill (Figure 1c) can add up and provide compressive forces large enough for the activation of glycosidic bonds [47].

In the same work, Kobayashi, Fukuoka, and co-workers concluded that “if a new mechanical method [different from ball milling] is developed to apply tensile forces to samples selectively and efficiently, it will probably improve the reaction efficiency” [47]. Along these lines, ring-and-puck mills (often called vibrating disc mills, Figure 1d) are a type of milling equipment in which the number of collisions is low, but the friction, and therefore the tensile force transduced to the milled sample, is high. Experimental studies focused on the oxidative mechanochemical depolymerization of lignin have found that mechanical treatment of this biomacromolecule by ring-and-puck milling can lead to the cleavage of lignin linkages more effectively and in a shorter time as compared to the reaction carried out in ball mills [48,49]. Probably, the compression and particularly the tension exerted on the sample by the disc is transduced with better directionality to the biopolymer, which acts as a force transmission medium (Figure 4b). Hence, widespread mechanical methods such as ring-and-puck milling are already available to mechanochemically activate polymeric materials with an enhanced control over the direction in which the mechanical force is applied. However, it remains to be seen whether ring-and-puck milling, or similar technologies, will be able to trigger the mechanical activation of multimechanophore polymers. If successful, this approach could actually enable the activation of functional polymers on a scale of up to a hundred grams per run.



Piezoelectric materials as mechanophores

Mechanophores were initially described as molecular units that chemically respond in a selective manner to a mechanical perturbation preferentially transduced through polymers [1]. As mentioned above, force-sensitive molecular mechanophores are now complemented by organometallic-based force-responsive mechanophores that are not purely organic molecular fragments [16–18]. In fact, the concept of a mechanophore is now broader and may include any force-reactive functional unit, whether it possesses mechanically labile bonds or not, and whether it is a hydrocarbon [50], contains heteroatoms [51], or is inorganic in nature. With regards to the latter, ceramic piezoelectric materials such as barium titanate (BaTiO_3) or zinc oxide (ZnO) are materials that can accumulate electric charge in the structure in response to applied mechanical stress, and thus they could well be considered as force-reactive functional units (i.e., a new class of mechanophores) [52]. Interestingly, techniques based on ultrasound and ball milling have recently been used to activate piezoelectric materials, hinting at the similarities of these two different experimental approaches in the development of mechanochemical reactions. For example, Li and co-workers showed that piezoelectric nanoparticles such as BaTiO_3 and ZnO could trigger water electrolysis under ultrasonication [53]. Sonication caused deformation of, or strain on the material, which induced a nonzero dipole moment in the crystal lattice. As a consequence, a strain-induced charge potential of at least 1.23 eV was produced on the surface of the material, leading to the conversion of mechanical energy into chemi-

cal energy. Mechanistically, the ZnO and BaTiO_3 participated in the formation of H_2 and O_2 from the water splitting reaction by donating strain-induced electrons and holes [53]. The piezoelectricity obtained upon ultrasonication of BaTiO_3 has also been used to trigger and sustain atom transfer radical polymerization (ATRP) reactions of acrylate monomers by mechano-redox reduction of inactive Cu(II) salts to catalytically active Cu(I) species (Figure 5a) [54].

Complementarily, ball milling of BaTiO_3 has been used for mechano-redox ATRC reactions in which highly polarized BaTiO_3 particles produced by the collisions of the milling balls were proposed to reduce the Cu(II) precatalyst to the catalytically active Cu(I) form (Figure 5b) [55].

Other examples have also shown how mechanical activation of piezoelectric materials by ultrasonication and by ball milling is equally appropriate for mechanochemical reactions. For instance, in the field of environmental remediation, the degradation of dye pollutants (e.g., rhodamine) has been accomplished using BaTiO_3 as a mechanophore in solution with ultrasonication [52] or under solvent-free ball milling reaction conditions [56]. These reports complement recent studies on piezocatalysis, such as on chain-growth polymerizations [57–59], arylations and borylations [60], trifluoromethylations [61], as well as dehydrogenative couplings and cycloadditions [62], among others [63,64] in which mechanically polarized piezoelectric materials triggered redox chemistry.

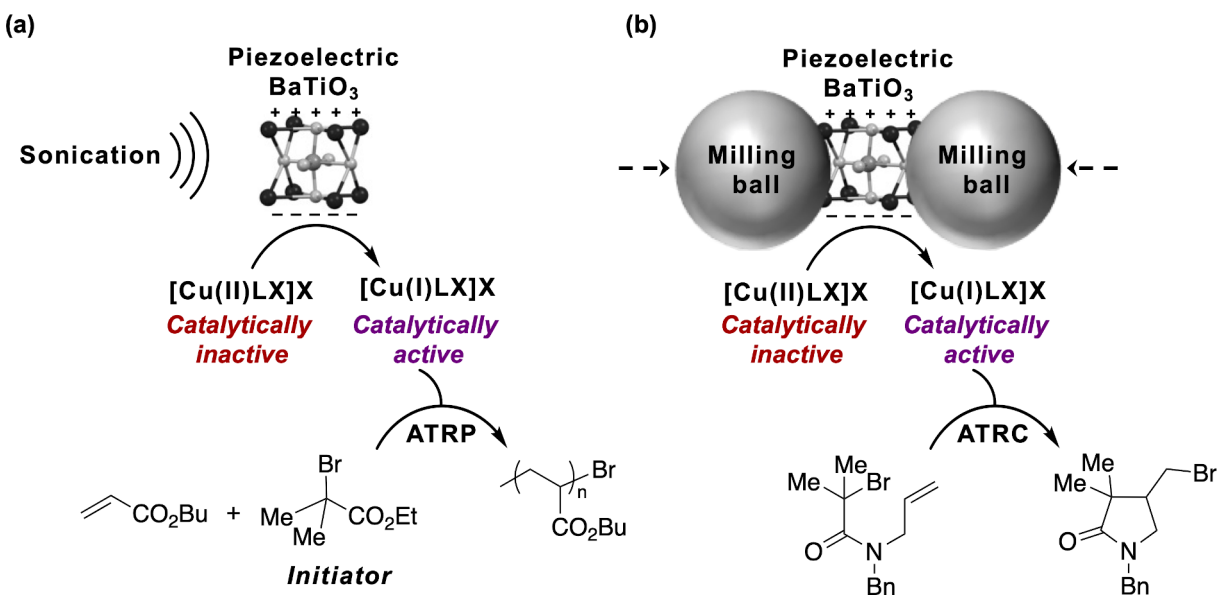


Figure 5: (a) Ultrasound-induced ATRP using piezoelectric BaTiO_3 and (b) mechanochemical atom transfer radical cyclization (ATRC) using BaTiO_3 by ball milling.

Alternative strategies to transduce mechanical force to mechanophores

As evidenced in previous paragraphs, the concept of a mechanophore, which was originally associated with polymer mechanochemistry, has reached the field of small molecule mechanochemistry. However, not only the definition of a mechanophore has evolved in recent years but also the means to transduce mechanical energy to the mechanophores. Typically, polymers were the force transmission medium of choice, but in a recent study, Potrzebowksi, Szumna, and co-workers have shown that molecular capsules can behave as stress-sensitive units [65]. The authors demonstrated the effective complexation of the covalent capsule **5** (made from resorcinarene caps connected by four dihydrazone units of L-cysteine) with C₆₀ and C₇₀ fullerenes upon neat ball milling in a planetary ball mill (Figure 6).

The mechanochemical complexation is remarkable since the porous capsule does not possess large enough openings for the fullerenes to pass through. However, the capsule **5** is sensitive to mechanochemical stress due to the porosity, conformational rigidity, and due to the presence of hydrazone and/or disulfide moieties that act as mechanophores. Therefore, during ball milling, **5** gets partially disintegrated at the weakest covalent connections, enabling the access of fullerenes. As a result, besides polymeric matrices, also porous, semirigid molecules [65] and molecular anvils [66] could eventually become effective transducers of mechanical forces to mechanophores.

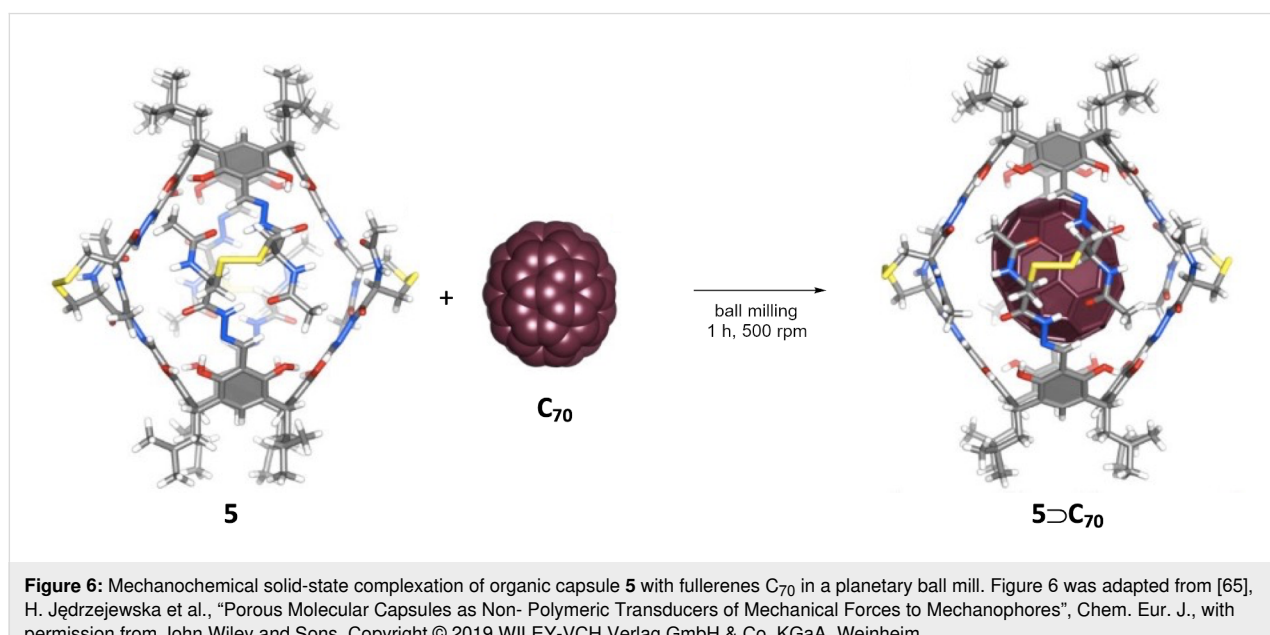
Simpler strategies to circumvent the need for polymers as force transmission media have been investigated. In 2021, Otsuka

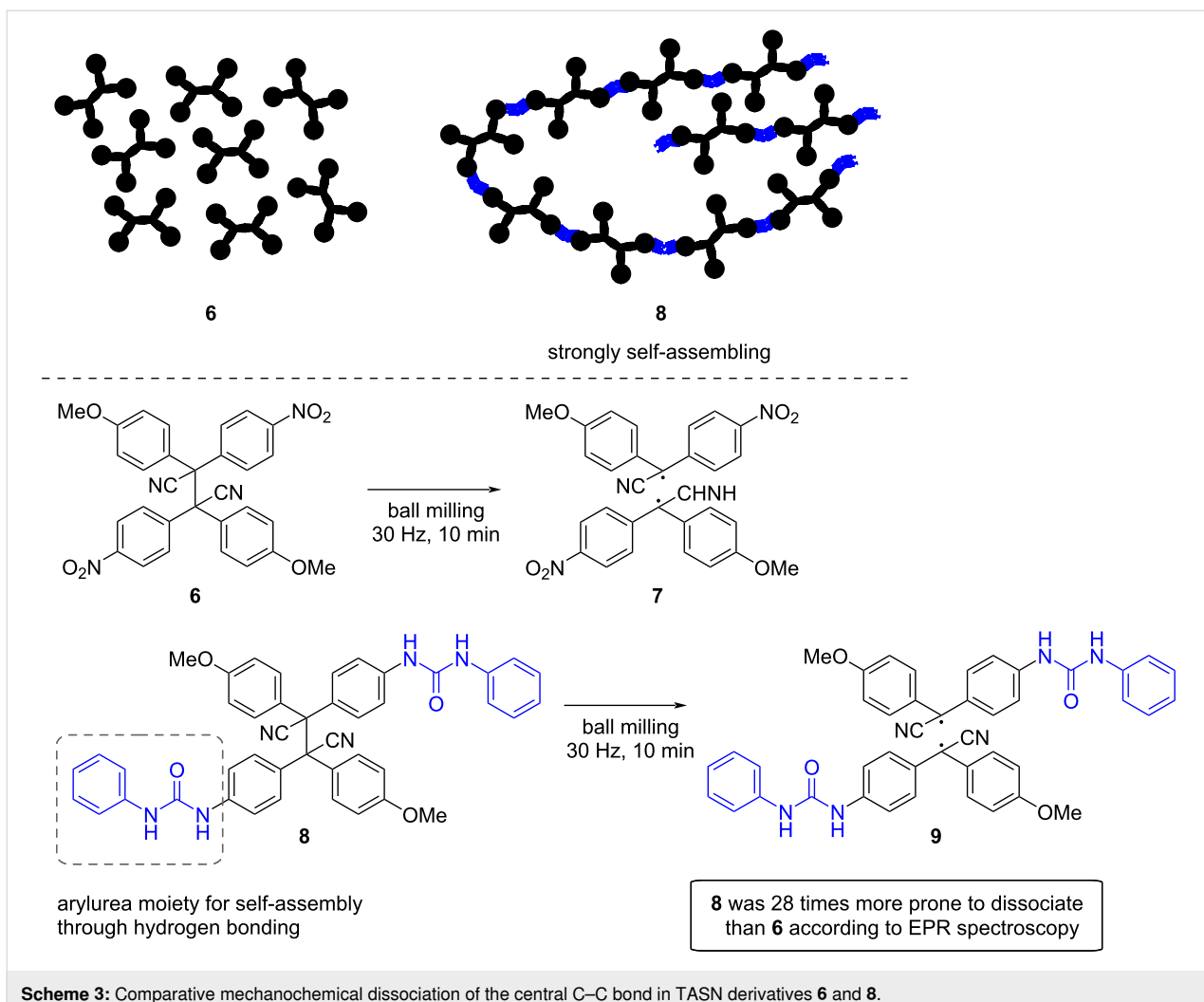
and co-workers reported supramolecular hydrogen-bonding systems as alternative mechanical force transducers [67]. Specifically, the authors synthesized tetraarylsuccinonitrile (TASN) derivatives **6** and **8**. TASN is a well-known mechanophore that generates diarylacetonitrile radicals under force. Hence, when TASN derivative **8**, bearing diarylurea moieties, was ball milled, the corresponding radical **9** was detected by electron paramagnetic resonance (EPR) spectroscopy. Similar treatment proved that **6** was 28 times less prone to generate radicals (Scheme 3) [67].

The difference in the C–C bond scission between **6** and **8** was explained based on the ability of diarylurea moieties in **8** to form strong self-assemblies through hydrogen bonding. In the solid state, this enabled the transduction of mechanical force to the mechanophores. Moreover, it was demonstrated that the hydrogen bonds of the diarylurea linkages also acted as supporting units to maintain the activated mechanophores (radicals) for a longer time [67]. Overall, this new strategy, which harnesses the power of noncovalent interactions by ball milling [68–70], could become an alternative to enhance mechanochemical bond scission in mechanophores without the need to incorporate them into polymeric matrices.

Conclusion

Ultrasonication and ball milling have historically been the flagship techniques in the fields of polymer and small molecule mechanochemistry, respectively. At the same time, examples of crossover in the literature were scarce. However, recent studies have evidenced that not only ultrasound but also ball milling can trigger the activation of mechanophores incorporated into





Scheme 3: Comparative mechanochemical dissociation of the central C–C bond in TASN derivatives **6** and **8**.

polymeric matrices. Conversely, ultrasonication in solution has proven highly effective to mechanically polarize redox active mechanophores such as piezoelectric materials, for which the activation in solid state by ball milling is becoming more frequent. Therefore, despite the apparent differences between both methodological approaches, which is partially attributed to the ability of each method to strain chemical systems on different length- and timescales, new studies have proven that the disparity is slowly becoming less pronounced. For example, with regards to the accepted higher directionality to induce mechanical deformation at the molecular level exhibited by ultrasonication experiments, a new body of evidence indicates that tensile and compressive forces exerted by ball and ring-and-puck milling can also be transduced through the backbone of large molecules. This is accompanied by a certain degree of directionality and can therefore influence the scission of specific bonds within the material. Moreover, research at the interface of polymer and small molecule mechanochemistry has opened new avenues towards the activation of mechanophores

without the need for incorporation into polymeric materials. This is particularly true for porous, semirigid capsules and molecular anvils, which hold promise to become standard low-molecular effective transducers of mechanical forces. This, together with the ability of ball milling to facilitate the formation of covalent and noncovalent supramolecular assemblies, could lead to the direct activation of small mechanophores via the formation of permanent or transient structural aggregates to simplify the transduction of mechanical force to force-reactive functional units. Looking into the future, one could expect that additional comparative studies between sonication and ball milling experiments will occur. At the same time, research into new modes to activate matter by force (e.g., twin-screw extrusion [71], resonant acoustic mixing [72], vortex fluidic mixing [73], laminar flow [74], etc.) will continue to unveil similarities and complementarities, rather than disparities, between the ways polymer and small molecule mechanochemical reactions occur. As a result, the field of mechanochemistry as a whole will ultimately be strengthened.

Acknowledgements

I thank Dr. Karen J. Ardila-Fierro (Universidad de Antioquia, Colombia) for helpful discussions and proofreading.

ORCID® IDs

José G. Hernández - <https://orcid.org/0000-0001-9064-4456>

References

- Li, J.; Nagamani, C.; Moore, J. S. *Acc. Chem. Res.* **2015**, *48*, 2181–2190. doi:10.1021/acs.accounts.5b00184
- De Bo, G. *Macromolecules* **2020**, *53*, 7615–7617. doi:10.1021/acs.macromol.0c01683
- Ghanem, M. A.; Basu, A.; Behrou, R.; Boechler, N.; Boydston, A. J.; Craig, S. L.; Lin, Y.; Lynde, B. E.; Nelson, A.; Shen, H.; Storti, D. W. *Nat. Rev. Mater.* **2021**, *6*, 84–98. doi:10.1038/s41578-020-00249-w
- Chen, Y.; Mellot, G.; van Luijk, D.; Creton, C.; Sijbesma, R. P. *Chem. Soc. Rev.* **2021**, *50*, 6659–6660. doi:10.1039/d1cs90042k
- Bowser, B. H.; Craig, S. L. *Polym. Chem.* **2018**, *9*, 3583–3593. doi:10.1039/c8py00720a
- Akulatov, S.; Boulatov, R. *ChemPhysChem* **2017**, *18*, 1422–1450. doi:10.1002/cphc.201601354
- James, S. L.; Adams, C. J.; Bolm, C.; Braga, D.; Collier, P.; Friščić, T.; Grepioni, F.; Harris, K. D. M.; Hyett, G.; Jones, W.; Krebs, A.; Mack, J.; Maini, L.; Orpen, A. G.; Parkin, I. P.; Shearouse, W. C.; Steed, J. W.; Waddell, D. C. *Chem. Soc. Rev.* **2012**, *41*, 413–447. doi:10.1039/c1cs15171a
- Hernández, J. G.; Bolm, C. J. *Org. Chem.* **2017**, *82*, 4007–4019. doi:10.1021/acs.joc.6b02887
- Howard, J. L.; Cao, Q.; Browne, D. L. *Chem. Sci.* **2018**, *9*, 3080–3094. doi:10.1039/c7sc05371a
- Friščić, T.; Mottillo, C.; Titi, H. M. *Angew. Chem., Int. Ed.* **2020**, *59*, 1018–1029. doi:10.1002/anie.201906755
- Cintas, P.; Tabasso, S.; Veselov, V. V.; Cravotto, G. *Curr. Opin. Green Sustainable Chem.* **2020**, *21*, 44–49. doi:10.1016/j.cogsc.2019.11.007
- Calcio Gaudino, E.; Cravotto, G.; Manzoli, M.; Tabasso, S. *Chem. Soc. Rev.* **2021**, *50*, 1785–1812. doi:10.1039/d0cs01152e
- O’Neill, R. T.; Boulatov, R. *Nat. Rev. Chem.* **2021**, *5*, 148–167. doi:10.1038/s41570-020-00249-y
- Versaw, B. A.; Zeng, T.; Hu, X.; Robb, M. J. *J. Am. Chem. Soc.* **2021**, *143*, 21461–21473. doi:10.1021/jacs.1c11868
- Thieme WebCheminar #2: Mechanochemistry. Thieme, 2022; <https://www.youtube.com/watch?v=jFdw9qt9g5w> (accessed May 12, 2022).
- Di Giannantonio, M.; Ayer, M. A.; Verde-Sesto, E.; Lattuada, M.; Weder, C.; Fromm, K. M. *Angew. Chem., Int. Ed.* **2018**, *57*, 11445–11450. doi:10.1002/anie.201803524
- Sha, Y.; Zhang, Y.; Xu, E.; Wang, Z.; Zhu, T.; Craig, S. L.; Tang, C. *ACS Macro Lett.* **2018**, *7*, 1174–1179. doi:10.1021/acsmacrolett.8b00625
- Sha, Y.; Zhang, H.; Zhou, Z.; Luo, Z. *Polym. Chem.* **2021**, *12*, 2509–2521. doi:10.1039/d1py00311a
- Küng, R.; Göstl, R.; Schmidt, B. M. *Chem. – Eur. J.* **2022**, *28*, e202103860. doi:10.1002/chem.202103860
- Shen, H.; Cao, Y.; Lv, M.; Sheng, Q.; Zhang, Z. *Chem. Commun.* **2022**, *58*, 4813–4824. doi:10.1039/d2cc00147k
- Beedle, A. E. M.; Mora, M.; Davis, C. T.; Snijders, A. P.; Stirnemann, G.; Garcia-Manyes, S. *Nat. Commun.* **2018**, *9*, 3155. doi:10.1038/s41467-018-05115-6
- May, P. A.; Munaretto, N. F.; Hamoy, M. B.; Robb, M. J.; Moore, J. S. *ACS Macro Lett.* **2016**, *5*, 177–180. doi:10.1021/acsmacrolett.5b00855
- Staudinger, H.; Heuer, W. *Ber. Dtsch. Chem. Ges. B* **1934**, *67*, 1159–1164. doi:10.1002/cber.19340670708
- Yamamoto, T.; Kato, S.; Aoki, D.; Otsuka, H. *Angew. Chem., Int. Ed.* **2021**, *60*, 2680–2683. doi:10.1002/anie.202013180
- Kubota, K.; Toyoshima, N.; Miura, D.; Jiang, J.; Maeda, S.; Jin, M.; Ito, H. *Angew. Chem., Int. Ed.* **2021**, *60*, 16003–16008. doi:10.1002/anie.202105381
- Krusenbaum, A.; Grätz, S.; Tigineh, G. T.; Borchardt, L.; Kim, J. G. *Chem. Soc. Rev.* **2022**, *51*, 2873–2905. doi:10.1039/d1cs01093j
- Turksoy, A.; Yıldız, D.; Aydonat, S.; Bedük, T.; Canyurt, M.; Baytekin, B.; Akkaya, E. U. *RSC Adv.* **2020**, *10*, 9182–9186. doi:10.1039/d0ra00831a
- Lu, Y.; Sugita, H.; Mikami, K.; Aoki, D.; Otsuka, H. *J. Am. Chem. Soc.* **2021**, *143*, 17744–17750. doi:10.1021/jacs.1c08533
- Noh, J.; Peterson, G. I.; Choi, T.-L. *Angew. Chem., Int. Ed.* **2021**, *60*, 18651–18659. doi:10.1002/anie.202104447
- Peterson, G. I.; Lee, J.; Choi, T.-L. *Macromolecules* **2019**, *52*, 9561–9568. doi:10.1021/acs.macromol.9b01996
- Yanada, K.; Kato, S.; Aoki, D.; Mikami, K.; Sugita, H.; Otsuka, H. *Chem. Commun.* **2021**, *57*, 2899–2902. doi:10.1039/d0cc08048a
- Ishizuki, K.; Aoki, D.; Otsuka, H. *Macromol. Rapid Commun.* **2021**, *42*, 2000429. doi:10.1002/marc.202000429
- Watabe, T.; Ishizuki, K.; Aoki, D.; Otsuka, H. *Chem. Commun.* **2019**, *55*, 6831–6834. doi:10.1039/c9cc03011e
- Watabe, T.; Aoki, D.; Otsuka, H. *Macromolecules* **2021**, *54*, 1725–1731. doi:10.1021/acs.macromol.0c02497
- Hajiali, F.; Jin, T.; Yang, G.; Santos, M.; Lam, E.; Moores, A. *ChemSusChem* **2022**, *15*, e202102535. doi:10.1002/cssc.202102535
- Hick, S. M.; Griebel, C.; Restrepo, D. T.; Truitt, J. H.; Buker, E. J.; Bylda, C.; Blair, R. G. *Green Chem.* **2010**, *12*, 468–474. doi:10.1039/b923079c
- Hilger, J.; Meine, N.; Rinaldi, R.; Schüth, F. *Energy Environ. Sci.* **2013**, *6*, 92–96. doi:10.1039/c2ee23057g
- Yabushita, M.; Kobayashi, H.; Kuroki, K.; Ito, S.; Fukuoka, A. *ChemSusChem* **2015**, *8*, 3760–3763. doi:10.1002/cssc.201501224
- Chen, X.; Yang, H.; Zhong, Z.; Yan, N. *Green Chem.* **2017**, *19*, 2783–2792. doi:10.1039/c7gc00089h
- Kleine, T.; Buendia, J.; Bolm, C. *Green Chem.* **2013**, *15*, 160–166. doi:10.1039/c2gc36456e
- Brittain, A. D.; Chrisandina, N. J.; Cooper, R. E.; Buchanan, M.; Cort, J. R.; Olarte, M. V.; Sievers, C. *Catal. Today* **2018**, *302*, 180–189. doi:10.1016/j.cattod.2017.04.066
- Amirjalayer, S.; Fuchs, H.; Marx, D. *Angew. Chem., Int. Ed.* **2019**, *58*, 5232–5235. doi:10.1002/anie.201811091
- Patel, D. H.; Marx, D.; East, A. L. L. *ChemPhysChem* **2020**, *21*, 2660–2666. doi:10.1002/cphc.202000671
- Ribas-Arino, J.; Shiga, M.; Marx, D. *Angew. Chem., Int. Ed.* **2009**, *48*, 4190–4193. doi:10.1002/anie.200900673
- De Chavez, D.; Kobayashi, H.; Fukuoka, A.; Hasegawa, J.-y. *J. Phys. Chem. A* **2021**, *125*, 187–197. doi:10.1021/acs.jpca.0c09030
- Einbu, A.; Vårum, K. M. *Biomacromolecules* **2007**, *8*, 309–314. doi:10.1021/bm0608535
- Kobayashi, H.; Suzuki, Y.; Sagawa, T.; Kuroki, K.; Hasegawa, J.-y.; Fukuoka, A. *Phys. Chem. Chem. Phys.* **2021**, *23*, 15908–15916. doi:10.1039/d1cp01650d

48. Dabral, S.; Wotruba, H.; Hernández, J. G.; Bolm, C. *ACS Sustainable Chem. Eng.* **2018**, *6*, 3242–3254. doi:10.1021/acssuschemeng.7b03418

49. Fang, Z.; Mobley, J. K.; Meier, M. S. *Energy Fuels* **2018**, *32*, 11632–11638. doi:10.1021/acs.energyfuels.8b02993

50. Chen, Z.; Mercer, J. A. M.; Zhu, X.; Romaniuk, J. A. H.; Pfattner, R.; Cegelski, L.; Martinez, T. J.; Burns, N. Z.; Xia, Y. *Science* **2017**, *357*, 475–479. doi:10.1126/science.aan2797

51. Jung, S.; Yoon, H. J. *Synlett* **2022**, *33*, 863–874. doi:10.1055/a-1703-2608

52. Wang, M.; Wang, B.; Huang, F.; Lin, Z. *Angew. Chem., Int. Ed.* **2019**, *58*, 7526–7536. doi:10.1002/anie.201811709

53. Hong, K.-S.; Xu, H.; Konishi, H.; Li, X. *J. Phys. Chem. Lett.* **2010**, *1*, 997–1002. doi:10.1021/jz100027t

54. Mohapatra, H.; Kleiman, M.; Esser-Kahn, A. P. *Nat. Chem.* **2017**, *9*, 135–139. doi:10.1038/nchem.2633

55. Schumacher, C.; Hernández, J. G.; Bolm, C. *Angew. Chem., Int. Ed.* **2020**, *59*, 16357–16360. doi:10.1002/anie.202003565

56. Zhou, S.; Hao, J.; Zhou, M.; Qiao, X.; Pang, X. *Appl. Catal., A* **2022**, *629*, 118406. doi:10.1016/j.apcata.2021.118406

57. Mohapatra, H.; Ayarza, J.; Sanders, E. C.; Scheuermann, A. M.; Griffin, P. J.; Esser-Kahn, A. P. *Angew. Chem., Int. Ed.* **2018**, *57*, 11208–11212. doi:10.1002/anie.201804451

58. Wang, Z.; Ayarza, J.; Esser-Kahn, A. P. *Angew. Chem., Int. Ed.* **2019**, *58*, 12023–12026. doi:10.1002/anie.201903956

59. Ayarza, J.; Wang, Z.; Wang, J.; Huang, C.-W.; Esser-Kahn, A. P. *ACS Macro Lett.* **2020**, *9*, 1237–1248. doi:10.1021/acsmacrolett.0c00477

60. Kubota, K.; Pang, Y.; Miura, A.; Ito, H. *Science* **2019**, *366*, 1500–1504. doi:10.1126/science.aay8224

61. Pang, Y.; Lee, J. W.; Kubota, K.; Ito, H. *Angew. Chem., Int. Ed.* **2020**, *59*, 22570–22576. doi:10.1002/anie.202009844

62. Huang, M.; Deng, L.; Lao, T.; Zhang, Z.; Su, Z.; Yu, Y.; Cao, H. *J. Org. Chem.* **2022**, *87*, 3265–3275. doi:10.1021/acs.joc.1c02940

63. Sharma, H.; Kaur, N.; Singh, N.; Jang, D. O. *Green Chem.* **2015**, *17*, 4263–4270. doi:10.1039/c5gc00536a

64. Wang, Y.; Zhang, Z.; Deng, L.; Lao, T.; Su, Z.; Yu, Y.; Cao, H. *Org. Lett.* **2021**, *23*, 7171–7176. doi:10.1021/acs.orglett.1c02575

65. Jędrzejewska, H.; Wielgus, E.; Kaźmierski, S.; Rogala, H.; Wierzbicki, M.; Wróblewska, A.; Pawlak, T.; Potrzebowski, M. J.; Szumna, A. *Chem. – Eur. J.* **2020**, *26*, 1558–1566. doi:10.1002/chem.201904024

66. Yan, H.; Yang, F.; Pan, D.; Lin, Y.; Hohman, J. N.; Solis-Ibarra, D.; Li, F. H.; Dahl, J. E. P.; Carlson, R. M. K.; Tkachenko, B. A.; Fokin, A. A.; Schreiner, P. R.; Galli, G.; Mao, W. L.; Shen, Z.-X.; Melosh, N. A. *Nature* **2018**, *554*, 505–510. doi:10.1038/nature25765

67. Kida, J.; Aoki, D.; Otsuka, H. *Aggregate* **2021**, *2*, e50. doi:10.1002/agt2.50

68. Lukin, S.; Tireli, M.; Lončarić, I.; Barišić, D.; Šket, P.; Vrsaljko, D.; di Michiel, M.; Plavec, J.; Užarević, K.; Halasz, I. *Chem. Commun.* **2018**, *54*, 13216–13219. doi:10.1039/c8cc07853j

69. Kralj, M.; Lukin, S.; Miletić, G.; Halasz, I. *J. Org. Chem.* **2021**, *86*, 14160–14168. doi:10.1021/acs.joc.1c01817

70. Ardila-Fierro, K. J.; Rubčić, M.; Hernández, J. G. *Chem. – Eur. J.* **2022**, *28*, e202200737. doi:10.1002/chem.202200737

71. Bolt, R. R. A.; Leitch, J. A.; Jones, A. C.; Nicholson, W. I.; Browne, D. L. *Chem. Soc. Rev.* **2022**, *51*, 4243–4260. doi:10.1039/d1cs00657f

72. Gonnet, L.; Lennox, C. B.; Do, J.-L.; Malvestiti, I.; Koenig, S. G.; Nagapudi, K.; Friščić, T. *Angew. Chem., Int. Ed.* **2022**, *61*, e202115030. doi:10.1002/anie.202115030

73. Jellicoe, M.; Igder, A.; Chuah, C.; Jones, D. B.; Luo, X.; Stubbs, K. A.; Crawley, E. M.; Pye, S. J.; Joseph, N.; Vimalanathan, K.; Gardner, Z.; Harvey, D. P.; Chen, X.; Salvemini, F.; He, S.; Zhang, W.; Chalker, J. M.; Quinton, J. S.; Tang, Y.; Raston, C. L. *Chem. Sci.* **2022**, *13*, 3375–3385. doi:10.1039/d1sc05829k

74. Willis-Fox, N.; Rognin, E.; Baumann, C.; Aljohani, T. A.; Göstl, R.; Daly, R. *Adv. Funct. Mater.* **2020**, *30*, 2002372. doi:10.1002/adfm.202002372

License and Terms

This is an open access article licensed under the terms of the Beilstein-Institut Open Access License Agreement (<https://www.beilstein-journals.org/bjoc/terms>), which is identical to the Creative Commons Attribution 4.0 International License

(<https://creativecommons.org/licenses/by/4.0>). The reuse of material under this license requires that the author(s), source and license are credited. Third-party material in this article could be subject to other licenses (typically indicated in the credit line), and in this case, users are required to obtain permission from the license holder to reuse the material.

The definitive version of this article is the electronic one which can be found at:

<https://doi.org/10.3762/bjoc.18.128>



Mechanochemical synthesis of unsymmetrical salens for the preparation of Co–salen complexes and their evaluation as catalysts for the synthesis of α -aryloxy alcohols via asymmetric phenolic kinetic resolution of terminal epoxides

Shengli Zuo¹, Shuxiang Zheng¹, Jianjun Liu^{*1} and Ang Zuo^{*2}

Letter

Open Access

Address:

¹State Key Laboratory of Chemical Resource Engineering, Department of Applied Chemistry, College of Chemistry, Beijing University of Chemical Technology, Beijing 100029, China and ²Department of Pharmaceutical Sciences, College of Pharmacy and UICentre, University of Illinois at Chicago, Chicago, Illinois 60612, United States

Email:

Jianjun Liu^{*} - ljj-717@163.com; Ang Zuo^{*} - azuo@uic.edu

* Corresponding author

Keywords:

α -aryloxy alcohols; chiral Co–salen; HKR; mechanochemistry; phenolic KR

Beilstein J. Org. Chem. **2022**, *18*, 1416–1423.

<https://doi.org/10.3762/bjoc.18.147>

Received: 21 April 2022

Accepted: 07 September 2022

Published: 10 October 2022

This article is part of the thematic issue "Mechanochemistry III".

Guest Editors: J. G. Hernández and L. Borchardt

© 2022 Zuo et al.; licensee Beilstein-Institut.

License and terms: see end of document.

Abstract

In this paper, we report the mechanochemical synthesis of unsymmetrical salens using grinding and ball milling technologies, respectively, both of which were afforded in good yield. The chelating effect of the unsymmetrical salens with zinc, copper, and cobalt was studied and the chiral Co–salen complex **2f** was obtained in 98% yield. Hydrolytic kinetic resolution (HKR) of epichlorohydrin with water catalyzed by complex **2f** (0.5 mol %) was explored and resulted in 98% ee, suggesting complex **2f** could serve as an enantioselective catalyst for the asymmetric ring opening of terminal epoxides by phenols. A library of α -aryloxy alcohols **3** was thereafter synthesized in good yield and high ee using **2f** via the phenolic KR of epichlorohydrin.

Introduction

In the past decade, more than twenty chiral small molecule drugs were approved by the FDA, including ruxolitinib, afatinib, sonidegib, encorafenib, lorlatinib, darolutamide, alpelisib, artesunate, maribavir, ponesimod, daridorexant and others [1–3]. The enantioselective synthesis in modern chem-

istry turns out to be accumulatively essential for the preparation of chiral drugs, which is a huge growing market in the future. Indeed, the asymmetric ring opening of terminal epoxides is one of the most important strategies for synthesizing drug-like building blocks and key organic intermediates in the drug

discovery and process chemistry [4–6]. Chiral metal–salen complexes were designed for catalyzing reaction processes that resulted in good yield, high regioselective and enantioselective control for the asymmetric ring opening of terminal epoxides. Various metals have been explored to optimize the catalytic properties of chiral metal–salens, such as Cr [7], Co [8], Fe [9], Ti [10], Al [11], Y [12], and Mn [13] and investigated with numerous nucleophiles to afford chiral molecules. In addition to the variation of metals, salen ligands have also been studied with regard to conformational differences, for instance, oligo-salen [14], macrocyclic oligosalen [15], and polymeric salen [16].

Jacobsen and co-workers reported the first synthesis of α -aryloxy alcohols through the phenolic kinetic resolution (KR) of terminal epoxides using a Co–salen catalyst [17]. Since their discovery, researchers have investigated several Co–salen complexes for the KR of epoxides with phenols as nucleophiles

(Figure 1) [18,19]. Kim et al. described a catalytic system of a chiral Co–salen immobilized on meso/macroporous silica monoliths for the ring opening of epoxides [20]. Jones et al. designed a cyclooctene-based Co–salen macrocycle catalyst for the phenolic KR of epichlorohydrin and 1,2-epoxyhexane [21]. However, these Co–salen systems suffer from several limitations such as tedious preparation of salen scaffolds, excess use of epoxides, high catalyst loadings, narrow scope and the need of Lewis acidic or basic co-catalysts [22–24]. A more efficient preparation of Co–salen catalysts is therefore of a great need for the asymmetric ring opening of epoxides, and thus became extremely attractive to us.

The synthesis of novel Co–salen catalysts begins with the design and preparation of suitable salen compounds, sometimes are described as bis-imine Schiff bases. Imines were originally synthesized by Schiff from the condensation of carbonyls with amines [25]. Thereafter, syntheses of salens were exten-

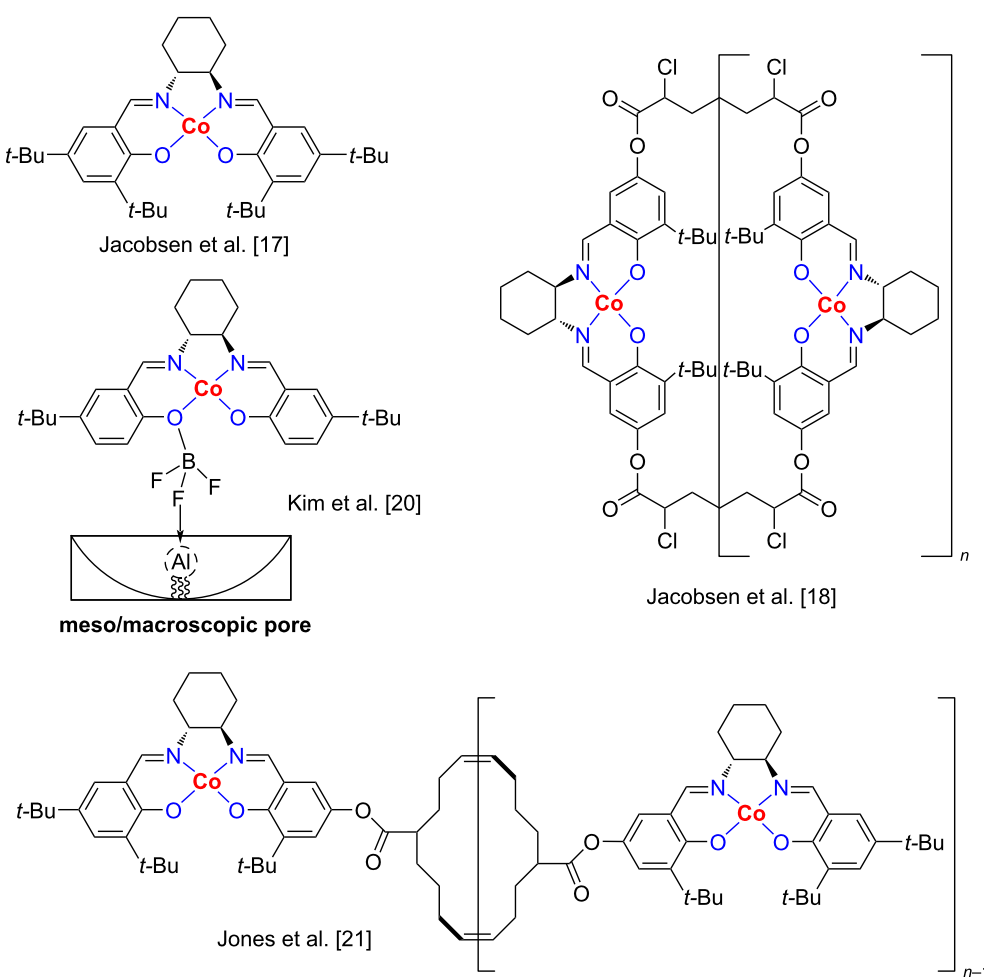


Figure 1: Representative asymmetric Co–salen catalysts.

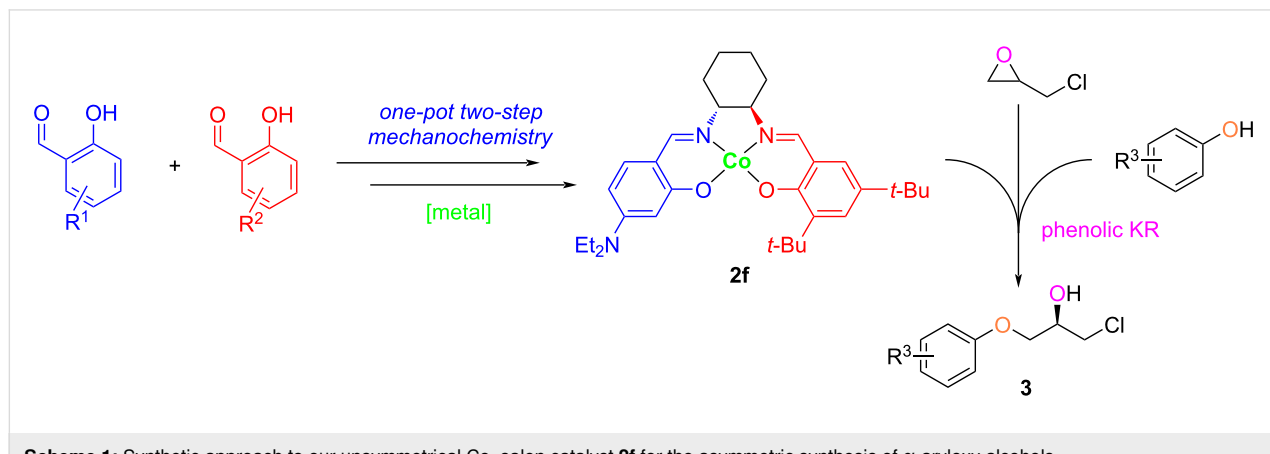
sively reported using timely technologies [26–29]. Inspired by the mechanochemical chemistry technology to simplify chemical processes and eliminate the use of organic solvents, salen compounds have been synthesized by the “green” grinding strategy previously [30–39]. Herein, we report a one-pot two-step mechanochemical synthesis of unsymmetrical salens for the preparation of Co–salen complexes and their evaluation as catalyst for the synthesis of α -aryloxy alcohols through the phenolic KR of terminal epoxides (Scheme 1). Indeed, advantages to break the C_2 -symmetry in Co–salen complexes were reported before [23,40]. In addition, a Lewis basic NEt_2 ($-\text{N}(\text{CH}_2\text{CH}_3)_2$) group was introduced to the salen scaffold to facilitate purification, enhance catalytic efficiency, and improve the thermal stability, as was shown in the synthesis of fluorescent probes [41,42]. The chelating effect of salen compounds **1** with different metals were explored as well. Furthermore, we present the hydrolytic kinetic resolution (HKR) of epichlorohydrin with water using Co–salen complexes **2**, and α -aryloxy alcohols were synthesized by the **2f** catalytic system through the asymmetric ring opening of epichlorohydrin and phenols.

Results and Discussion

The mechanochemical study examined the synthesis of several unsymmetrical salens using monoammonium salts and salicylaldehydes (Scheme 2). Agate mortar and pestle were used for the one-pot two-step mechanochemical reactions (see Supporting Information File 1). Initially, 1,2-diaminocyclohexane or ethylenediamine monohydrochlorides were grinded with a half equivalent of 4-diethylamino ($\text{Et}_2\text{N}-$), 3,5-dichloro ($\text{Cl}-$), or 3,5-di-*tert*-butyl (*t*-Bu–) salicylaldehydes (blue moieties in Scheme 2) for 10 minutes. The synthesis of diamine monohydrochlorides and characterization data of mono-imine ammonium salts were described before [30–33,36]. This process generates mono-imine ammonium salts as the stable intermediates in the mortar. Without implementing treatment such as

filtration, evaporation of solvents, or further purification, mono-imine ammonium salts were subsequently treated with triethylamine (Et_3N), half equivalent of 5-bromo ($\text{Br}-$), 5-methyl, 4-diethylamino ($\text{Et}_2\text{N}-$), 3,5-dichloro ($\text{Cl}-$), or 3,5-di-*tert*-butyl (*t*-Bu–) salicylaldehydes (red moieties in Scheme 2), and trace methanol, followed by grinding for 20 minutes for the second reaction step to complete, monitored by TLC. A trace amount of methanol was used to lubricate the molecular surface for an improved performance (known as liquid-assisted grinding, LAG) [42]. Unsymmetrical salens **1a–h** were obtained in the yield of 72% to 95% after being purified by column chromatography. Bromo-containing salen **1a** was yielded the best (95%), presumably due to the strong electron-withdrawing effect of bromine, enhancing the electrophilic property of bromo-substituted salicylaldehyde. Because of the poor solubility in the eluent, the yield of dichloro-containing **1c** (88%) was lower than **1a** after isolating by column chromatography. This was also found between **1g** (81%) and **1h** (76%). Yields of **1d** (79%), **1e** (81%), and **1f** (72%) were less than **1a–c**, caused by the steric hindrance of di-*tert*-butyl groups. In the aspect of characterization of salens, two singlets were shown at around 8 ppm in the ^1H NMR spectrum, indicating two unsymmetrical imines. The broad peak at around 13 ppm was assigned to the phenolic OH groups. The signal at around 1615 cm^{-1} in the IR spectrum could also indicate the formation of imine (see Supporting Information File 1).

In addition to the use of grinding technology, a self-made ball mill was applied to the synthesis of unsymmetrical salens by us. The method and its principle were described previously [43–45]. Ball mill systems have several advantages including superior mixing, continuous operation, and enclosed reaction environment. Our ball mill system was designed to mount a 40 mL glass reactor with zirconia and/or alumina composite balls (3.20 mm and 2.16 mm in diameter, respectively). Considering the safety in the synthesis of unsymmetrical salens, the working



speed was set to be 700 rev/min. Similarly to the above reaction conditions, amounts of chemicals and workup, the first reaction step between amino monohydrochlorides and salicylaldehydes (blue in Scheme 2) took 1 hour for reaction completion. After adding another salicylaldehyde (red in Scheme 2), Et₃N, and methanol, the second reaction step was completed in an additional hour, monitored by TLC. Yields of unsymmetrical salens using grinding and ball milling were summarized in

Table 1. We were surprised that the overall yield from ball milling was lower than the overall yield from grinding, suggesting a higher revolution per minute (RPM) could be necessary to increase the reaction yield using ball milling. It is assumed that the forces are not equivalent in both techniques and probably pressure-induced activation and shearing deformation of reactant particles are more efficient using the grinding.

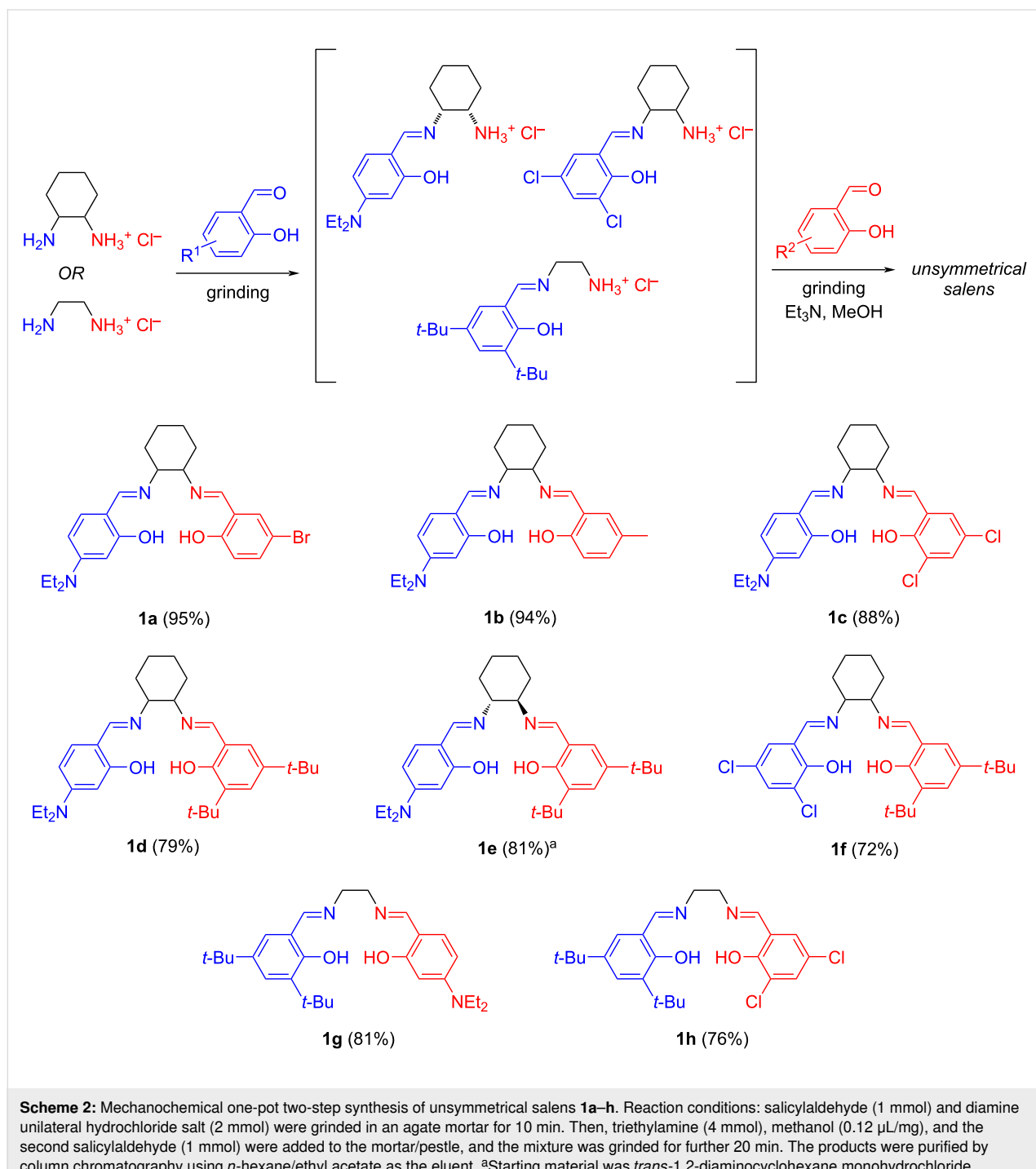
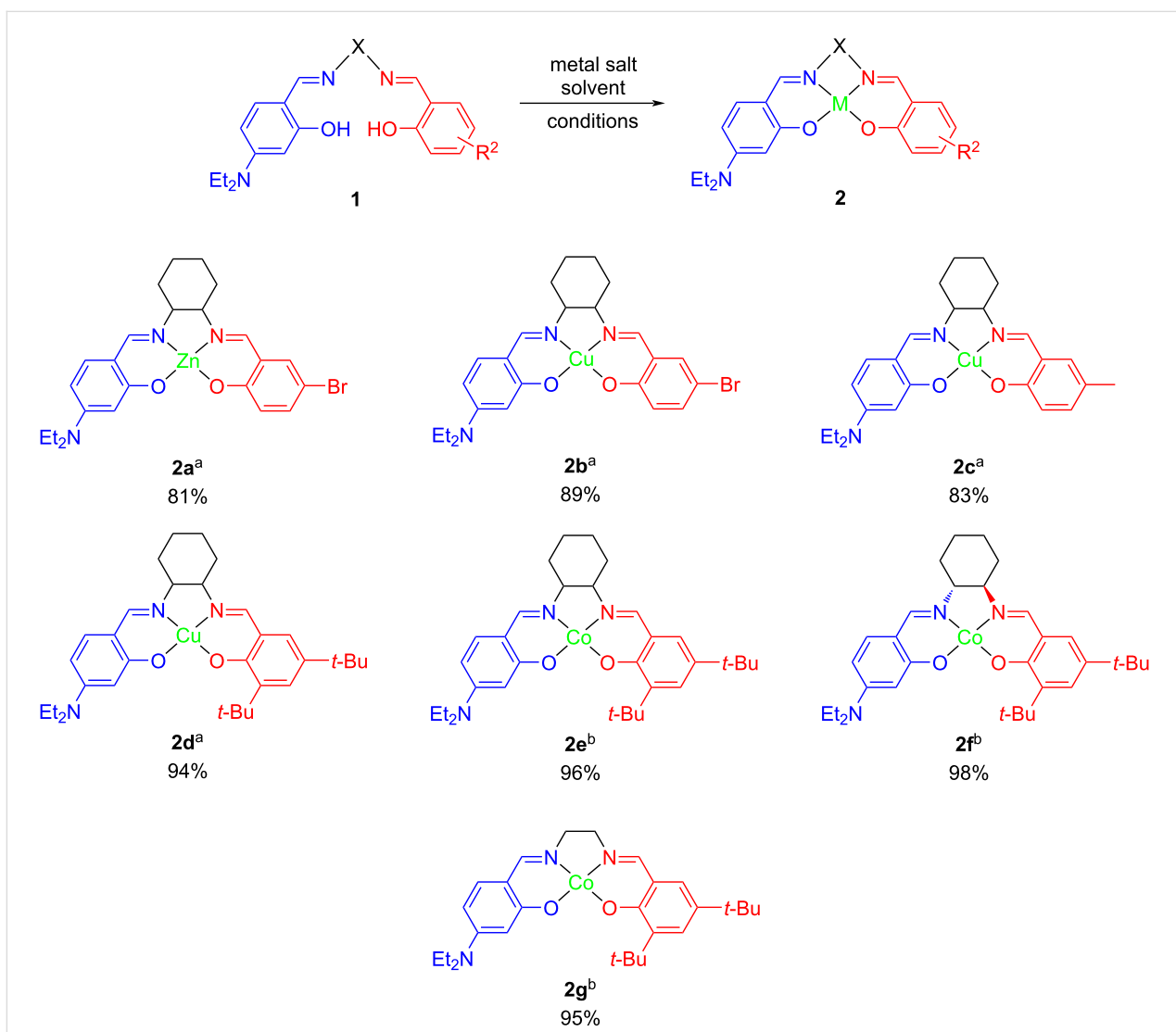


Table 1: Yields of unsymmetrical salens **1** using grinding and ball milling.

Entry	ID	Grinding/yield (%)	Ball milling/yield (%)
1	1a	95	82
2	1b	94	71
3	1c	88	77
4	1d	79	66
5	1e	81	68
6	1f	72	57
7	1g	81	72
8	1h	76	61

We next examined the chelating effect of the above salens **1** with different transition metals. A library of metal–salen complexes was synthesized as outlined in Scheme 3. Reaction conditions were described previously [17,46]. For reactions using Zn and Cu, $Zn(OAc)_2 \cdot 2H_2O$ or $Cu(OAc)_2 \cdot H_2O$ in methanol was dropwise added to **1a**, **b**, or **d** in ethanol under nitrogen gas. The reaction mixture was refluxed for 4 hours and a light yellow or dark green solid was formed. Complexes **2a–d** were obtained by filtration and washed with cold methanol. For reactions using Co salt, $Co(OAc)_2 \cdot 4H_2O$ and **1d**, **g**, or **e** was gradually added to methanol under nitrogen gas. The reaction mixture was stirred at $0\text{ }^\circ\text{C}$ for 40 min and a brick-red precipitate was formed. Complexes **2e–g** were isolated by the similar puri-

**Scheme 3:** Synthesis of unsymmetrical metal–salen complexes **2**. Reaction conditions a: metal acetate hydrate (1 mmol) and MeOH (12 mL) were dropwise added to compound **1** (1 mmol) in EtOH (7 mL) in a round-bottomed flask, and refluxed for 4 hours under nitrogen gas. Products were afforded by filtration and washed with cold methanol (20 mL \times 2); Reaction conditions b: ligand **1** (1 mmol), cobalt(II) acetate tetrahydrate (1.2 mmol), and MeOH (10 mL) were gradually added to a round-bottomed flask, and stirred at $0\text{ }^\circ\text{C}$ for 40 min under nitrogen gas. Products were isolated by filtration and washed with cold methanol (2 \times 20 mL).

fying method as described above. The yield of Zn complex **2a** (81%) is slightly lower than the Cu complex **2b** (89%). Compounds **1b** and **1d** reacted with Cu to afford **2c** and **2d** in the yields of 83% and 94%, respectively. The reaction affinity between Co and selected salens was higher than Zn and Cu complexes, for instance, **2e** (96%), **2f** (98%), and **2g** (95%). A *tert*-butyl group played an important role as an electron-donating moiety for increasing the yield (**2d–g**). The slightly higher yield of **2f** over **2e** suggested a relatively more effective preparation for chiral salen complexes.

The HKR of epichlorohydrin with water was selected as a classical model to evaluate the catalytic activity of Co-unsymmetrical salen complexes **2e**, **2f**, and **2g** for the asymmetric ring opening of epoxides. Enantiomeric excess (ee) results of 3-chloro-1,2-propanediol from the HKR reactions were summarized in Table 2. The complex **2** (0.5 mmol) and trace amount of glacial acetic acid were added to dry dichloromethane. The mixture solution was evaporated after the reaction color changed from orange-red to dark brown in 30 minutes. Racemic epichlorohydrin and deionized water were subsequently added to the reaction and stirred for 18 hours at 0 °C. Upon the reaction completion, 3-chloro-1,2-propanediol in highly enantioenriched structure was afforded using chiral catalyst **2f**, while non-chiral catalysts **2e** and **2g** displayed nonenantioselective results (Table 2).

To broaden the use of our chiral catalyst, α -aryloxy alcohols were thereafter synthesized through the KR of epichlorohydrin with different phenols using chiral Co-salen catalyst **2f**

(Table 3). *meta*-Substituted methylphenol showed less reactivity and selectivity (Table 3, entry 2), while *tert*-butyl monosubstitution at the *para*-position on the phenol slightly increased in light of the yield and ee (Table 3, entry 3). Bulky phenol afforded no product (**3e**), which is in good agreement with the suggested Co-salen catalytic mechanism [6]. Phenols with both electron-donating and electron-withdrawing moieties participated in the asymmetric ring opening of epichlorohydrin and provided α -aryloxy alcohols in an overall high yield and a complete enantioselectivity.

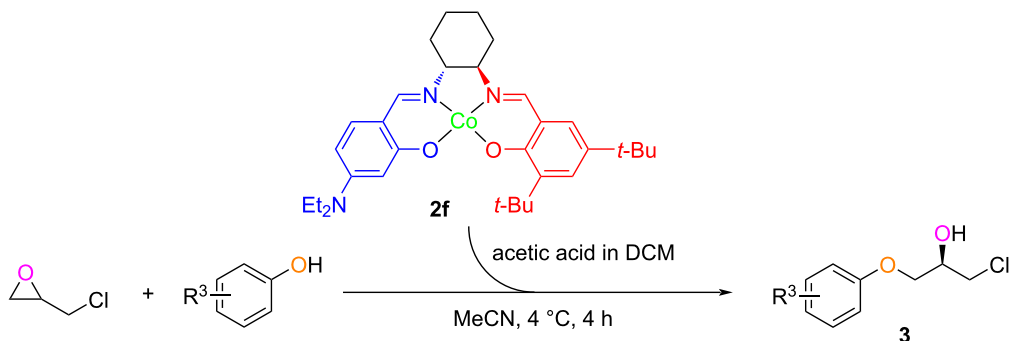
Conclusion

In summary, we mechanochemically synthesized unsymmetrical salens **1** for preparing metal-salen catalysts **2** for the first time. The use of grinding technology provided salens **1** in an overall higher yield in comparison to the self-made ball milling. Faster RPM (over 700 rev/min) might be necessary to increase the reaction efficiency through a ball milling technology. Chelating ability of **1** with different metals was explored and metal-salen complexes **2a–g** were highly yielded, demonstrating an intimate affinity of unsymmetrical salens chelating with metals. The HKR of epichlorohydrin with water catalyzed by Co-salen **2** was studied and chiral **2f** showed an outstanding catalytic ability to afford the diol product in high ee (98%). A library of α -aryloxy alcohols was thereafter synthesized through the asymmetric ring opening of epichlorohydrin with different phenols in the presence of **2f** (0.5 mol %), resulting in good yields and high ee (up to 99%). Further application of chiral Co-salen complexes and their reaction mechanism will be addressed in the due course.

Table 2: HKR of epichlorohydrin with water catalyzed by **2**.^a

Entry	Catalyst	ee (%) ^b
1	2e	0
2	2f	98
3	2g	0

^aReaction conditions: **2** (0.5 mmol, 0.5 mol % of deionized water), DCM (8 mL), acetic acid (5 mmol) were stirred for 30 min at rt, epichlorohydrin (167 mmol, 1.8 equiv) in deionized water (1.65 mL, 92 mmol, 1 equiv) was added to the reaction system at 0 °C and stirred for 18 h for completion; ^bdetermined by chiral HPLC analysis, $[\alpha]_D^{23} +22.30$ (c 1, MeOH).

Table 3: Synthesis of α -aryloxy alcohols **3** by KR of epichlorohydrin with phenols catalyzed by complex **2f**.^{a,b}

Entry	ID	R ³	Yield (%) ^c	ee (%) ^d
1	3a	H	60	98
2	3b	<i>m</i> -CH ₃	67	93
3	3c	<i>p</i> - <i>t</i> -Bu	75	99
4	3d	<i>p</i> -CHO	56	96
5	3e	di- <i>o</i> - <i>t</i> -Bu; <i>p</i> -CH ₃	0	—

^aReaction conditions: Complex **2f** (0.1 mmol, 0.5 mol % of phenol), DCM (2 mL), and acetic acid (1 mmol) were stirred for 30 min at rt, epichlorohydrin (44.4 mmol, 2.22 equiv) in MeCN (1.1 mL) was added to the reaction system at 4 °C and stirred for 20 min, followed by the addition of the phenol (20 mmol, 1 equiv) and stirring at 4 °C for 4 h for completion; ^bsee ref. [21] for method development; ^cisolated yields based on alcohol; ^ddetermined by chiral HPLC analysis.

Supporting Information

Supporting Information File 1

Experimental section and copies of spectra.

[<https://www.beilstein-journals.org/bjoc/content/supplementary/1860-5397-18-147-S1.pdf>]

ORCID® IDs

Ang Zuo - <https://orcid.org/0000-0002-4075-8786>

Preprint

A non-peer-reviewed version of this article has been previously published as a preprint: <https://doi.org/10.3762/bxiv.2022.27.v1>

References

- Chu, X.; Bu, Y.; Yang, X. *Front. Oncol.* **2021**, *11*, 785855. doi:10.3389/fonc.2021.785855
- Nguyen, L. A.; He, H.; Pham-Huy, C. *Int. J. Biomed. Sci. (Pomona, CA, U. S.)* **2006**, *2*, 85–100.
- Yoon, T. P.; Jacobsen, E. N. *Science* **2003**, *299*, 1691–1693. doi:10.1126/science.1083622
- Schettini, R.; Della Sala, G. *Catalysts* **2021**, *11*, 306. doi:10.3390/catal11030306
- Lidskog, A.; Li, Y.; Wärnmark, K. *Catalysts* **2020**, *10*, 705. doi:10.3390/catal10060705
- Jacobsen, E. N. *Acc. Chem. Res.* **2000**, *33*, 421–431. doi:10.1021/ar960061v
- Lindbäck, E.; Norouzi-Arasi, H.; Sheibani, E.; Ma, D.; Dawaigher, S.; Wärnmark, K. *ChemistrySelect* **2016**, *1*, 1789–1794. doi:10.1002/slct.201600457
- White, D. E.; Tadross, P. M.; Lu, Z.; Jacobsen, E. N. *Tetrahedron* **2014**, *70*, 4165–4180. doi:10.1016/j.tet.2014.03.043
- Roy, S.; Bhanja, P.; Safikul Islam, S.; Bhaumik, A.; Manirul Islam, S. *Chem. Commun.* **2016**, *52*, 1871–1874. doi:10.1039/c5cc08675b
- Kureshy, R. I.; Kumar, M.; Agrawal, S.; Khan, N.-U. H.; Dangi, B.; Abdi, S. H. R.; Bajaj, H. C. *Chirality* **2011**, *23*, 76–83. doi:10.1002/chir.20868
- Pakulski, Z.; Pietrusiewicz, K. M. *Tetrahedron: Asymmetry* **2004**, *15*, 41–45. doi:10.1016/j.tetasy.2003.10.015
- Saha, B.; Lin, M.-H.; RajanBabu, T. V. *J. Org. Chem.* **2007**, *72*, 8648–8655. doi:10.1021/jo071076h
- Kawthekar, R. B.; Bi, W.; Kim, G.-J. *Bull. Korean Chem. Soc.* **2008**, *29*, 313–318. doi:10.5012/bkcs.2008.29.2.313
- Ready, J. M.; Jacobsen, E. N. *Angew. Chem., Int. Ed.* **2002**, *41*, 1374–1377. doi:10.1002/1521-3773(20020415)41:8<1374::aid-anie1374>3.0.co;2-8
- Kahn, M. G. C.; Weck, M. *Catal. Sci. Technol.* **2012**, *2*, 386–389. doi:10.1039/c1cy00290b
- Dandachi, H.; Nasrallah, H.; Ibrahim, F.; Hong, X.; Mellah, M.; Jaber, N.; Schulz, E. *J. Mol. Catal. A: Chem.* **2014**, *395*, 457–462. doi:10.1016/j.molcata.2014.09.012
- Ready, J. M.; Jacobsen, E. N. *J. Am. Chem. Soc.* **1999**, *121*, 6086–6087. doi:10.1021/ja9910917
- Ready, J. M.; Jacobsen, E. N. *J. Am. Chem. Soc.* **2001**, *123*, 2687–2688. doi:10.1021/ja005867b

19. Kamble, R. B.; Devalankar, D.; Suryavanshi, G. *New J. Chem.* **2018**, *42*, 10414–10420. doi:10.1039/c8nj01616j

20. Kim, Y.-S.; Guo, X.-f.; Kim, G.-J. *Top. Catal.* **2009**, *52*, 197–204. doi:10.1007/s11244-008-9140-x

21. Zhu, X.; Venkatasubbaiah, K.; Weck, M.; Jones, C. W. *J. Mol. Catal. A: Chem.* **2010**, *329*, 1–6. doi:10.1016/j.molcata.2010.06.015

22. Dhakshinamoorthy, A.; Alvaro, M.; Garcia, H. *Chem. – Eur. J.* **2010**, *16*, 8530–8536. doi:10.1002/chem.201000588

23. Zheng, X.; Jones, C. W.; Weck, M. *J. Am. Chem. Soc.* **2007**, *129*, 1105–1112. doi:10.1021/ja0641406

24. Surendra, K.; Krishnaveni, N. S.; Nageswar, Y. V. D.; Rao, K. R. *J. Org. Chem.* **2003**, *68*, 4994–4995. doi:10.1021/jo034194n

25. Nic, M.; Jirat, J.; Kosata, B. *Schiff bases. IUPAC Compendium of Chemical Terminology*; International Union of Pure and Applied Chemistry (IUPAC): Research Triangle Park, NC, USA, 2006.

26. Leon, F.; Li, C.; Reynes, J. F.; Sigh, V. K.; Xiao, L.; Ong, H. C.; Hum, G.; Sun, H.; García, F. *ChemRxiv* **2022**. doi:10.26434/chemrxiv-2022-gm12z

27. Mohan, N.; Sreejith, S. S.; George, R.; Mohanan, P. V.; Kurup, M. R. P. *J. Mol. Struct.* **2021**, *1229*, 129779. doi:10.1016/j.molstruc.2020.129779

28. Rawajfeh, R. S.; Awwadi, F. F.; Bardawel, S. K.; Hodali, H. A. *J. Struct. Chem.* **2020**, *61*, 1985–1992. doi:10.1134/s0022476620120173

29. Cívicos, J. F.; Coimbra, J. S. M.; Costa, P. R. R. *Synthesis* **2017**, *49*, 3998–4006. doi:10.1055/s-0036-1588446

30. Bento, O.; Luttringer, F.; Mohy El Dine, T.; Pétry, N.; Bantrel, X.; Lamaty, F. *Eur. J. Org. Chem.* **2022**, e202101516. doi:10.1002/ejoc.202101516

31. Singh, V. K.; Chamberlain-Clay, A.; Ong, H. C.; León, F.; Hum, G.; Par, M. Y.; Daley-Dee, P.; García, F. *ACS Sustainable Chem. Eng.* **2021**, *9*, 1152–1160. doi:10.1021/acssuschemeng.0c06374

32. León, F.; García, F. Metal Complexes in Mechanochemistry. In *Comprehensive Coordination Chemistry III*; Constable, E. C.; Parkin, G.; Que, L., Jr., Eds.; Elsevier: Amsterdam, Netherlands, 2021; pp 620–679. doi:10.1016/b978-0-08-102688-5.00031-3

33. Friščić, T.; Mottillo, C.; Titi, H. M. *Angew. Chem., Int. Ed.* **2020**, *59*, 1018–1029. doi:10.1002/anie.201906755

34. Tan, D.; García, F. *Chem. Soc. Rev.* **2019**, *48*, 2274–2292. doi:10.1039/c7cs00813a

35. Bolm, C.; Hernández, J. G. *Angew. Chem., Int. Ed.* **2019**, *58*, 3285–3299. doi:10.1002/anie.201810902

36. Hernández, J. G.; Bolm, C. *J. Org. Chem.* **2017**, *82*, 4007–4019. doi:10.1021/acs.joc.6b02887

37. Rightmire, N. R.; Hanusa, T. P. *Dalton Trans.* **2016**, *45*, 2352–2362. doi:10.1039/c5dt03866a

38. Wang, J.; Ganguly, R.; Yongxin, L.; Díaz, J.; Soo, H. S.; García, F. *Dalton Trans.* **2016**, *45*, 7941–7946. doi:10.1039/c6dt00978f

39. Hernández, J. G.; Butler, I. S.; Friščić, T. *Chem. Sci.* **2014**, *5*, 3576–3582. doi:10.1039/c4sc01252f

40. Renahan, M. F.; Schanz, H.-J.; McGarrigle, E. M.; Dalton, C. T.; Daly, A. M.; Gilheany, D. G. *J. Mol. Catal. A: Chem.* **2005**, *231*, 205–220. doi:10.1016/j.molcata.2004.12.034

41. Gaston, A. J.; Navickaite, G.; Nichol, G. S.; Shaver, M. P.; Garden, J. A. *Eur. Polym. J.* **2019**, *119*, 507–513. doi:10.1016/j.eurpolymj.2019.07.017

42. Bowmaker, G. A. *Chem. Commun.* **2013**, *49*, 334–348. doi:10.1039/c2cc35694e

43. Milbeo, P.; Quintin, F.; Moulat, L.; Didierjean, C.; Martinez, J.; Bantrel, X.; Calmès, M.; Lamaty, F. *Tetrahedron Lett.* **2021**, *63*, 152706. doi:10.1016/j.tetlet.2020.152706

44. Crawford, D.; Casaban, J.; Haydon, R.; Giri, N.; McNally, T.; James, S. L. *Chem. Sci.* **2015**, *6*, 1645–1649. doi:10.1039/c4sc03217a

45. Ferguson, M.; Giri, N.; Huang, X.; Apperley, D.; James, S. L. *Green Chem.* **2014**, *16*, 1374–1382. doi:10.1039/c3gc42141d

46. Shen, Y.-M.; Duan, W.-L.; Shi, M. *J. Org. Chem.* **2003**, *68*, 1559–1562. doi:10.1021/jo020191j

License and Terms

This is an open access article licensed under the terms of the Beilstein-Institut Open Access License Agreement (<https://www.beilstein-journals.org/bjoc/terms>), which is identical to the Creative Commons Attribution 4.0 International License

(<https://creativecommons.org/licenses/by/4.0>). The reuse of material under this license requires that the author(s), source and license are credited. Third-party material in this article could be subject to other licenses (typically indicated in the credit line), and in this case, users are required to obtain permission from the license holder to reuse the material.

The definitive version of this article is the electronic one which can be found at:

<https://doi.org/10.3762/bjoc.18.147>